

MR11-05  
(27 June.- 4 August.2011)  
Preliminary Cruise Report



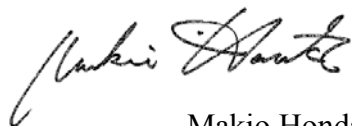
September.2011  
**JAMSTEC**

### **Note**

This cruise report is a preliminary documentation published in approximately a month after the end of this cruise. It may not be corrected even if changes on contents are found after publication. It may also be changed without notice. Data on the cruise report may be raw or not processed. Please ask the principal investigator and parsons in charge of respective observations for the latest information and permission before using. Users of data are requested to submit their results to JAMSTEC Data Integration and Analysis Group (DIAG).

August 2011

Principal Investigator of MR11-05

A handwritten signature in black ink, appearing to read 'Makio Honda', with a stylized, cursive script.

Makio Honda  
JAMSTEC

## Contents of MR11-05 Preliminary Cruise Report

### A. Cruise summary

#### 1. Cruise information

(1) Cruise designation	A1
(2) Cruise title	A1
(3) Principal investigator	A1
(4) Science proposal of cruise	A1
(5) Cruise period (port call)	A2
(6) Cruise region (geographical boundary)	A2
(7) Cruise track and stations	A3

#### 2. Overview of MR11-05

(1) Objective of this cruise	A4
(2) Cruise summary	A4 - A9

### B. Text

#### 1. Outline of MR11-05

1.1 Cruise summary	
(1) Introduction of principal science proposal	1
(2) Objective of this cruise	1
(3) Cruise summary	1
(4) Scientific gears	7
1.2 Track and log	8
1.3 Cruise participants	13-14

#### 2. General observation

2.1 Meteorological observations	
2.1.1 Surface meteorological observation	15
2.1.2 Ceilometer observation	23
2.1.3 Lidar observations of clouds and aerosols	25
2.1.4 Optical characteristics of aerosol observed by Ship-borne Sky radiometer	28
2.1.5 Tropospheric aerosol and gas observations on a research vessel by MAX-DOAS and auxiliary techniques	30
2.1.6 Rain, water vapor and surface water sampling	32
2.1.7 Air-Sea surface eddy flux measurement	37
2.2 Physical oceanographic observations	
2.2.1 CTD cast and water sampling	38
2.2.2 Salinity measurement	43
2.2.3 Shipboard ADCP	47
2.3 Sea surface water monitoring	51
2.4 Dissolved oxygen (MWJ)	55

2.5 Nutrients	59
2.6 pH measurement	75
2.7 Dissolved inorganic carbon –DIC-	78
2.8 Total alkalinity	80
2.9 Underway pCO <sub>2</sub>	83
<b>3. Special observation</b>	
3.1 BGC mooring Recovery and deployment	
3.1.1 Recovery and deployment	85
3.1.2 Instruments	95
3.1.3 Sampling schedule	98
3.1.4 Preliminary results	99
3.2 Underwater profiling buoy system	101
3.3 WHOI ST mooring system	107
3.4 Phytoplankton	
3.4.1 Chlorophyll a measurements by fluorometric determination	111
3.4.2 HPLC measurements of marine phytoplankton pigments	116
3.4.3 Phytoplankton abundance	121
3.4.4 Primary production and new production	124
3.4.5 P vs E curve	130
3.4.6 Oxygen evolution (gross primary production)	133
3.5 Optical measurement	136
3.6 Drifting sediment trap	
3.6.1 Drifting mooring system	139
3.6.2 Drifting sediment trap of JAMSTEC	143
3.6.3 Vertical changes of fecal pellets	144
3.7 Po-210 and export flux	148
3.8 Settling velocity of particles in the twilight zone	149
3.9 Zooplankton	
3.9.1 Community structure and ecological roles	150
3.9.2 Grazing pressure of microzooplankton	153
3.10 Effects of zooplankton on sinking carbon flux	
3.10.1 Active carbon flux	155
3.10.2 Production and consumption of fecal pellets	157
3.11 Biological study for phytoplankton and zooplankton	
3.11.1 Planktic Foraminifers and radiolarians	159
3.11.2 Shell-bearing phytoplankton studies in the western North Pacific	162
3.12 Community structures and metabolic activities of microbes	163
3.13 Dissolved organic carbon	165
3.14 Chlorofluorocarbons	166
3.15 Argo float	169
3.16 Optical measurement of marine snow: VPR	175
3.17 Observational research on air-sea interaction in the Kuroshio-Oyashio Extension region	178



3.18 Temporal changes in water properties of abyssal water in the western North Pacific	188
---	-----

#### **4. Studies of artificial radioactive nuclide**

4.1 Verification of DNA damage in microorganisms by the radioactive contamination	191
4.2 The concentrations of radionuclides in the western North Pacific	194
4.3 Estimation of radionuclides' deposition into the ocean in the western Pacific by using a regional chemical model	195
4.4 Model-observation comparison study on upper-ocean conditions and radionuclide dispersion off Tohoku	3; 9
4.5 Geochemical behavior of radionuclides from Fukushima Daiichi Nuclear Power Plant in marine environment	198
4.6 Distribution of radioisotopes in sediments off Fukushima, Japan	199
4.7 Detection of radioactive sulfur in the maritime air and surface seawater	200
4.8 Multiple Corer (MC)	203

#### **5. Geophysical observation**

5.1 Swath bathymetry	208
5.2 Sea surface gravity	210
5.3 Sea surface magnetic field	211

#### **6. Satellite image acquisition (MCSST from NOAA/HPRT)** 213

Cover sheet: the first prize of “MR11-05 CRUISE REPORT COVER SHEET CONTEST”  
The winner is Mr. Shintaro Abe, who is not the former Japanese prime minister, but a young man of ship crews (engine room).

## A. Cruise summary

### 1. Cruise information

(1) Cruise designation (research vessel)

MR11-05 (R/V MIRAI)

(2) Cruise title (principal science proposal) and introduction

Change in material cycles and ecosystem by the climate change and its feedback

#### *Introduction*

Some disturbing effects are progressively coming to the fore in the ocean by climate change, such as rising water temperature, intensification of upper ocean stratification and ocean acidification. It is supposed that these effects result in serious damage to the ocean ecosystems. Disturbed ocean ecosystems will change a material cycle through the change of biological pump efficiency, and it will be fed back into the climate. We are aimed at clarifying the mechanisms of changes in the ocean structure in ocean ecosystems derived from the climate change,

We arranged the time-series observation stations in the subarctic gyre (K2: 47°N 160°E) and the subtropical gyre (S1: 30°N, 145°E) in the western North Pacific. In general, biological pump is more efficient in the subarctic gyre than the subtropical gyre because large size phytoplankton (diatom) is abundant in the subarctic gyre by its eutrophic oceanic condition. It is suspected that the responses against climate change are different for respective gyres. To elucidate the oceanic structures in ocean ecosystems and material cycles at both gyres is important to understand the relationship between ecosystem, material cycle and climate change in the global ocean.

There are significant seasonal variations in the ocean environments in both gyres. The seasonal variability of oceanic structures will be estimated by the mooring systems and by the seasonally repetitive ship observations scheduled for next several years.

(3) Principal Investigator (PI)

Makio Honda

Research Institute for Global Change (RIGC)

Japan Agency for Marine-Earth Science and Technology (JAMSTEC)

(4) Science proposals of cruise

Affiliation	PI	Proposal titles
AORI / The Univ. Tokyo	Koji HAMASAKI	Studies on the microbial-geochemical processes that regulate the operation of the biological pump in the subarctic and subtropical regions of the western North Pacific
Kagoshima Univ.	Toru KOBARI	Effects of meso-zooplankton on food web and vertical flux
JAMSTEC RIGC	Hiroshi UCHIDA	Temporal changes in water properties of abyssal water in the western North Pacific
JAMSTEC RIGC	Yoshimi KAWAI	Observational research on air-sea interaction in the Kuroshio-Oyashio Extension region
JAMSTEC RIGC	Toshio SUGA	Study of ocean circulation and heat and freshwater transport and their variability, and experimental comprehensive study of physical, chemical, and biochemical processes in the western North Pacific by the deployment of Argo floats and using

		Argo data
JAMSTEC RIGC	Hideki KOBAYASHI	Verification of DNA damage in microorganisms by the radioactive contamination
not onboard study		
NIES	Nobuo SUGIMOTO	Study of distribution and optical characteristics of ice/water clouds and marine aerosols
Okayama Univ.	Osamu TSUKAMOTO	Onboard continuous air-sea eddy flux measurement
JAMSTEC	Hisanori TAKASHIMA	Tropospheric aerosol and gas profile observations by MAX-DOAS on a research vessel
Toyama Univ.	Kazuma AOKI	Maritime aerosol optical properties from measurements of Ship-borne sky radiometer
Chiba Univ.	Masao NAKANISHI	Tectonics of the mid-Cretaceous Pacific Plate
Ryukyu Univ.	Takeshi MATSUMOTO	Standardization of marine geophysical data and its application to the ocean floor geodynamics studies
JAMSTEC	Naoyuki KURITA	Rain and seawater sampling for stable isotopes
National Institute of Radiological Sciences	Tatsuo AONO	The concentrations of radionuclides in the western North Pacific
JAMSTEC RIGC	Masayuki TAKIGAWA	Estimation of radionuclides' deposition into the ocean in the western Pacific by using a regional chemical transport model
JAMSTEC RIGC	Yukio MASUMOTO	Model-observation comparison study on upper-ocean conditions and radionuclide dispersion off Tohoku
Kanazawa Univ.	Seiya NAGAO	Geochemical behavior of radionuclides released from Fukushima Daiichi NPP in marine environment
Tokai Univ.	Yoshihisa KATO	Distribution of radioisotopes in sediments off Fukushima, Japan
Tokyo Institute of Technology	Naohiro YOSHIDA	Detection of radioactive sulfur in the maritime air and surface seawater

(5) Cruise period (port call)

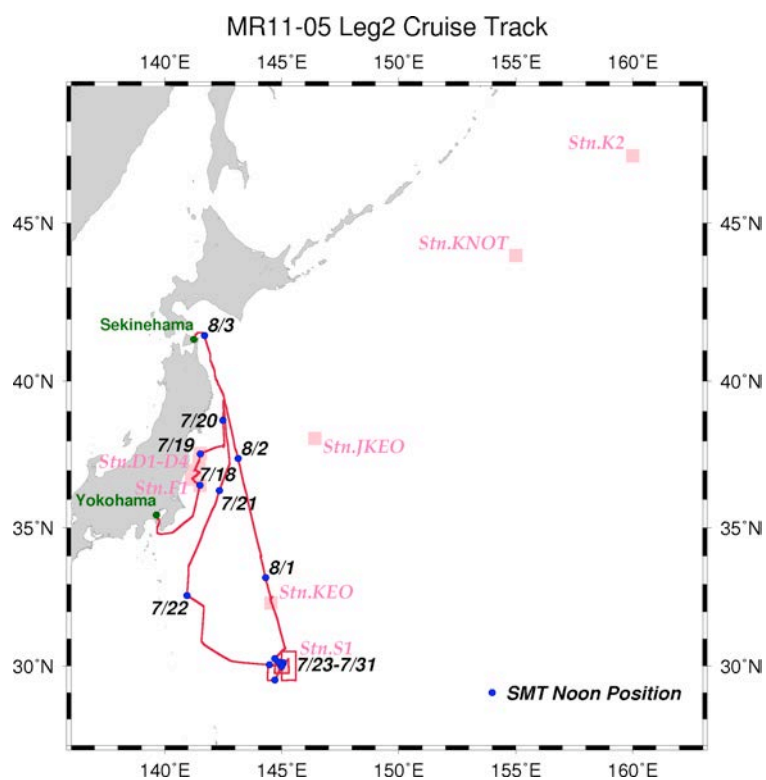
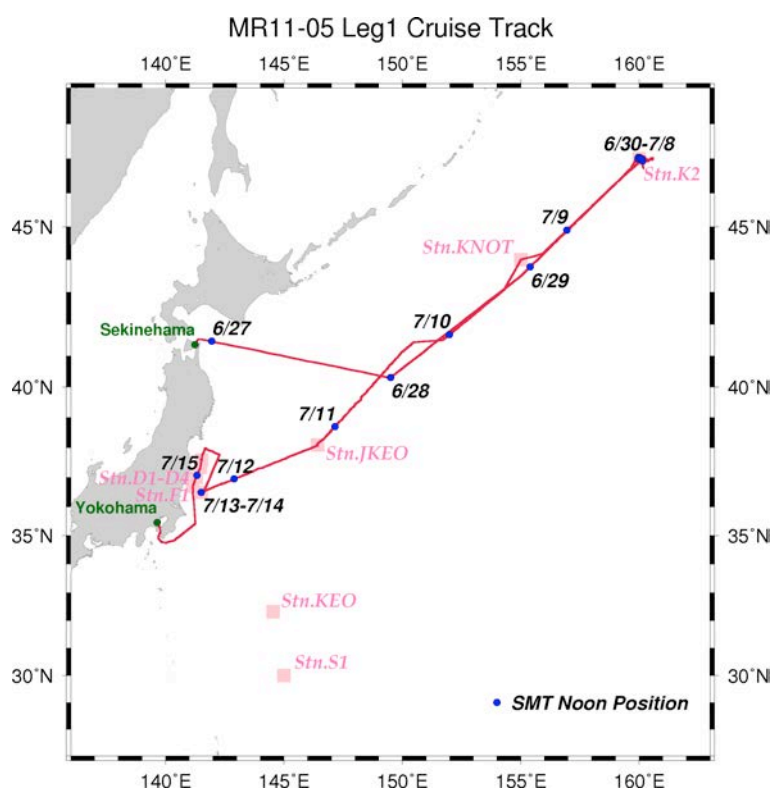
Leg.1: 27 June 2011 (Sekinehama) – 16 July 2011 (Yokohama)

Leg.2: 17 July 2011 (Yokohama) – 4 August 2011 (Sekinehama)

(6) Cruise region (geographical boundary)

The western North Pacific (50°N – 30°N, 140°E – 160°W)

### (7) Cruise truck and stations



## 2. Outline of MR11-05

### (1) Objective of this cruise

Objective of this cruise is to observe summer ecosystem and biogeochemical cycle at time-series stations in the sub-arctic and sub-tropical gyres. Additional purpose is to collect samples for measurement of artificial radioactive nuclides (ARN) accidentally emitted from the Fukushima Daiichi nuclear power plant caused by the Tohoku great earthquake and its induced tsunami on 11 March 2011 in order to verify mechanism of transport and circulation of ARN in the ocean.

### (2) Cruise summary

#### 1) Time-series observation at stations K2 and S1

Since last autumn 2010, time-series observation of ecosystem and biogeochemistry has been conducted at time-series stations (K2: sub-arctic gyre, S1: sub-tropical gyre). In this cruise, comprehensive oceanography in summer was observed and many samples were collected for analysis of ecosystem and biogeochemistry in summer at both stations.

#### a) Station K2

We stayed at station K2 for ca. 10 days and comprehensive observations were conducted. Sea surface temperature was ca. 7°C. Surface mixed layer was ca. 20 – 25 m and the shallowest among time-series cruises since winter 2010 (Fig. 1a). Chlorophyll-a in the surface water was ca. 1 mg L<sup>-1</sup> on average and subsurface maximum was observed at around 30 m just below surface mixed layer (1b). Chlorophyll-a in the surface water was the maximum among time-series cruises (Fig. 2a). Integrated chlorophyll-a was estimated to be 70-80 mg m<sup>-2</sup> and also the maximum. Integrated primary productivity was estimated 460 - 820 mg-C m<sup>-2</sup> day<sup>-1</sup> (average: 660 mg-C m<sup>-2</sup> day<sup>-1</sup>) (Fig. 2b). To sum up, biological activity and productivity was the greatest in this cruise among time-series cruises. In addition, sediment trap mooring system deployed last October 2010 was successfully recovered at station K2. Time-series sediment traps at 200m, 500m and 4810m collected seasonal sinking particles each 6 – 12 days interval. At 200m, relatively higher flux was observed in the early period after sediment trap started sampling in autumn. However amount of collected materials decreased since then (Fig. 3a). Distinct seasonal variability in sediment trap materials at 500 m and 4810 m did not appear. Compared to other years, amount and seasonal variability of sinking materials collected looked smaller. Moreover synchronization of seasonal variability between different depths was not seen either.

#### b) Station S1

We started observation at S1 just after typhoon passed. It was expected that primary productivity was high because nutrient in subsurface layer was supplied by increase of surface mixing. However chlorophyll-a maximum at subsurface (~ 100 m) was at most 0.6 µg kg<sup>-1</sup> (Fig. 4a) and surface chlorophyll-a was only 0.06 µg kg<sup>-1</sup> and the smallest among time-series cruises (Fig. 2a). Primary productivity (PP) was low (Fig. 4b) and integrated PP of approximately 220 mg-C m<sup>-2</sup> day<sup>-1</sup> was the second smallest among time-series cruises. Sediment trap mooring system deployed in October 2010 was also recovered successfully at station S1. At 200m, relatively higher flux was observed in late February and April 2011 (Fig. 3b). At 500m, similar seasonal variability was observed although variability was small. At 4810 m, high flux was observed in May 2011. Distinct synchronization of seasonal variability between different depths was not observed.

Seasonal observation at stations K2 and S1 since winter 2010 showed similar seasonal variability to previous one (Fig. 2a, 2b). However winter chlorophyll-a and primary productivity was higher than previous data. Especially its trend at station S1 was noteworthy and sinking particles were higher than that at station K2. Future chemical analysis will reveal this characteristic quantitatively.



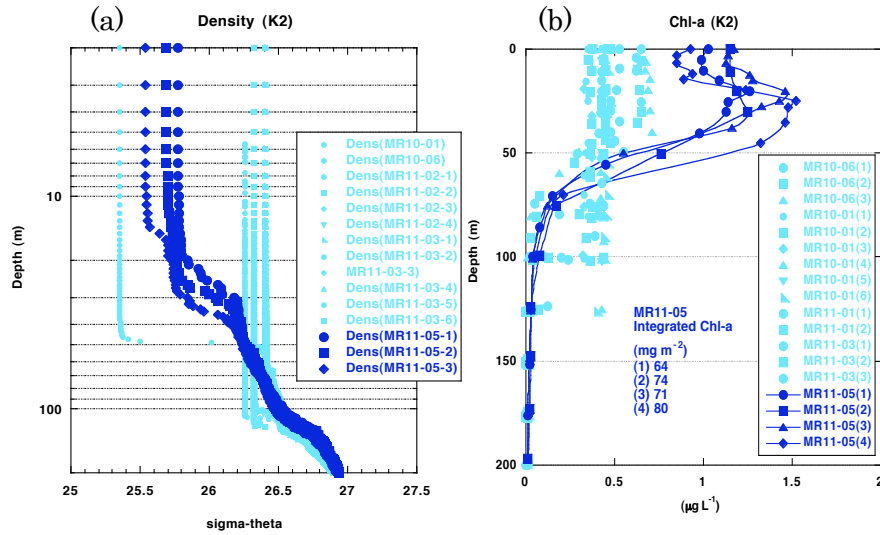


Fig.1 Seasonal variability in vertical profiles of (a) density (b)chlorophyll-a at station K2

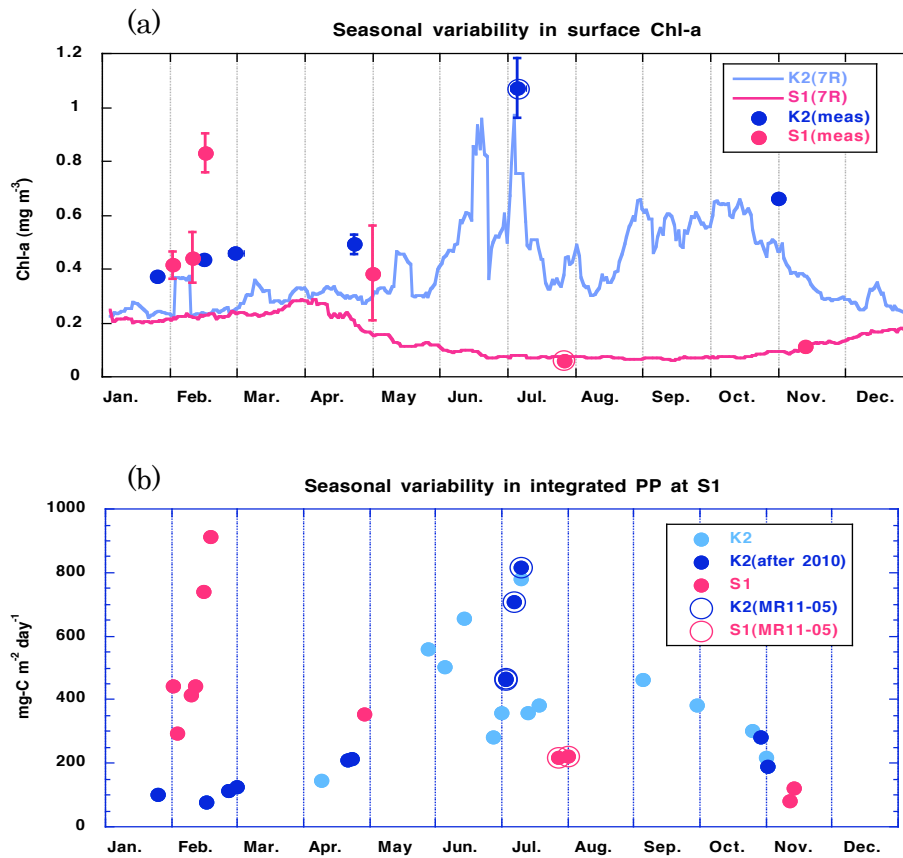


Fig. 2 Seasonal variability in (a) surface chlorophyll-a and (b) integrated primary productivity. Line graph in (a) is previous average of satellite based chlorophyll –a.

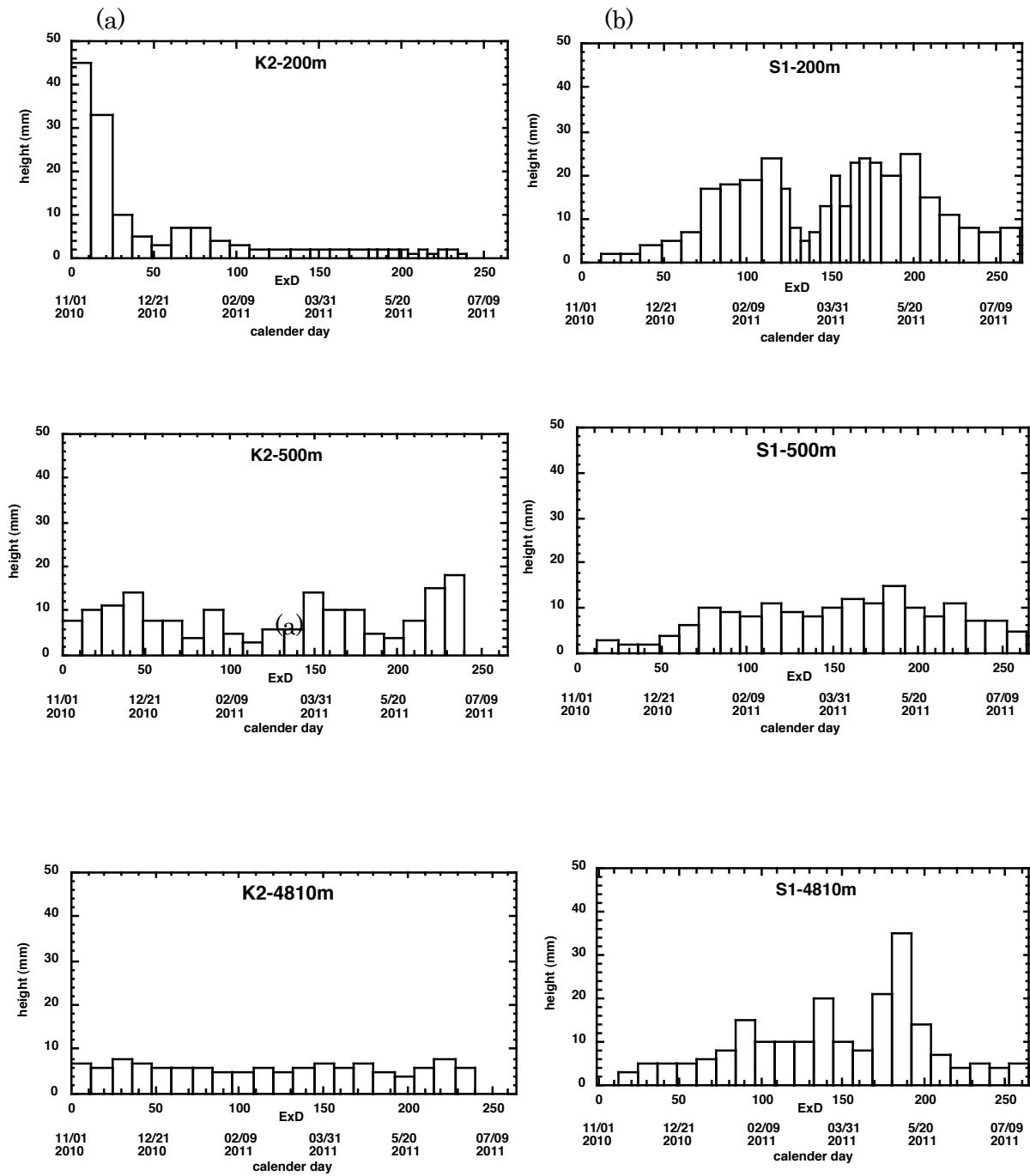


Fig. 3 Seasonal variability in sinking particle flux (a) K2-200m (upper) K2-500m (middle) K2-4810m (lower) and (b) S1-200m (upper) S1-500m (middle) S1-4810m (lower) . Vertical axis is height of collected materials in collecting cups.

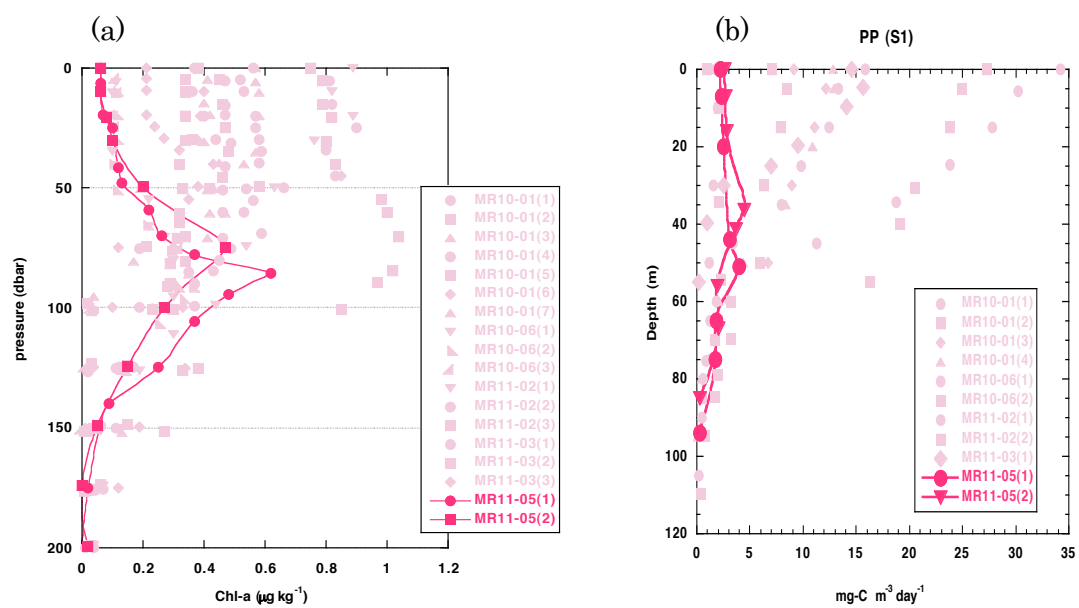


Fig. 4 Vertical profiles of (a) chlorophyll-a and (b) primary productivity at station S1

## 2) Observation of artificial radioactive nuclides

Along the cruise track and at stations K2, S1 and brand-new station F1, seawater, aerosol, suspended matter and seafloor sediment were collected in order to measure artificial radioactive nuclides (Fig. 5). At station F1, where is ca. 90 km southeast from the Fukushima Daiichi nuclear power plant, the small decrease of beam transmittance was observed at not only near surface, but also middle layer (around 700 m) and near bottom (1200 m) (Fig. 6). It was indicative of that there exist materials transported horizontally at station F1. The mooring system with time-series sediment traps at 500 m and 1000 m was deployed under cooperation with Woods Hole Oceanographic Institution. This mooring system will be recovered in June 2012.

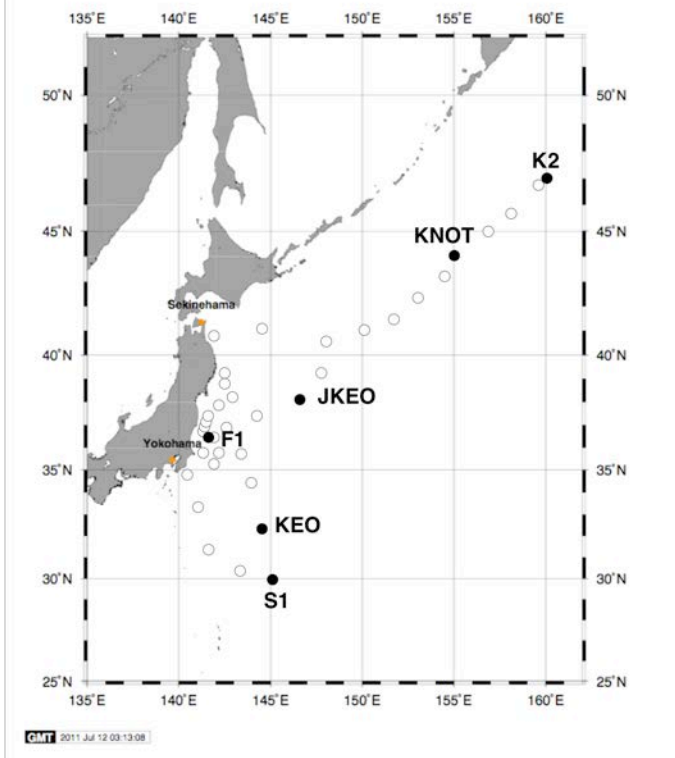


Fig. 5 Sampling stations of sea surface water for measurement of radioactive nuclides

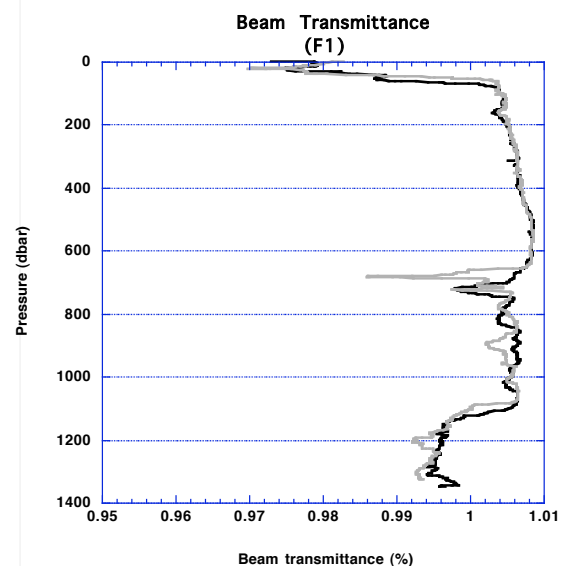


Fig. 6 Vertical profile of beam transmittance at station F1

## **B. Text**

### **1. Outline of MR11-05**

**Makio HONDA (JAMSTEC RIGC)**

**Principal Investigator of MR11-05**

#### **1.1 Cruise summary**

##### **(1) Introduction of principal science proposal**

Some disturbing effects are progressively coming to the fore in the ocean by climate change, such as rising water temperature, intensification of upper ocean stratification and oceanic acidification. It is supposed that these effects result in serious damage to the ocean ecosystems. Disturbed ocean ecosystems will change a material cycle through the change of biological pump efficiency, and it will be fed back into the climate. We are aimed at clarifying the mechanisms of changes in the oceanic structure in ocean ecosystems derived from the climate change,

We arranged the time-series observation stations in the subarctic gyre (K2: 47°N 160°E) and the subtropical gyre (S1: 30°N, 145°E) in the western North Pacific. In general, biological pump is more efficient in the subarctic gyre than the subtropical gyre because large size phytoplankton (diatom) is abundant in the subarctic gyre by its eutrophic oceanic condition. It is suspected that the responses against climate change are different for respective gyres. To elucidate the oceanic structures in ocean ecosystems and material cycles at both gyres is important to understand the relationship between ecosystem, material cycle and climate change in the global ocean.

There are significant seasonal variations in the ocean environments in both gyres. The seasonal variability of oceanic structures will be estimated by the mooring systems and by the seasonally repetitive ship observations scheduled for next several years.

##### **(2) Objective of this cruise**

Objective of this cruise is to observe summer ecosystem and biogeochemical cycle at time-series stations in the sub-arctic and sub-tropical gyres. Additional purpose is to collect samples for measurement of artificial radioactive nuclides (ARN) accidentally emitted from the Fukushima Daiichi nuclear power plant caused by the Tohoku great earthquake and its induced tsunami on 11 March 2011 in order to verify mechanism of transport and circulation of ARN in the ocean.

##### **(3) Cruise summary**

###### **1) Time-series observation at stations K2 and S1**

Since last autumn 2010, time-series observation of ecosystem and biogeochemistry has been conducted at time-series stations (K2: sub-arctic gyre, S1: sub-tropical gyre). In this cruise, comprehensive oceanography in summer was observed and many samples were collected for analysis of ecosystem and biogeochemistry in summer at both stations.

###### **a) Station K2**

We stayed at station K2 for ca. 10 days and comprehensive observations were conducted. Sea surface temperature was ca. 7°C. Surface mixed layer was ca. 20 – 25 m and the shallowest among time-series cruises since winter 2010 (Fig. 1a). Chlorophyll-a in the surface

water was ca.  $1 \text{ mg L}^{-1}$  on average and subsurface maximum was observed at around 30 m just below surface mixed layer (1b). Chlorophyll-a in the surface water was the maximum among time-series cruises (Fig. 2a). Integrated chlorophyll-a was estimated to be  $70\text{-}80 \text{ mg m}^{-2}$  and also the maximum. Integrated primary productivity was estimated  $460 - 820 \text{ mg-C m}^{-2} \text{ day}^{-1}$  (average:  $660 \text{ mg-C m}^{-2} \text{ day}^{-1}$ ) (Fig. 2b). To sum up, biological activity and productivity was the greatest in this cruise among time-series cruises. In addition, sediment trap mooring system deployed last October 2010 was successfully recovered at station K2. Time-series sediment traps at 200m, 500m and 4810m collected seasonal sinking particles each 6 – 12 days interval. At 200m, relatively higher flux was observed in the early period after sediment trap started sampling in autumn. However amount of collected materials decreased since then (Fig. 3a). Distinct seasonal variability in sediment trap materials at 500 m and 4810 m did not appear. Compared to other years, amount and seasonal variability of sinking materials collected looked smaller. Moreover synchronization of seasonal variability between different depths was not seen either.

#### b) Station S1

We started observation at S1 just after typhoon passed. It was expected that primary productivity was high because nutrient in subsurface layer was supplied by increase of surface mixing. However chlorophyll-a maximum at subsurface ( $\sim 100 \text{ m}$ ) was at most  $0.6 \mu\text{g kg}^{-1}$  (Fig. 4a) and surface chlorophyll-a was only  $0.06 \mu\text{g kg}^{-1}$  and the smallest among time-series cruises (Fig. 2a). Primary productivity (PP) was low (Fig. 4b) and integrated PP of approximately  $220 \text{ mg-C m}^{-2} \text{ day}^{-1}$  was the second smallest among time-series cruises. Sediment trap mooring system deployed in October 2010 was also recovered successfully at station S1. At 200m, relatively higher flux was observed in late February and April 2011 (Fig. 3b). At 500m, similar seasonal variability was observed although variability was small. At 4810 m, high flux was observed in May 2011. Distinct synchronization of seasonal variability between different depths was not observed.

Seasonal observation at stations K2 and S1 since winter 2010 showed similar seasonal variability to previous one (Fig. 2a, 2b). However winter chlorophyll-a and primary productivity was higher than previous data. Especially its trend at station S1 was noteworthy and sinking particles were higher than that at station K2. Future chemical analysis will reveal this characteristic quantitatively.



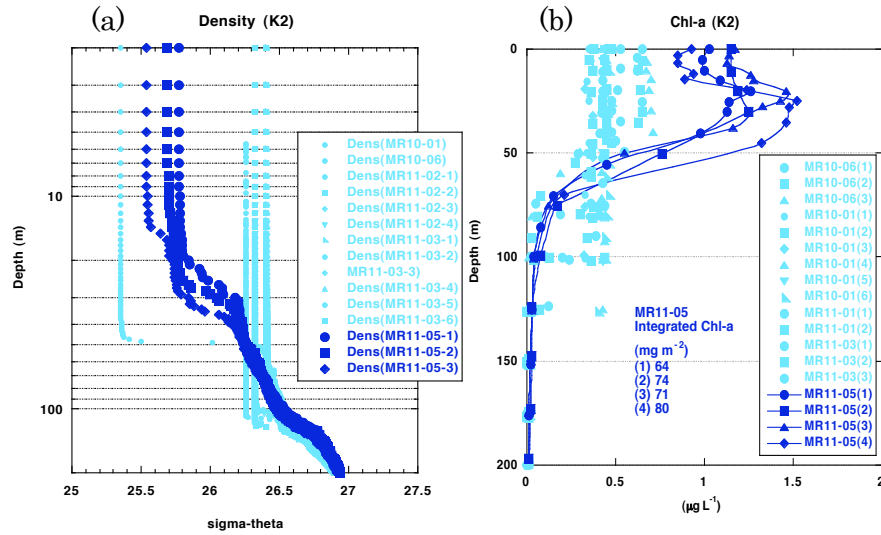


Fig.1 Seasonal variability in vertical profiles of (a) density (b)chlorophyll-a at station K2

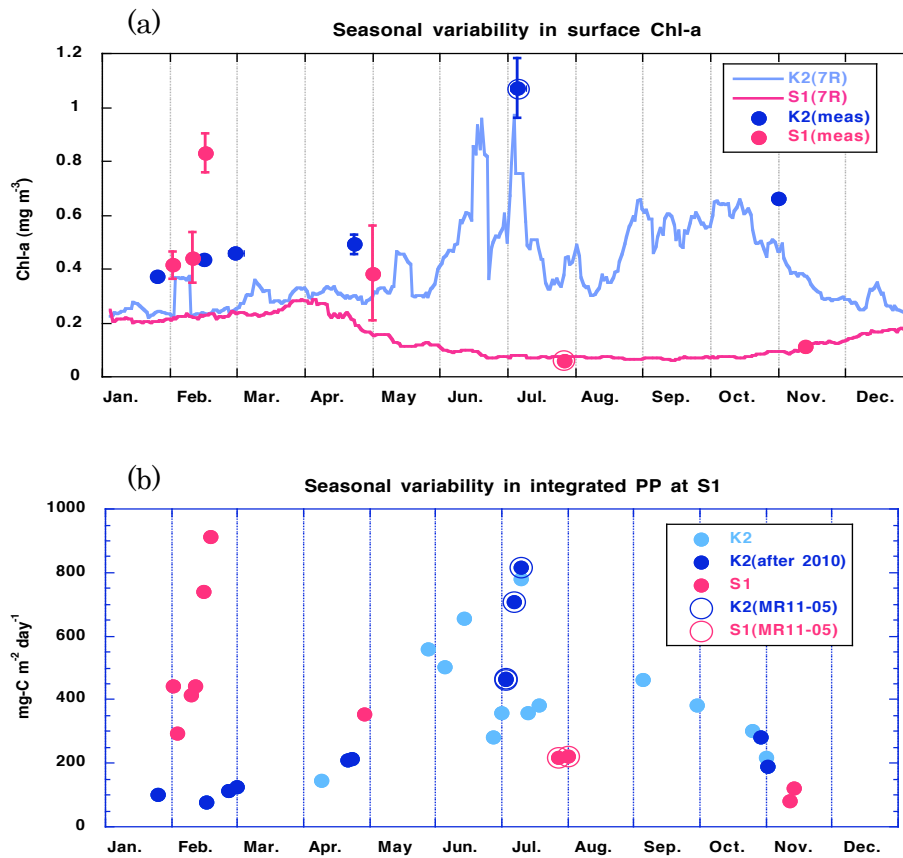


Fig. 2 Seasonal variability in (a) surface chlorophyll-a and (b) integrated primary productivity. Line graph in (a) is previous average of satellite based chlorophyll -a.

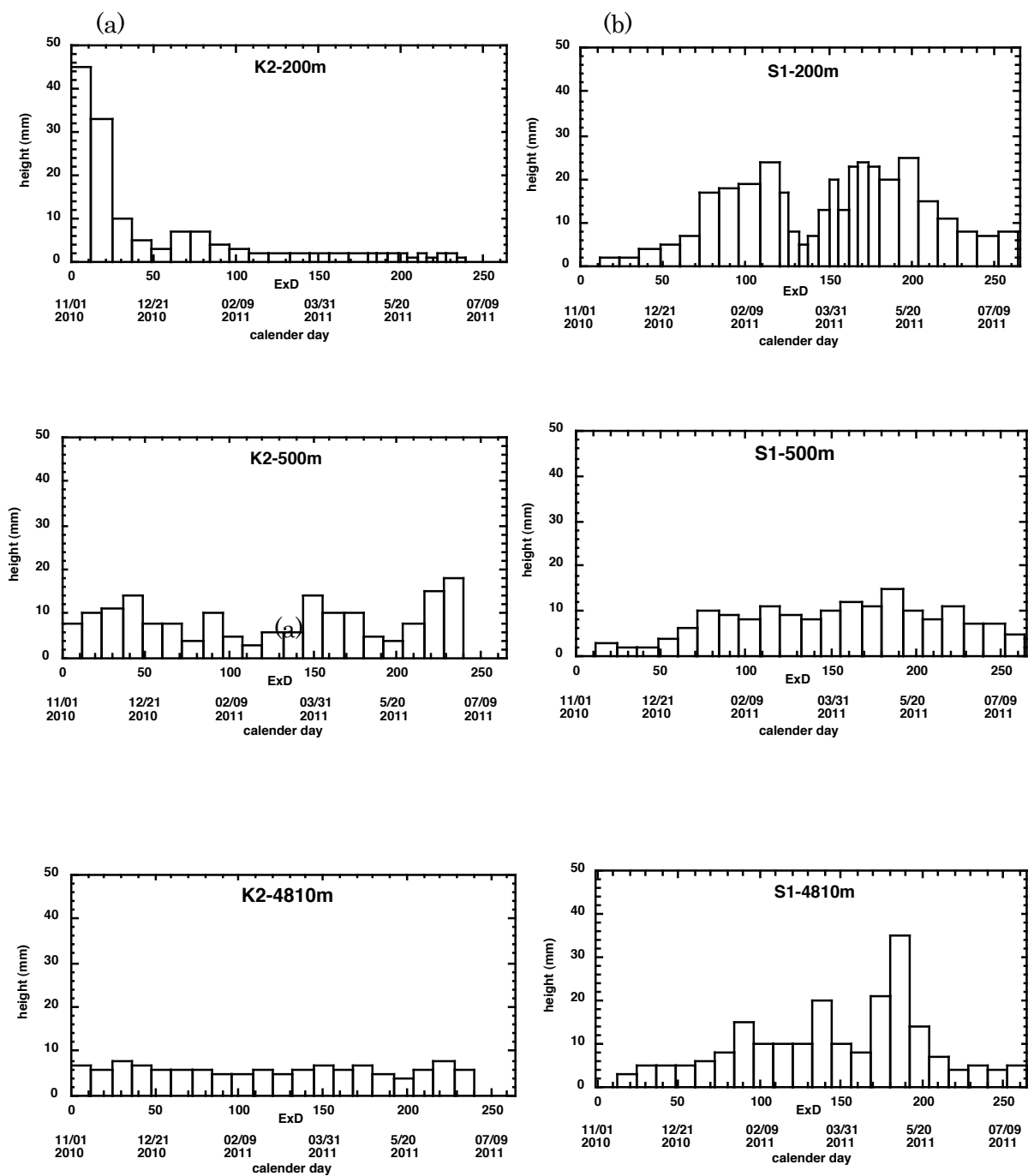


Fig. 3 Seasonal variability in sinking particle flux (a) K2-200m (upper) K2-500m (middle) K2-4810m (lower) and (b) S1-200m (upper) S1-500m (middle) S1-4810m (lower) . Vertical axis is height of collected materials in collecting cups.

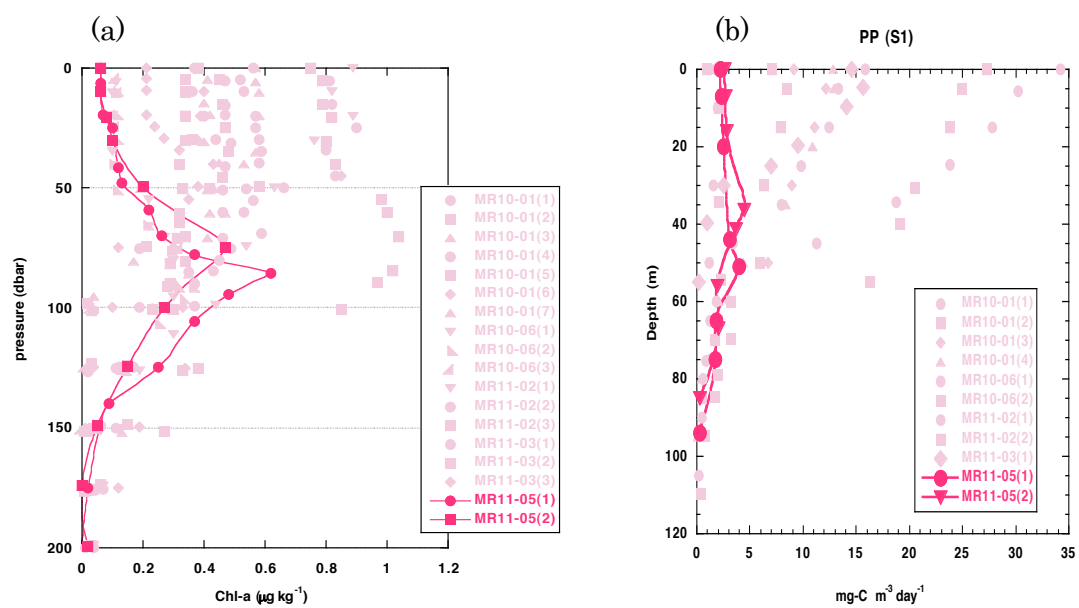


Fig. 4 Vertical profiles of (a) chlorophyll-a and (b) primary productivity at station S1

## 2) Observation of artificial radioactive nuclides

Along the cruise track and at stations K2, S1 and brand-new station F1, seawater, aerosol, suspended matter and seafloor sediment were collected in order to measure artificial radioactive nuclides (Fig. 5). At station F1, where is ca. 90 km southeast from the Fukushima Daiichi nuclear power plant, the small decrease of beam transmittance was observed at not only near surface, but also middle layer (around 700 m) and near bottom (1200 m) (Fig. 6). It was indicative of that there exist materials transported horizontally at station F1. The mooring system with time-series sediment traps at 500 m and 1000 m was deployed under cooperation with Woods Hole Oceanographic Institution. This mooring system will be recovered in June 2012.

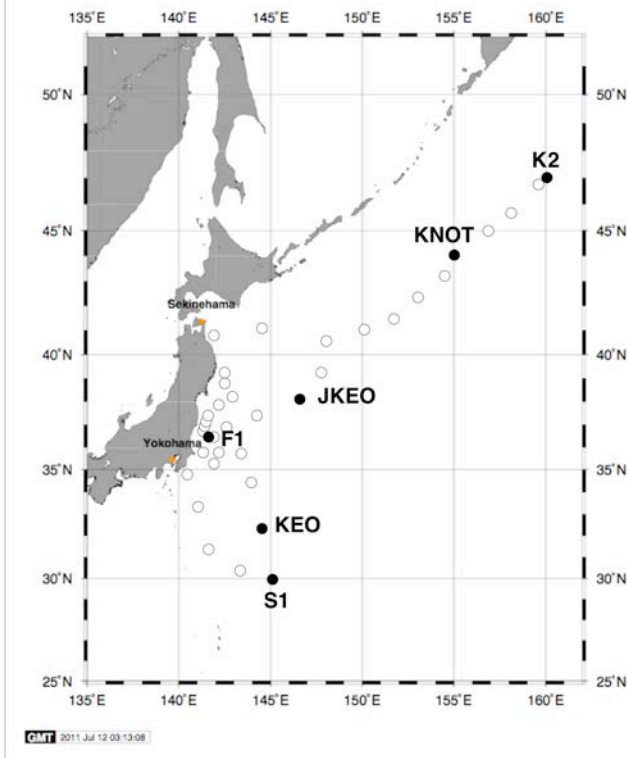


Fig. 5 Sampling stations of sea surface water for measurement of radioactive nuclides

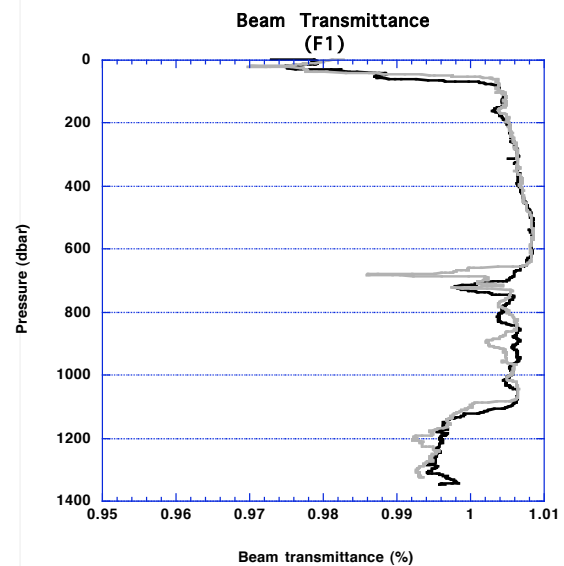


Fig. 6 Vertical profile of beam transmittance at station F1

#### (4) Scientific gears

All hydrocasts were conducted using 36-position 12 liter Niskin bottles carousel system with SBE CTD-DO system, fluorescence and transmission sensors. JAMSTEC scientists and MWJ (Marine Work Japan Co. Ltd.) technician group were responsible for analyzing water sample for salinity, dissolved oxygen, nutrients, CFCs, total carbon contents, alkalinity and pH. Cruise participants from JAMSTEC, University of Tokyo, and Kochi University helped to divide seawater from Niskin bottles to sample bottles for analysis. Surface water was collected with bucket.

Optical measurement in air and underwater was conducted with PAR sensor (RAMSES-ACC) and PAR sensor on CTD, respectively.

For collecting suspended particles at station K2 and S1, Large Volume Pump (LVP) was deployed. For observing in situ particles, optical sensor called LISST (Laser In Situ Scattering and Transmissometer) and VPR (Visual Plankton recorder) were deployed by University of Tokyo and JAMSTEC, respectively.

GODI technicians group undertook responsibility for underway current direction and velocity measurements using an Acoustic Current Profiler (ADCP), geological measurements (topography, geo-magnetic field and gravity), and collecting meteorological data.

Radio zonde observation were conducted by JAMSTEC.

For collection of zooplankton, NORPAC plankton net, and IONESS were deployed.

For conducting in situ incubation for measurement of primary productivity and collecting sinking particles at station K2, drifter was deployed at station K2 and S1.

For observing vertical profile of primary productivity optically, FRRF was deployed.

In order to conduct time-series observation in biogeochemical cycle, JAMSTEC POPPS mooring was recovered and re-deployed at station S1.

For observation of atmospheric chemistry (aerosol and gas), various instruments including “sky-radiometer” and “MAX-DOAS” were onboard and automatic measurement was conducted.

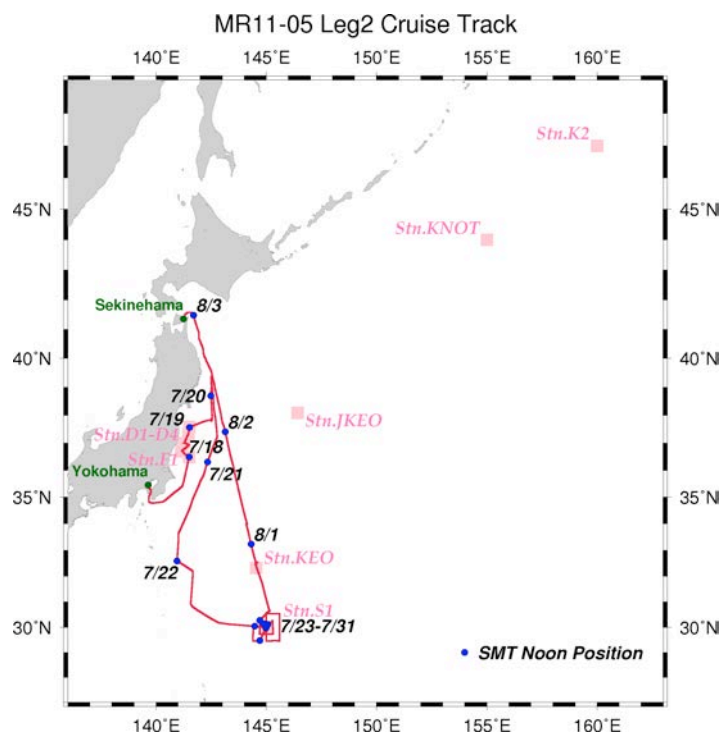
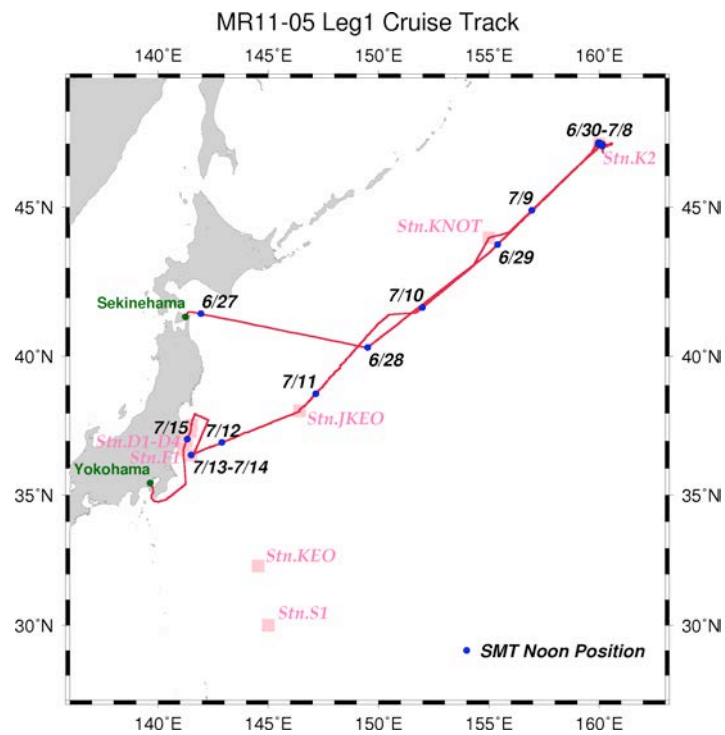
Please read text for more detail information and other instruments used for oceanographic and meteorological or atmospheric observation.

## 1.2 Track and log

### 1.2.1 Research Area

The western North Pacific (47°N – 30°N, 140°E – 160°W)

### 1.2.2 Cruise track





## MR11-05 Cruise log

(Leg.1)

U.T.C.		S.M.T.		Position		Event logs
Date	Time	Date	Time	Lat.	Lon.	
6.26	23:50	6.27	8:50	41-22N	141-14E	Departure from Sekinehama
6.27	5:30		14:30	-	-	Sea surface water analysis start
6.28	13:00	6.28	22:00	-	-	Time adjustment +1 hour (SMT=UTC+10h)
6.29	12:00	6.29	22:00	-	-	Time adjustment +1 hour (SMT=UTC+11h)
	23:24	6.30	10:24	47-00N	160-00E	Arrival at Station K2
	23:31		10:31	47-03.88N	159-58.43E	Free fall optical measruements #01
6.30	0:20		11:20	47-02.48N	159-58.44E	Free fall optical measruements #02
	0:41		11:41	47-02.25N	159-58.43E	CTD cast #01 (150 m)
	2:51		13:51	47-00.85N	159-58.56E	BGC mooring recovery
	7:00		18:00	46-59.99N	160-05.11E	Plankton net #01-1 (NORPAC: 20-0 m)
	7:08		18:08	46-59.96N	160-05.18E	Plankton net #01-2 (NORPAC: 50-20 m)
	7:23		18:23	46-59.93N	160-05.29E	Plankton net #01-3 (NORPAC: 100-50 m)
	7:37		18:37	46-59.95N	160-05.40E	Plankton net #01-4 (NORPAC: 150-100 m)
	7:52		18:52	46-59.91N	160-05.50E	Plankton net #01-5 (NORPAC: 200-150 m)
	8:09		19:09	46-59.88N	160-05.57E	Plankton net #01-6 (NORPAC: 300-200 m)
	10:53		21:53	46-59.92N	160-05.09E	Plankton net #02-1 (NORPAC: 100 m)
	11:04		22:04	46-59.89N	160-05.11E	Plankton net #02-2 (NORPAC: 100 m)
	11:16		22:16	46-59.87N	160-05.15E	Plankton net #02-3 (NORPAC: 200 m)
	14:58	7.1	1:58	46-59.92N	160-12.11E	CTD cast #02 (300 m)
	16:01		3:01	46-59.93N	160-12.54E	FRRF #01 (100 m)
	17:03		4:03	46-59.91N	160-12.06E	Surface drifting float buoy deployment
	18:07		5:07	46-59.58N	160-11.26E	FRRF #02 (100 m)
	19:01		6:01	46-59.73N	160-06.18E	CTD cast #03 (5,231 m)
	23:30		10:30	46-59.69N	160-04.81E	Radio sonde #01
	23:55		10:55	47-00.25N	160-05.26E	Free fall optical measruements #03
7.1	0:29		11:29	47-00.00N	160-05.50E	Plankton net #03-1 (NORPAC: 100 m)
	0:41		11:41	46-59.99N	160-05.53E	Plankton net #03-2 (NORPAC: 200 m)
	1:26		12:26	46-59.99N	160-05.53E	FRRF #03 (100 m)
	2:30		13:30	47-00.08N	160-05.02E	Radio sonde #02
	3:26		14:26	46-59.97N	160-05.06E	FRRF #04 (100 m)
	3:54		14:54	46-59.93N	160-05.16E	Plankton net #04-1 (NORPAC: 500-300 m)
	4:28		15:28	46-59.94N	160-05.27E	Plankton net #04-2 (NORPAC: 700-500 m)
	5:10		16:10	46-59.99N	160-05.42E	Plankton net #04-3 (NORPAC: 1000-700 m)

		7:53	18:53	47-00.05N	160-04.99E	FRRF #05 (100 m)
		10:49	21:49	47-00.03N	160-05.00E	Plankton net #05-1 (NORPAC: 200 m)
		11:02	22:02	47-00.05N	160-05.06E	Plankton net #05-2 (NORPAC: 100 m)
		11:11	22:11	47-00.05N	160-05.11E	Plankton net #05-3 (NORPAC: 100 m)
7.2		17:04	7.2 4:04	47-00.06N	160-15.39E	Surface drifting float buoy recovery
		17:39	4:39	46-59.87N	160-14.88E	Drifting sediment trap buoy deployment
		20:54	7:54	47-00.00N	160-04.93E	CTD cast #04 (2,000 m)
		23:59	10:59	47-00.04N	160-04.87E	IONESS #01 (1,000 m)
		3:16	14:16	46-55.26N	160-08.84E	Plankton net #06-1 (NORPAC: 20-0 m)
		3:22	14:22	46-55.31N	160-08.91E	Plankton net #06-2 (NORPAC: 50-20 m)
		3:31	14:31	46-55.38N	160-08.99E	Plankton net #06-3 (NORPAC: 100-50 m)
		3:42	14:42	46-55.47N	160-09.08E	Plankton net #06-4 (NORPAC: 150-100 m)
		3:55	14:55	46-55.56N	160-09.19E	Plankton net #06-5 (NORPAC: 200-150 m)
		4:11	15:11	46-55.66N	160-09.32E	Plankton net #06-6 (NORPAC: 300-200 m)
		4:59	15:59	160-09.63E	160-09.63E	Large Volume Pump (LVP) #01 (200 m)
		8:06	19:06	46-59.40N	160-05.56E	CTD cast #05 (200 m)
		11:01	22:01	46-59.87N	160-04.91E	IONESS #02 (1,000 m)
7.3		14:23	7.3 1:23	46-54.68N	160-08.02E	Atmospheric turbulent flux observation #1
		20:59	7:59	46-57.96N	160-05.65E	Plankton net #07-1 (NORPAC: 500-300 m)
		21:27	8:27	46-57.93N	160-05.73E	Plankton net #07-2 (NORPAC: 700-500 m)
		22:03	9:03	46-57.91N	160-05.83E	Plankton net #07-3 (NORPAC: 1000-700 m)
		23:56	10:56	46-59.98N	160-05.04E	IONESS #03 (1,000 m)
		3:55	14:55	46-55.52N	160-08.31E	CTD cast #06 (1,000 m)
		10:56	21:56	46-59.93N	160-04.72E	IONESS #04 (1,000 m)
7.4		14:20	7.4 1:20	46-54.63N	160-03.62E	Atmospheric turbulent flux observation #2
		21:14	8:14	47-05.17N	160-04.28E	BGC mooring deployment
		0:38	11:38	46-59.83N	159-57.65E	Free fall optical measurements #04
		1:44	12:44	47-00.34N	159-58.42E	BGC mooring fixed position
		2:57	13:57	46-58.88N	159-58.42E	CTD cast #07 (5,000 m)
		6:13	17:13	46-58.82N	159-59.21E	LISST #01 (200 m)
		9:53	20:53	46-59.78N	160-05.01E	Plankton net #08-1 (NORPAC: 150 m)
		10:05	21:05	46-59.75N	160-05.02E	Plankton net #08-2 (NORPAC: 50 m)
		10:12	21:12	46-59.73N	160-05.01E	Plankton net #08-3 (NORPAC: 50 m)
		10:19	21:19	46-59.72N	160-04.99E	Plankton net #08-4 (NORPAC: 100 m)
		10:29	21:29	46-59.69N	160-04.98E	Plankton net #08-5 (NORPAC: 150 m)
		10:44	21:44	46-59.66N	160-04.96E	Plankton net #08-6 (NORPAC: 150 m)
		10:59	21:59	46-59.63N	160-04.95E	Plankton net #08-7 (NORPAC: 200 m)
		15:27	7.5 2:27	47-00.01N	160-04.97E	CTD cast #08 (300 m)
		16:24	3:24	47-00.08N	160-05.00E	FRRF #06 (100 m)
		20:55	7:55	46-59.99N	160-05.23E	FRRF #07 (100 m)

7.5	21:26		8:26	46-59.93N	160-05.46E	CTD cast #09 (200 m)
	23:56		10:56	46-59.81N	160-04.92E	Free fall optical measruements #05
	0:32		11:32	46-59.43N	160-04.91E	Plankton net #09-1 (NORPAC: 50 m)
	0:40		11:40	46-59.40N	160-04.91E	Plankton net #09-2 (NORPAC: 200 m)
	0:52		11:52	46-59.41N	160-04.93E	Plankton net #09-3 (NORPAC: 100 m)
	1:26		12:26	46-59.69N	160-04.96E	FRRF #08 (100 m)
	3:25		14:25	47-00.01N	160-05.03E	FRRF #09 (100 m)
	3:50		14:50	47-00.02N	160-05.05E	Plankton net #10-1 (NORPAC: 300-200 m)
	4:10		15:10	47-00.03N	160-05.12E	Plankton net #10-2 (NORPAC: 200-150 m)
	4:24		15:24	47-00.04N	160-05.19E	Plankton net #10-3 (NORPAC: 150-100 m)
	4:35		15:35	47-00.05N	160-05.26E	Plankton net #10-4 (NORPAC: 100-50 m)
	4:46		15:46	47-00.06N	160-05.33E	Plankton net #10-5 (NORPAC: 50-20 m)
	4:57		15:57	47-00.07N	160-05.43E	Plankton net #10-6 (NORPAC: 20 m)
	5:02		16:02	47-00.08N	160-05.47E	Plankton net #10-7 (NORPAC: 50 m)
	5:10		16:10	47-00.09N	160-05.55E	Plankton net #10-8 (NORPAC: 50 m)
	7:54		18:54	46-59.95N	160-05.17E	FRRF #10 (100 m)
	11:01		22:01	46-59.85N	160-04.96E	IONESS #05 (200 m)
7.6	14:25	7.6	1:25	46-54.65N	160-02.64E	Atmospheric turbulent flux observation #2
	18:02		5:02	46-55.99N	160-09.65E	LVP #02 (1,000 m)
	0:45		11:45	46-55.78N	160-09.13E	Plankton net #11-1 (NORPAC: 100 m)
	0:55		11:55	46-55.81N	160-09.22E	Plankton net #11-2 (NORPAC: 100 m)
	1:06		12:06	46-55.82N	160-09.27E	Plankton net #11-3 (NORPAC: 200 m)
	2:01		13:01	46-55.78N	160-09.50E	Plankton net #12-1 (NORPAC: 1,000-500 m)
	2:51		13:51	46-55.77N	160-09.64E	Plankton net #12-2 (NORPAC: 500-300 m)
	3:17		14:17	46-55.76N	160-09.70E	Plankton net #12-3 (NORPAC: 300-200 m)
	3:35		14:35	46-55.76N	160-09.74E	Plankton net #12-4 (NORPAC: 200-100 m)
	3:50		14:50	46-55.75N	160-09.80E	Plankton net #12-5 (NORPAC: 100-50 m)
	3:59		14:59	46-55.74N	160-09.84E	Plankton net #12-6 (NORPAC: 50-0 m)
	4:17		15:17	46-55.73N	160-09.89E	CTD cast #10 (200 m)
7.7	17:45	7.7	4:45	46-58.35N	160-33.85E	Drifting sediment trap buoy recovery
	20:57		7:57	46-59.95N	160-05.12E	Plankton net #13-1 (NORPAC: 300-200 m)
	21:16		8:16	46-59.91N	160-05.18E	Plankton net #13-2 (NORPAC: 200-150 m)
	21:32		8:32	46-59.85N	160-05.22E	Plankton net #13-3 (NORPAC: 150-100 m)
	21:44		8:44	46-59.79N	160-05.30E	Plankton net #13-4 (NORPAC: 100-50 m)
	21:52		8:52	46-59.75N	160-05.35E	Plankton net #13-5 (NORPAC: 50-20 m)
	22:04		9:04	46-59.71N	160-05.42E	Plankton net #13-6 (NORPAC: 20-0 m)
	23:58		10:58	46-59.94N	160-04.89E	Free fall optical measruements #06
	0:38		11:38	46-59.81N	160-04.38E	IONESS #06 (300 m)
	3:11		14:11	46-55.85N	160-09.73E	LVP #03 (1,000 m)
	9:25		20:25	46-55.95N	160-09.47E	Plankton net #14-1 (NORPAC: 100 m)
	9:33		20:33	46-55.93N	160-09.45E	Plankton net #14-2 (NORPAC: 100 m)
	9:39		20:39	46-55.91N	160-09.44E	Plankton net #14-3 (NORPAC: 100 m)
	9:45		20:45	46-55.90N	160-09.43E	Plankton net #14-4 (NORPAC: 100 m)

		9:51	20:51	46-55.88N	160-09.43E	Plankton net #14-5 (NORPAC: 100 m)
		9:58	20:58	46-55.87N	160-09.43E	Plankton net #14-6 (NORPAC: 100 m)
		10:03	21:03	46-55.86N	160-09.42E	Plankton net #14-7 (NORPAC: 100 m)
		15:30	7.8 2:30	47-00.32N	160-04.72E	CTD cast #11 (300 m)
		16:27	3:27	47-00.25N	160-04.82E	FRRF #11 (100 m)
		16:48	3:48	47-00.21N	160-04.89E	Plankton net #15-1 (NORPAC: 100 m)
		16:58	3:58	47-00.18N	160-04.93E	Plankton net #15-2 (NORPAC: 100 m)
		17:07	4:07	47-00.17N	160-04.95E	Plankton net #15-3 (NORPAC: 100 m)
		20:54	7:54	46-59.97N	160-05.07E	FRRF #12 (100 m)
		23:56	10:56	46-59.90N	160-05.13E	Free fall optical measruements #07
7.8		1:24	12:24	47-00.06N	160-04.84E	FRRF #13 (100 m)
		3:24	14:24	47-00.12N	160-05.08E	FRRF #14 (100 m)
		3:45	14:45	47-00.18N	160-05.06E	Plankton net #16-1 (NORPAC: 10,00-500 m)
		4:41	15:41	47-00.31N	160-05.14E	Plankton net #16-2 (NORPAC: 500-300 m)
		5:09	16:09	47-00.39N	160-05.21E	Plankton net #16-3 (NORPAC: 300-150 m)
		5:30	16:30	47-00.44N	160-05.29E	Plankton net #16-4 (NORPAC: 150-50 m)
		5:44	16:44	47-00.47N	160-05.36E	Plankton net #16-5 (NORPAC: 50-0 m)
		7:55	18:55	47-00.05N	160-05.09E	FRRF #15 (100 m)
		8:16	19:16	47-00.10N	160-05.21E	Plankton net #17-1 (NORPAC: 100 m)
		8:25	19:25	47-00.11N	160-05.25E	Plankton net #17-2 (NORPAC: 100 m)
		8:34	19:34	47-00.12N	160-05.30E	Plankton net #17-3 (NORPAC: 100 m)
		11:58	22:58	47-00.00N	160-05.10E	IONESS #07 (300 m)
		13:18	7.9 0:18	47-00N	160-00E	Departure from Station K2
7.9		7:48	18:48	44-00N	155-00E	Arrival at Station KNOT
		7:50	18:50	43-59.93N	155-00.05E	CTD cast #12 (5,300 m)
		8:07	19:07	43-59.86N	155-00.15E	Plankton net (Maual: Kagoshima university) #01
		11:36	22:36	44-00N	155-00E	Departure from Station KNOT
		12:23	23:23	43-51.74N	154-54.43E	Cesium magnetometer towing start #01
7.10	7.10	6:06	17:06	41-26.03N	150-29.03E	Radio sonde #03
		6:13	17:13	41-25.54N	150-27.97E	XCTD #01
		7:31	18:31	41-16.94N	150-14.51E	Radio sonde #04
		7:38	18:38	41-16.47N	150-13.51E	XCTD #02
		8:59	19:59	41-07.89N	149-59.82E	Radio sonde #05
		9:08	20:08	41-07.24N	149-59.00E	XCTD #03
		10:30	21:30	40-54.93N	149-45.03E	Radio sonde #06
		10:38	21:38	40-54.50N	149-43.78E	XCTD #04
		11:00	22:00			Time adjustment -1 hours (SMT=UTC+10h)
		11:59	21:59	40-42.99N	149-29.98E	Radio sonde #07
		12:07	22:07	40-42.66N	149-28.80E	XCTD #05
		13:30	23:30	40-29.98N	149-15.24E	Radio sonde #08
		13:38	23:38	40-29.74N	149-14.30E	XCTD #06

7.11	15:01	7.11	1:01	40-17.43N	149-00.26E	Radio sonde #09
	15:08		1:08	40-16.96N	148-59.47E	XCTD #07
	16:30		2:30	40-04.37N	148-45.79E	Radio sonde #10
	16:35		2:35	40-03.86N	148-46.17E	XCTD #08
	18:00		4:00	39-50.70N	148-29.82E	Radio sonde #11
	18:07		4:07	39-49.95N	148-30.24E	XCTD #09
	19:31		5:31	39-37.18N	148-15.56E	Radio sonde #12
	19:37		5:37	39-36.21N	148-15.94E	XCTD #10
	20:59		6:59	39-24.38N	147-59.91E	Radio sonde #13
	22:29		8:29	39-12.08N	147-45.00E	Radio sonde #14
	0:02		10:02	38-58.46N	147-30.18E	Radio sonde #15
	1:27		11:27	38-46.44N	147-14.76E	Radio sonde #16
	2:59		12:59	38-33.35N	147-00.21E	Radio sonde #17
	4:29		14:29	38-20.36N	146-44.93E	Radio sonde #18
	4:59		14:59	38-15.92N	146-38.62E	Cesium magnetometer towing finish #01
	6:25		16:25	38-05.99N	146-25.39E	Radio sonde #19
	6:30		16:30	38-05N	146-25E	Arrival at Station J-KEO
	6:41		16:41	38-04.00N	146-25.52E	CTD cast #13 (5,380 m)
	6:45		16:45	38-04.03N	146-25.53E	Plankton net (Mauul: Kagoshima university) #02
	10:00		20:00	38-04.11N	146-25.41E	Radio sonde #20
	10:24		20:24	38-04.10N	146-25.44E	Departure from Station J-KEO
	10:35		20:35	38-03.69N	146-23.98E	Cesium magnetometer towing start #02
	11:30		21:30	38-01.02N	146-14.82E	Radio sonde #21
	12:00		22:00	37-58.83N	146-08.73E	Time adjustment -1 hours (SMT=UTC+9h)
	12:59		21:59	37-55.91N	145-59.85E	Radio sonde #22
	14:29		23:29	37-50.02N	145-40.22E	Radio sonde #23
7.12	15:58	7.12	0:58	37-43.95N	145-19.72E	Radio sonde #24
	17:30		2:30	37-36.98N	145-00.34E	Radio sonde #25
	18:59		3:59	37-30.97N	144-39.81E	Radio sonde #26
	20:30		5:30	37-24.05N	144-19.83E	Radio sonde #27
	21:59		6:59	37-18.46N	144-00.09E	Radio sonde #28
	23:29		8:29	37-11.95N	143-39.96E	Radio sonde #29
	0:59		9:59	37-05.02N	143-19.81E	Radio sonde #30
	2:29		11:29	36-58.97N	142-59.88E	Radio sonde #31
	3:59		12:59	36-52.02N	142-40.13E	Radio sonde #32
	5:29		14:29	36-45.99N	142-19.94E	Radio sonde #33
	6:30		15:30	36-40.64N	142-03.05E	Cesium magnetometer towing finish #02
	6:59		15:59	36-40.16N	142-01.13E	Radio sonde #34
	7:03		16:03	36-40.15N	142-01.08E	Free fall optical measruements #08
	8:59		17:59	36-32.87N	141-39.98E	Radio sonde #35
	9:48		18:48	36-29N	141-30E	Arrival at Station F1
	10:29		19:29	36-29.40N	141-29.84E	Radio sonde #36

	17:39	7.13	2:39	36-28.94N	141-30.17E	CTD cast #14 (1,334 m)
	19:15		4:15	36-29.09N	141-30.22E	FRRF #16 (100 m)
	22:54		7:54	36-29.01N	141-30.06E	FRRF #17 (100 m)
	23:57		8:57	36-29.07N	141-30.20E	CTD cast #15 (1,315 m)
7.13	1:58		10:58	36-29.05N	141-29.97E	Free fall optical measruements #08
	2:30		11:30	36-28.76N	141-29.73E	FRRF #18 (100 m)
	5:25		14:25	36-29.05N	141-30.01E	FRRF #19 (100 m)
	9:20		18:20	36-28.98N	141-30.03E	FRRF #20 (100 m)
	13:02		22:02	36-28.90N	141-30.14E	IONESS #08 (200 m)
	23:17	7.14	8:17	36-29.07N	141-29.90E	LVP #04 (100 m)
	23:52		8:52	37-36.28N	141-29.73E	Calibration for magnetometer #1
7.14	4:58		13:58	36-30.03N	141-24.23E	Site survey start (Station F1: MBES)
	7:18		16:18	36-26.01N	141-34.13E	Site survey finish (Station F1: MBES)
	7:18		16:18	36-29N	141-30E	Departure from Station F1
7.15	0:21	7.15	9:21	37-34.86N	141-30.99E	Site survey start (Station D1-D4: MBES&SBP)
	5:00		14:00	36-40.79N	141-08.66E	Site survey finish (Station D1-D4: MBES&SBP)
	21:00	7.16	6:00	-	-	Sea surface water analysis finish
7.17	0:00		9:00	35-27N	139-40E	Arrival at Yokohama

(Leg.2)

U.T.C.		S.M.T.		Position		Event logs
Date	Time	Date	Time	Lat.	Lon.	
7.16	23:50	7.17	8:50	35-27N	139-40E	Departure from Yokohama
7.17	4:40		13:40	-	-	Sea surface water analysis start
	17:18	7.18	2:18	36-29N	141-30E	Arrival at Station F1
	21:30		6:30	36-29.00N	141-29.97E	CTD cast #01 (200 m)
	23:06		8:06	36-28.66N	141-27.85E	WHOI mooring deployment
7.18	0:42		9:42	36-27.1252N	141-27.1596E	WHOI mooring fixed position
	2:29		11:29	36-29.00N	141-29.97E	Multipul corer #01
	3:42		12:42	36-28.88N	141-29.84E	Departure from Station F1
	5:36		14:36	36-41.46N	141-09.06E	Arrival at Station D4
	5:56		14:56	36-41.46N	141-09.02E	Multipul corer #02
	6:31		15:31	36-41.49N	141-09.05E	CTD cast #02 (192 m)
	7:48		16:48	36-41.61N	141-09.46E	Departure from Station D4
	20:30	7.19	5:30	36-59.93N	141-16.97E	Arrival at Station D3
	20:56		5:56	36-59.99N	141-16.98E	Multipul corer #03
	21:34		6:34	37-00.02N	141-16.92E	CTD cast #03 (140 m)
	22:06		7:06	36-59.98N	141-16.98E	Departure from Station D3



7.19	0:00		9:00	37-19.98N	141-28.01E	Arrival at Station D2
	0:06		9:06	37-19.93N	141-27.94E	Multipul corer #04
	0:38		9:38	37-19.93N	141-27.96E	CTD cast #04 (146 m)
	1:06		10:06	37-19.73N	141-28.06E	Departure from Station D2
	3:42		12:42	37-35.06N	141-30.98E	Arrival at Station D1
	3:58		12:58	37-35.01N	141-30.96E	Multipul corer #05
	4:31		13:31	37-35.00N	141-30.93E	CTD cast #05 (126 m)
	5:00		14:00	37-34.98N	141-31.15E	Departure from Station D1
7.22	13:00	7.22	22:00	-	-	Time adjustment +1 hour (SMT=UTC+10h)
7.23	3:54	7.23	13:54	29-59.99N	144-59.99E	Arrival at Station S1
	5:38		15:38	29-44.31N	144-59.71E	ARGO Float #01
	6:55		16:55	29-28.61N	145-00.03E	ARGO Float #02
	8:16		18:16	29-28.00N	145-17.92E	ARGO Float #03
	9:29		19:29	29-27.81N	145-35.62E	ARGO Float #04
	10:48		20:48	29-43.77N	145-35.96E	ARGO Float #05
	12:15		22:15	29-59.95N	145-35.97E	ARGO Float #06
	13:39		23:39	30-15.79N	145-35.99E	ARGO Float #07
	14:58	7.24	0:58	30-31.97N	145-35.94E	ARGO Float #08
	16:13		2:13	30-32.01N	145-18.15E	ARGO Float #09
	17:31		3:31	30-32.06N	145-00.22E	ARGO Float #10
	18:55		4:55	30-16.09N	145-00.00E	ARGO Float #11
	22:04		8:04	29-59.97N	144-24.63E	ARGO Float #12
	23:24		9:24	29-44.37N	144-24.06E	ARGO Float #13
7.24	0:46		10:46	29-28.19N	144-24.01E	ARGO Float #14
	1:56		11:56	29-28.04N	144-41.77E	ARGO Float #15
	2:57		12:57	29-38.14N	144-47.98E	Free fall optical measruements #01
	5:24		15:24	30-00.03N	144-59.99E	CTD cast #06 (5,943 m)
	10:21		20:21	29-59.58N	144-59.98E	Plankton net #01-1 (NORPAC: 50 m)
	10:29		20:29	29-59.58N	144-59.98E	Plankton net #01-2 (NORPAC: 150 m)
	10:42		20:42	29-59.63N	144-59.94E	Plankton net #01-3 (NORPAC: 200 m)
	10:53		20:53	29-59.67N	144-59.91E	Plankton net #01-4 (NORPAC: 100 m)
	11:03		21:03	29-59.71N	144-59.89E	Plankton net #01-5 (NORPAC: 100 m)
	11:14		21:14	29-59.74N	144-59.88E	Plankton net #01-6 (NORPAC: 100 m)
	17:27	7.25	3:27	30-00.14N	144-59.98E	CTD cast #07 (300 m)
	18:28		4:28	30-00.44N	144-59.99E	FRRF #01 (200 m)
	19:58		5:58	30-04.88N	144-58.10E	FRRF #02 (200 m)
	22:23		8:23	30-04.50N	144-58.03E	BGC mooring recovery
7.25	1:28		11:28	30-03.59N	144-58.02E	Free fall optical measruements #02
	1:56		11:56	30-03.36N	144-58.04E	Plankton net #02-1 (NORPAC: 200 m)
	2:08		12:08	30-03.43N	144-58.07E	Plankton net #02-2 (NORPAC: 100 m)

		2:18	12:18	30-03.50N	144-58.11E	Plankton net #02-3 (NORPAC: 100 m)
		2:28	12:28	30-03.56N	144-58.17E	Plankton net #02-4 (NORPAC: 100 m)
		2:41	12:41	30-03.62N	144-58.24E	FRRF #03 (200 m)
		4:25	14:25	30-00.06N	145-00.01E	FRRF #04 (200 m)
		5:08	15:08	30-00.15N	145-00.01E	Plankton net #03-1 (NORPAC: 1000-700 m)
		5:59	15:59	30-00.27N	144-59.99E	Plankton net #03-2 (NORPAC: 700-500 m)
		6:34	16:34	30-00.29N	144-59.97E	Plankton net #03-3 (NORPAC: 500-300 m)
		7:07	17:07	30-00.29N	144-59.92E	CTD cast #08 (200 m)
		8:23	18:23	29-59.98N	144-59.95E	FRRF #05 (200 m)
		9:28	19:28	29-59.90N	144-59.76E	Plankton net #04-1 (NORPAC: 300-200 m)
		9:47	19:47	29-59.93N	144-59.67E	Plankton net #04-2 (NORPAC: 200-150 m)
		10:02	20:02	29-59.96N	144-59.63E	Plankton net #04-3 (NORPAC: 150-100 m)
		10:13	20:13	29-59.97N	144-59.59E	Plankton net #04-4 (NORPAC: 100-50 m)
		10:24	20:24	29-59.98N	144-59.54E	Plankton net #04-5 (NORPAC: 50-20 m)
		10:32	20:32	29-59.99N	144-59.49E	Plankton net #04-6 (NORPAC: 20-0 m)
		10:38	20:38	29-59.99N	144-59.47E	Plankton net #05-1 (NORPAC: 200 m)
		10:49	20:49	30-00.00N	144-59.41E	Plankton net #05-2 (NORPAC: 100 m)
		10:59	20:59	30-00.02N	144-59.34E	Plankton net #05-3 (NORPAC: 100 m)
		19:27	7.26 5:27	30-04.07N	145-09.94E	Drifting sediment trap buoy deployment
		20:30	6:30	30-07.32N	145-08.47E	Plankton net #06-1 (NORPAC: 100 m)
		20:40	6:40	30-07.44N	145-08.42E	Plankton net #06-2 (NORPAC: 100 m)
		21:57	7:57	30-11.95N	145-05.97E	Multipul corer #06
7.26		2:29	12:29	30-02.29N	145-01.21E	CTD cast #09 (5,000 m)
		5:38	15:38	30-02.29N	145-01.20E	LISST #01 (200 m)
		6:38	16:38	30-02.26N	145-01.08E	CTD cast #10 (2,000 m)
		10:57	20:57	29-59.97N	144-59.67E	IONESS #01 (1,000 m)
		18:59	7.27 4:59	29-57.54N	144-56.10E	Plankton net #07-1 (NORPAC: 300-150 m)
		19:20	5:20	29-57.66N	144-56.01E	Plankton net #07-2 (NORPAC: 150-100 m)
		19:32	5:32	29-57.74N	144-55.95E	Plankton net #07-3 (NORPAC: 150-100 m)
		19:45	5:45	29-57.83N	144-55.89E	Plankton net #07-4 (NORPAC: 100-50 m)
		19:55	5:55	29-57.88N	144-55.88E	Plankton net #07-5 (NORPAC: 100-50 m)
		20:06	6:06	29-57.92N	144-55.85E	Plankton net #07-6 (NORPAC: 50-0 m)
		20:13	6:13	29-57.95N	144-55.85E	Plankton net #07-7 (NORPAC: 50-0 m)
		21:53	7:53	29-56.82N	144-57.78E	POPPS mooring recovery
7.27		0:55	10:55	29-58.53N	144-58.27E	Free fall optical measruements #03
		1:36	11:36	29-58.23N	144-58.48E	IONESS #02 (1,000 m)
		4:35	14:35	30-02.48N	145-02.49E	CTD cast #11 (200 m)
		5:05	15:05	30-02.56N	145-02.45E	Large Volume Pump (LVP) #01 (1,000 m)
		11:25	21:25	30-01.60N	145-02.87E	Plankton net #08-1 (NORPAC: 200 m)
		11:35	21:35	30-01.61N	145-02.80E	Plankton net #08-2 (NORPAC: 100 m)
		11:47	21:47	30-02.00N	145-02.69E	Plankton net #08-3 (NORPAC: 100 m)
		11:57	21:57	30-01.59N	145-03.00E	Plankton net #08-4 (NORPAC: 100 m)

7.28	17:26	7.28	3:26	30-00.09N	144-59.88E	CTD cast #12 (300 m)
	18:22		4:22	30-00.39N	144-59.57E	FRRF #06 (200 m)
	19:50		5:50	30-00.01N	144-59.98E	LVP #02 (200 m)
	21:54		7:54	30-00.18N	144-59.91E	FRRF #07 (200 m)
	22:59		8:59	30-00.52N	144-59.76E	CTD cast #13 (200 m)
	0:30		10:30	29-59.99N	144-59.86E	Free fall optical measruements #04
	0:58		10:58	29-59.84N	144-59.76E	Plankton net #09-1 (NORPAC: 200 m)
	1:09		11:09	29-59.84N	144-59.78E	Plankton net #09-2 (NORPAC: 100 m)
	1:20		11:20	29-59.84N	144-59.84E	Plankton net #09-3 (NORPAC: 100 m)
	1:30		11:30	29-59.85N	144-59.90E	Plankton net #09-4 (NORPAC: 100 m)
	1:52		11:52	29-59.87N	145-00.06E	FRRF #08 (200 m)
	3:52		13:52	29-59.98N	145-00.03E	FRRF #09 (200 m)
	4:53		14:53	29-59.77N	144-59.93E	LVP #03 (100 m)
	9:58		19:58	29-59.90N	144-59.78E	Visual Plankton Recorder (VPR) #01-1 (500 m)
	10:31		20:31	29-59.89N	144-59.55E	VPR #01-2 (500 m)
	11:11		21:11	29-59.87N	144-59.26E	IONESS #03 (150 m)
7.29	14:20	7.29	0:20	30-02.67N	145-02.93E	Atmospheric turbulent flux observation #1
	20:10		6:10	30-07.12N	145-02.58E	BGC mooring deployment
	23:56		9:56	30-03.9344N	144-58.0250E	BGC mooring fixed position
	1:56		11:56	30-00.00N	144-59.86E	IONESS #04 (1,000 m)
	5:00		15:00	30-02.00N	144-54.41E	CTD cast #14 (1,000 m)
	6:15		16:15	30-01.79N	144-54.13E	Plankton net #10-1 (NORPAC: 100 m)
	6:24		16:24	30-01.70N	144-54.14E	Plankton net #10-2 (NORPAC: 100 m)
	6:34		16:34	30-01.63N	144-54.09E	Plankton net #10-3 (NORPAC: 100 m)
	7:26		17:26	30-01.46N	144-53.98E	Plankton net #11-1 (NORPAC: 200-120 m)
	7:40		17:40	30-01.41N	144-53.90E	Plankton net #11-2 (NORPAC: 120-80 m)
	7:51		17:51	30-01.38N	144-53.81E	Plankton net #11-3 (NORPAC: 120-80 m)
	8:02		18:02	30-01.35N	144-53.74E	Plankton net #11-4 (NORPAC: 120-80 m)
	8:13		18:13	30-01.33N	144-53.67E	Plankton net #11-5 (NORPAC: 80-40 m)
	8:22		18:22	30-01.31N	144-53.61E	Plankton net #11-6 (NORPAC: 80-40 m)
	8:32		18:32	30-01.26N	144-53.53E	Plankton net #11-7 (NORPAC: 40-0 m)
	10:01		20:01	30-00.10N	144-56.85E	VPR #02 (500 m)
	10:54		20:54	29-59.90N	144-56.36E	IONESS #05 (1,000 m)
7.30	20:01	7.30	6:01	29-57.36N	144-55.12E	POPPS mooring deployment
	23:55		9:55	29-55.58N	145-00.07E	POPPS mooring fixed position
	2:50		12:50	30-10.17N	144-50.67E	Drifting sediment trap buoy recovery
	3:57		13:57	30-07.75N	144-52.54E	Plankton net #12-1 (NORPAC: 200-120 m)
	4:13		14:13	30-07.69N	144-52.59E	Plankton net #12-2 (NORPAC: 120-80 m)
	4:23		14:23	30-07.66N	144-52.60E	Plankton net #12-3 (NORPAC: 120-80 m)
	4:33		14:33	30-07.62N	144-52.62E	Plankton net #12-4 (NORPAC: 120-80 m)
	4:47		14:47	30-07.54N	144-52.63E	Plankton net #12-5 (NORPAC: 80-40 m)

	4:57		14:57	30-07.52N	144-52.63E	Plankton net #12-6 (NORPAC: 80-40 m)
	5:06		15:06	30-07.47N	144-52.64E	Plankton net #12-7 (NORPAC: 80-40 m)
	5:15		15:15	30-07.42N	144-52.64E	Plankton net #12-8 (NORPAC: 80-40 m)
	5:24		15:24	30-07.35N	144-52.62E	Plankton net #12-9 (NORPAC: 40-0 m)
	6:29		16:29	29-59.83N	145-00.09E	CTD cast #15 (2,000 m)
	8:28		18:28	29-59.53N	145-00.18E	ARGO Float #16
	10:13		20:13	30-15.96N	145-17.94E	CTD cast #16 (2,000 m)
	12:17		22:17	30-15.64N	145-17.67E	ARGO Float #17
	13:39		23:39	30-00.01N	145-17.96E	ARGO Float #18
	15:03	7.31	1:03	29-44.22N	145-17.98E	CTD cast #17 (2,000 m)
	16:59		2:59	29-44.04N	145-17.47E	ARGO Float #19
	19:38		5:38	29-44.01N	144-42.02E	CTD cast #18 (2,000 m)
	21:35		7:35	29-44.46N	144-41.65E	ARGO Float #20
	22:49		8:49	29-59.91N	144-41.99E	ARGO Float #21
7.31	0:12		10:12	30-15.98N	144-41.98E	CTD cast #19 (2,000 m)
	2:07		12:07	30-16.01N	144-42.07E	ARGO Float #22
	4:30		14:30	30-39.75N	145-09.47E	ARGO Float search start
	6:11		16:11	30-38.06N	145-09.23E	ARGO Float recovery
	6:23		16:23	30-37.94N	145-09.07E	ARGO Float search finish
	6:30		16:30	30-37.97N	145-09.17E	Departure from Station S1
	16:48	8.1	2:48	32-30.54N	144-32.63E	Arrival at Station KEO
	20:32		6:32	32-29.89N	144-33.54E	CTD cast #20 (1,000 m)
	22:06		8:06	32-28.16N	144-32.80E	Departure from Station KEO
8.2	12:00	8.2	22:00	-	-	Time adjustment -1 hours (SMT=UTC+9h)
8.3	5:30	8.3	14:30	-	-	Sea surface water analysis finish
	3:59		12:59	41-28.86N	141-42.62E	Calibration for magnetometer #2
8.4	0:10	8.4	9:10	41-22N	141-14E	Arrival at Sekinehama

### 1.3 Cruise Participants

	Name	Affiliation	Appointment	Leg .1	Leg. 2
1	Makio HONDA (Principal Investigator)	Research Institute for Global Change (RIGC), Japan Agency for Marine-Earth Science and Technology (JAMSTEC)	Team Leader	○	○
2	Kazuhiko MATSUMOTO (Deputy PI)	RIGC, JAMSTEC	Research scientist	○	○
3	Minoru KITAMURA	Institute of Biogeoscience (BIOGEOS) , JAMSTEC	Scientist	○	○
4	Hajime KAWAKAMI	Mutsu Institute for Oceanography (MIO), JAMSTEC	Research scientist	○	○
5	Masahide WAKITA	Same as above	Scientist	○	○
6	Tetsuichi FUJIKI	RIGC, JAMSTEC	Scientist	○	○
7	Katsunori KIMOTO	Same as above	Research scientist	○	○
8	Michell TIGCHELAAR	Same as above	Graduate student	○	○
9	Kenichi SASAKI	MIO, JAMSTEC	Research scientist	○	○
10	Taiyo KOBAYASHI	RIGC, JAMSTEC	Senior Scientist		○
11	Yoshimi KAWAI	RIGC, JAMSTEC	Team Leader	○	
12	Yoshihisa MINO	Nagoya Univ. (Additional post: RIGC, JAMSTEC)	Assistant professor	○	○
13	Hideki KOBAYASHI	BioGeoss, JAMSTEC	Senior Scientist		○
14	Toru KOBARI	Kagoshima Univ.	Associate professor	○	○
15	Rie NAKAMURA	Same as above	Undergraduate student	○	○
16	Yuichi HAYASAKI	Same as above	Undergraduate student	○	○
17	Sachi MIYAKE	Same as above	Undergraduate student	○	○
18	Hideki FUKUDA	The Univ. Tokyo	Assistant professor	○	○
19	Mario UCHIMIYA	Same as above	Graduate student	○	○
20	JeHO	Same as above	Graduate student	○	○

21	Shotaro SUZUKI	Same as above	Graduate student	○	○
22	Minoru KAMATA (Principal Marine Tech.)	Marine Works Japan Inc. (MWJ)	Marin Technician	○	○
23	Toru IDAI	Same as above	Same as above	○	○
24	Naoko MIYAMOTO	Same as above	Same as above	○	○
25	Tomoyuki TAKAMORI	Same as above	Same as above	○	○
26	Daiki USHIROMURA	Same as above	Same as above	○	○
27	Shungo OSHITANI	Same as above	Same as above	○	○
28	Yasuhiro ARII	Same as above	Same as above	○	○
29	Yoshiko ISHIKAWA	Same as above	Same as above	○	○
30	Hatsumi AOYAMA	Same as above	Same as above	○	○
31	Shin TAKADA	Same as above	Same as above	○	○
32	Hideki YAMAMOTO	Same as above	Same as above	○	○
33	Miyo IKEDA	Same as above	Same as above	○	○
34	Shoko TATAMISASHI	Same as above	Same as above	○	○
35	Misato KUWAHARA	Same as above	Same as above	○	○
36	Hiroyasu SATO	Same as above	Same as above	○	○
37	Kanako YOSHIDA	Same as above	Same as above	○	○
38	Masaki FURUHATA	Same as above	Same as above	○	○
39	Masanori ENOKI	Same as above	Same as above	○	○
40	Sayaka KAWAMURA	Same as above	Same as above		○
41	Katsuhisa MAENO (Principal Marine Tech.)	Global Ocean Development Inc. (GODI)	Same as above	○	○
42	Harumi Ohta	Same as above	Same as above	○	○

## **2 General observation**

### **2.1 Meteorological observations**

#### **2.1.1 Surface Meteorological Observation**

<b>Makio HONDA</b>	<b>(JAMSTEC): Principal Investigator</b>
<b>Katsuhisa MAENO</b>	<b>(Global Ocean Development Inc., GODI)</b>
<b>Harumi OTA</b>	<b>(GODI)</b>
<b>Ryo OYAMA</b>	<b>(Mirai Crew)</b>

##### **(1) Objectives**

Surface meteorological parameters are observed as a basic dataset of the meteorology. These parameters bring us the information about the temporal variation of the meteorological condition surrounding the ship.

##### **(2) Methods**

Surface meteorological parameters were observed throughout the MR11-05 cruise. During this cruise, we used three systems for the observation.

- i. MIRAI Surface Meteorological observation (SMet) system
  - ii. Shipboard Oceanographic and Atmospheric Radiation (SOAR) system
- 
- i. MIRAI Surface Meteorological observation (SMet) system  
Instruments of SMet system are listed in Table.2.1.1-1 and measured parameters are listed in Table.2.1.1-2. Data were collected and processed by KOAC-7800 weather data processor made by Koshin-Denki, Japan. The data set consists of 6-second averaged data.
  - ii. Shipboard Oceanographic and Atmospheric Radiation (SOAR) measurement system  
SOAR system designed by BNL (Brookhaven National Laboratory, USA) consists of major three parts.
    - a) Portable Radiation Package (PRP) designed by BNL – short and long wave downward radiation.
    - b) Zeno Meteorological (Zeno/Met) system designed by BNL – wind, air temperature, relative humidity, pressure, and rainfall measurement.
    - c) Scientific Computer System (SCS) developed by NOAA (National Oceanic and Atmospheric Administration, USA) – centralized data acquisition and logging of all data sets.SCS recorded PRP data every 6 seconds, while Zeno/Met data every 10 seconds. Instruments and their locations are listed in Table.2.1.1-3 and measured parameters are listed in Table.2.1.1-4.

For the quality control as post processing, we checked the following sensors, before and

after the cruise.

i. Young Rain gauge (SMet and SOAR)

Inspect of the linearity of output value from the rain gauge sensor to change Input value by adding fixed quantity of test water.

ii. Barometer (SMet and SOAR)

Comparison with the portable barometer value, PTB220CASE, VAISALA.

iii. Thermometer (air temperature and relative humidity) (SMet and SOAR)

Comparison with the portable thermometer value, HMP41/45, VAISALA.

(3) Preliminary results

Figure 2.1.1-1 shows the time series of the following parameters;

Wind (SMet)

Air temperature (SMet)

Relative humidity (SMet)

Precipitation (SOAR, rain gauge)

Short/long wave radiation (SOAR)

Pressure (SMet)

Sea surface temperature (SMet)

Significant wave height (SMet)

(4) Data archives

These meteorological data will be submitted to the Data Management Group (DMG) of JAMSTEC just after the cruise.

(5) Remarks

i. SST (Sea Surface Temperature) data were available in the following periods.

05:30UTC 27 Jun. - 21:00UTC 16 Jul.

04:32UTC 17 Jul. - 05:30UTC 03 Aug.

ii. SMet ORG cleaning

21:59UTC 16 Jul.

08:17UTC 24 Jul.

iii. SMet Young rain gauge includes invalid data at the following time due to MF/HF transmit.

07:22UTC 30 Jun.

07:38UTC 27 Jul.

iv. SOAR ORG cleaning

05:40UTC 16 Jul.

v. PRP cleaning

05:39UTC 16 Jul.



Table.2.1.1-1 Instruments and installations of MIRAI Surface Meteorological observation system

Sensors	Type	Manufacturer	Location (altitude from surface)
Anemometer	KE-500	Koshin Denki, Japan	foremast (24 m)
Tair/RH	HMP45A	Vaisala, Finland	
with 43408 Gill aspirated radiation shield		R.M. Young, USA	compass deck (21 m) starboard side and port side
Thermometer: SST	RFN1-0	Koshin Denki, Japan	4th deck (-1m, inlet -5m)
Barometer	Model-370	Setra System, USA	captain deck (13 m) weather observation room
Rain gauge	50202	R. M. Young, USA	compass deck (19 m)
Optical rain gauge	ORG-815DR	Osi, USA	compass deck (19 m)
Radiometer (short wave)	MS-801	Eiko Seiki, Japan	radar mast (28 m)
Radiometer (long wave)	MS-200	Eiko Seiki, Japan	radar mast (28 m)
Wave height meter	MW-2	Tsurumi-seiki, Japan	bow (10 m)

Table.2.1.1-2 Parameters of MIRAI Surface Meteorological observation system

Parameter	Units	Remarks
1 Latitude	degree	
2 Longitude	degree	
3 Ship's speed	knot	Mirai log, DS-30 Furuno
4 Ship's heading	degree	Mirai gyro, TG-6000, Tokimec
5 Relative wind speed	m/s	6sec./10min. averaged
6 Relative wind direction	degree	6sec./10min. averaged
7 True wind speed	m/s	6sec./10min. averaged
8 True wind direction	degree	6sec./10min. averaged
9 Barometric pressure	hPa	adjusted to sea surface level 6sec. averaged
10 Air temperature (starboard side)	degC	6sec. averaged
11 Air temperature (port side)	degC	6sec. averaged
12 Dewpoint temperature (starboard side)	degC	6sec. averaged
13 Dewpoint temperature (port side)	degC	6sec. averaged
14 Relative humidity (starboard side)	%	6sec. averaged
15 Relative humidity (port side)	%	6sec. averaged
16 Sea surface temperature	degC	6sec. averaged
17 Rain rate (optical rain gauge)	mm/hr	hourly accumulation
18 Rain rate (capacitive rain gauge)	mm/hr	hourly accumulation
19 Down welling shortwave radiation	W/m2	6sec. averaged
20 Down welling infra-red radiation	W/m2	6sec. averaged
21 Significant wave height (bow)	m	hourly
22 Significant wave height (aft)	m	hourly
23 Significant wave period (bow)	second	hourly
24 Significant wave period (aft)	second	hourly

Table.2.1.1-3 Instruments and installation locations of SOAR system

<u>Sensors (Zeno/Met)</u>	<u>Type</u>	<u>Manufacturer</u>	<u>Location (altitude from surface)</u>
Anemometer	05106	R.M. Young, USA	foremast (25 m)
Tair/RH	HMP45A	Vaisala, Finland	
with 43408 Gill aspirated radiation shield		R.M. Young, USA	foremast (23 m)
Barometer	61202V	R.M. Young, USA	
with 61002 Gill pressure port		R.M. Young, USA	foremast (23 m)
Rain gauge	50202	R.M. Young, USA	foremast (24 m)
Optical rain gauge	ORG-815DA	Osi, USA	foremast (24 m)
<u>Sensors (PRP)</u>	<u>Type</u>	<u>Manufacturer</u>	<u>Location (altitude from surface)</u>
Radiometer (short wave)	PSP	Epply Labs, USA	foremast (25 m)
Radiometer (long wave)	PIR	Epply Labs, USA	foremast (25 m)
Fast rotating shadowband radiometer		Yankee, USA	foremast (25 m)

Table.2.1.1-4 Parameters of SOAR system

<u>Parameter</u>	<u>Units</u>	<u>Remarks</u>
1 Latitude	degree	
2 Longitude	degree	
3 SOG	knot	
4 COG	degree	
5 Relative wind speed	m/s	
6 Relative wind direction	degree	
7 Barometric pressure	hPa	
8 Air temperature	degC	
9 Relative humidity	%	
10 Rain rate (optical rain gauge)	mm/hr	
11 Precipitation (capacitive rain gauge)	mm	reset at 50 mm
12 Down welling shortwave radiation	W/m2	
13 Down welling infra-red radiation	W/m2	
14 Defuse irradiance	W/m2	

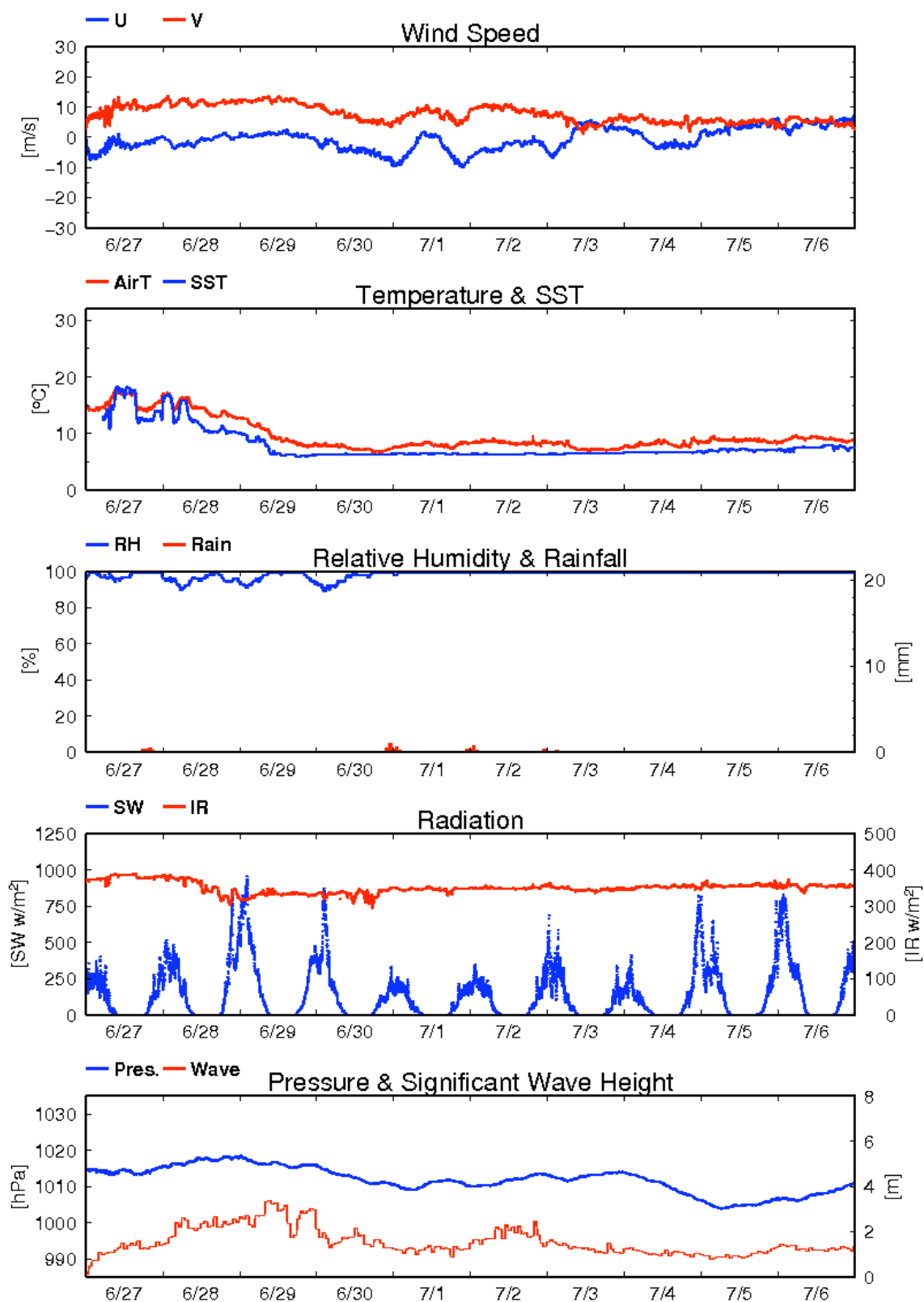


Fig.2.1.1-1 Time series of surface meteorological parameters during the MR11-03 cruise

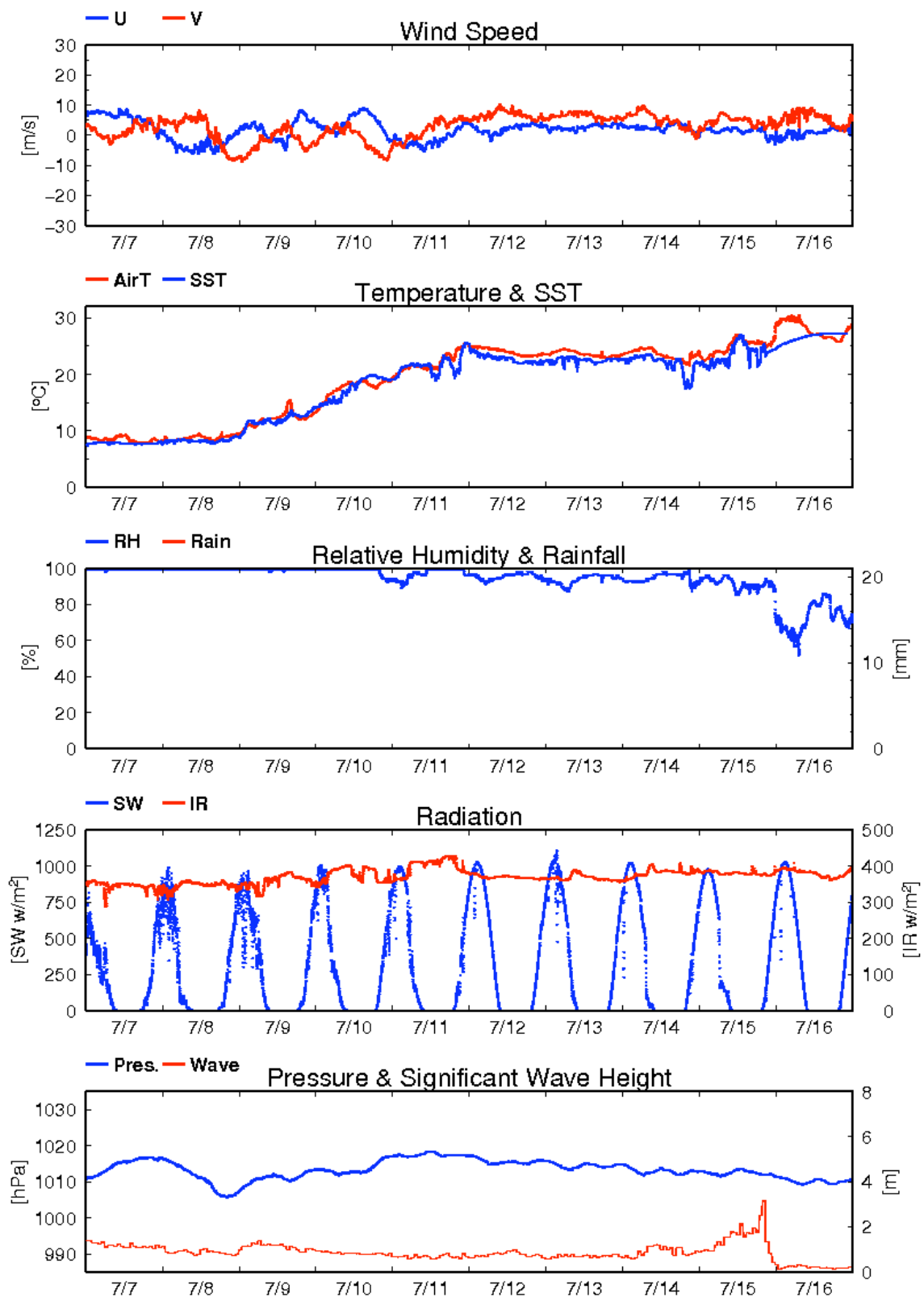


Fig.2.1.1-1 Continued

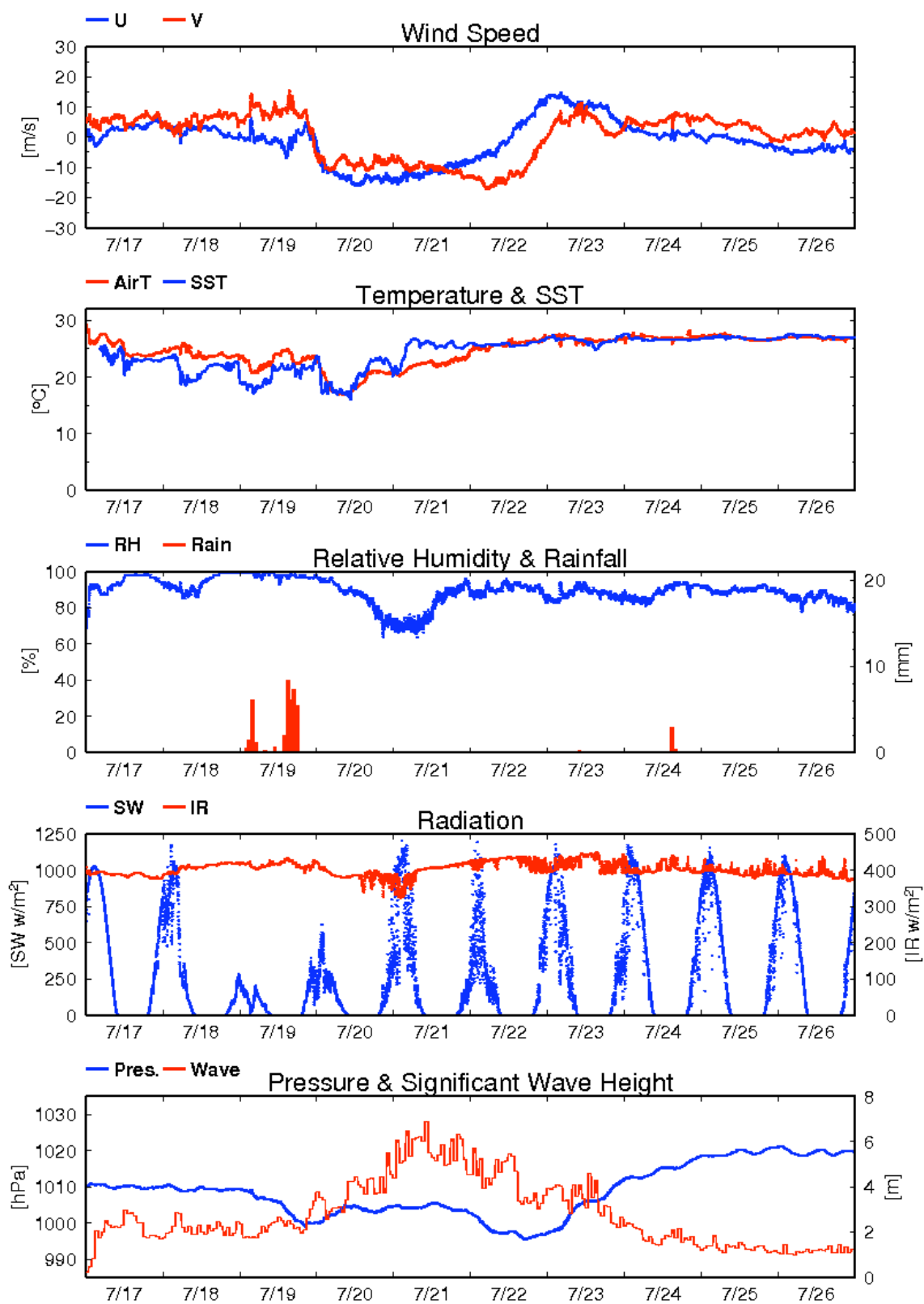


Fig.2.1.1-1 Continued

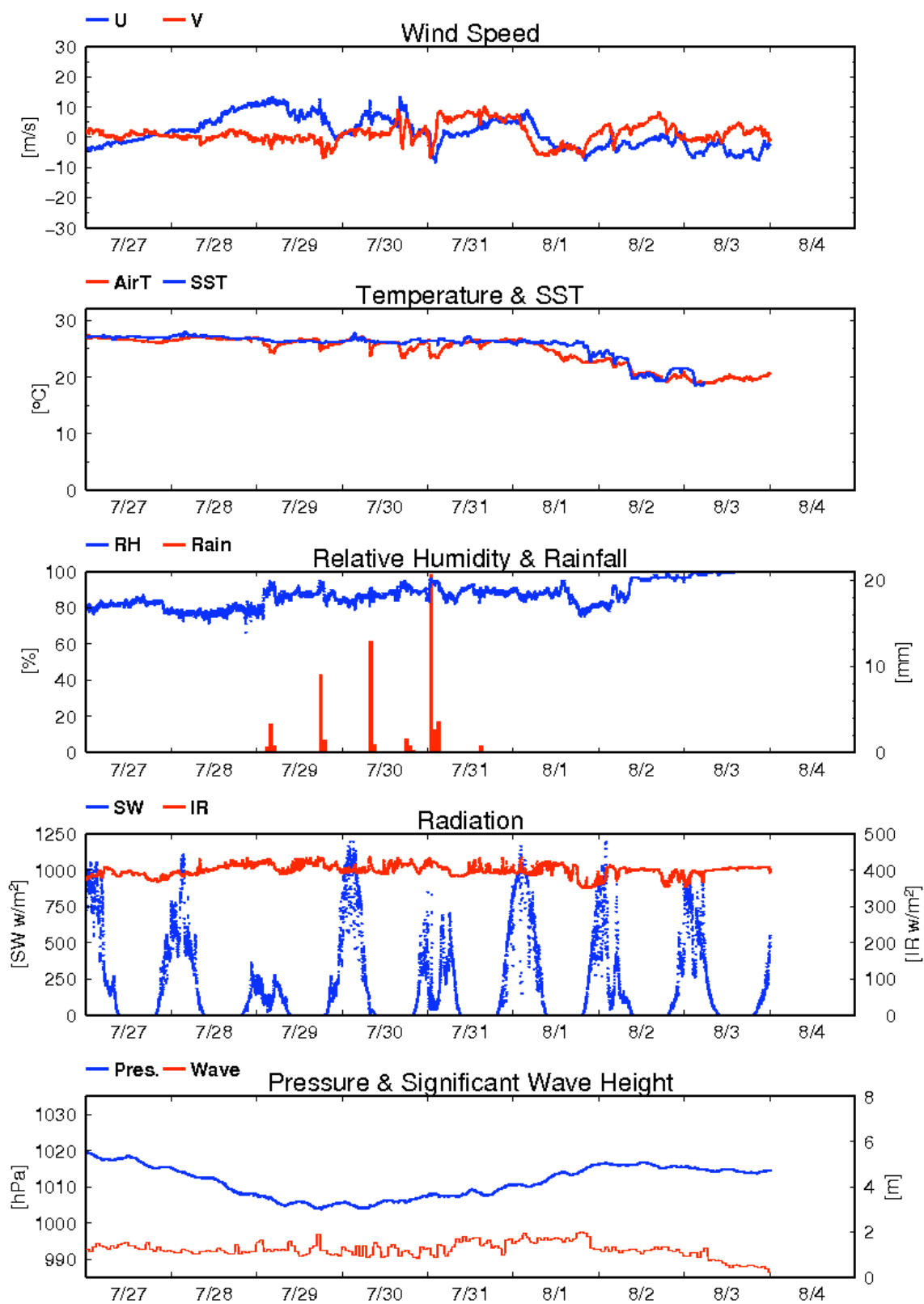


Fig.2.1.1-1 Continued

## 2.1.2 Ceilometer Observation

**Makio HONDA** (JAMSTEC): Principal Investigator  
**Katsuhisa MAENO** (Global Ocean Development Inc., GODI)  
**Harumi OTA** (GODI)  
**Ryo OYAMA** (Mirai Crew)

### (1) Objectives

The information of cloud base height and the liquid water amount around cloud base is important to understand the process on formation of the cloud. As one of the methods to measure them, the ceilometer observation was carried out.

### (2) Parameters

1. Cloud base height [m].
2. Backscatter profile, sensitivity and range normalized at 30 m resolution.
3. Estimated cloud amount [oktas] and height [m]; Sky Condition Algorithm.

### (3) Methods

We measured cloud base height and backscatter profile using ceilometer (CT-25K, VAISALA, Finland) throughout the MR11-05 cruise from the departure of Sekinehama on 27 June 2011 to arrival of Sekinehama on 4 August 2011.

Major parameters for the measurement configuration are as follows;

Laser source:	Indium Gallium Arsenide (InGaAs) Diode
Transmitting wavelength:	905±5 nm at 25 degC
Transmitting average power:	8.9 mW
Repetition rate:	5.57 kHz
Detector:	Silicon avalanche photodiode (APD)
	Responsibility at 905 nm: 65 A/W
Measurement range:	0 ~ 7.5 km
Resolution:	50 ft in full range
Sampling rate:	60 sec
Sky Condition	0, 1, 3, 5, 7, 8 oktas (9: Vertical Visibility)
	(0: Sky Clear, 1: Few, 3: Scattered, 5-7: Broken, 8: Overcast)

On the archive dataset, cloud base height and backscatter profile are recorded with the resolution of 30 m (100 ft).

### (4) Preliminary results

Figure 2.1.2-1 shows the time series of the lowest, second and third cloud base height.

### (5) Data archives

The raw data obtained during this cruise will be submitted to the Data Management Group (DMG) in JAMSTEC.

### (6) Remarks

1. Window cleaning;  
09:23UTC 8 Jul., 21:59UTC 16 Jul., 08:17UTC 24 Jul.

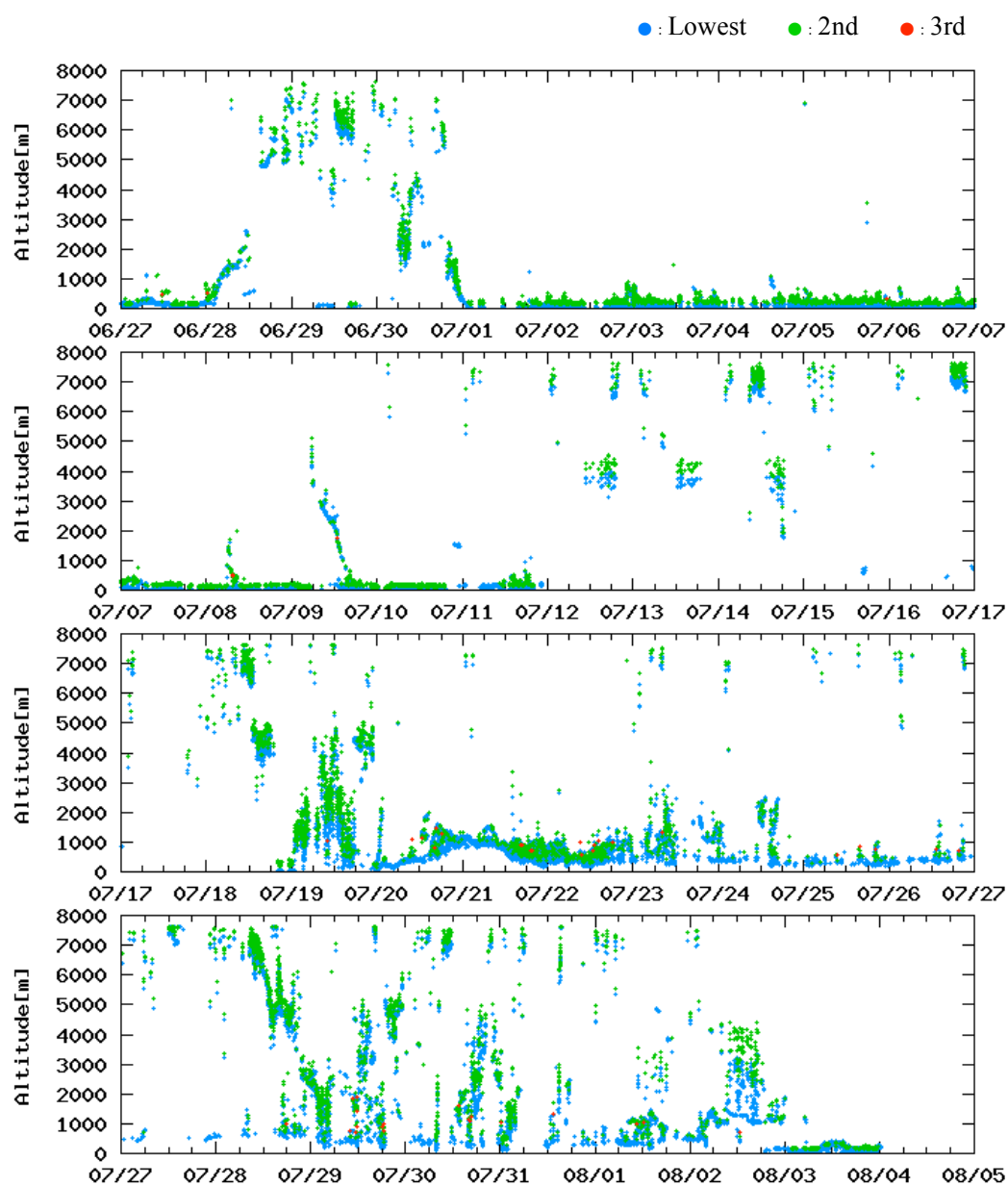


Fig.2.1.2-1 Lowest (blue), 2nd (green) and 3rd(red) cloud base height during the cruise.



### 2.1.3 Lidar observations of clouds and aerosols

**Nobuo SUGIMOTO (National Institute for Environmental Studies: NIES, not on board)**

**Ichiro MATSUI (NIES, not on board)**

**Atsushi SHIMIZU (NIES, not on board)**

**Tomoaki NISHIZAWA (NIES, not on board)**

**\* lidar operation was supported by Global Ocean Development Inc.**

#### (1) Objectives

Objectives of the observations in this cruise is to study distribution and optical characteristics of ice/water clouds and marine aerosols using a two-wavelength lidar.

#### (2) Measured parameters

- Vertical profiles of backscattering coefficient at 532 nm
- Vertical profiles of backscattering coefficient at 1064 nm
- Depolarization ratio at 532 nm

#### (3) Method

Vertical profiles of aerosols and clouds were measured with a two-wavelength lidar. The lidar employs a Nd:YAG laser as a light source which generates the fundamental output at 1064 nm and the second harmonic at 532 nm. Transmitted laser energy is typically 30 mJ per pulse at both of 1064 and 532 nm. The pulse repetition rate is 10 Hz. The receiver telescope has a diameter of 20 cm. The receiver has three detection channels to receive the lidar signals at 1064 nm and the parallel and perpendicular polarization components at 532 nm. An analog-mode avalanche photo diode (APD) is used as a detector for 1064 nm, and photomultiplier tubes (PMTs) are used for 532 nm. The detected signals are recorded with a transient recorder and stored on a hard disk with a computer. The lidar system was installed in a container which has a glass window on the roof, and the lidar was operated continuously regardless of weather. Every 10 minutes vertical profiles of four channels (532 parallel, 532 perpendicular, 1064, 532 near range) are recorded.

#### (4) Results

Figure 1 is an example of one-day quicklook figure of lidar observation. It displays time-height sections of backscatter intensity and depolarization ratio for 27 July. In top panel cirrus are frequently observed in height range of 6 km -- 14 km. Their intensity and depolarization varies with time/height, and more precise analysis on these optical properties of cirrus is indispensable to understand the radiation budget in this region. Although there are little backscatter signal from aerosols in the free troposphere, certain amount of aerosols are confirmed in marine boundary layer below 500 m. As depolarization ratio in this layer is very low, dominant component is considered as sea salt.

## Mirai lidar 2011-07-27

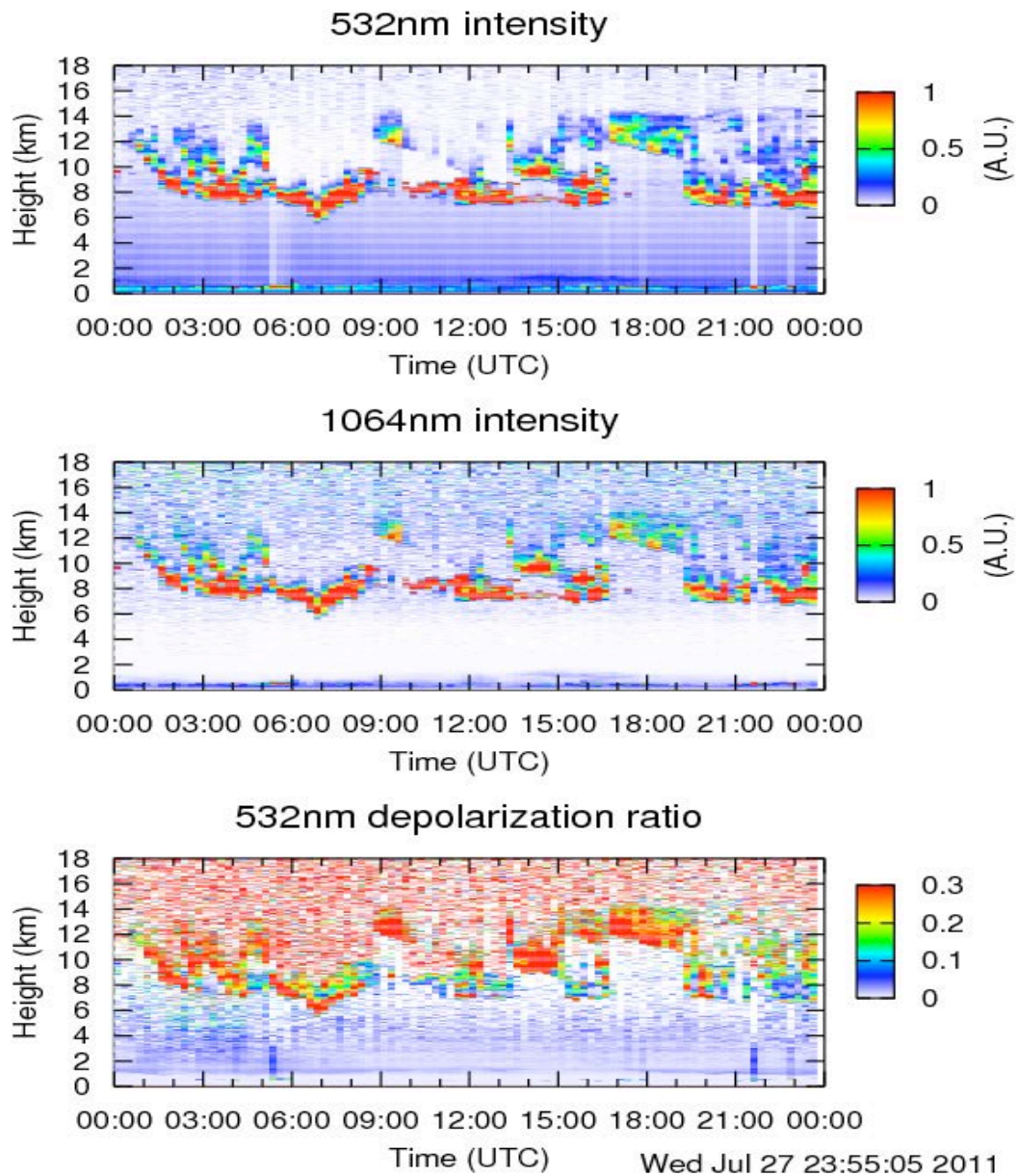


Figure 1: Time-height sections of (top) backscatter intensity at 532 nm, (middle) backscatter intensity at 1064 nm, and (bottom) volume depolarization ratio at 532 nm on 27 July 2011, respectively.

### (5) Data archive

#### - raw data

lidar signal at 532 nm

lidar signal at 1064 nm

depolarization ratio at 532 nm

temporal resolution 10min/ vertical resolution 6 m

data period (UTC): June, 27, 2011 - August 3, 2011

#### - processed data (plan)

cloud base height, apparent cloud top height  
phase of clouds (ice/water)  
cloud fraction  
boundary layer height (aerosol layer upper boundary height)  
backscatter coefficient of aerosols  
particle depolarization ratio

(6) Data policy and Citation

Contact NIES lidar team ([nsugimot/i-matsui/shimizua/nisizawa@nies.go.jp](mailto:nsugimot/i-matsui/shimizua/nisizawa@nies.go.jp)) to utilize lidar data for productive use.

## 2.1.4 Optical characteristics of aerosol observed by Ship-borne Sky radiometer

**Kazuma AOKI** (University of Toyama) Principal Investigator / not onboard

**Tadahiro HAYASAKA** (Tohoku University) Co-worker / not onboard

**Masataka SHIOBARA** (NIPR) Co-worker / not onboard

Sky radiometer operation was supported by Global Ocean Development Inc.

### (1) Objective

Objective of the observations in this aerosol is to study distribution and optical characteristics of marine aerosols by using a ship-borne sky radiometer (POM-01 MKII: PREDE Co. Ltd., Japan). Furthermore, collections of the data for calibration and validation to the remote sensing data were performed simultaneously.

### (2) Methods and Instruments

Sky radiometer is measuring the direct solar irradiance and the solar aureole radiance distribution, has seven interference filters (0.34, 0.4, 0.5, 0.675, 0.87, 0.94, and 1.02  $\mu\text{m}$ ). Analysis of these data is performed by SKYRAD.pack version 4.2 developed by Nakajima *et al.* 1996.

#### @ Measured parameters

- Aerosol optical thickness at five wavelengths (400, 500, 675, 870 and 1020 nm)
- Ångström exponent
- Single scattering albedo at five wavelengths
- Size distribution of volume (0.01  $\mu\text{m}$  – 20  $\mu\text{m}$ )

# GPS provides the position with longitude and latitude and heading direction of the vessel, and azimuth and elevation angle of sun. Horizon sensor provides rolling and pitching angles.

### (3) Preliminary results

Figure 1 shows preliminary result of temporal variation of aerosol optical thickness at 0.5  $\mu\text{m}$  during MR11-05 cruise. All data obtained in this cruise will be analyzed at University of Toyama.

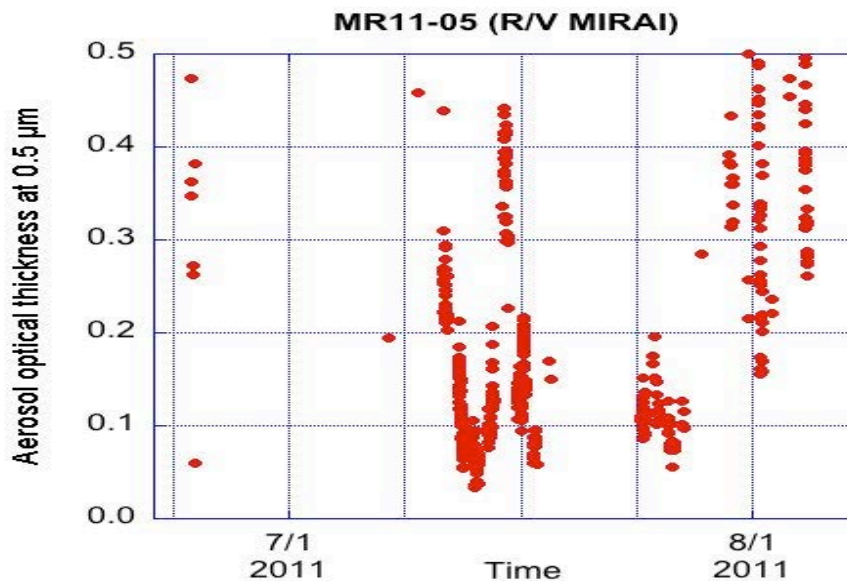


Fig.1 Temporal variation of aerosol optical thickness at 0.5  $\mu\text{m}$  during MR11-05 cruise.

(4) Data archives

Measurements of aerosol optical data are not archived so soon and developed, examined, arranged and finally provided as available data after certain duration. All data will archived at University of Toyama (K.Aoki, SKYNET/SKY: <http://skyrad.sci.u-toyama.ac.jp/>) after the quality check and submitted to JAMSTEC.

## **2.1.5 Tropospheric aerosol and gas observations on a research vessel by MAX-DOAS and auxiliary techniques**

**Hisahiro TAKASHIMA (PI, JAMSTEC/RIGC, not on board)**

**Fumikazu TAKETANI (JAMSTEC/RIGC, not on board)**

**Hitoshi IRIE (JAMSTEC/RIGC, not on board)**

**Yugo KANAYA (JAMSTEC/RIGC, not on board)**

### **(1) Objectives**

- To quantify typical background values of atmospheric aerosol and gas over the ocean
- To clarify transport processes from source over Asia to the ocean (and also clarify the gas emission from the ocean)
- To validate satellite measurements as well as chemical transport model over the ocean
- To quantify fluorescent aerosol over the ocean

### **(2) Methods**

#### **(2-1) MAX-DOAS**

Multi-Axis Differential Optical Absorption Spectroscopy (MAX-DOAS) is a passive remote sensing technique designed for atmospheric aerosol and gas profile measurements using scattered visible and ultraviolet (UV) solar radiation at several elevation angles. Our MAX-DOAS instrument for R/V *Mirai* consists of two main parts: an outdoor telescope unit and an indoor spectrometer (Acton SP-2358 with Princeton Instruments PIXIS-400B). These two parts are connected by a 10-m bundle cable that consists of 12 cores with 100-mm radii. On the roof top of the anti-rolling system of R/V *Mirai*, the telescope unit was installed on a gimbal mount, which compensates for the pitch and roll of the ship. A sensor measuring pitch and roll of the telescope unit (10Hz) is used together to measure an offset of elevation angle due to incomplete compensation by the gimbal. The line of sight was in directions of the starboard and portside of the vessel.

The MAX-DOAS system records spectra of scattered solar radiation every 0.2-0.4 second. Measurements were made at several elevation angles of 0, 1.5, 3, 5, 10, 20, 30, 70, 110, 150, 160, 170, 175, 177 and 178.5 degrees using a movable mirror, which repeated the same sequence of elevation angles every 30-min. The UV/visible spectra range was changed every minute (284-423 nm and 391-528 nm).

After measurements were made, we first selected spectrum data with an elevation angle offset less than  $\pm 0.2$  degrees. For those spectra, DOAS spectral fitting was performed to quantify the slant column density (SCD), defined as the concentration integrated along the light path, for each elevation angle. In this analysis, SCDs of NO<sub>2</sub> (and other gases) and O<sub>4</sub> (O<sub>2</sub>-O<sub>2</sub>, collision complex of oxygen) were obtained together. Next, O<sub>4</sub> SCDs were converted to the aerosol optical depth (AOD) and the vertical profile of aerosol extinction coefficient (AEC) at a wavelength of 476 nm using an optimal estimation inversion method with a radiative transfer model. Using derived aerosol information, another inversion is performed to retrieve the tropospheric vertical column/profile of NO<sub>2</sub> and other gases.

#### **(2-2) CO, O<sub>3</sub>, and aerosol size distribution**

Carbon monoxide (CO), ozone (O<sub>3</sub>), and aerosol size distribution measurements were also continually conducted during the cruise. For CO and O<sub>3</sub> measurements, ambient air was continually sampled on the compass deck and drawn through ~20-m-long Teflon tubes connected to gas filter correlation CO analyzer (Model 48C, Thermo Fisher Scientific) and UV photometric based ozone

analyzer (Model 49C, Thermo Fisher Scientific) in the *Research Information Center*. For aerosol size distribution measurement, air was also sample on the compass deck and drawn through ~5-m-long tube connected to optical particle counter (KR-12A, Lion). All measurement data was recorded by both laptop and data logger.

#### (2-3) Fluorescent aerosol particle

To investigate the fluorescent aerosol particle on the ocean, we have continually measured fluorescent particle by the single particle fluorescence sensor, WIBS4. Ambient air is pumped through the instrument at 0.38 L/min. When a particle passes through the sensing region it encounters a 635 nm continuous-wave laser beam and the intensity of scattering light is measured to allow particle diameter to be estimated. Two optically filtered Xenon flash-lamps then sequentially provide ultraviolet radiation at wavelengths of 280 nm and 370 nm to particle by the scattering light of 635 nm. The fluorescence from the particle are detected by two photomultiplier tubes (PMTs) which can measure the wavelength in the range of 310-400 nm and 420-650 nm using optical filter, respectively. In this cruise, we detected >30,000,000 particles in which size are >0.5  $\mu\text{m}$ . After the elimination of data affected the ship's funnel period using wind data, fluorescent particles were about 5% in the total. We are planning to analyze the relationship fluorescent intensity of wavelength in the range of 310-400 nm and 420-650 nm.

#### (3) Preliminary results

These data for the whole cruise period will be analyzed.

#### (4) Data archives

The data will be submitted to the Marine-Earth Data and Information Department (MEDID) of JAMSTEC after the full analysis of the raw spectrum data is completed, which will be <2 years after the end of the cruise.

## **2.1.6 Rain, water vapor and surface water sampling**

**Naoyuki KURITA (JAMSTEC) Principal Investigator (not on-board)**  
**Katsuhisa MAENO (Global Ocean Development Inc.: GODI) Operator**

### **(1) Objective**

It is well known that the variability of stable water isotopes (HDO and H<sub>2</sub><sup>18</sup>O) is closely related with the moisture origin and hydrological processes during the transportation from the source region to deposition site. Thus, water isotope tracer is recognized as the powerful tool to study of the hydrological cycles in the atmosphere. However, oceanic region is one of sparse region of the isotope data, it is necessary to fill the data to identify the moisture sources by using the isotope tracer. In this study, to fill this sparse observation area, intense water isotopes observation was conducted along the cruise track of MR11-05.

### **(2) Method**

Following observation was carried out throughout this cruise.

#### **- Atmospheric moisture sampling:**

Water vapor was sampled from the height about 20m above the sea level. The air was drawn at rate of 1.2-3.0L/min through a plastic tube attached to top of the compass deck. The flow rate is regulated according to the water vapor content to collect the sample amount 12-28ml. The water vapor was trapped in a glass trap submerged into an ethanol cooled to 100 degree C by radiator, and then they are collected every 12 hour during the cruise. After collection, water in the trap was subsequently thawed and poured into the 6ml glass bottle.

#### **- Rainwater sampling**

Rainwater samples gathered in rain/snow collector were collected just after precipitation events have ended. The collected sample was then transferred into glass bottle (6ml) immediately after the measurement of precipitation amount.

#### **- Surface seawater sampling**

Seawater sample taken by the pump from 4m depth were collected in glass bottle (6ml) around the noon at the local time.

### **(3) Results**

Sampling of water vapor for isotope analysis is summarized in Table 2.1.6-1 (74 samples). The detail of rainfall sampling (13 samples) is summarized in Table 2.1.6-2. Described rainfall amount is calculated from the collected amount of precipitation. Sampling of surface seawater taken by pump from 4m depths is summarized in Table 2.1.6-3 (34 samples).

### **(4) Data archive**

Isotopes (HDO, H<sub>2</sub><sup>18</sup>O) analysis will be done at RIGC/JAMSTEC, and then analyzed isotopes data will be submitted to JAMSTEC Data Integration and Analysis Group (DIAG).



Table 2.1.6-1 Summary of water vapor sampling for isotope analysis

Sample	Date	Time (UT)	Date	Time (UT)	Lon	Lat	T.M. (m <sup>3</sup> )	Sam. (ml)	H2O ppm
V-1	6.26	23:45	6.27	12:01	144-43.03	41-01.94	2.35	25.0	13239
V-2	6.27	12:01	6.28	0:01	148-33.39	40-26.35	2.35	27.0	14298
V-3	6.28	0:04	6.28	12:01	151-52.59	41-42.34	2.28	23.5	12827
V-4	6.28	12:02	6.29	0:23	155-02.18	43-31.42	2.15	20.0	11576
V-5	6.29	0:24	6.29	12:00	157-39.47	45-21.34	1.99	18.0	11256
V-6	6.29	12:01	6.30	0:00	159-58.52	47-03.37	2.07	17.0	10220
V-7	6.30	0:02	6.30	12:00	160-09.26	46-59.89	2.06	13.0	7853
V-8	6.30	12:01	7.1	0:00	160-05.27	47-00.258	2.06	12.3	7430
V-9	7.1	0:00	7.1	12:02	160-07.99	47-01.17	2.07	14.0	8417
V-10	7.1	12:03	7.2	0:00	160-04.88	47-00.01	2.06	13.8	8337
V-11	7.2	0:01	7.2	12:00	160-05.74	46-58.46	2.06	14.5	8759
V-12	7.2	12:01	7.3	0:00	160-05.04	46-59.95	2.08	16.0	9573
V-13	7.3	0:02	7.3	12:00	160-04.33	46-58.16	2.06	14.2	8578
V-14	7.3	12:01	7.4	00:00	159-58.62	47-00.59	2.07	17.0	10220
V-15	7.4	00:03	7.4	12:05	160-05.23	47-00.05	2.08	15.0	8974
V-16	7.4	12:05	7.5	00:00	160-04.91	46-59.74	2.06	15.0	9061
V-17	7.5	0:01	7.5	12:00	160-04.30	46-58.34	2.07	16.0	9619
V-18	7.5	12:01	7.6	00:00	160-09.39	46-55.99	2.09	15.5	9229
V-19	7.6	0:02	7.6	12:00	160-20.33	46-55.05	2.07	17.0	10220
V-20	7.6	12:00	7.7	00:03	160-04.76	46-59.90	2.08	18.0	10769
V-21	7.7	0:04	7.7	12:00	160-04.65	47-00.14	2.07	16.0	9619
V-22	7.7	12:00	7.8	00:55	160-04.99	46-49.87	2.26	18.0	9912
V-23	7.8	0:56	7.8	12:01	160-05.11	46-59.98	1.93	15.0	9672
V-24	7.8	12:02	7.9	00:02	157-12.82	45-04.05	2.08	18.2	10889
V-25	7.9	0:03	7.9	12:53	154-50.84	43-47.05	2.23	20.2	11273
V-26	7.9	12:54	7.10	00:01	152-13.35	41-48.95	1.93	19.4	12509
V-27	7.10	0:03	7.10	12:02	149-29.35	40-43.11	2.01	23.0	14240
V-28	7.10	12:03	7.11	00:16	147-27.05	38-55.86	2.07	30.5	18336
V-29	7.11	0:18	7.11	12:00	146-08.64	37-58.80	1.86	25.0	16726
V-30	7.11	12:00	7.12	00:00	143-32.42	37-09.29	1.49	28.5	23803
V-31	7.12	0:01	7.12	12:02	141-32.47	36-29.61	1.41	25.0	22065
V-32	7.12	12:03	7.13	00:00	141-32.20	36-29.09	1.26	21.5	21235
V-33	7.13	0:02	7.13	12:00	141-29.37	36-28.52	1.12	20.0	22222
V-34	7.13	12:01	7.14	00:00	141-29.89	36-29.08	1.11	20.5	22983
V-35	7.14	0:00	7.14	12:00	141-59.52	37-13.83	1.10	21.0	23758
V-36	7.14	12:00	7.15	00:00	141-30.94	37-36.04	1.10	19.5	22061

V-37	7.15	0:00	7.15	12:03	141-08.18	35-20.19	1.11	20.5	22983
V-38	7.15	12:04	7.16	00:00	139-39.92	35-26.92	1.10	22.5	25455
V-39	7.17	0:00	7.17	12:00	141-16.99	35-42.19	1.08	22.5	25926
V-40	7.17	12:00	7.18	00:00	141-27.25	36-27.45	1.08	20.5	23621
V-41	7.18	0:03	7.18	12:01	141-20.45	36-49.34	1.07	20.0	23261
V-42	7.18	12:01	7.19	00:00	141-28.05	37-19.94	1.07	20.5	23842
V-43	7.19	0:00	7.19	12:01	142-31.43	37-52.26	1.07	19.0	22098
V-44	7.19	12:01	7.20	00:00	142-31.57	38-09.71	1.07	20.0	23261
V-45	7.20	0:01	7.20	12:00	142-34.05	38-47.13	1.07	14.0	16282
V-46	7.20	12:01	7.21	00:00	142-33.30	36-47.33	1.08	14.0	16132
V-47	7.21	0:01	7.21	12:02	141-44.90	35-05.31	1.06	13.0	15262
V-48	7.21	12:02	7.22	00:01	140-59.61	33-07.06	1.09	18.0	20550
V-49	7.22	0:03	7.22	12:00	141-36.08	31-16.21	1.05	20.0	23704
V-50	7.22	12:01	7.23	00:24	144-00.63	30-04.49	1.09	23.5	26830
V-51	7.23	0:25	7.23	12:00	145-35.93	29-57.41	1.03	22.0	26580
V-52	7.23	12:01	7.24	00:00	144-24.00	29-35.84	1.03	23.0	27789
V-53	7.24	0:03	7.24	12:00	144-59.90	29-59.97	1.06	20.5	24067
V-54	7.24	12:00	7.25	00:00	144-57.91	30-03.38	1.00	23.0	28622
V-55	7.25	0:02	7.25	12:00	145-05.47	30-02.33	1.00	22.0	27378
V-56	7.25	12:01	7.26	00:00	145-05.97	30-11.97	1.06	23.0	27002
V-57	7.26	0:03	7.26	12:00	145-01.50	30-00.13	1.06	20.5	24067
V-58	7.26	12:00	7.27	00:45	144-58.30	29-58.67	1.11	21.5	24104
V-59	7.27	0:45	7.27	12:00	145-02.55	30-01.58	1.00	19.0	23644
V-60	7.27	12:03	7.28	00:30	145-00.01	30-02.50	1.09	20.0	22834
V-61	7.28	0:31	7.28	12:11	145-00.66	30-00.68	1.03	19.5	23560
V-62	7.28	12:12	7.29	00:43	144-58.77	30-03.27	1.12	20.0	22222
V-63	7.29	0:44	7.29	12:55	144-53.92	30-02.84	1.08	21.5	24774
V-64	7.29	12:55	7.30	00:00	144-59.95	29-55.40	0.98	18.0	22857
V-65	7.30	0:00	7.30	12:00	145-17.80	30-15.81	1.07	22.0	25587
V-66	7.30	12:00	7.31	00:00	144-42.08	30-15.06	1.07	20.0	23261
V-67	7.31	0:01	7.31	12:00	144-49.54	31-40.46	1.06	20.0	23480
V-68	7.31	12:01	8.1	00:16	144-24.41	32-53.43	1.09	23.5	26830
V-69	8.1	0:16	8.1	12:00	143-49.06	35-00.62	1.05	20.0	23704
V-70	8.1	12:01	8.2	00:00	143-14.31	37-01.87	1.06	17.8	20897
V-71	8.2	0:01	8.2	12:00	142-39.24	39-02.70	1.07	18.0	20935
V-72	8.2	12:00	8.3	00:00	141-56.43	40-52.85	1.07	16.0	18609
V-73	8.3	0:01	8.3	12:00	141-18.41	41-30.54	1.07	14.5	16864
V-74	8.3	12:01	8.3	23:59	141-14.31	41-21.99	1.07	16.0	18609

Table 2.1.6-2 Summary of precipitation sampling for isotope analysis.

	Date	Time (UT)	Lon	Lat	Date	Time (UT)	Lon	Lat	Rain (mm)	R/S
R-1	6.26	23:50	141-14.37E	41-21.97N	7.1	01:38	160-05.59E	47-00.02N	5.3	R
R-2	7.1	01:38	160-05.59E	47-00.02N	7.2	08:15	160-05.66E	46-59.36N	1.4	R
R-3	7.2	08:16	160-05.66E	46-59.36N	7.3	12:05	160-04.25E	46-57.93N	0.1	R
R-4	7.3	12:05	160-04.25E	46-57.93N	7.4	08:41	160-05.24E	46-59.72N	1.0	R
R-5	7.4	08:41	160-05.24E	46-59.72N	7.4	21:13	160-05.34E	46-59.97N	0.6	R
R-6	7.4	21:13	160-05.34E	46-59.97N	7.7	12:08	160-04.71E	47-00.29N	mist	R
R-7	7.7	12:08	160-04.71E	47-00.29N	7.10	05:16	150-38.68E	41-26.48N	0.2	R
R-8	7.10	05:16	150-38.68E	41-26.48N	7.19	12:08	142-31.59E	37-52.53N	13.3	R
R-9	7.19	12:08	142-31.59E	37-52.53N	7.23	12:09	145-35.95E	29-59.31N	25.4	R
R-10	7.23	12:09	145-35.95E	29-59.31N	7.26	00:37	145-05.98E	30-11.98N	4.1	R
R-11	7.26	00:37	145-05.98E	30-11.98N	7.29	00:49	144-58.85E	30-02.85N	0.3	R
R-12	7.29	00:49	144-58.85E	30-02.85N	7.30	22:49	144-41.98E	29-59.99N	25.3	R
R-13	7.30	22:49	144-41.98E	29-59.99N	7.31	10:19	144-55.42E	31-20.59N	21.5	R

Table 2.1.6-3 Summary of water vapor sampling for isotope analysis

Sampling No.		Date	Time (UTC)	Position	
				LON	LAT
MR11-05 O-	1	6.28	03:04	149-31.62E	40-18.84N
MR11-05 O-	2	6.29	02:02	155-24.80E	43-47.63N
MR11-05 O-	3	6.30	01:01	159-58.57E	47-02.17N
MR11-05 O-	4	7.1	01:00	160-05.60E	46-59.98N
MR11-05 O-	5	7.2	01:00	160-06.14E	46-58.54N
MR11-05 O-	6	7.3	01:01	160-05.64E	46-58.86N
MR11-05 O-	7	7.4	01:00	159-57.56E	46-59.54E
MR11-05 O-	8	7.5	01:00	160-04.93E	46-59.44N
MR11-05 O-	9	7.6	01:02	160-09.26E	46-55.82N
MR11-05 O-	10	7.7	01:05	160-03.36E	46-59.38N
MR11-05 O-	11	7.8	01:00	160-04.94E	46-59.87N
MR11-05 O-	12	7.9	01:00	156-57.55E	44-53.40N
MR11-05 O-	13	7.10	01:00	151-58.92E	41-40.22N
MR11-05 O-	14	7.11	02:01	147-08.38E	38-41.38N
MR11-05 O-	15	7.12	03:02	142-51.80E	36-55.71N
MR11-05 O-	16	7.13	03:11	141-29.73E	36-28.81N
MR11-05 O-	17	7.14	03:03	141-30.00E	36-29.00N
MR11-05 O-	18	7.15	03:02	141-18.67E	37-03.13N
MR11-05 O-	19	7.18	03:00	141-29.92E	36-28.97N

MR11-05 O-	20	7.19	03:02	141-30.76E	37-33.62N
MR11-05 O-	21	7.20	03:02	142-29.28E	38-41.53N
MR11-05 O-	22	7.21	03:02	142-19.86E	36-17.38N
MR11-05 O-	23	7.22	03:02	140-56.99E	32-34.72N
MR11-05 O-	24	7.23	02:00	144-28.95E	30-02.22N
MR11-05 O-	25	7.24	02:02	144-42.61E	29-28.71N
MR11-05 O-	26	7.25	02:01	144-58.06E	30.03.38N
MR11-05 O-	27	7.26	02:04	145-03.06E	30-05.80N
MR11-05 O-	28	7.27	02:07	144-59.03E	29-58.82N
MR11-05 O-	29	7.28	02:08	145-00.09E	29-59.88N
MR11-05 O-	30	7.29	04:56	144-54.41E	30-02.01N
MR11-05 O-	31	7.30	02:47	144-50.61E	30-10.17N
MR11-05 O-	32	8.1	02:59	144-15.17E	33-25.07N
MR11-05 O-	33	8.2	05:28	142-56.64E	38-00.53N
MR11-05 O-	34	8.3	03:00	141-42.03E	41-28.61N

---

### 2.1.7 Air-sea surface eddy flux measurement

<b>Osamu TSUKAMOTO</b> (Okayama University)	<b>Principal Investigator</b>	<b>* not on board</b>
<b>Fumiyoshi KONDO</b> (University of Tokyo)		<b>* not on board</b>
<b>Hiroshi ISHIDA</b> (Kobe University)		<b>* not on board</b>
<b>Satoshi OKUMURA</b> (Global Ocean Development Inc. (GODI))		

#### (1) Objective

To better understand the air-sea interaction, accurate measurements of surface heat and fresh water budgets are necessary as well as momentum exchange through the sea surface. In addition, the evaluation of surface flux of carbon dioxide is also indispensable for the study of global warming. Sea surface turbulent fluxes of momentum, sensible heat, latent heat, and carbon dioxide were measured by using the eddy correlation method that is thought to be most accurate and free from assumptions. These surface heat flux data are combined with radiation fluxes and water temperature profiles to derive the surface energy budget.

#### (2) Instruments and Methods

The surface turbulent flux measurement system (Fig. 1) consists of turbulence instruments (Kaijo Co., Ltd.) and ship motion sensors (Kanto Aircraft Instrument Co., Ltd.). The turbulence sensors include a three-dimensional sonic anemometer-thermometer (Kaijo, DA-600) and an infrared hygrometer (LICOR, LI-7500). The sonic anemometer measures three-dimensional wind components relative to the ship. The ship motion sensors include a two-axis inclinometer (Applied Geomechanics, MD-900-T), a three-axis accelerometer (Applied Signal Inc., QA-700-020), and a three-axis rate gyro (Systron Donner, QRS-0050-100). LI7500 is a CO<sub>2</sub>/H<sub>2</sub>O turbulence sensor that measures turbulent signals of carbon dioxide and water vapor simultaneously. These signals are sampled at 10 Hz by a PC-based data logging system (Labview, National Instruments Co., Ltd.). By obtaining the ship speed and heading information through the Mirai network system it yields the absolute wind components relative to the ground. Combining wind data with the turbulence data, turbulent fluxes and statistics are calculated in a real-time basis. These data are also saved in digital files every 0.1 second for raw data and every 1 minute for statistic data.

#### (3) Observation log

The observation was carried out throughout this cruise.

#### (4) Data Policy and citation

All data are archived at Okayama University, and will be open to public after quality checks and corrections. Corrected data will be submitted to JAMSTEC Marine-Earth Data and Information Department.



Fig. 1 Turbulent flux measurement system on the top deck of the foremast.

## 2.2 Physical oceanographic observation

### 2.2.1 CTD cast and water sampling

**Masahide WAKITA (JAMSTEC RIGC)**

**Naoko MIYAMOTO (MWJ)**

**Shungo OSHITANI (MWJ)**

**Hiroki USHIROMURA (MWJ)**

**Toru IDAI (MWJ)**

**Tomoyuki TAKAMORI (MWJ)**

**Masaki FURUBATA (MWJ)**

#### (1) Objective

Investigation of oceanic structure and water sampling.

#### (2) Parameters

Temperature (Primary and Secondary)

Conductivity (Primary and Secondary)

Pressure

Dissolved Oxygen

Fluorescence

Transmission Voltage

Dissolved Oxygen Voltage

Photosynthetically Active Radiation

Altimeter

#### (3) Instruments and Methods

CTD/Carousel Water Sampling System, which is a 36-position Carousel water sampler (CWS) with Sea-Bird Electronics, Inc. CTD (SBE9plus), was used during this cruise. 12-liter Niskin Bottles, which were washed by alkaline detergent and 1 N HCl, were used for sampling seawater. The sensors attached on the CTD were temperature (Primary and Secondary), conductivity (Primary and Secondary), pressure, fluorescence, transmission voltage, RINKO-III (dissolved oxygen sensor), dissolved oxygen, altimeter, PAR sensor and deep ocean standards thermometer. The Practical Salinity was calculated by measured values of pressure, conductivity and temperature. The CTD/CWS was deployed from starboard on working deck.

The CTD raw data were acquired on real time using the Seasave-Win32 (ver.7.20g) provided by Sea-Bird Electronics, Inc. and stored on the hard disk of the personal computer. Seawater was sampled during the up cast by sending fire commands from the personal computer. We usually stop at each layer for 30 seconds to stabilize then fire.

35 casts of CTD measurements were conducted (table 2.2.1-1).

The data shifts observed are listed as follows.

K02M03 (down cast 4400-4450, 4700-4800dbar): Dissolved Oxygen

K02M04 (down cast 1850-2025dbar): Temperature, Conductivity (Primary)

K02M06 (up cast 535-360dbar): Temperature, Conductivity (Primary) and Dissolved Oxygen

S01M10 (up cast 900-1dbar): Temperature, Conductivity (Primary) and Dissolved Oxygen

Data processing procedures and used utilities of SBE Data Processing-Win32 (ver.7.18d) and SEASOFT were as follows:

(The process in order)

DATCNV: Convert the binary raw data to engineering unit data. DATCNV also extracts bottle information where scans were marked with the bottle confirm bit during acquisition. The duration was set to 4.4 seconds, and the offset was set to 0.0 seconds.

RINKOCOR (original module): Corrected of the hysteresis of RINK-III voltage.

RINKOCORROS (original module): Corrected of the hysteresis of RINKO-III voltage bottle data.

BOTTLESUM: Create a summary of the bottle data. The data were averaged over 4.4 seconds.

ALIGNCTD: Convert the time-sequence of sensor outputs into the pressure sequence to ensure that all calculations were made using measurements from the same parcel of water. Dissolved oxygen data are systematically delayed with respect to depth mainly because of the long time constant of the dissolved oxygen sensor and of an additional delay from the transit time of water in the pumped plumbing line. This delay was compensated by 6 seconds advancing dissolved oxygen sensor (SBE43) output (dissolved oxygen voltage) relative to the temperature data. RINKO-III data and transmission voltage data are also delayed by slightly slow response time to the sensor. The delay was compensated by 1 second or 2 seconds advancing.

WILDEDIT: Mark extreme outliers in the data files. The first pass of WILDEDIT obtained an accurate estimate of the true standard deviation of the data. The data were read in blocks of 1000 scans. Data greater than 10 standard deviations were flagged. The second pass computed a standard deviation over the same 1000 scans excluding the flagged values. Values greater than 20 standard deviations were marked bad. This process was applied to pressure, depth, temperature, conductivity and dissolved oxygen voltage (SBE43).

CELLTM: Remove conductivity cell thermal mass effects from the measured conductivity. Typical values used were thermal anomaly amplitude  $\alpha = 0.03$  and the time constant  $1/\beta = 7.0$ .

FILTER: Perform a low pass filter on pressure with a time constant of 0.15 second. In order to produce zero phase lag (no time shift) the filter runs forward first then backward

WFILTER: Perform a median filter to remove spikes in the fluorescence data and transmission voltage data. A median value was determined by 49 scans of the window.

SECTIONU (original module of SECTION): Select a time span of data based on scan number in order to reduce a file size. The minimum number was set to be the starting time when the CTD package was beneath the sea-surface after activation of the pump.

The maximum number of was set to be the end time when the package came up from the surface.

LOOPEDIT: Mark scans where the CTD was moving less than the minimum velocity of 0.0 m/s (traveling backwards due to ship roll).

DESPIKE (original module): Remove spikes of the data. A median and mean absolute deviation was calculated in 1-dbar pressure bins for both down and up cast, excluding the flagged values. Values greater than 4 mean absolute deviations from the median were marked bad for each bin. This process was performed 2 times for temperature, conductivity, dissolved oxygen voltage (SBE43) and RINKO-III voltage.

DERIVE: Compute dissolved oxygen (SBE43).

BINAVG: Average the data into 1-dbar pressure bins.

DERIVE: Compute the Practical Salinity, potential temperature, and sigma-theta.

SPLIT: Separate the data from an input .cnv file into down cast and up cast files.

Configuration file: MR1105A.con

Specifications of the sensors are listed below.

CTD: SBE911plus CTD system

Under water unit:

SBE9plus (S/N 09P54451-1027, Sea-Bird Electronics, Inc.)

Pressure sensor: Digiquartz pressure sensor (S/N 117457)

Calibrated Date: 05 May. 2011

Temperature sensors:

Primary: SBE03Plus (S/N 03P4815, Sea-Bird Electronics, Inc.)

Calibrated Date: 25 Jan. 2011

Secondary: SBE03-04/F (S/N 031359, Sea-Bird Electronics, Inc.)

Calibrated Date: 18 May. 2011

Conductivity sensors:

Primary: SBE04-04/0 (S/N 041203, Sea-Bird Electronics, Inc.)

Calibrated Date: 25 May. 2011

Secondary: SBE04-04/0 (S/N 042435, Sea-Bird Electronics, Inc.)

Calibrated Date: 02 Mar. 2011

Fluorescence:

Chlorophyll Fluorometer (S/N 3054, Seapoint Sensors, Inc.)

Altimeter:

Benthos PSA-916T (S/N 1100, Teledyne Benthos, Inc.)

Dissolved Oxygen sensor:

SBE43 (S/N 430394, Sea-Bird Electronics, Inc.)

Calibrated Date: 10 Dec. 2010

Dissolved Oxygen sensors:



RINK-III (S/N 0024, Alec Electronics Co. Ltd.)  
RINK-III (S/N 0037, Alec Electronics Co. Ltd.)  
Photosynthetically Active Radiation:  
PAR sensor (S/N 0049, Satlantic Inc.)  
Calibrated Date: 22 Jan. 2009  
Deep Ocean Standards Thermometer:  
SBE35 (S/N 0022, Sea-Bird Electronics, Inc.)  
Calibrated Date: 23 Jan. 2011  
Carousel water sampler:  
SBE32 (S/N 3221746-0278, Sea-Bird Electronics, Inc.)

Deck unit: SBE11plus (S/N 11P7030-0272, Sea-Bird Electronics, Inc.)

(4) Preliminary Results

During this cruise, 35 casts of CTD observation were carried out. Date, time and locations of the CTD casts are listed in Table 2.2.1-1.

(5) Data archive

All raw and processed data files were copied onto CD-ROM. The data will be submitted to the Data Management office (DMO), JAMSTEC, and will be opened to public via “JAMSTEC Data Site for Research Cruises”.

Table 2.2.1-1 MR11-05 CTD Casttable

Stnnbr	Castno	Date(UTC)	Time(UTC)		BottomPosition		Depth	Wire Out	HT Above Bottom	Max Depth	Max Pressure	CTD Filename	Remark
		(mmddyy)	Start	End	Latitude	Longitude							
K02	1	063011	00:48	00:58	47-02.25N	159-58.50E	5182.0	147.1	-	151.7	152.6	K02M01	FF Ref.
K02	2	063011	15:04	15:45	46-59.88N	160-12.22E	5275.0	297.6	-	301.3	304.0	K02M02	Shallow(P.P.)
K02	3	063011	19:06	22:33	46-59.72N	160-06.28E	5256.0	5236.6	9.2	5231.2	5340.4	K02M03	Deep(routine)
K02	4	070111	21:02	22:33	47-00.18N	160-04.93E	5248.0	2002.7	-	2000.7	2026.7	K02M04	Shallow(trap/paleo/sf6)
K02	5	070211	08:11	08:38	46-59.35N	160-05.65E	5256.0	196.9	-	201.3	203.1	K02M05	Shallow(KU/POC)
K02	6	070311	04:01	05:09	46-55.53N	160-08.39E	5206.0	1000.7	-	1001.0	1012.5	K02M06	Shallow(RI)
K02	7	070411	03:03	06:00	46-58.89N	159-58.90E	5222.0	5008.6	-	5000.5	5102.5	K02M07	Bacteria
K02	8	070411	15:33	16:15	47-00.01N	160-04.98E	5245.0	297.3	-	300.6	303.3	K02M08	Shallow(P.P.)
K02	9	070411	21:31	22:01	46-59.92N	160-05.55E	5250.0	198.6	-	200.5	202.2	K02M09	Shallow(PE)
K02	10	070611	04:19	04:44	46-55.72N	160-09.91E	5211.0	197.5	-	201.2	203.0	K02M10	Shallow(KU/POC)
K02	11	070711	15:35	16:18	47-00.31N	160-04.73E	5243.0	297.3	-	300.6	303.5	K02M11	Shallow(P.P.)
KNT	1	070911	07:56	11:31	43-59.75N	155-00.20E	5317.0	5304.8	9.4	5300.2	5410.5	KNTM01	Deep(routine)
JKO	1	071111	06:46	10:20	38-04.10N	146-25.57E	5394.0	5392.1	9.7	5381.1	5491.0	JKOM01	Deep(routine)
F01	1	071211	17:44	19:05	36-28.99N	141-30.18E	1340.0	1336.6	9.6	1334.9	1349.8	F01M01	Deep(P.P. & routine)
F01	2	071311	00:03	01:00	36-29.15N	141-30.13E	1320.0	1315.3	10.2	1313.6	1327.6	F01M02	Deep(RI)
F01	3	071711	21:35	21:55	36-28.98N	141-29.97E	1332.0	195.8	-	200.9	202.3	F01M03	Shallow(RI)
D04	1	071811	06:37	06:59	36-41.49N	141-09.08E	208.0	190.7	9.8	193.2	195.2	D04M01	Shallow(RI)
D03	1	071811	21:39	21:58	37-00.01N	141-16.94E	154.0	137.2	9.8	140.2	140.9	D03M01	Shallow(RI)
D02	1	071911	00:43	01:02	37-19.85N	141-27.99E	159.0	144.9	8.8	147.3	148.6	D02M01	Shallow(RI)
D01	1	071911	04:36	04:55	37-35.01N	141-30.97E	141.0	122.9	10.5	126.1	127.1	D01M01	Shallow(RI)
S01	1	072411	05:31	09:26	29-59.92N	145-00.22E	5969.0	5940.6	10.2	5942.7	6067.3	S01M01	Deep(routine)
S01	2	072411	17:33	18:18	30-00.22N	144-59.95E	5965.0	296.9	-	300.6	302.6	S01M02	Shallow(P.P.)
S01	3	072511	07:12	07:37	30-00.25N	144-59.91E	5970.0	196.6	-	201.5	203.0	S01M03	Shallow(KU/POC)
S01	4	072611	02:34	05:29	30-02.43N	145-01.31E	5939.0	4998.5	-	5000.3	5094.5	S01M04	Deep(Bacteria)
S01	5	072611	06:43	08:17	30-02.29N	145-00.99E	5910.0	2003.4	-	2002.2	2025.8	S01M05	Shallow(trap/paleo/sf6)
S01	6	072711	04:40	05:05	30-02.51N	145-02.49E	5973.0	195.8	-	200.0	201.5	S01M06	Shallow(KU/POC)
S01	7	072711	17:31	18:13	30-00.18N	144-59.75E	5969.0	297.6	-	300.4	302.9	S01M07	Shallow(P.P.)
S01	8	072711	23:04	23:33	30-00.58N	144-59.75E	5983.0	197.5	-	200.4	201.8	S01M08	Shallow(PE)
S01	9	072911	05:05	06:06	30-01.90N	144-54.32E	5910.0	1000.5	-	1002.5	1011.8	S01M09	Shallow(RI)
S01	10	073011	06:34	08:19	29-59.74N	145-00.05E	5953.0	1977.5	-	1977.9	2000.8	S01M10	Deep(ARGO)
S01	11	073011	10:18	12:10	30-15.90N	145-17.88E	5940.0	1977.7	-	1976.6	2000.3	S01M11	Deep(ARGO)
S01	12	073011	15:08	16:52	29-44.18N	145-17.88E	5791.0	1980.8	-	1978.6	2001.6	S01M12	Deep(ARGO)
S01	13	073011	19:43	21:28	29-44.01N	144-41.93E	5908.0	1976.6	-	1977.3	2000.0	S01M13	Deep(ARGO)
S01	14	073111	00:18	02:00	30-15.98N	144-42.02E	5910.0	1980.5	-	1979.0	2001.9	S01M14	Deep(ARGO)
KEO	1	073111	20:37	21:20	32-29.91N	144-33.59E	5654.0	1001.1	-	1001.9	1011.9	KEOM01	Deep(RI)

## 2.2.2 Salinity measurement

**Masahide WAKITA (JAMSTEC MIO)**

**Hiroki USHIROMURA (MWJ)**

### (1) Objective

To measure bottle salinity obtained by CTD casts, bucket sampling, and The Continuous Sea Surface Water Monitoring System (TSG).

### (2) Methods

#### a. Salinity Sample Collection

Seawater samples were collected with 12 liter Niskin-X bottles, bucket, and TSG. The salinity sample bottles of the 250ml brown glass bottles with screw caps were used for collecting the sample water. Each bottle was rinsed three times with the sample water, and was filled with sample water to the bottle shoulder. The salinity sample bottles for TSG were sealed with plastic inner caps and screw caps because we took into consideration the possibility of storage for about a month. These caps were rinsed three times with the sample water before use. The bottle was stored for more than 18 hours in the laboratory before the salinity measurement.

The number of samples is shown as follows;

Table 2.2.2-1 The number of samples

Sampling type	Number of samples
CTD and Bucket	443
TSG	48
Total	491

#### b. Instruments and Method

The salinity analysis on R/V MIRAI was carried out during the cruise of MR11-05 using the salinometer (Model 8400B “AUTOSAL”; Guildline Instruments Ltd.: S/N 62827) with an additional peristaltic-type intake pump (Ocean Scientific International, Ltd.). A pair of precision digital thermometers (Model 9540; Guildline Instruments Ltd.: S/N 62525 and 62521) were used. The thermometer monitored the ambient temperature and the bath temperature of the salinometer.

The specifications of AUTOSAL salinometer and thermometer are shown as follows;

Salinometer (Model 8400B “AUTOSAL”; Guildline Instruments Ltd.)

Measurement Range : 0.005 to 42 (PSU)

Accuracy : Better than  $\pm 0.002$  (PSU) over 24 hours  
without re-standardization

Maximum Resolution : Better than  $\pm 0.0002$  (PSU) at 35 (PSU)

Thermometer (Model 9540: Guildline Instruments Ltd.)

Measurement Range	: -40 to +180 deg C
Resolution	: 0.001
Limits of error $\pm$ deg C	: 0.01 (24 hours @ 23 deg C $\pm$ 1 deg C)
Repeatability	: $\pm$ 2 least significant digits

The measurement system was almost the same as Aoyama *et al.* (2002). The salinometer was operated in the air-conditioned ship's laboratory at a bath temperature of 24 deg C. The ambient temperature varied from approximately 20.5 deg C to 23.4 deg C, while the bath temperature was very stable and varied within  $\pm$  0.004 deg C on rare occasion.

The measurement for each sample was done with the double conductivity ratio and defined as the median of 31 readings of the salinometer. Data collection was started 5 seconds after filling the cell with the sample and it took about 10 seconds to collect 31 readings by a personal computer. Data were taken for the sixth and seventh filling of the cell after rinsing five times. In the case of the difference between the double conductivity ratio of these two fillings being smaller than 0.00002, the average value of the double conductivity ratio was used to calculate the bottle salinity with the algorithm for practical salinity scale, 1978 (UNESCO, 1981). If the difference was greater than or equal to 0.00003, an eighth filling of the cell was done. In the case of the difference between the double conductivity ratio of these two fillings being smaller than 0.00002, the average value of the double conductivity ratio was used to calculate the bottle salinity. In the case of the double conductivity ratio of eighth filling did not satisfy the criteria above, we measured a ninth filling of the cell and calculated the bottle salinity. The measurement was conducted in about 4 - 12 hours per day and the cell was cleaned with soap after the measurement of the day.

### (3) Preliminary Result

#### a. Standard Seawater

Standardization control of the salinometer was set to 468 and all measurements were done at this setting. The value of STANDBY was 24+5396  $\pm$  0.0002 and that of ZERO was 0.0-0000  $\pm$  0.0001. The conductivity ratio of IAPSO Standard Seawater batch P152 was 0.99981 (the double conductivity ratio was 1.99962) and was used as the standard for salinity. We measured 35 bottles of P152.

The specifications of SSW used in this cruise are shown as follows ;

Batch	: P152
conductivity ratio	: 0.99981
salinity	: 34.993
Use by	: 5 <sup>th</sup> May 2013

Fig.2.2.2-1 shows the history of the double conductivity ratio of the Standard Seawater batch P152 before correction. The average of the double conductivity ratio was 1.99959 and the standard deviation was 0.00002, which is equivalent to 0.0004 in salinity.

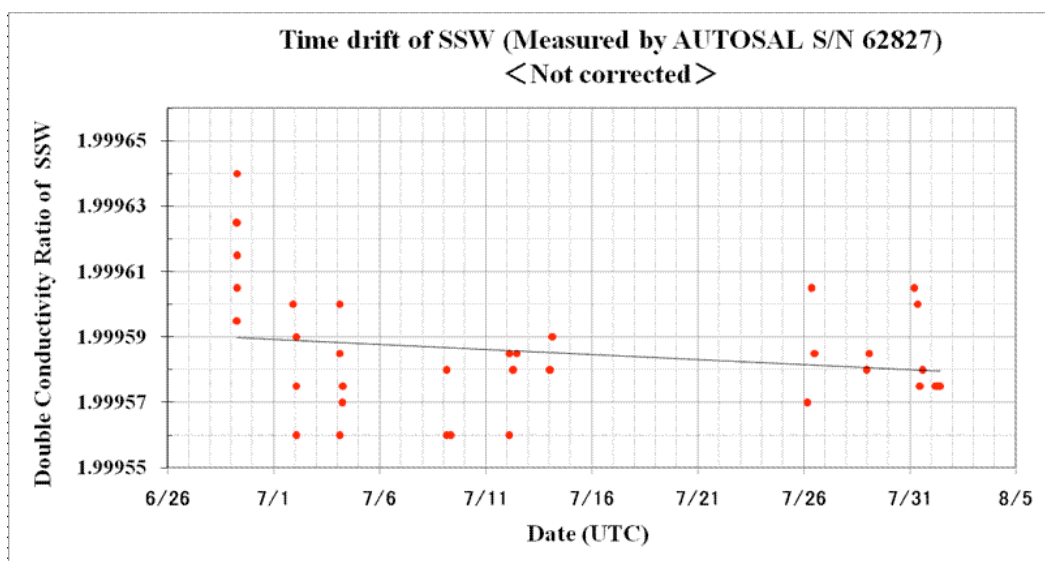


Fig. 2.2.2-1 The history of the double conductivity ratio for the Standard Seawater batch P152 (Before correction)

Fig.2.2.2-2 shows the history of the double conductivity ratio of the Standard Seawater batch P152 after correction. The average of the double conductivity ratio after correction was 1.99962 and the standard deviation was 0.00001, which is equivalent to 0.0003 in salinity.

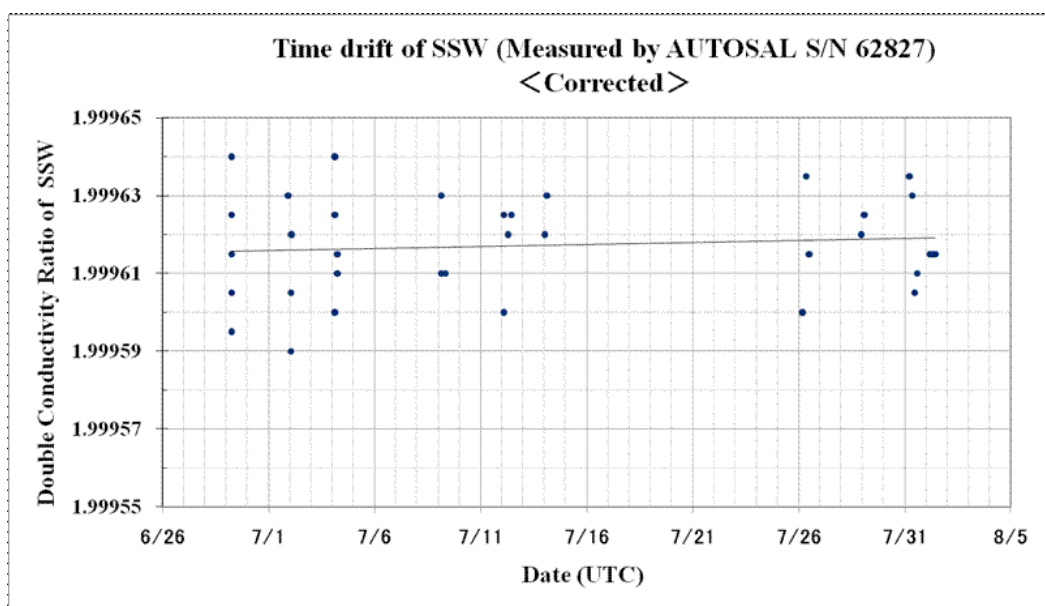


Fig. 2.2.2-2 The history of the double conductivity ratio for the Standard Seawater batch P152 (After correction)

#### b. Sub-Standard Seawater

Sub-standard seawater was made from deep-sea water filtered by a pore size of 0.45 micrometer and stored in a 20-liter container made of polyethylene and stirred for at least 24 hours before measuring. It was measured about every 6 samples in order to check for the possible sudden drifts of the salinometer.

#### c. Replicate Samples

We estimated the precision of this method using 41 pairs of replicate samples taken from the same Niskin bottle. Fig.2.2.2-3 shows the histogram of the absolute difference between each pair of the replicate samples. The average and the standard deviation of absolute difference among 41 pairs of replicate samples were 0.0002 and 0.0001 in salinity, respectively.

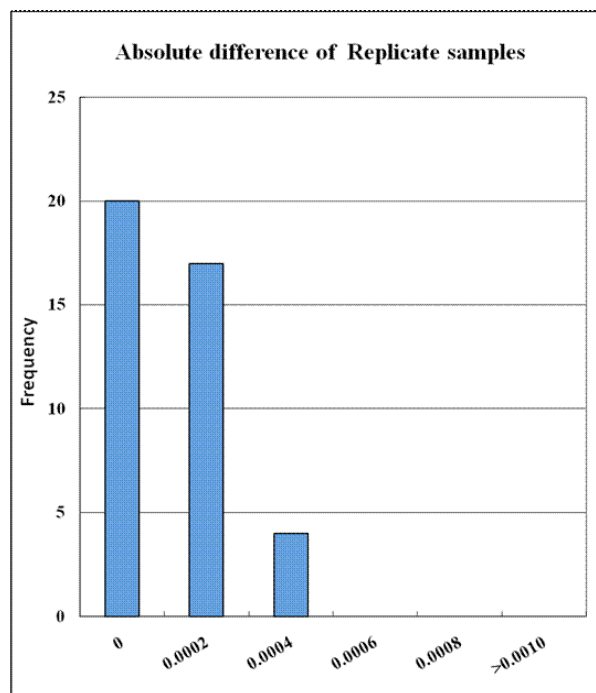


Fig. 2.2.2-3 The histogram of the double conductivity ratio for the absolute difference of replicate samples

#### (4) Data archive

These raw datasets will be submitted to JAMSTEC Data Management Office (DMO).

#### (5) Reference

- Aoyama, M. , T. Joyce, T. Kawano and Y. Takatsuki: Standard seawater comparison up to P129. Deep-Sea Research, I, Vol. 49, 1103~1114, 2002
- UNESCO : Tenth report of the Joint Panel on Oceanographic Tables and Standards. UNESCO Tech. Papers in Mar. Sci., 36, 25 pp., 1981

### 2.2.3 Shipboard ADCP

<b>Makio HONDA</b>	<b>(JAMSTEC RIGC)</b>
<b>Katsuhisa MAENO</b>	<b>(Global Ocean Development Inc., GODI)</b>
<b>Harumi OTA</b>	<b>(GODI)</b>
<b>Ryo OYAMA</b>	<b>(MIRAI Crew)</b>

#### (1) Objective

To obtain continuous measurement of the current profile along the ship's track.

#### (2) Methods

Upper ocean current measurements were made in MR11-05 cruise, using the hull-mounted Acoustic Doppler Current Profiler (ADCP) system. For most of its operation the instrument was configured for water-tracking mode. Bottom-tracking mode, interleaved bottom-ping with water-ping, was made to get the calibration data for evaluating transducer misalignment angle in the shallow water. The system consists of following components;

1. R/V MIRAI has installed the Ocean Surveyor for vessel-mount ADCP (frequency 75 kHz; Teledyne RD Instruments, USA). It has a phased-array transducer with single ceramic assembly and creates 4 acoustic beams electronically. We mounted the transducer head rotated to a ship-relative angle of 45 degrees azimuth from the keel
2. For heading source, we use ship's gyro compass (Tokimec, Japan), continuously providing heading to the ADCP system directory. Additionally, we have Inertial Navigation System which provide high-precision heading, attitude information, pitch and roll, are stored in ".N2R" data files with a time stamp.
3. DGPS system (Trimble SPS751 & Fugro Multifix ver.5) providing precise ship's position.
4. We used VmDas software version 1.4.6 (TRDI) for data acquisition.
5. To synchronize time stamp of ping with GPS time, the clock of the logging computer is adjusted to GPS time every 1 minute
6. Fresh water is charged in the sea chest to prevent biofouling at transducer face.
7. The sound speed at the transducer does affect the vertical bin mapping and vertical velocity measurement, is calculated from temperature, salinity (constant value; 35.0 psu) and depth (6.5 m; transducer depth) by equation in Medwin (1975).

Data was configured for 8-m intervals starting 23-m below sea surface. Data was recorded every ping as raw ensemble data (.ENR). Also, 60 seconds and 300 seconds averaged data were recorded as short-term average (.STA) and long-term average (.LTA) data, respectively. Major parameters for the measurement, Direct Command, are shown in Table 2.2.3-1.

#### (3) Preliminary results

Fig.2.2.3-1 and Fig.2.2.3-2 shows the current profile along the ship's track.

#### (4) Data archive

These data obtained in this cruise will be submitted to The Data Management Group (DMG) of JAMSTEC, and will be opened to the public via JAMSTEC home page.

(5) Remarks

Following periods, GPS data was invalid.

03:46:14 09 Jul. 2011 - 03:46:16 09 Jul. 2011

03:51:16 09 Jul. 2011

23:38:53 15 Jul. 2011 - 23:41:36 15 Jul. 2011

00:11:36 17 Jul. 2011 - 00:14:03 17 Jul. 2011

01:32:35 17 Jul. 2011 - 01:34:43 17 Jul. 2011

03:07:51 17 Jul. 2011

02:33:34 23 Jul. 2011 - 02:52:03 23 Jul. 2011

02:58:50 24 Jul. 2011

03:24:11 24 Jul. 2011

Table 2.2.3-1 Major parameters

---

***Bottom-Track Commands***

BP = 001                      Pings per Ensemble (almost less than 1000m depth)

***Environmental Sensor Commands***

EA = +04500                  Heading Alignment (1/100 deg)  
EB = +00000                  Heading Bias (1/100 deg)  
ED = 00065                   Transducer Depth (0 - 65535 dm)  
EF = +001                      Pitch/Roll Divisor/Multiplier (pos/neg) [1/99 - 99]  
EH = 00000                   Heading (1/100 deg)  
ES = 35                          Salinity (0-40 pp thousand)  
EX = 00000                   Coord Transform (Xform:Type; Tilts; 3Bm; Map)  
EZ = 10200010                Sensor Source (C; D; H; P; R; S; T; U)  
C (1): Sound velocity calculates using ED, ES, ET (temp.)  
D (0): Manual ED  
H (2): External synchro  
P (0), R (0): Manual EP, ER (0 degree)  
S (0): Manual ES  
T (1): Internal transducer sensor  
U (0): Manual EU

***Timing Commands***

TE = 00:00:02.00            Time per Ensemble (hrs:min:sec.sec/100)  
TP = 00:02.00                Time per Ping (min:sec.sec/100)

***Water-Track Commands***

WA = 255                      False Target Threshold (Max) (0-255 count)  
WB = 1                          Mode 1 Bandwidth Control (0=Wid, 1=Med, 2=Nar)  
WC = 120                       Low Correlation Threshold (0-255)  
WD = 111 100 000            Data Out (V; C; A; PG; St; Vsum; Vsum^2; #G; P0)  
WE = 1000                      Error Velocity Threshold (0-5000 mm/s)  
WF = 0800                      Blank After Transmit (cm)  
WG = 001                       Percent Good Minimum (0-100%)  
WI = 0                           Clip Data Past Bottom (0 = OFF, 1 = ON)  
WJ = 1                           Rcvr Gain Select (0 = Low, 1 = High)  
WM = 1                           Profiling Mode (1-8)



WN = 100	Number of depth cells (1-128)
WP = 00001	Pings per Ensemble (0-16384)
WS = 800	Depth Cell Size (cm)
WT = 000	Transmit Length (cm) [0 = Bin Length]
WV = 0390	Mode 1 Ambiguity Velocity (cm/s radial)

---

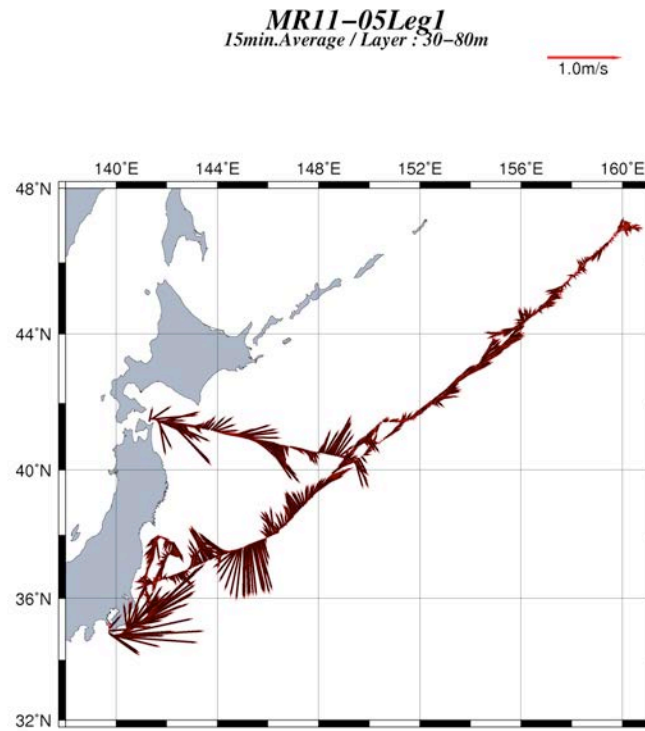


Fig 2.2.3-1. Current profile along the ship's track.(leg1)

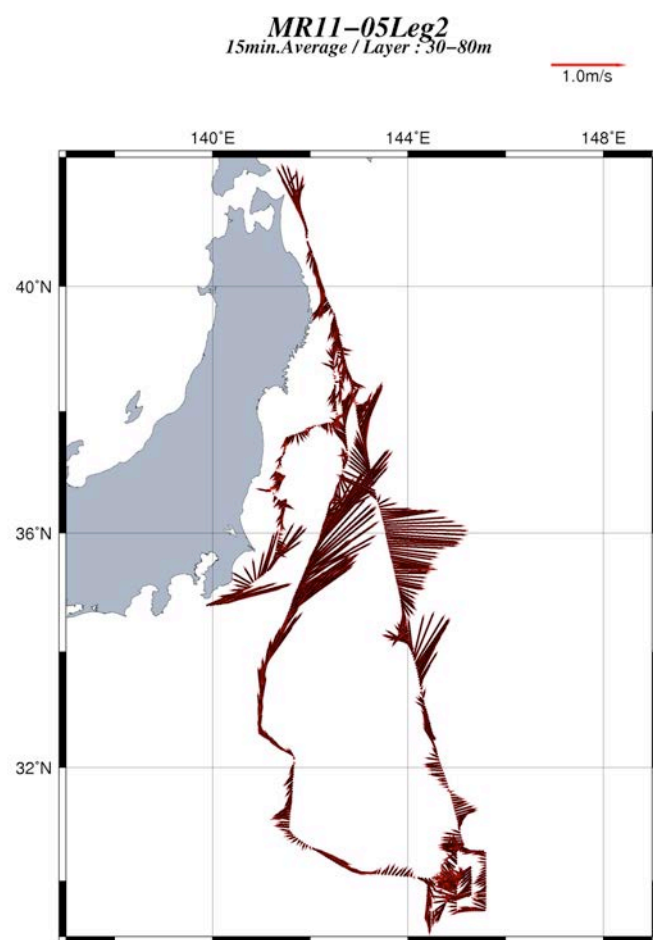


Fig 2.2.3-2. Current profile along the ship's track.(leg2)

## 2.3 Sea surface water monitoring

**Masahide WAKITA (JAMSTEC): Principal Investigator**

**Misato KUWAHARA (Marine Works Japan Co. Ltd): Operation Leader**

**Hideki YAMAMOTO (Marine Works Japan Co. Ltd)**

### (1) Objective

Our purpose is to obtain temperature, salinity, dissolved oxygen, and fluorescence data continuously in near-sea surface water.

### (2) Parameters

Temperature (surface water)

Salinity (surface water)

Dissolved oxygen (surface water)

Fluorescence (surface water)

### (3) Instruments and Methods

The Continuous Sea Surface Water Monitoring System (Marine Works Japan Co. Ltd.) has four sensors and automatically measures temperature, conductivity, dissolved oxygen and fluorescence in near-sea surface water every one minute. This system is located in the “*sea surface monitoring laboratory*” and connected to shipboard LAN-system. Measured data, time, and location of the ship were stored in a data management PC. The near-surface water was continuously pumped up to the laboratory from about 4.5 m water depth and flowed into the system through a vinyl-chloride pipe. The flow rate of the surface seawater was adjusted to be 5 dm<sup>3</sup> min<sup>-1</sup>.

#### a. Instruments

##### Software

Seamoni-kun Ver.1.10.52

##### Sensors

Specifications of the each sensor in this system are listed below.

#### 1) Temperature and Conductivity sensor

Model:	SBE-45, SEA-BIRD ELECTRONICS, INC.
Serial number:	4552788-0264
Measurement range:	Temperature -5 to +35 °C Conductivity 0 to 7 S m <sup>-1</sup>
Initial accuracy:	Temperature 0.002 °C Conductivity 0.0003 S m <sup>-1</sup>
Typical stability (per month):	Temperature 0.0002 °C Conductivity 0.0003 S m <sup>-1</sup>
Resolution:	Temperatures 0.0001 °C Conductivity 0.00001 S m <sup>-1</sup>

#### 2) Bottom of ship thermometer

Model:	SBE 38, SEA-BIRD ELECTRONICS, INC.
Serial number:	3852788-0457

Measurement range: -5 to +35 °C  
 Initial accuracy:  $\pm 0.001$  °C  
 Typical stability (per 6 month): 0.001 °C  
 Resolution: 0.00025 °C

3) Dissolved oxygen sensor

Model: OPTODE 3835, AANDERAA Instruments.  
 Serial number: 1519  
 Measuring range: 0 - 500  $\mu\text{mol dm}^{-3}$   
 Resolution:  $<1 \mu\text{mol dm}^{-3}$   
 Accuracy:  $<8 \mu\text{mol dm}^{-3}$  or 5% whichever is greater  
 Settling time:  $<25$  s

4) Fluorometer

Model: C3, TURNER DESIGNS  
 Serial number: 2300123

b. Measurements

Periods of measurement during MR 11-05 are listed in Table 2.3-1.

Table 2.3-1 Events list of the Sea surface water monitoring during MR11-05

System Date [UTC]	System Time [UTC]	Events	Remarks
2011/6/27	06:27	All the measurements were started and data was available.	Cruise start
2011/07/15	20:56	All the measurements were stopped.	Yokohama port
2011/7/17	05:19	All the measurements were started and data was available.	Cruise restart
2011/08/03	00:06	All the measurements were stopped.	Cruise end

(5) Preliminary Result

Preliminary data of temperature, salinity, dissolved oxygen and fluorescence at sea surface is shown in Fig. 2.3-1.

Fig. 2.3-1. Spatial and temporal distribution of (a) temperature, (b) salinity, (c) dissolved oxygen and (d) fluorescence in MR11-05 cruise.

We took the surface water samples to compare sensor data with bottle data of salinity, dissolved oxygen and fluorescence. The results are shown in Figs. 2.3-2 - 4. All the salinity samples were analyzed by the Guideline 8400B “AUTOSAL” (see 2.2.2), and dissolve oxygen samples were analyzed by Winkler method (see 2.4), and fluorescence were analyzed by 10-AU (see 3.4.1).

(6) Data archive

All data will be submitted to Chief Scientist.

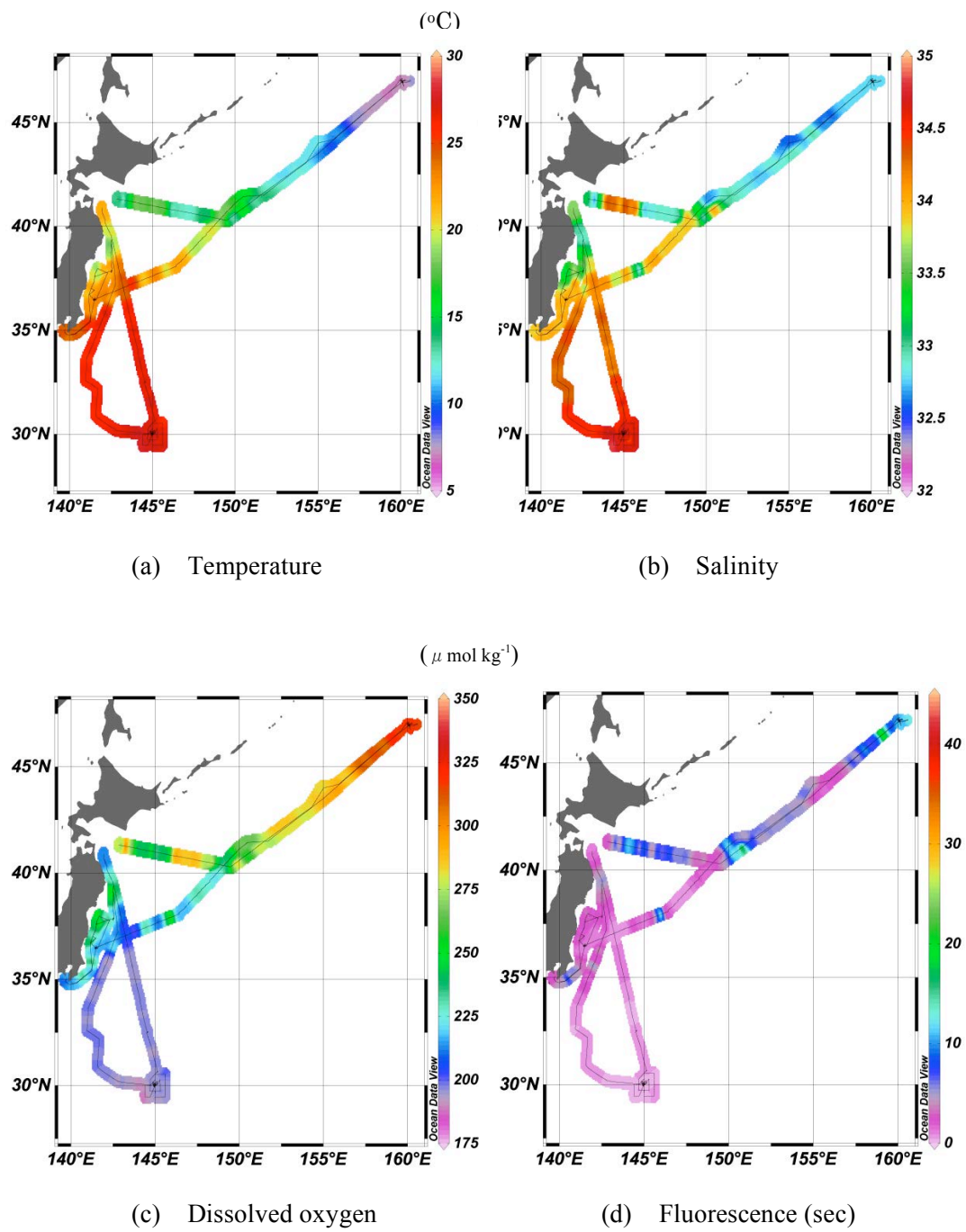


Fig. 2.3-1. Spatial and temporal distribution of (a) temperature, (b) salinity, (c) dissolved oxygen and (d) fluorescence in MR11-05 cruise.

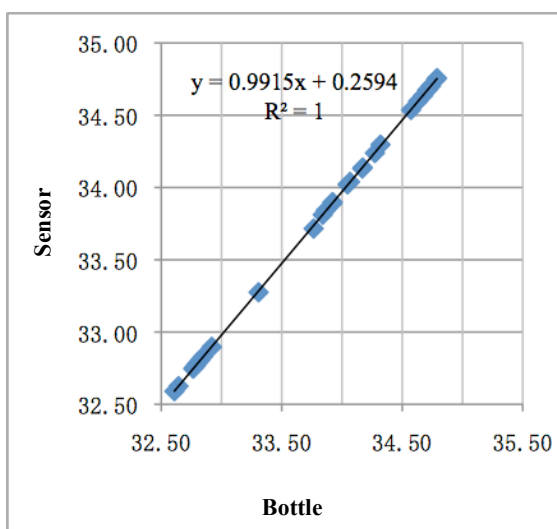


Fig. 2.3-2. Correlation of salinity between bottle data and sensor

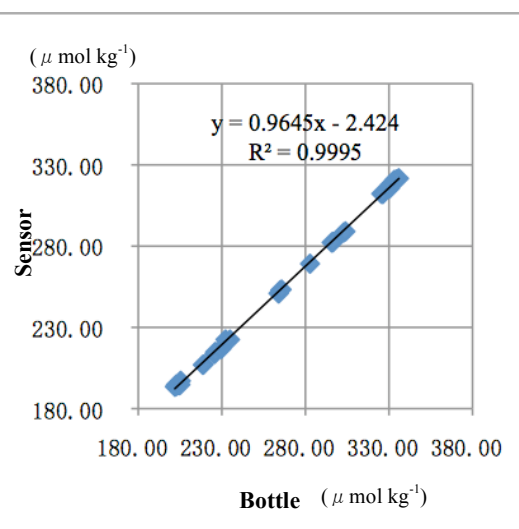


Fig. 2.3-3. Correlation of dissolved oxygen between bottle data and sensor

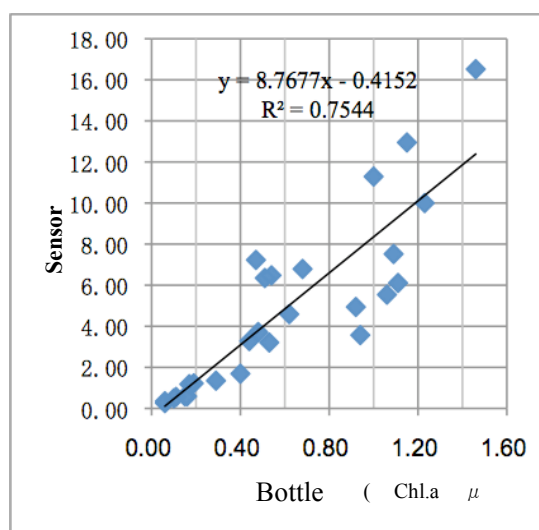


Fig. 2.3-4. Correlation of fluorescence between bottle data and sensor

## 2.4 Dissolved oxygen

**Masahide WAKITA (JAMSTEC): Principal Investigator**

**Misato KUWAHARA (Marine Works Japan Co. Ltd): Operation Leader**

**Hideki YAMAMOTO (Marine Works Japan Co. Ltd)**

### (1) Objectives

Determination of dissolved oxygen in seawater by Winkler titration.

### (2) Parameter

Dissolved Oxygen

### (3) Instruments and Methods

Following procedure is based on an analytical method, entitled by “Determination of dissolved oxygen in sea water by Winkler titration”, in the WHP Operations and Methods (Dickson, 1996).

#### a. Instruments

Burette for sodium thiosulfate and potassium iodate;

APB-510 and APB-620 of both manufactured by Kyoto Electronic Co. Ltd. / 10 cm<sup>3</sup> of titration vessel

Detector;

Automatic photometric titrator (DOT-01) manufactured by Kimoto Electronic Co. Ltd.

Software;

DOT controller Ver.2.2.1

#### b. Reagents

Pickling Reagent I: Manganese chloride solution (3 mol dm<sup>-3</sup>)

Pickling Reagent II: Sodium hydroxide (8 mol dm<sup>-3</sup>) / sodium iodide solution (4 mol dm<sup>-3</sup>)

Sulfuric acid solution (5 mol dm<sup>-3</sup>)

Sodium thiosulfate (0.025 mol dm<sup>-3</sup>)

Potassium iodide (0.001667 mol dm<sup>-3</sup>)

CSK standard of potassium iodide:

Lot EPJ3885, Wako Pure Chemical Industries Ltd., 0.0100N

#### c. Sampling

Seawater samples were collected with Niskin bottle attached to the CTD-system and surface bucket sampler. Seawater for oxygen measurement was transferred from sampler to a volume calibrated flask (ca. 100 cm<sup>3</sup>). Three times volume of the flask of seawater was overflowed. Temperature was measured by digital thermometer during the overflowing. Then two reagent solutions (Reagent I and II) of 0.5 cm<sup>3</sup> each were added immediately into the sample flask and the stopper was inserted carefully into the flask. The sample flask was then shaken vigorously to mix the contents and to disperse the precipitate finely throughout. After the precipitate has settled at least halfway down the flask, the flask was shaken again vigorously to disperse the precipitate. The sample flasks containing pickled samples were stored in a laboratory until they were titrated.

#### d. Sample measurement

At least two hours after the re-shaking, the pickled samples were measured on board. 1 cm<sup>3</sup> sulfuric acid solution and a magnetic stirrer bar were added into the sample flask and stirring began. Samples were titrated by sodium thiosulfate solution whose morality was determined by potassium iodate solution. Temperature of sodium thiosulfate during titration was recorded by a digital thermometer. During this cruise, we measured dissolved oxygen concentration using 2 sets of the titration apparatus. Dissolved oxygen concentration (μmol kg<sup>-1</sup>) was calculated by sample temperature during seawater sampling, salinity, flask volume, and titrated volume of sodium thiosulfate solution without the blank. When we measured low concentration samples, titration procedure was adjusted manually.

#### e. Standardization and determination of the blank

Concentration of sodium thiosulfate titrant was determined by potassium iodate solution. Pure potassium iodate was dried in an oven at 130 °C. 1.7835 g potassium iodate weighed out accurately was dissolved in deionized water and diluted to final volume of 5 dm<sup>3</sup> in a calibrated volumetric flask (0.001667 mol dm<sup>-3</sup>). 10 cm<sup>3</sup> of the standard potassium iodate solution was added to a flask using a volume-calibrated dispenser. Then 90 cm<sup>3</sup> of deionized water, 1 cm<sup>3</sup> of sulfuric acid solution, and 0.5 cm<sup>3</sup> of pickling reagent solution II and I were added into the flask in order. Amount of titrated volume of sodium thiosulfate (usually 5 times measurements average) gave the morality of sodium thiosulfate titrant.

The oxygen in the pickling reagents I (0.5 cm<sup>3</sup>) and II (0.5 cm<sup>3</sup>) was assumed to be 3.8 × 10<sup>-8</sup> mol (Murray *et al.*, 1968). The blank due to other than oxygen was determined as follows. 1 and 2 cm<sup>3</sup> of the standard potassium iodate solution were added to two flasks respectively using a calibrated dispenser. Then 100 cm<sup>3</sup> of deionized water, 1 cm<sup>3</sup> of sulfuric acid solution, and 0.5 cm<sup>3</sup> of pickling reagent solution II and I each were added into the flask in order. The blank was determined by difference between the first (1 cm<sup>3</sup> of KIO<sub>3</sub>) titrated volume of the sodium thiosulfate and the second (2 cm<sup>3</sup> of KIO<sub>3</sub>) one. The results of 3 times blank determinations were averaged.

Table 2.4-1 shows results of the standardization and the blank determination during this cruise.

Date	KIO <sub>3</sub> ID	Na <sub>2</sub> S <sub>2</sub> O <sub>3</sub>	DOT-01(No.1)		DOT-01(No.2)		Stations
			E.P.	Blank	E.P.	Blank	
2011/6/30	20110523-01-02	20110602-20	3.947	-0.004	3.949	0.000	K02 cast 02, 03
2011/6/30	CSK	20110602-20	3.945	-0.004	3.947	0.000	
2011/7/3	20110523-01-03	20110602-20	3.946	-0.004	3.950	-0.002	K02 cast 08
2011/7/7	20110523-01-04	20110602-20	3.946	-0.005	3.949	-0.002	K02 cast 11, KNT
2011/7/10	20110523-01-05	20110602-20	3.948	-0.004	3.948	-0.001	JKO, F01
2011/7/22	20110523-01-07	20110602-21	3.949	-0.005	3.953	0.000	S01 cast 01, 02
2011/7/26	20110523-01-08	20110602-21	3.950	-0.004	3.953	-0.001	S01 cast 07, 10, 11, 12, 13, 14
2011/7/31	20110523-01-09	20110602-21	3.948	-0.007	3.951	0.001	(operation finished)

#### f. Repeatability of sample measurement

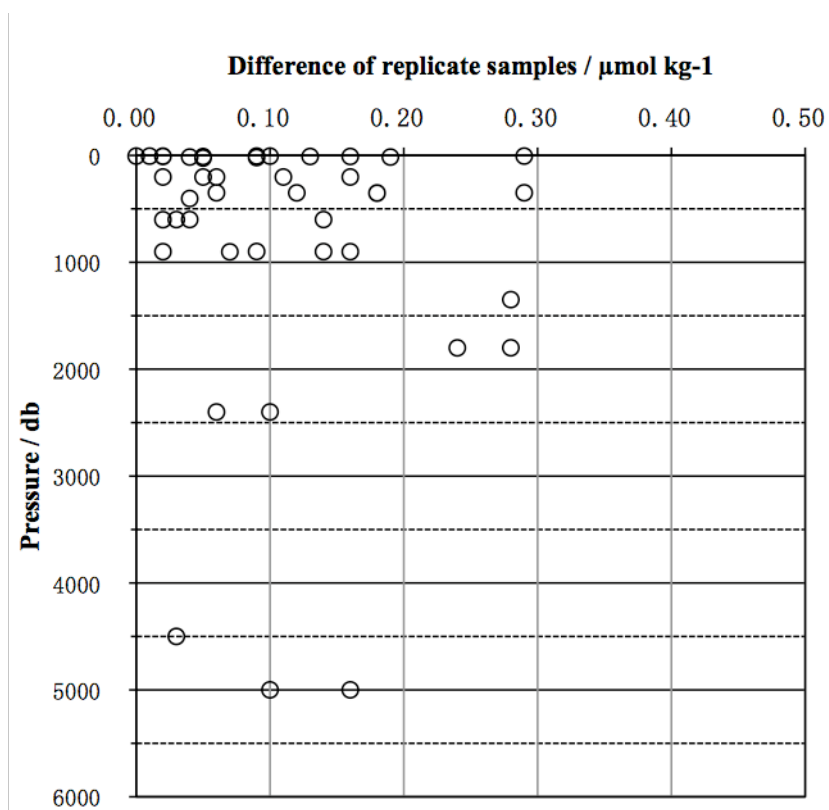


Replicate samples were taken at every CTD casts. Total amount of the replicate sample pairs of good measurement was 44. The standard deviation of the replicate measurement was  $0.09 \mu\text{mol kg}^{-1}$  that was calculated by a procedure in Guide to best practices for ocean  $\text{CO}_2$  measurements Chapter4 SOP23 Ver.3.0 (2007). Results of replicate samples were shown in Table 2.4-2 and this diagram shown in Fig. 2.4-1 and-2.

Table 2.4-2 Results of the replicate samples

Layer	Number of replicate sample pairs	Oxygen concentration ( $\mu\text{mol kg}^{-1}$ ) Standard Deviation.
1000m>=	35	0.08
>1000m	9	0.12
All	44	0.09

Fig. 2.4-1 Difference of replicate samples against pressure



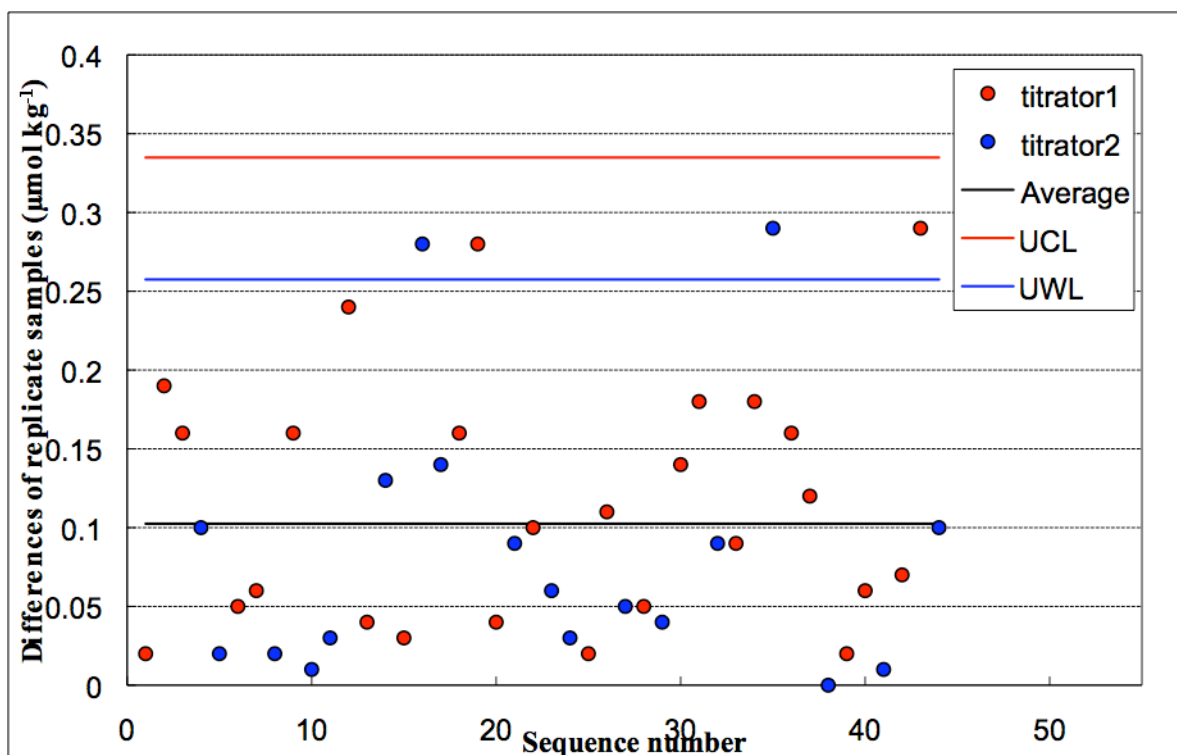


Fig. 2.4-2 Difference of replicate samples against sequence number

(4) Data archive

All data will be submitted to Chief Scientist.

(5) References

- Dickson, A.G., Determination of dissolved oxygen in sea water by Winkler titration. (1996)
- Dickson, A.G., Sabine, C.L. and Christian, J.R. (Eds.), Guide to best practices for ocean CO<sub>2</sub> measurements. (2007)
- Culberson, C.H., WHP Operations and Methods July-1991 "Dissolved Oxygen", (1991)
- Japan Meteorological Agency, Oceanographic research guidelines (Part 1). (1999)
- KIMOTO electric CO. LTD., Automatic photometric titrator DOT-01 Instruction manual

## 2.5 Nutrients

**Michio AOYAMA (Meteorological Research Institute) Principal investigator**

**Masahide WAKITA (JAMSTEC MIO)**

**Masanori ENOKI (Department of Marine Science, Marine Works Japan Ltd.)**

**Yasuhiro ARII (Department of Marine Science, Marine Works Japan Ltd.)**

### (1) Objectives

The objectives of nutrients analyses during the R/V Mirai MR11-05 cruise in the Western North Pacific Ocean are as follows:

- Describe the present status of nutrients concentration with excellent comparability.
- Provide excellent nutrients data to biologist onboard MR11-05 to help their study.

### (2) Parameters

The determinants are nitrate, nitrite, phosphate, silicate and ammonia in the western North Pacific Ocean.

### (3) Summary of nutrients analysis

We made 13 runs for the samples at 5 stations (17 casts) in MR11-05. The total amount of layers of the seawater sample reached up to 383 for MR11-05. We made duplicate measurement at all layers (stn. S01 cast 11, 12, 13, and 14 were single measurement). The station locations for nutrients measurement is shown in Figure 2.5.1

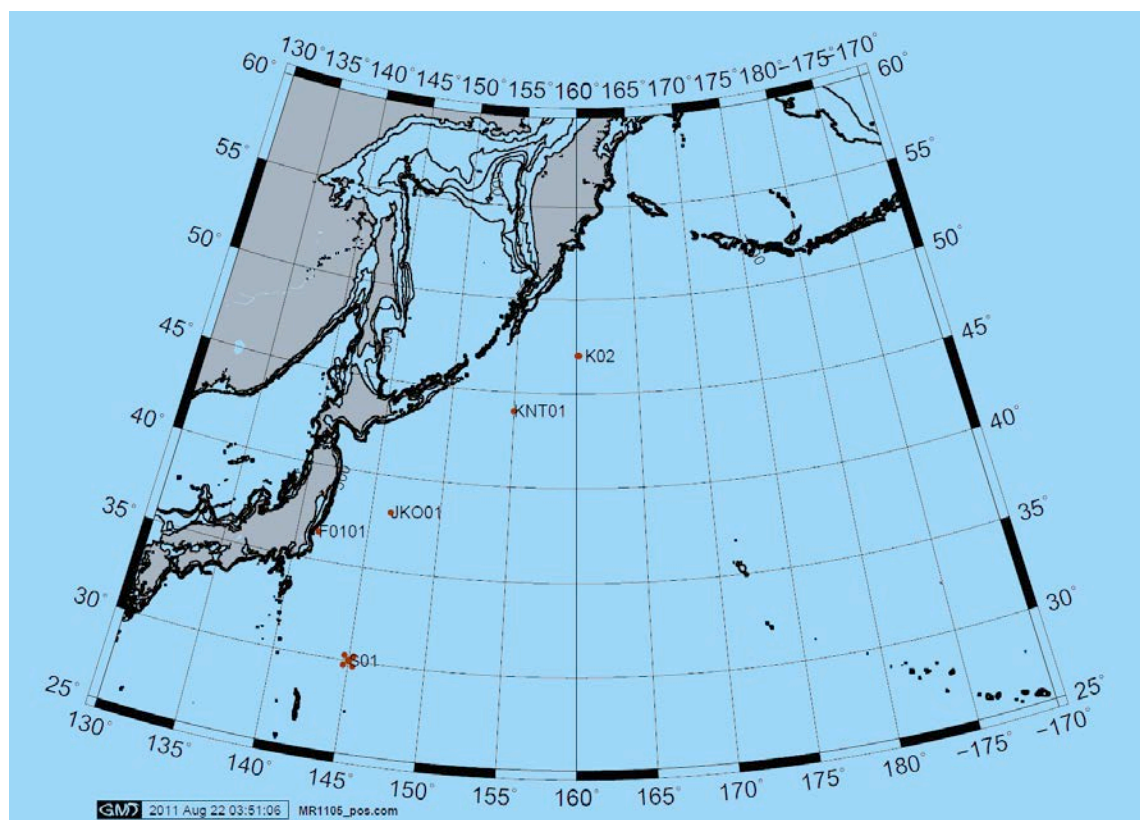


Figure 2.5.1 Sampling positions of nutrients sample.

#### (4) Instrument and methods

##### a). Analytical detail using QuAAtro system

The phosphate analysis was a modification of the procedure of Murphy and Riley (1962). Molybdic acid was added to the seawater sample to form phosphomolybdic acid which was in turn reduced to phosphomolybdous acid using L-ascorbic acid as the reductant.

Nitrate + nitrite and nitrite were analyzed according to the modification method of Grasshoff (1970). The sample nitrate was reduced to nitrite in a cadmium tube inside of which was coated with metallic copper. The sample stream with its equivalent nitrite was treated with an acidic, sulfanilamide reagent and the nitrite forms nitrous acid which reacted with the sulfanilamide to produce a diazonium ion. N-1-Naphthylethylene-diamine added to the sample stream then coupled with the diazonium ion to produce a red, azo dye. With reduction of the nitrate to nitrite, both nitrate and nitrite reacted and were measured; without reduction, only nitrite reacted. Thus, for the nitrite analysis, no reduction was performed and the alkaline buffer was not necessary. Nitrate was computed by difference.

The silicate method was analogous to that described for phosphate. The method used was essentially that of Grasshoff et al. (1983), wherein silicomolybdic acid was first formed from the silicate in the sample and added molybdic acid; then the silicomolybdic acid was reduced to silicomolybdous acid, or "molybdenum blue" using ascorbic acid as the reductant. The analytical methods of the nutrients, nitrate, nitrite, silicate and phosphate, during this cruise were same as the methods used in (Kawano et al. 2009).

The details of modification of analytical methods used in this cruise are also compatible with the methods described in nutrients section in GO-SHIP repeat hydrography manual (Hydes et al., 2010)

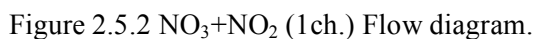
The ammonia in seawater was mixed with an alkaline containing EDTA, ammonia as gas state was formed from seawater. The ammonia (gas) was absorbed in sulfuric acid by way of 0.5 µm pore size membrane filter (ADVANTEC PTFE) at the dialyzer attached to analytical system. The ammonia absorbed in sulfuric acid was determined by coupling with phenol and hypochlorite to form indophenols blue. Wavelength using ammonia analysis was 630 nm, which was absorbance of indophenols blue.

The flow diagrams and reagents for each parameter are shown in Figures 2.5.2 to 2.5.6.

Imidazole (buffer), 0.06 M (0.4 % w/v)  
Dissolved 4 g imidazole,  $\text{C}_3\text{H}_4\text{N}_2$ , in ca. 1000 ml DIW; added 2 ml concentrated HCl. After mixing, 1 ml Triton®X-100 (50 % solution in ethanol) was added.

Dissolved 10 g sulfanilamide, 4-NH<sub>2</sub>C<sub>6</sub>H<sub>4</sub>SO<sub>3</sub>H, in 900 ml of DIW, added 100 ml concentrated HCl. After mixing, 2 ml Triton®X-100 (50 % solution in ethanol) was added.

Dissolved 1 g NED,  $C_{10}H_7NHCH_2CH_2NH_2 \cdot 2HCl$ , in 1000 ml of DIW and added 10 ml concentrated HCl. After mixing, 1 ml Triton®X-100 (50 % solution in ethanol) was added. This reagent was stored in a dark bottle.



c). Nitrite Reagents

Sulfanilamide, 0.06 M (1 % w/v) in 1.2 M HCl

Dissolved 10g sulfanilamide, 4-NH<sub>2</sub>C<sub>6</sub>H<sub>4</sub>SO<sub>3</sub>H, in 900 ml of DIW, added 100 ml concentrated HCl. After mixing, 2 ml Triton®X-100 (50 % solution in ethanol) was added.

N-1-Naphthylethylene-diamine dihydrochloride, 0.004 M (0.1 % w/v)

Dissolved 1 g NED, C<sub>10</sub>H<sub>7</sub>NHCH<sub>2</sub>CH<sub>2</sub>NH<sub>2</sub>•2HCl, in 1000 ml of DIW and added 10 ml concentrated HCl. After mixing, 1 ml Triton®X-100 (50 % solution in ethanol) was added. This reagent was stored in a dark bottle.

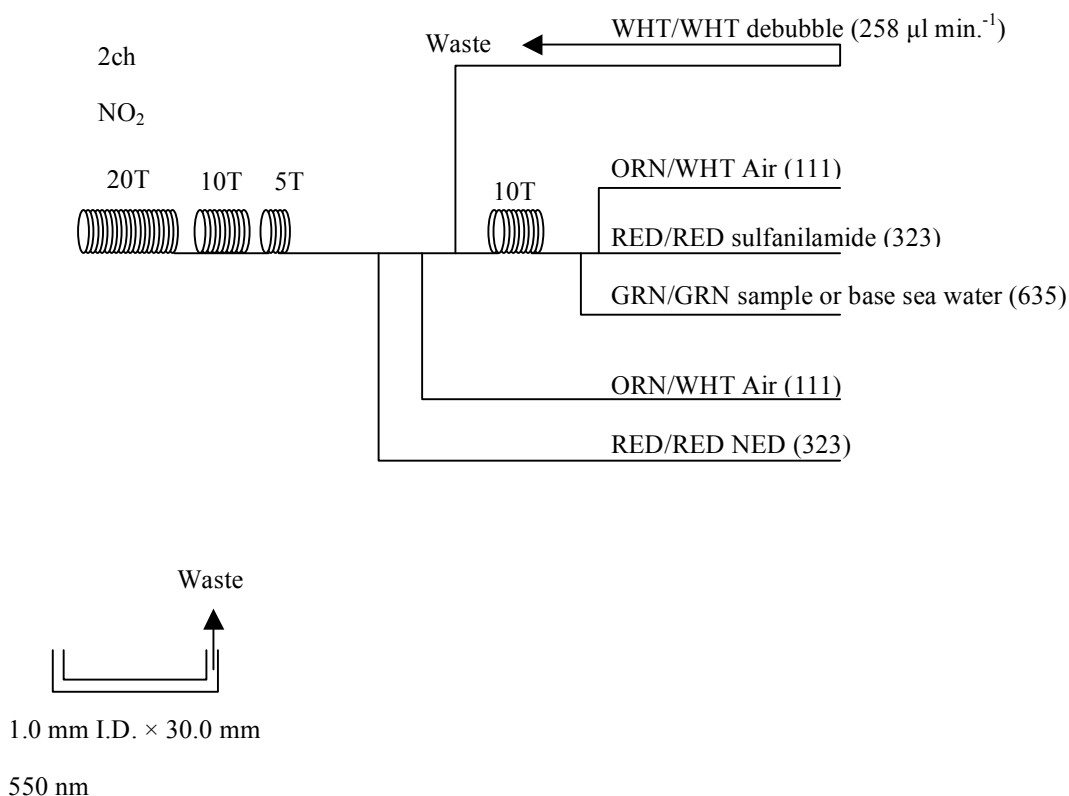


Figure 2.5.3 NO<sub>2</sub> (2ch.) Flow diagram.

d). Silicate Reagents

Molybdic acid, 0.06 M (2 % w/v)

Dissolved 15 g disodium molybdate (VI) dihydrate,  $\text{Na}_2\text{MoO}_4 \cdot 2\text{H}_2\text{O}$ , in 980 ml DIW, added 8 ml concentrated  $\text{H}_2\text{SO}_4$ . After mixing, 20 ml sodium dodecyl sulphate (15 % solution in water) was added.

Oxalic acid, 0.6 M (5 % w/v)

Dissolved 50 g oxalic acid anhydrous,  $\text{HOOC:COOH}$ , in 950 ml of DIW.

Ascorbic acid, 0.01M (3 % w/v)

Dissolved 2.5 g L (+)-ascorbic acid,  $\text{C}_6\text{H}_8\text{O}_6$ , in 100 ml of DIW. This reagent was freshly prepared before every measurement.

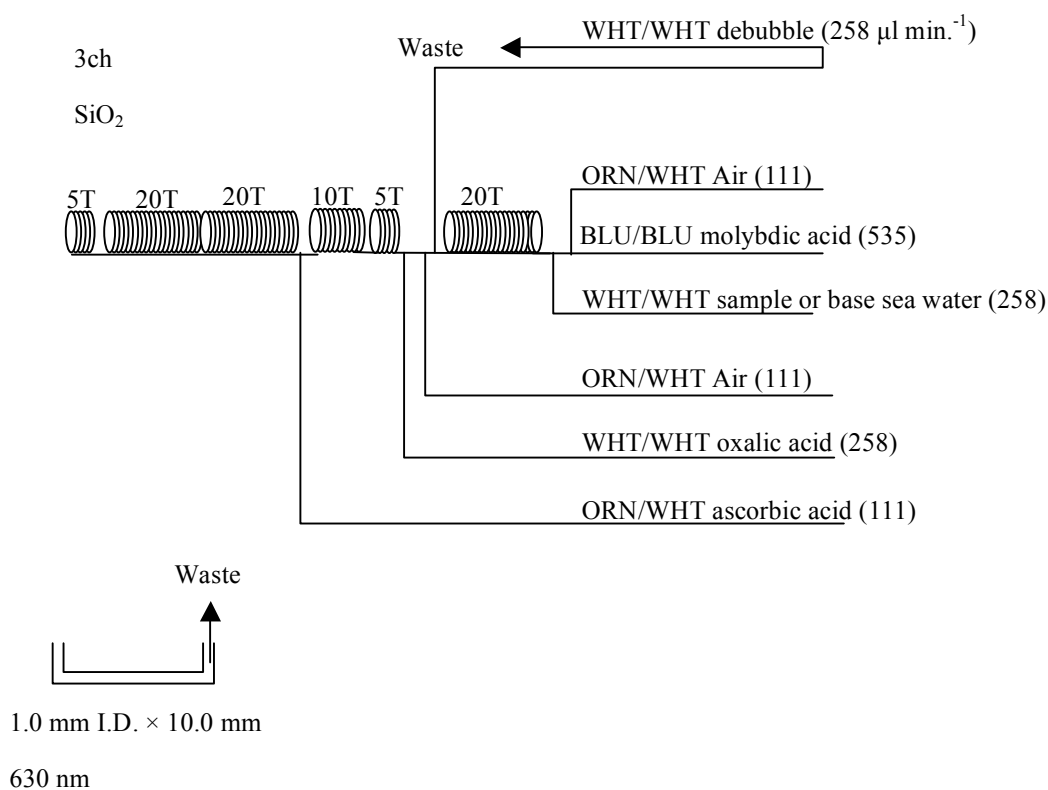


Figure 2.5.4  $\text{SiO}_2$  (3ch.) Flow diagram.

e). Phosphate Reagents

Stock molybdate solution, 0.03M (0.8 % w/v)

Dissolved 8 g disodium molybdate (VI) dihydrate,  $\text{Na}_2\text{MoO}_4 \cdot 2\text{H}_2\text{O}$ , and 0.17 g antimony potassium tartrate,  $\text{C}_8\text{H}_4\text{K}_2\text{O}_{12}\text{Sb}_2 \cdot 3\text{H}_2\text{O}$ , in 950 ml of DIW and added 50 ml concentrated  $\text{H}_2\text{SO}_4$ .

Mixed Reagent

Dissolved 1.2 g L (+)-ascorbic acid,  $\text{C}_6\text{H}_8\text{O}_6$ , in 150 ml of stock molybdate solution. After mixing, 3 ml sodium dodecyl sulphate (15 % solution in water) was added. This reagent was freshly prepared before every measurement.

Reagent for sample dilution

Dissolved sodium chloride,  $\text{NaCl}$ , 10 g in ca. 950 ml of DIW, added 50 ml acetone and 4 ml concentrated  $\text{H}_2\text{SO}_4$ . After mixing, 5 ml sodium dodecyl sulphate (15 % solution in water) was added.

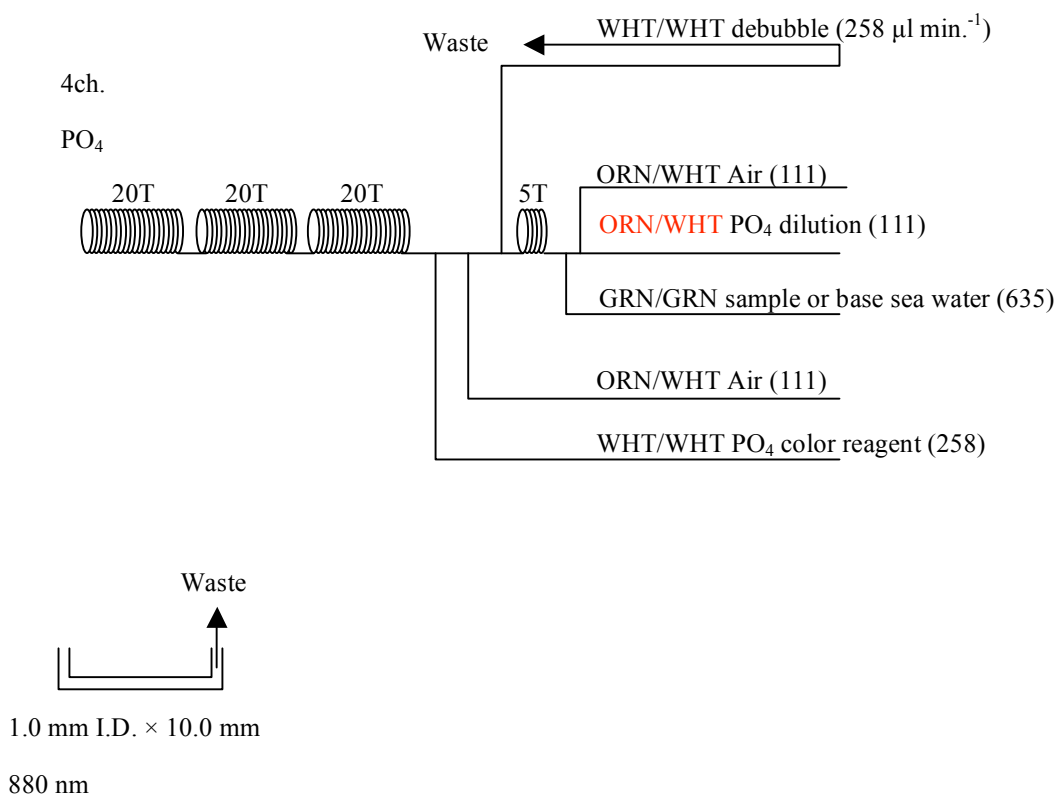


Figure 2.5.5  $\text{PO}_4$  (4ch.) Flow diagram.



f). Ammonia Reagents

EDTA

Dissolved 41 g EDTA (ethylenediaminetetraacetic acid tetrasodium salt),  $C_{10}H_{12}N_2O_8Na_4 \cdot 4H_2O$ , and 2 g boric acid,  $H_3BO_3$ , in 200 ml of DIW. After mixing, 1 ml Triton®X-100 (30 % solution in DIW) was added. This reagent was prepared at a week about.

NaOH

Dissolved 5 g sodium hydroxide, NaOH, and 16 g EDTA in 100 ml of DIW. This reagent was prepared at a week about.

Stock Nitroprusside

Dissolved 0.25 g sodium pentacyanonitrosylferrate (II),  $Na_2[Fe(CN)_5NO]$ , in 100 ml of DIW and added 0.2 ml 1N  $H_2SO_4$ . Stored in a dark bottle and prepared at a month about.

Nitroprusside solution

Mixed 4 ml stock nitroprusside and 5 ml 1N  $H_2SO_4$  in 500 ml of DIW. After mixing, 1 ml Triton®X-100 (30 % solution in DIW) was added. This reagent was stored in a dark bottle and prepared at every 2 or 3 days.

Alkaline phenol

Dissolved 10 g phenol,  $C_6H_5OH$ , 5 g sodium hydroxide and citric acid,  $C_6H_8O_7$ , in 200 ml DIW. Stored in a dark bottle and prepared at a week about.

NaClO solution

Mixed 3 ml sodium hypochlorite solution, NaClO, in 47 ml DIW. Stored in a dark bottle and freshly prepared before every measurement. This reagent was prepared 0.3% available chlorine.

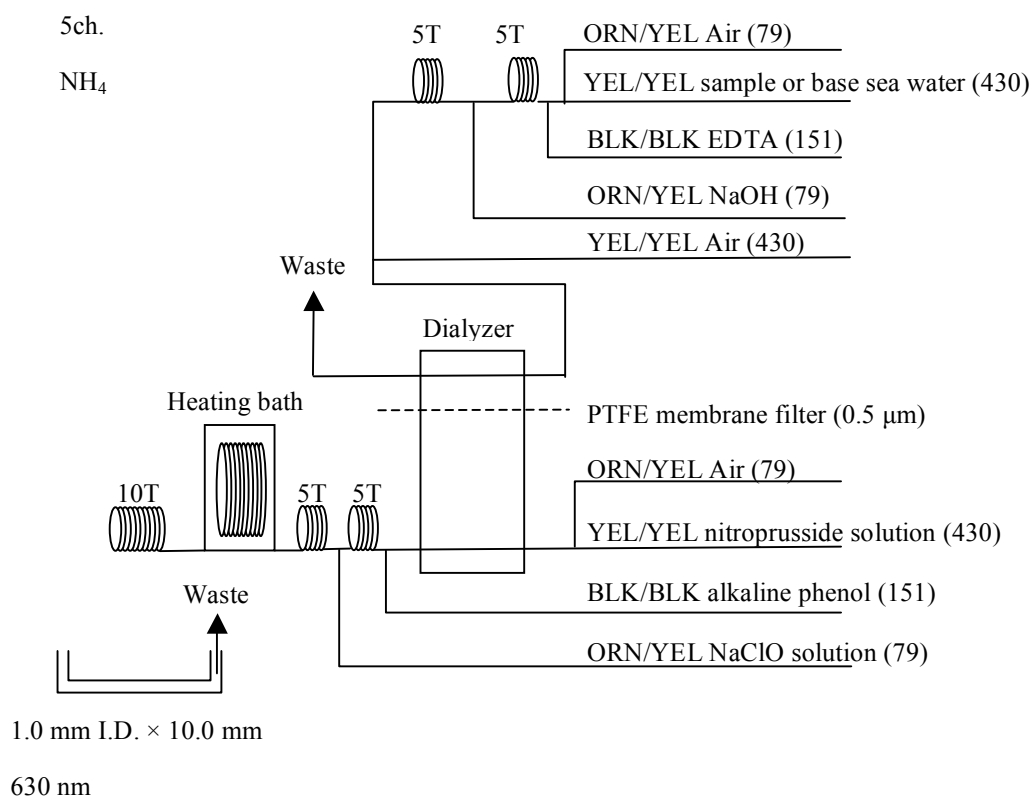


Figure 2.5.6 NH<sub>4</sub> (5ch.) Flow diagram.

g). Sampling procedures

Sampling of nutrients followed that oxygen, salinity and trace gases. Samples were drawn into two of virgin 10 ml polyacrylates vials without sample drawing tubes. These were rinsed three times before filling and vials were capped immediately after the drawing. The vials were put into water bath adjusted to ambient temperature,  $24 \pm 2$  deg. C, in about 30 minutes before use to stabilize the temperature of samples in MR11-05.

No transfer was made and the vials were set an auto sampler tray directly. Samples were analyzed after collection basically within 24 hours in MR11-05.

h). Data processing

Raw data from QuAAtro was treated as follows:

- Checked baseline shift.
- Checked the shape of each peak and positions of peak values taken, and then changed the positions of peak values taken if necessary.
- Carry-over correction and baseline drift correction were applied to peak heights of each samples followed by sensitivity correction.
- Baseline correction and sensitivity correction were done basically using liner regression.
- Loaded pressure and salinity from CTD data to calculate density of seawater.
- Calibration curves to get nutrients concentration were assumed second order equations.

## (5) Nutrients standards

### a). Volumetric laboratory ware of in-house standards

All volumetric glass ware and polymethylpentene (PMP) ware used were gravimetrically calibrated. Plastic volumetric flasks were gravimetrically calibrated at the temperature of use within 0 to 4 K.

#### Volumetric flasks

Volumetric flasks of Class quality (Class A) were used because their nominal tolerances are 0.05 % or less over the size ranges likely to be used in this work. Class A flasks were made of borosilicate glass, and the standard solutions were transferred to plastic bottles as quickly as possible after they were made up to volume and well mixed in order to prevent excessive dissolution of silicate from the glass. PMP volumetric flasks were gravimetrically calibrated and used only within 0 to 4 K of the calibration temperature.

The computation of volume contained by glass flasks at various temperatures other than the calibration temperatures were done by using the coefficient of linear expansion of borosilicate crown glass.

Because of their larger temperature coefficients of cubical expansion and lack of tables constructed for these materials, the plastic volumetric flasks were gravimetrically calibrated over the temperature range of intended use and used at the temperature of calibration within 0 to 4 K. The weights obtained in the calibration weightings were corrected for the density of water and air buoyancy.

#### Pipettes and pipettors

All pipettes had nominal calibration tolerances of 0.1 % or better. These were gravimetrically calibrated in order to verify and improve upon this nominal tolerance.

### b). Reagents, general considerations

#### Specifications

For nitrate standard, “potassium nitrate 99.995 suprapur®” provided by Merck, CAS No.: 7757-91-1, was used.

For phosphate standard, “potassium dihydrogen phosphate anhydrous 99.995 suprapur®” provided by Merck, CAS No.: 7778-77-0, was used.

For nitrite standard, “sodium nitrite” provided by Wako, CAS No.: 7632-00-0, was used. The assay of nitrite salts was determined according to JIS K8019 were 98.31% (used at stations K0202, K0203, K0208 and K0209) and 97.75% (used at the others stations). We used that value to adjust the weights taken.

For the silicate standard, we use “Silicon standard solution SiO<sub>2</sub> in NaOH 0.5 mol/l CertiPUR®” provided by Merck, CAS No.: 1310-73-2, of which lot number HC074650 was used. The silicate concentration was certified by NIST-SRM3150 with the uncertainty of 0.5 %. Factor of HC074650 was signed 1.000, however we reassigned the factor as 0.975 from the result of comparison among HC814662, HC074650 and RMNS in MR10-05 cruise.

For ammonia standard, “ammonia sulfate” provided by Wako, CAS No.: 7783-20-2, was used.

#### Ultra pure water

Ultra pure water (Milli-Q) freshly drawn was used for preparation of reagent, standard solutions and for measurement of reagent and system blanks.

#### Low-nutrients seawater (LNSW)

Surface water having low nutrient concentration was taken and filtered using 0.45  $\mu\text{m}$  pore size membrane filter. This water was stored in 20 liter cubitainer with paper box. The concentrations of nutrient of this water were measured carefully in Jul 2008.

#### Treatment of silicate standard due to high alkalinity

Since the silicon standard solution Merck CertiPUR® is in NaOH 0.5 mol/l, we need to dilute and neutralize to avoid make precipitation of  $\text{MgOH}_2$  etc. When we make B standard, silicon standard solution is diluted by factor 12 with pure water and neutralized by HCl 1.0 mol/l to be about 7. After that B standard solution is used to prepare C standards.

#### c). Concentrations of nutrients for A, B and C standards

Concentrations of nutrients for A, B and C standards (working standards) were set as shown in Table 2.5.1. The working standard was prepared according recipes as shown in Table 2.5.2. All volumetric laboratory tools were calibrated prior the cruise as stated in chapter (5). Then the actual concentration of nutrients in each fresh standard was calculated based on the ambient, solution temperature and determined factors of volumetric laboratory wares.

The calibration curves for each run were obtained using 5 levels working standards, C-1, C-2, C-3, C-4 and C-5.

Table 2.5.1 Nominal concentrations of nutrients for A, B and C standards.

	A	B	C-1	C-2	C-3	C-4	C-5
$\text{NO}_3$ ( $\mu\text{M}$ )	22000	900	0.03	9.2	18.3	36.6	55.0
$\text{NO}_2$ ( $\mu\text{M}$ )	4000	20	0.00	0.2	0.4	0.8	1.2
$\text{SiO}_2$ ( $\mu\text{M}$ )	36000	2800	0.80	28	56	111	167
$\text{PO}_4$ ( $\mu\text{M}$ )	3000	60	0.04	0.6	1.2	2.4	3.6
$\text{NH}_4$ ( $\mu\text{M}$ )	4000	200	0.00	0.0	2.0	4.0	6.0

Table 2.5.2 Working standard recipes.

C Std.	B-1 Std.	B-2 Std.	B-3 Std.	DIW
C-1	0 ml	0 ml	0 ml	75 ml
C-2	5 ml	5 ml	0 ml	65 ml
C-3	10 ml	10 ml	5 ml	40 ml
C-4	20 ml	20 ml	10 ml	25 ml
C-5	30 ml	30 ml	15 ml	0 ml

B-1 Std.: Mixture of nitrate, silicate and phosphate.

B-2 Std.: Nitrite.

B-3 Std.: Ammonia.

## d). Renewal of in-house standard solutions

In-house standard solutions as stated in paragraph c) were renewed as shown in Table 2.5.3(a) to (c).

Table 2.5.3(a) Timing of renewal of in-house standards.

NO <sub>3</sub> , NO <sub>2</sub> , SiO <sub>2</sub> , PO <sub>4</sub> , NH <sub>4</sub>	Renewal
A-1 Std. (NO <sub>3</sub> )	maximum 1 month
A-2 Std. (NO <sub>2</sub> )	maximum 1 month
A-3 Std. (SiO <sub>2</sub> )	commercial prepared solution
A-4 Std. (PO <sub>4</sub> )	maximum 1 month
A-5 Std. (NH <sub>4</sub> )	maximum 1 month
B-1 Std. (mixture of NO <sub>3</sub> , SiO <sub>2</sub> , PO <sub>4</sub> )	8 days
B-2 Std. (NO <sub>2</sub> )	8 days
B-3 Std. (NH <sub>4</sub> )	8 days

Table 2.5.3(b) Timing of renewal of working calibration standards.

Working standards	Renewal
C Std. (mixture of B-1, B-2 and B-3 Std.)	24 hours

Table 2.5.3(c) Timing of renewal of in-house standards for reduction estimation.

Reduction estimation	Renewal
D-1 Std. (3600 µM NO <sub>3</sub> )	8 days
43 µM NO <sub>3</sub>	when C Std. renewed
47 µM NO <sub>2</sub>	when C Std. renewed

## (6) Reference material of nutrients in seawater

To get the more accurate and high quality nutrients data to achieve the objectives stated above, huge numbers of the bottles of the reference material of nutrients in seawater (hereafter RMNS) are prepared (Aoyama et al., 2006, 2007, 2008, 2009). In the previous worldwide expeditions, such as CLIVAR cruises, the higher reproducibility and precision of nutrients measurements were required (Joyce and Corry, 1994). Since no standards were

available for the measurement of nutrients in seawater at that time, the requirements were described in term of reproducibility. The required reproducibility was 1 %, 1 to 2 %, 1 to 3 % for nitrate, phosphate and silicate, respectively. Although nutrient data from the WOCE one-time survey was of unprecedented quality and coverage due to much care in sampling and measurements, the differences of nutrients concentration at crossover points are still found among the expeditions (Aoyama and Joyce, 1996, Mordy et al., 2000, Gouretski and Jancke, 2001). For instance, the mean offset of nitrate concentration at deep waters was  $0.5 \mu\text{mol kg}^{-1}$  for 345 crossovers at world oceans, though the maximum was  $1.7 \mu\text{mol kg}^{-1}$  (Gouretski and Jancke, 2001). At the 31 crossover points in the Pacific WHP one-time lines, the WOCE standard of reproducibility for nitrate of 1 % was fulfilled at about half of the crossover points and the maximum difference was 7 % at deeper layers below 1.6 deg. C in potential temperature (Aoyama and Joyce, 1996).

During the period from 2003 to 2010, RMNS were used to keep comparability of nutrients measurement among the 8 cruises of CLIVAR project (Sato et al., 2010), MR10-05 cruise for Arctic research (Aoyama et al., 2010) and MR10-06 cruise for “Change in material cycles and ecosystem by the climate change and its feedback” (Aoyama et al., 2011).

a). RMNS for this cruise

RMNS lots BA, AS, AY, BT, BD, BE, AZ and BF, which cover full range of nutrients concentrations in the North Pacific Ocean are prepared. These RMNS assignment were completely done based on random number. The RMNS bottles were stored at a room in the ship, REAGENT STORE, where the temperature was maintained 19 - 27 deg. C.

b). Assigned concentration for RMNSs

We assigned nutrients concentrations for RMNS lots BA, AS, AY, BT, BD, BE, AZ and BF as shown in Table 2.5.4.

Table 2.5.4 Assigned concentration of RMNSs.

	unit: $\mu\text{mol kg}^{-1}$				
	Nitrate	Phosphate	Silicate	Nitrite	Ammonia
BA	0.07	0.068	1.60	0.02	0.97
AS	0.11	0.077	1.58	0.02	-
AY	5.60	0.516	29.42	0.62	0.81
BT	17.99	1.310	40.85	0.44	-
BD	29.83	2.182	64.41	0.04	2.93
BE	36.70	2.662	99.20	0.03	-
AZ	42.36	3.017	133.93	0.03	-
BF	41.39	2.809	150.23	0.02	-

(7) Quality control

a). Precision of nutrients analyses during the cruise

Precision of nutrients analyses during the cruise was evaluated based on the 5 to 7 measurements, which are measured every 9 to 13 samples, during a run at the concentration of C-5 std. Summary of precisions are shown as shown in Table 2.5.5. Analytical precisions previously evaluated were 0.08 % for nitrate, 0.10 % for phosphate and 0.07 % for silicate in

CLIVAR P21 revisited cruise of MR09-01 cruise in 2009, respectively. During this cruise, analytical precisions were 0.09 % for nitrate, 0.18 % for phosphate, 0.11 % for silicate, 0.20 % for nitrite and 0.18 % for ammonia in terms of median of precision, respectively. Then we can conclude that the analytical precisions for nitrate, phosphate and silicate were maintained throughout this cruise.

Table 2.5.5 Summary of precision based on the replicate analyses.

	Nitrate CV %	Nitrite CV %	Phosphate CV %	Silicate CV %	Ammonia CV%
Median	0.09	0.19	0.17	0.10	0.18
Mean	0.09	0.21	0.18	0.10	0.26
Maximum	0.18	0.39	0.28	0.17	0.59
Minimum	0.04	0.14	0.11	0.03	0.06
N	17	17	17	17	7

b). Carry over

We can also summarize the magnitudes of carry over throughout the cruise. These are small enough within acceptable levels as shown in Table 2.5.6.

Table 2.5.6 Summary of carry over throughout MR11-05.

	Nitrate %	Nitrite %	Phosphate %	Silicate %	Ammonia %
Median	0.34	0.16	0.33	0.28	0.71
Mean	0.36	0.21	0.35	0.26	0.79
Maximum	0.51	0.58	0.89	0.33	1.56
Minimum	0.12	0.00	0.10	0.12	0.31
N	17	17	17	17	7

c). Estimation of uncertainty of phosphate, nitrate and silicate concentrations

Empirical equations, eq. (1), (2) and (3) to estimate uncertainty of measurement of phosphate, nitrate and silicate are used based on measurements of 140 sets of RMNSs during the cruise MR09-01 in 2009. These empirical equations are as follows, respectively.

Phosphate Concentration  $C_p$  in  $\mu\text{mol kg}^{-1}$ :

$$\text{Uncertainty of measurement of phosphate (\%)} = 0.000 + 0.378 * (1/C_p) + 0.00430 * (1/C_p) * (1/C_p) \quad \text{--- (1)}$$

where  $C_p$  is phosphate concentration of sample.

Nitrate Concentration  $C_n$  in  $\mu\text{mol kg}^{-1}$ :

$$\text{Uncertainty of measurement of nitrate (\%)} = 0.142 + 0.431 * (1/C_n) + 0.114 * (1/C_n) * (1/C_n) \quad \text{--- (2)}$$

where  $C_n$  is nitrate concentration of sample.

Silicate Concentration  $C_s$  in  $\mu\text{mol kg}^{-1}$ :

$$\text{Uncertainty of measurement of silicate (\%)} = 0.047 + 4.99 * (1/C_s) + 1.879 * (1/C_s) * (1/C_s) \quad \text{--- (3)}$$

where  $C_s$  is silicate concentration of sample.

d). Empirical equation for uncertainty of ammonia

Since we do not have RM for ammonia, empirical equation of uncertainty of ammonia is created based on differences of duplicate measurements of samples taken from same niskin bottles during the cruise MR10-05. We use 102 pair of duplicate measurements and concentration of ammonia ranged from 0.02 to 1.1  $\mu\text{mol kg}^{-1}$  among all 122 pair.

Based on differences between two measurements, we estimated an empirical equation between uncertainty of measurement of ammonia and ammonia concentration where we adapted  $k = 1$  as follows;

Ammonia Concentration Ca in  $\mu\text{mol kg}^{-1}$ :

$$\text{Uncertainty of measurement of ammonia (\%)} = 1.233 + 1.15 * (1/\text{Ca}) - 0.00338 * (1/\text{Ca}) * (1/\text{Ca}) \quad \text{--- (4)}$$

where Ca is ammonia concentration of sample.

For 28 pair, we see larger uncertainty than that estimated using empirical equation above.

(8) Problems/improvements occurred and solutions.

The smoothing is smoothed by averaging successive data points of chart peaks on AACE which is QuAAtro operating software. By the setting value of smoothing changed from 4 to 16, the base linenoise due to rolling and pitching of the ship was canceled.

(9) Station list

Table 2.5.7 List of stations

Cruise	Station	Cast	Year	Month	Date	Latitude	Longitude
MR11-05	K02	02	2011	6	30	46.998 N	160.204 E
MR11-05	K02	03	2011	6	30	46.995 N	160.105 E
MR11-05	K02	08	2011	7	4	47.000 N	160.083 E
MR11-05	K02	09	2011	7	4	46.999 N	160.093 E
MR11-05	K02	11	2011	7	7	47.005 N	160.079 E
MR11-05	KNT	01	2011	7	9	43.996 N	155.003 E
MR11-05	JKO	01	2011	7	11	38.068 N	146.426 E
MR11-05	F01	01	2011	7	12	36.483 N	141.503 E
MR11-05	S01	01	2011	7	24	29.999 N	145.004 E
MR11-05	S01	02	2011	7	24	30.004 N	144.999 E
MR11-05	S01	07	2011	7	27	30.003 N	144.996 E
MR11-05	S01	08	2011	7	27	30.010 N	144.996 E
MR11-05	S01	10	2011	7	30	29.996 N	145.001 E
MR11-05	S01	11	2011	7	30	30.265 N	145.298 E
MR11-05	S01	12	2011	7	30	29.736 N	145.298 E
MR11-05	S01	13	2011	7	30	29.734 N	144.699 E
MR11-05	S01	14	2011	7	31	30.266 N	144.700 E

(10) Data archive

All data will be submitted to JAMSTEC Data Management Office (DMO) and is currently under its control.



## References

- Aminot, A. and Kerouel, R. 1991. Autoclaved seawater as a reference material for the determination of nitrate and phosphate in seawater. *Anal. Chim. Acta*, 248: 277-283.
- Aminot, A. and Kirkwood, D.S. 1995. Report on the results of the fifth ICES intercomparison exercise for nutrients in sea water, ICES coop. Res. Rep. Ser., 213.
- Aminot, A. and Kerouel, R. 1995. Reference material for nutrients in seawater: stability of nitrate, nitrite, ammonia and phosphate in autoclaved samples. *Mar. Chem.*, 49: 221-232.
- Aoyama M., and Joyce T.M. 1996, WHP property comparisons from crossing lines in North Pacific. In Abstracts, 1996 WOCE Pacific Workshop, Newport Beach, California.
- Aoyama, M., 2006: 2003 Intercomparison Exercise for Reference Material for Nutrients in Seawater in a Seawater Matrix, Technical Reports of the Meteorological Research Institute No.50, 91pp, Tsukuba, Japan.
- Aoyama, M., Susan B., Minhan, D., Hideshi, D., Louis, I. G., Kasai, H., Roger, K., Nurit, K., Doug, M., Murata, A., Nagai, N., Ogawa, H., Ota, H., Saito, H., Saito, K., Shimizu, T., Takano, H., Tsuda, A., Yokouchi, K., and Agnes, Y. 2007. Recent Comparability of Oceanographic Nutrients Data: Results of a 2003 Intercomparison Exercise Using Reference Materials. *Analytical Sciences*, 23: 1151-1154.
- Aoyama M., J. Barwell-Clarke, S. Becker, M. Blum, Braga E. S., S. C. Coverly, E. Czobik, I. Dahllöf, M. H. Dai, G. O. Donnell, C. Engelke, G. C. Gong, Gi-Hoon Hong, D. J. Hydes, M. M. Jin, H. Kasai, R. Kerouel, Y. Kiyomono, M. Knockaert, N. Kress, K. A. Kroglund, M. Kumagai, S. Leterme, Yarong Li, S. Masuda, T. Miyao, T. Moutin, A. Murata, N. Nagai, G. Nausch, M. K. Ngirchchol, A. Nybakk, H. Ogawa, J. van Ooijen, H. Ota, J. M. Pan, C. Payne, O. Pierre-Duplessix, M. Pujo-Pay, T. Raabe, K. Saito, K. Sato, C. Schmidt, M. Schuett, T. M. Shammon, J. Sun, T. Tanhua, L. White, E.M.S. Woodward, P. Worsfold, P. Yeats, T. Yoshimura, A. Youenou, J. Z. Zhang, 2008: 2006 Intercomparison Exercise for Reference Material for Nutrients in Seawater in a Seawater Matrix, Technical Reports of the Meteorological Research Institute No. 58, 104pp.
- Aoyama, M., Nishino, S., Nishijima, K., Matsushita, J., Takano, A., Sato, K., 2010a. Nutrients, In: R/V Mirai Cruise Report MR10-05. JAMSTEC, Yokosuka, pp. 103-122.
- Aoyama, M., Matsushita, J., Takano, A., 2010b. Nutrients, In: MR10-06 preliminary cruise report. JAMSTEC, Yokosuka, pp. 69-83
- Gouretski, V.V. and Jancke, K. 2001. Systematic errors as the cause for an apparent deep water property variability: global analysis of the WOCE and historical hydrographic data • REVIEW ARTICLE, *Progress In Oceanography*, 48: Issue 4, 337-402.
- Grasshoff, K., Ehrhardt, M., Kremling K. et al. 1983. *Methods of seawater analysis*. 2nd rev. Weinheim: Verlag Chemie, Germany, West.
- Hydes, D.J., Aoyama, M., Aminot, A., Bakker, K., Becker, S., Coverly, S., Daniel, A., Dickson, A.G., Grosso, O., Kerouel, R., Ooijen, J. van, Sato, K., Tanhua, T., Woodward, E.M.S., Zhang, J.Z., 2010. Determination of Dissolved Nutrients (N, P, Si) in Seawater with High Precision and Inter-Comparability Using Gas-Segmented Continuous Flow Analysers, In: GO-SHIP Repeat Hydrography Manual: A Collection of Expert Reports and Guidelines. IOCCP Report No. 14, ICPO Publication Series No 134.
- Joyce, T. and Corry, C. 1994. Requirements for WOCE hydrographic programmed data reporting. WHPO Publication, 90-1, Revision 2, WOCE Report No. 67/91.
- Kawano, T., Uchida, H. and Doi, T. WHP P01, P14 REVISIT DATA BOOK, (Ryoin Co., Ltd., Yokohama, 2009).
- Kirkwood, D.S. 1992. Stability of solutions of nutrient salts during storage. *Mar. Chem.*, 38 :

151-164.

- Kirkwood, D.S. Aminot, A. and Perttila, M. 1991. Report on the results of the ICES fourth intercomparison exercise for nutrients in sea water. ICES coop. Res. Rep. Ser., 174.
- Mordy, C.W., Aoyama, M., Gordon, L.I., Johnson, G.C., Key, R.M., Ross, A.A., Jennings, J.C. and Wilson, J. 2000. Deep water comparison studies of the Pacific WOCE nutrient data set. Eos Trans-American Geophysical Union. 80 (supplement), OS43.
- Murphy, J., and Riley, J.P. 1962. *Analytica chim. Acta* 27, 31-36.
- Sato, K., Aoyama, M., Becker, S., 2010. RMNS as Calibration Standard Solution to Keep Comparability for Several Cruises in the World Ocean in 2000s. In: Aoyama, M., Dickson, A.G., Hydes, D.J., Murata, A., Oh, J.R., Roose, P., Woodward, E.M.S., (Eds.), *Comparability of nutrients in the world's ocean*. Tsukuba, JAPAN: MOTHER TANK, pp 43-56.
- Uchida, H. & Fukasawa, M. WHP P6, A10, I3/I4 REVISIT DATA BOOK Blue Earth Global Expedition 2003 1, 2, (Aiwa Printing Co., Ltd., Tokyo, 2005).

## 2.6 pH measurement

**Masahide WAKITA (JAMSTEC MIO): Principal Investigator**  
**Minoru KAMATA (MWJ)**

### (1) Objective

Since the global warming is becoming an issue world-widely, studies on the greenhouse gases such as CO<sub>2</sub> are drawing high attention. The ocean plays an important role in buffering the increase of atmospheric CO<sub>2</sub>, and studies on the exchange of CO<sub>2</sub> between the atmosphere and the sea becomes highly important. Oceanic biosphere, especially primary production, has an important role concerned to oceanic CO<sub>2</sub> cycle through its photosynthesis and respiration. However, the diverseness and variability of the biological system make difficult to reveal their mechanism and quantitative understanding of CO<sub>2</sub> cycle. Dissolved CO<sub>2</sub> in water alters its appearance into several species, but the concentrations of the individual species of CO<sub>2</sub> system in solution cannot be measured directly. However, two of the four measurable parameters (alkalinity, total dissolved inorganic carbon, pH and pCO<sub>2</sub>) can estimate each concentration of CO<sub>2</sub> system (Dickson et al., 2007). Seawater acidification associated with CO<sub>2</sub> uptake into the ocean possibly changes oceanic ecosystem and CO<sub>2</sub> garners in Ocean recently. We here report on board measurements of pH during MR11-05 cruise.

### (2) Methods, Apparatus and Performance

#### (2)-1 Seawater sampling

Seawater samples were collected by 12 liter Niskin bottles mounted on the CTD/Carousel Water Sampling System and a bucket at 5 stations. Among these stations, deep and shallow casts were carried out for 2 stations. Seawater was sampled in a 100 ml glass bottle that was previously soaked in 5 % non-phosphoric acid detergent (pH13) solution at least 3 hours and was cleaned by fresh water for 5 times and Milli-Q ultrapure water for 3 times. A sampling silicone rubber tube with PFA tip was connected to the Niskin bottle when the sampling was carried out. The glass bottles were filled from the bottom smoothly, without rinsing, and were overflowed for 2 times bottle volume (about 10 seconds) with care not to leave any bubbles in the bottle. The water in the bottle was sealed by a glass made cap gravimetrically fitted to the bottle mouth without additional force. After collecting the samples on the deck, the bottles were carried into the lab and put in the water bath kept about 25 deg C before the measurement.

#### (2)-2 Seawater analyses

pH (-log[H<sup>+</sup>]) of the seawater was measured potentiometrically in the glass bottles. The pH / Ion meter (Radiometer PHM240) is used to measure the electromotive force (e.m.f.) between the glass electrode cell (Radiometer pHG201) and the reference electrode cell (Radiometer REF201) in the sample with its temperature controlled to 25 +/- 0.05 deg C.

Ag, AgCl reference electrode | solution of KCl || test solution | H<sup>+</sup> -glass electrode.

To calibrate the electrodes, the TRIS buffer (Lot=100715-4: pH=8.0906 pH units at 25 deg C, Delvalls and Dickson, 1998) and AMP buffer (Lot=100720-4: pH=6.7838 pH units at 25 deg C, DOE, 1994) in the synthetic seawater (Total hydrogen ion concentration scale) were applied. pH<sub>T</sub> of seawater sample (pH<sub>sp</sub>) is calculated from the expression:

$$\text{pH}_{\text{spl}} = \text{pH}_{\text{TRIS}} + (E_{\text{TRIS}} - E_{\text{spl}}) / \text{ER}$$

where electrode response ER is calculated as follows:

$$\text{ER} = (E_{\text{AMP}} - E_{\text{TRIS}}) / (\text{pH}_{\text{TRIS}} - \text{pH}_{\text{AMP}})$$

ER value should be equal to the ideal Nernst value as follows:

$$\text{ER} = RT \ln(10) / F = 59.16 \text{ mV} / \text{pH units at 25 deg C}$$

### (3) Preliminary results

A replicate analysis of seawater sample was made at 4 layers (ex. 50, 300, 1600, and 3500 dbar depth) of deep cast or 2 layers (ex. 25 and 125 dbar depth) of shallow cast. The difference between each pair of analyses was plotted on a range control chart (see Figure 2.6-1). The average of the difference was 0.001 pH units (n = 31 pairs) with its standard deviation of 0.001 pH units. These values were lower than the value recommended by Guide (Dickson et al., 2007).

### (4) Data Archive

All data will be submitted to JAMSTEC and is currently under its control.

### (5) Reference

DOE (1994), Handbook of methods for the analysis of the various parameters of the carbon dioxide system in sea water; version 2, A. G. Dickson & C. Goyet, Eds., ORNS/CDIAC-74

DelValls, T. A. and Dickson, A. G., 1998. The pH of buffers based on 2-amino-2-hydroxymethyl-1,3-propanediol ( 'tris' ) in synthetic sea water. Deep-Sea Research I 45, 1541-1554.

Dickson, A. G., C. L. Sabine and J. R. Christian, Eds. (2007): Guide to best practices for ocean CO<sub>2</sub> measurements, PICES Special Publication 3, 199pp.

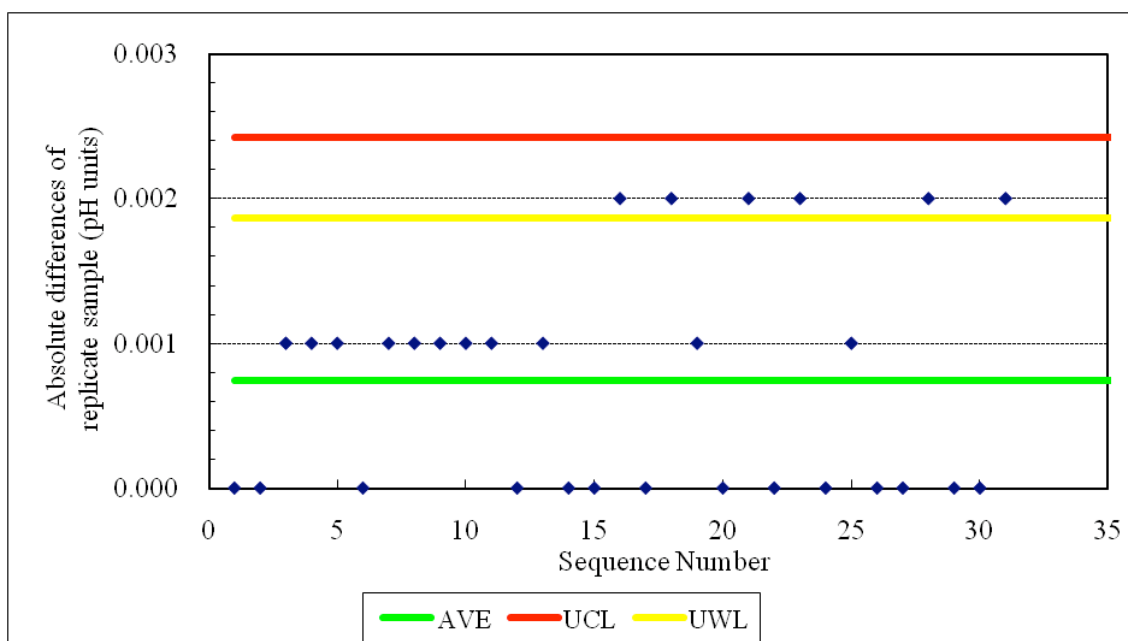


Figure 2.6-1 Range control chart of the absolute differences of replicate measurements of pH carried out during the cruise. AVE represents the average value, UCL upper control limit ( $UCL = AVE * 3.267$ ), and UWL upper warning limit ( $UWL = AVE * 2.512$ ) (Dickson et al., 2007).

## 2.7 Dissolved inorganic carbon-DIC-

**Masahide WAKITA (JAMSTEC MIO): Principal Investigator**

**Yoshiko ISHIKAWA (MWJ)**

**Makoto TAKADA (MWJ)**

### (1) Objective

Concentration of CO<sub>2</sub> in the atmosphere is now increasing at a rate of 1.5 ppmv yr<sup>-1</sup> owing to human activities such as burning of fossil fuels, deforestation, and cement production. The ocean plays an important role in buffering the increase of atmospheric CO<sub>2</sub>, therefore the urgent tasks are to clarify the mechanism of the oceanic CO<sub>2</sub> absorption and to estimate of CO<sub>2</sub> absorption capacity of the oceans. Oceanic biosphere, especially primary production, has an important role concerned to oceanic CO<sub>2</sub> cycle through its photosynthesis and respiration. However, the diverseness and variability of the biological system make difficult to reveal their mechanism and quantitative understanding of the CO<sub>2</sub> cycle. When CO<sub>2</sub> dissolves in water, chemical reaction takes place and CO<sub>2</sub> alters its appearance into several species. Concentrations of the individual species of the CO<sub>2</sub> system in solution cannot be measured directly, but calculated from two of four parameters: total alkalinity, total dissolved inorganic carbon, pH and pCO<sub>2</sub> (Dickson et al., 2007). We here report on-board measurements of DIC performed during the MR11-05 cruise.

### (2) Methods, Apparatus and Performance

#### (2)-1 Seawater sampling

Seawater samples were collected by 12 liter Niskin bottles mounted on the CTD/Carousel Water Sampling System and a bucket at 5 stations. Among these stations, deep and shallow casts were carried out for 2 stations. Seawater was sampled in a 300 ml glass bottle (SCHOTT DURAN) that was previously soaked in 5 % non-phosphoric acid detergent (pH = 13) solution at least 3 hours and was cleaned by fresh water for 5 times and Milli-Q deionized water for 3 times. A sampling silicone rubber tube with PFA tip was connected to the Niskin bottle when the sampling was carried out. The glass bottles were filled from the bottom, without rinsing, and were overflowed for 20 seconds. They were sealed using the polyethylene inner lids with its diameter of 29 mm with care not to leave any bubbles in the bottle. After collecting the samples on the deck, the glass bottles were carried to the laboratory to be measured. Within one hour after the sampling, 3 ml of the sample (1 % of the bottle volume) was removed from the glass bottle and poisoned with 100 µl of over saturated solution of mercury chloride. Then the samples were sealed by the polyethylene inner lids with its diameter of 31.9 mm and stored in a refrigerator at approximately 5 deg C until analyzed. Before the analysis, the samples were put in the water bath kept about 20 deg C for one hour.

#### (2)-2 Seawater analysis

Measurements of DIC were made with total CO<sub>2</sub> measuring system (Nippon ANS, Inc.). The system comprise of seawater dispensing unit, a CO<sub>2</sub> extraction unit and a coulometer (Model seacat2000, Nippon ANS, Inc.)

The seawater dispensing unit has an auto-sampler (6 ports), which dispenses the seawater from a glass bottle to a pipette of nominal 21 ml volume. The pipette was kept at 20 ± 0.05 deg C by a water jacket, in which water circulated through a thermostatic water bath (RTE 10, Thermo) set at 20 deg C.

The CO<sub>2</sub> dissolved in a seawater sample is extracted in a stripping chamber of the CO<sub>2</sub> extraction unit by adding phosphoric acid (10 % v/v). The stripping chamber is made approx. 25 cm long and has a fine frit at the bottom. First, the certain amount of acid is taken to the constant volume tube and added to the stripping chamber from its bottom by pressurizing an acid bottle with nitrogen gas (99.9999 %). Second, a seawater sample kept in a pipette is introduced to the stripping chamber by the same method as that for an acid. The seawater and phosphoric acid are stirred by the nitrogen bubbles through a fine frit at the bottom of the stripping chamber. The CO<sub>2</sub> stripped in the chamber is carried by the nitrogen gas (flow rates of 140 ml min<sup>-1</sup>) to the coulometer through two electric dehumidifiers (kept at 0.5 deg C) and a chemical desiccant (Mg(ClO<sub>4</sub>)<sub>2</sub>).

Measurements of 1.5 % CO<sub>2</sub> standard gas in a nitrogen base, system blank (phosphoric acid blank), and seawater samples (6 samples) were programmed to repeat. The variation of 1.5 % CO<sub>2</sub> standard gas signal was used to correct the signal drift results from chemical alternation of coulometer solutions.

### (3) Preliminary results

During the cruise, 322 samples were analyzed for DIC. A replicate analysis was performed at the interval decided beforehand and the difference between each pair of analyses was plotted on a range control chart (Figure 2.7-1). The average of the differences was 1.06 μmol kg<sup>-1</sup> (n = 30). The standard deviation was 0.95 μmol kg<sup>-1</sup>, which indicates that the analysis was accurate enough according to the Guide to best practices for ocean CO<sub>2</sub> measurements (Dickson et al., 2007).

### (4) Data Archive

These data obtained in this cruise will be submitted to the Data Management Office (DMO) of JAMSTEC, and will open to the public via “R/V Mirai Data Web Page” in JAMSTEC home page.

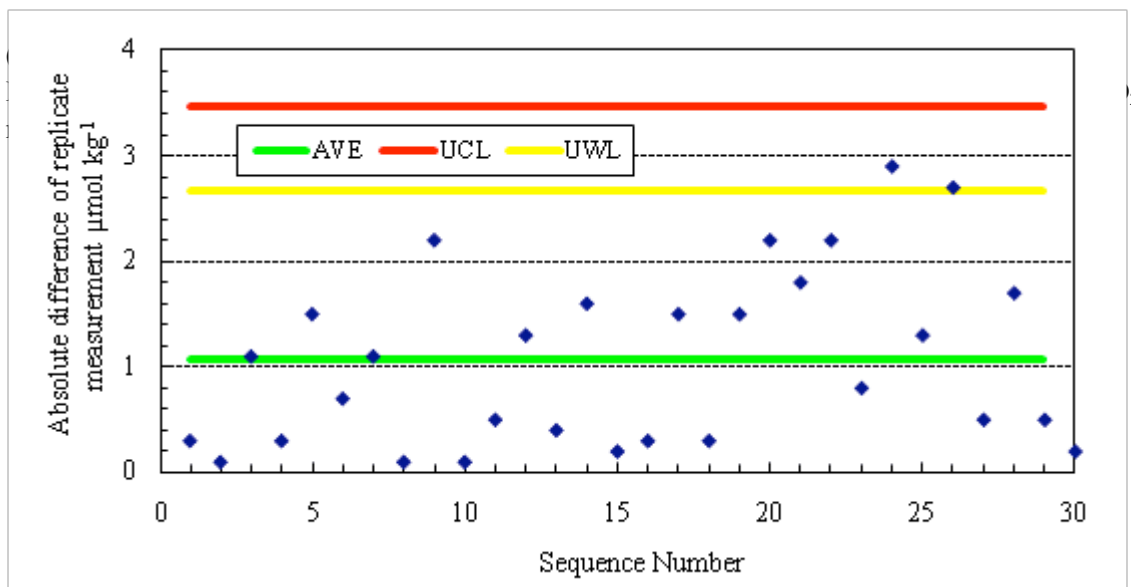


Figure 2.7-1 Range control chart of the absolute differences of replicate measurements of DIC carried out during this cruise. UCL and UWL represents the upper control limit (UCL=AVE\*3.267) and upper warning limit (UWL=AVE\*2.512), respectively.

## 2.8 Total Alkalinity

**Masahide WAKITA (JAMSTEC MIO): Principal Investigator**

**Yoshiko ISHIKAWA (MWJ)**

**Makoto TAKADA (MWJ)**

### (1) Objective

Global warming is becoming an issue world-widely, therefore studies on green house gases, especially carbon dioxide (CO<sub>2</sub>), are indispensable. The ocean currently absorbs one third of the 6 Gt of carbon emitted into the atmosphere each year by human activities, such as burning of fossil fuels, deforestation, and cement production. When CO<sub>2</sub> dissolves in sea water, chemical reaction takes place and CO<sub>2</sub> alters its appearance into several species and make the oceanic CO<sub>2</sub> cycle complicated. Furthermore, oceanic biological activity, especially oceanic primary production, plays an important role concerned to the CO<sub>2</sub> cycle through its photosynthesis and respiration. The concentrations of the individual CO<sub>2</sub> species cannot be measured directly, however, two of four measurable parameters: total alkalinity, total dissolved inorganic carbon, pH, and pCO<sub>2</sub>, can clarify the whole distribution of the CO<sub>2</sub> species (Dickson et al., 2007). We here report on-board measurements of total alkalinity performed during the MR11-05 cruise.

### (2) Methods, Apparatus and Performance

#### (2)-1 Seawater sampling

Seawater samples were collected by 12 liter Niskin bottles mounted on the CTD/Carousel Water Sampling System and a bucket at 5 stations. Among these stations, deep and shallow casts were carried out for 2 stations. A sampling silicone rubber tube with PFA tip was used to sample the seawater from the Niskin bottle. The 125 ml borosilicate glass bottles (SHOTT DURAN) were filled from the bottom smoothly, without rinsing, and were overflowed for 2 times bottle volume (10 seconds) with care not to leave any bubbles in the bottle. These bottles were pre-washed by soaking in 5 % non-phosphoric acid detergent (pH = 13) for more than 3 hours and then rinsed 5 times with tap water and 3 times with Milli-Q deionized water. After collecting the samples on the deck, the bottles were carried into the laboratory to be measured. The samples were stored in a refrigerator at approximately 5 deg C until being analyzed. Before the analysis, the samples were put in the water bath kept about 25 deg C for one hour.

#### (2)-2 Seawater analyses

The TA was measured using a spectrophotometric system (Nippon ANS, Inc.) using a scheme of Yao and Byrne (1998). The constant volume of sample seawater, with its value of approx. 42 ml, was transferred from a sample bottle into the titration cell kept at 25 deg C in a thermostated compartment. Then, the sample seawater was circulated through the tube connecting the titration cell and the pH cell in the spectrophotometer (Carry 50 Scan, Varian) by a peristaltic pump. The length and volume of the pH cell are 8 cm and 13 ml, respectively, and its temperature is also kept at 25 deg C in a thermostated compartment. The TA is calculated by measuring two sets of absorbance at three wavelengths (750, 616 and 444 nm). One is the absorbance of seawater sample before injecting an acid with indicator solution (bromocresol green sodium) and another is the one after the injection. For mixing the acid with indicator solution and the seawater, and for degassing CO<sub>2</sub> from the mixed solution sufficiently, they are



circulated between the titration and pH cell by a peristaltic pump for 7 and half minutes before the measurement.

The TA is calculated based on the following equation:

$$\begin{aligned} \text{pH}_T = & 4.2699 + 0.002578 * (35 - S) \\ & + \log ((R(25) - 0.00131) / (2.3148 - 0.1299 * R(25))) \\ & - \log (1 - 0.001005 * S), \end{aligned} \quad (1)$$

$$\begin{aligned} A_T = & (N_A * V_A - 10^{\text{pH}_T} * \text{DensSW}(T, S) * (V_S + V_A)) \\ & * (\text{DensSW}(T, S) * V_S)^{-1}, \end{aligned} \quad (2)$$

where R(25) represents the difference of absorbance at 616 and 444 nm between before and after the injection. The absorbance of wavelength at 750 nm is used to subtract the variation of absorbance caused by the system. DensSW (T, S) is the density of seawater at temperature (T) and salinity (S),  $N_A$  the concentration of the added acid,  $V_A$  and  $V_S$  the volume of added acid and seawater, respectively.

To keep the high analysis precision, some treatments were carried out during the cruise. The acid with indicator solution stored in 1 L DURAN bottle is kept in a bath with its temperature of 25 deg C, and about 10 ml of it is discarded at first before the batch of measurement. For mixing the seawater and the acid with indicator solution sufficiently, TYGON tube used on the peristaltic pump was periodically renewed. Absorbance measurements were done 10 times during each analysis, and the stable last five and three values are averaged and used for above listed calculation for before and after the injection, respectively.

### (3) Preliminary results

A few replicate samples were taken at most of stations and the difference between each pair of analyses was plotted on a range control chart (see Figure 2.8-1). The average of the difference was  $0.7 \mu\text{mol kg}^{-1}$  ( $n = 32$ ) with its standard deviation of  $0.6 \mu\text{mol kg}^{-1}$ , which indicates that the analysis was accurate enough according to the Guide to best practices for ocean CO<sub>2</sub> measurements (Dickson et al., 2007).

### (4) Data Archive

These data obtained in this cruise will be submitted to the Data Management Office (DMO) of JAMSTEC, and will be opened to the public via “R/V Mirai Data Web Page” in JAMSTEC home page.

### (5) References

Yao, W. and Byrne, R. H. (1998), Simplified seawater alkalinity analysis: Use of linear array spectrometers. Deep-Sea Research Part I, Vol. 45, 1383-1392.

Dickson, A. G., Sabine, C. L. & Christian, J. R. (2007), Guide to best practices for ocean CO<sub>2</sub> measurements; PICES Special Publication 3, 199pp.

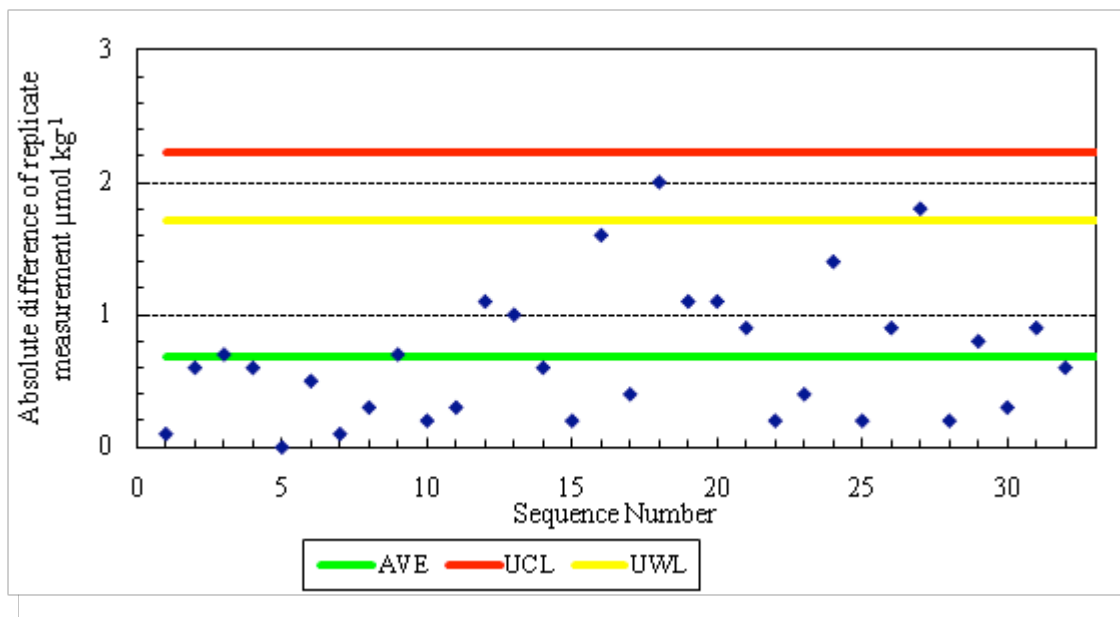


Figure 2.8-1 Range control chart of the absolute differences of replicate measurements carried out in the analysis of TA during the MR11-05 cruise. UCL and UWL represents the upper control limit ( $\text{UCL} = \text{AVE} \times 3.267$ ) and upper warning limit ( $\text{UWL} = \text{AVE} \times 2.512$ ), respectively.

## 2.9 Underway pCO<sub>2</sub>

**Masahide WAKITA (JAMSTEC MIO): Principal Investigator**

**Yoshiko ISHIKAWA (MWJ)**

**Makoto TAKADA (MWJ)**

### (1) Objectives

Concentrations of CO<sub>2</sub> in the atmosphere are increasing at a rate of 1.5 ppmv yr<sup>-1</sup> owing to human activities such as burning of fossil fuels, deforestation, and cement production. Oceanic CO<sub>2</sub> concentration is also considered to be increased with the atmospheric CO<sub>2</sub> increase, however, its variation is widely different by time and locations. Underway pCO<sub>2</sub> observation is indispensable to know the pCO<sub>2</sub> distribution, and it leads to elucidate the mechanism of oceanic pCO<sub>2</sub> variation. We here report the underway pCO<sub>2</sub> measurements performed during MR11-05 cruise.

### (2) Methods, Apparatus and Performance

Oceanic and atmospheric CO<sub>2</sub> concentrations were measured during the cruise using an automated system equipped with a non-dispersive infrared gas analyzer (NDIR; LI-7000, Li-Cor). Measurements were done every about one and a half hour, and 4 standard gasses, atmospheric air, and the CO<sub>2</sub> equilibrated air with sea surface water were analyzed subsequently in this hour. The concentrations of the CO<sub>2</sub> standard gases were 299.834, 350.002, 400.099 and 450.374 ppmv. Atmospheric air taken from the bow of the ship (approx.30 m above the sea level) was introduced into the NDIR by passing through a electrical cooling unit, a mass flow controller which controls the air flow rate of 0.5 L min<sup>-1</sup>, a membrane dryer (MD-110-72P, perma pure llc.) and chemical desiccant (Mg(ClO<sub>4</sub>)<sub>2</sub>). The CO<sub>2</sub> equilibrated air was the air with its CO<sub>2</sub> concentration was equivalent to the sea surface water. Seawater was taken from an intake placed at the approximately 4.5 m below the sea surface and introduced into the equilibrator at the flow rate of 4 - 5 L min<sup>-1</sup> by a pump. The equilibrated air was circulated in a closed loop by a pump at flow rate of 0.7 - 0.8 L min<sup>-1</sup> through two cooling units, a membrane dryer, the chemical desiccant, and the NDIR.

### (3) Preliminary results

Cruise track during pCO<sub>2</sub> observation is shown in Figure 2.9-1. Temporal variations of both oceanic and atmospheric CO<sub>2</sub> concentration (xCO<sub>2</sub>) are shown in Fig. 2.9-2.

### (4) Data Archive

Data obtained in this cruise will be submitted to the Data Management Office (DMO) of JAMSTEC, and will opened to the public via “R/V Mirai Data Web Page” in JAMSTEC home page.

### (5) Reference

Dickson, A. G., Sabine, C. L. & Christian, J. R. (2007), Guide to best practices for ocean CO<sub>2</sub> measurements; PICES Special Publication 3, 199pp.

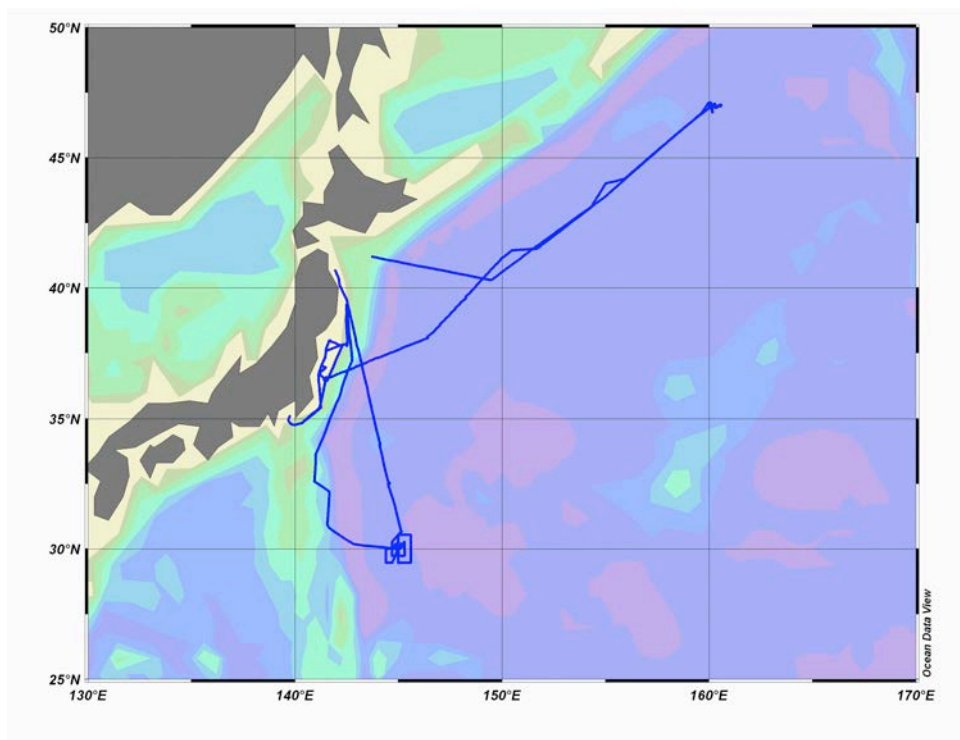


Figure 2.9-1 Observation map

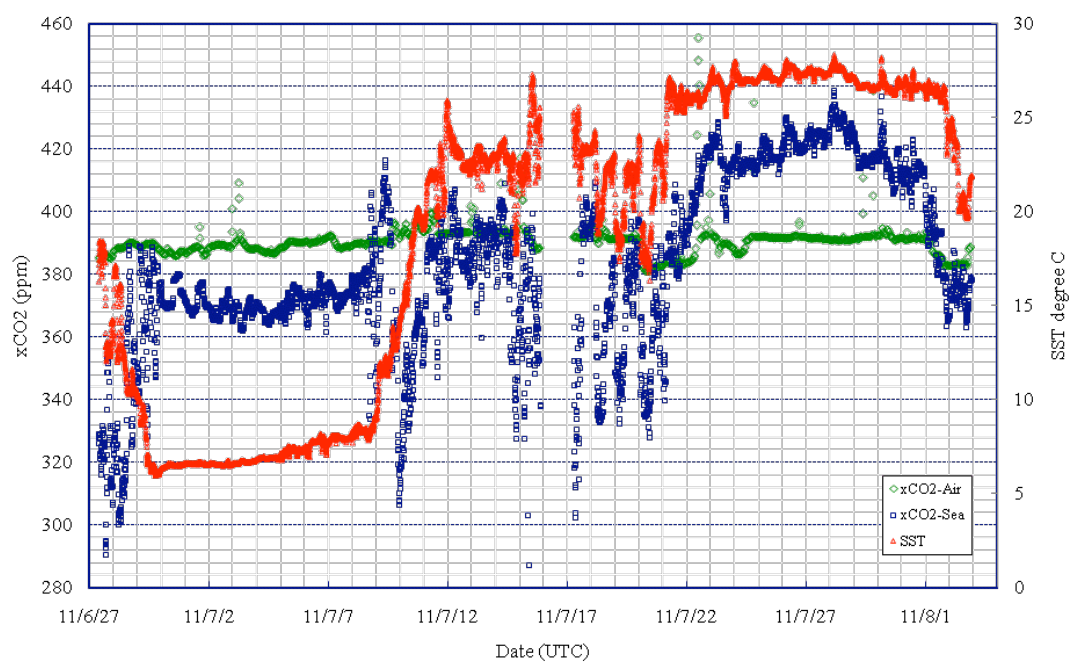


Figure 2.9-2 Temporal variations of oceanic and atmospheric CO<sub>2</sub> concentration (xCO<sub>2</sub>). Blue dots represent oceanic xCO<sub>2</sub> variation and green atmospheric xCO<sub>2</sub>. SST variation (red) is also shown.

### 3 Special observation

#### 3.1 BGC mooring Recovery and deployment

**Makio HONDA (JAMSTEC MIO)**

**Hajime KAWAKAMI (JAMSTEC MIO)**

**Toru IDAI (MWJ)**

**Masaki FURUHATA (MWJ)**

**Tomoyuki TAKAMORI (MWJ)**

##### 3.1.1 Recovery and deployment

The BGC mooring system was designed for biogeochemistry at Station K-2 and S-1 in the Western Subarctic Gyre. We recovered BGC mooring at Station K-2 and S-1 which were deployed at MR10-06 and deployed BGC mooring at Station K-2 and S-1. K-2 is 47N / 160E, where is close to station KNOT and, however, structure of water mass is more stable than station KNOT. Before deployment, sea floor topography was surveyed with Sea Beam. In order to place the top of mooring systems 150m depth, precise water depths for mooring positions was measured by an altimeter (Datasonics PSA900D) mounted on CTD / CWS. Mooring works took approximately 5 hours for each mooring system. After sinker was dropped, we positioned the mooring systems by measuring the slant ranges between research vessel and the acoustic releaser. The position of the mooring is finally determined as follow:

Table 3.1.1-1 Mooring positions for respective mooring systems

	Recovery	Deployment	Recovery	Deployment
Station & type	K-2 BGC	K-2 BGC	S-1 BGC	S-1 BGC
Mooring Number	K2BGC101031	K2BGC110703	S1BGC101110	S1BGC110729
Working Date	Jun.30 <sup>th</sup> 2011	Jul. 03 <sup>rd</sup> 2011	Jul. 25 <sup>th</sup> 2011	Jul. 29 <sup>th</sup> 2011
Latitude	47° 00.37 N	47° 00.34N	30° 03.92 N	30° 03.93 N
Longitude	159° 58.24 E	159° 58.42 E	144° 57.98 E	144° 58.03 E
Sea Beam Depth	5,218 m	5,218 m	5,927 m	5,924 m

The BGC mooring consists of a advance buoy with 30m pick up rope, a 64” syntactic top float with 3,000 lbs (1,360 kg) buoyancy, instruments, wire and nylon ropes, glass floats (Benthos 17” glass ball), dual releasers (Edgetech) and 4,660 lbs (2,116 kg) sinker with mace plate. Two ARGOS compact mooring locators and one submersible recovery strobe are mounted on the top float. This mooring system was planned to keep the following time-series observational instruments are mounted approximately 150 m below sea surface. It is 10 m longer than real depth because recovered depth sensor which was installed on the Sediment trap shows 10 m deeper than our expected by mooring tilt.

On the BGC mooring, 3 Sediment Traps are installed on the 200 m, 500 m and 5,000 m. Extra CTD (SBE-37) and DO Sensor (Arec) are mounted on the dual acoustic releasers. Also extra Depth Sensor(RIGO) is mounted on 200m Sediment Trap.

Details for each instrument are described later (section 3.1.2). Serial numbers for instruments are as follows:

Table 3.1.1-2 Serial numbers of instruments

	Recover		Deployment	
Station and type	K-2 BGC	S-1 BGC	K-2 BGC	S-1 BGC
Mooring Number	K2BGC101031	S1BGC10110	K2BGC110703	S1BGC110729
ARGOS	18842 / 52111	18841 / 52112	18842 / 52111	18841 / 52112
ARGOS ID	18577 / 5373	18570 / 5374	18577 / 5373	18570 / 5374
Strobe	N02-043	N02-044	Benthos 233	Benthos 234
Sediment Trap×3				
Nichiyu (200m)	ST98025	ST98080	ST98025	ST98080
Rigo Depth Sensor	DP1158	-	DP1158	DP1142
Mark7-21 (500m)	989	No ID	989	No ID
Mark7-21(5000m)	10558-01	878	10558-01	878
Releaser	27824	28533	27809	27864
Releaser	28531	27825	28386	27815
SBE-37	2731	2730	2731	2730
AREC DO sensor	05	03	05	03

Table 3.1.1-3 Recovery BGC Mooring Record at K-2

Project	Time-Series		Depth	5,206.2	m
Area	North Pacific		Planned Depth	5,216.2	m
Station	K2 BGC		Length	5,068.2	m
Target Position	47°00.350	N	Depth of Buoy	150	m
	159°58.326	E	Period	1	year
ACOUCTIC RELEASERS					
Type	Edgetech		Edgetech		
Serial Number	27824		28531		
Receive F.	11.0	kHz	11.0	kHz	
Transmit F.	14.0	kHz	12.0	kHz	
RELEASE C.	344674		223065		
Enable C.	361121		200405		
Disable C.	361167		200426		
Battery	2 years		2 years		
Release Test	OK		OK		
RECOVERY					
Recorder	Toru Idai		Work Distance	1.8	Nmile
Ship	R/V MIRAI		Send Enable C.	1:33	
Cruise No.	MR11-05		Slant Renge	3455	msec
Date	2011/6/30		Send Release C.	2:04	
Weather	○		Discovery Buoy	2:06	
Wave Hight	2.5	m	Pos. of Top Buoy	47°00.35	N
Seabeam Depth	5,217	m		159°58.29	E
Ship Heading	<030>		Pos. of Start	47°00.91	N
Ship Ave.Speed	0.6	knot		159°58.60	E
Wind	<165>	11.4 m/s	Pos. of Finish	47°02.39	N
Current	<128>	10.3 cm/sec		159°59.60	E

Table 3.1.1-4 Recovery BGC Mooring Record at S-1

Project	Time-Series		Depth	5,920.0	m
Area	North Pacific		Planned Depth	5,910.0	m
Station	S1 BGC		Length	5,752.3	m
Target Position	30°03.8656	N	Depth of Buoy	150	m
	144°58.0275	E	Period	1	year
ACOUCTIC RELEASERS					
Type	Edgetech		Edgetech		
Serial Number	28533		27825		
Receive F.	11.0	kHz	11.0	kHz	
Transmit F.	14.0	kHz	14.0	kHz	
RELEASE C.	223307		344176		
Enable C.	201054		356736		
Disable C.	201077		356770		
Battery	2 years		2 years		
Release Test	OK		OK		
RECOVERY					
Recorder	Toru Idai		Work Distance	0.9	Nmile
Ship	R/V MIRAI		Send Enable C.	21:16	
Cruise No.	MR11-05		Slant Renge	5869	m
Date	2011/7/25		Send Release C.	21:19	
Weather	bc		Discovery Buoy	21:21	
Wave Hight	2.0	m	Pos. of Top Buoy	30°03.97	N
Depth	5,926	m		144°57.95	E
Ship Heading	<180>		Pos. of Start	30°04.50	N
Ship Ave.Speed	0.3	knot		144°58.04	E
Wind	<200>	6.3 m/s	Pos. of Finish	30°03.61	N
Current	<340>	0.7 cm/sec		144°58.00	E

Table 3.1.1-5 Deployment BGC Mooring Record at K-2

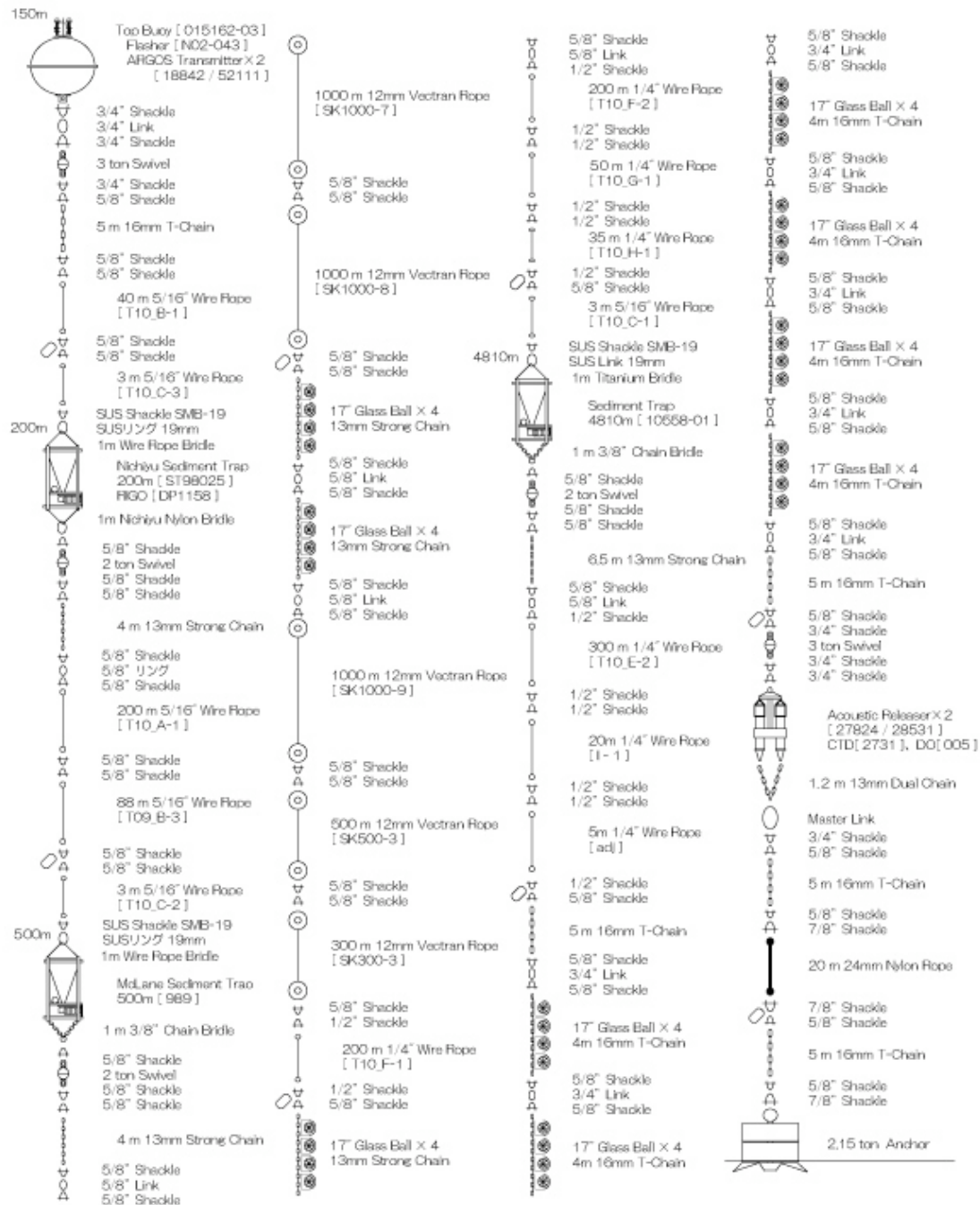
Project	Time-Series		Depth	5,206.2	m
Area	North Pacific		Planned Depth	5,216.2	m
Station	K2 BGC		Length	5,068.2	m
Target Position	47°00.350	N	Depth of Buoy	150	m
	159°58.326	E	Period	1	year
ACOUCTIC RELEASERS					
Type	Edgetech		Edgetech		
Serial Number	27809		28386		
Receive F.	11.0	kHz	11.0	kHz	
Transmit F.	14.0	kHz	14.0	kHz	
RELEASE C.	344535		354501		
Enable C.	360320		376513		
Disable C.	360366		376530		
Battery	2 years		2 years		
Release Test	OK		OK		
DEPLOYMENT					
Recorder	Toru Idai		Start	6.1	Nmile
Ship	R/V MIRAI		Overshoot	607	m
Cruise No.	MR11-05		Let go Top Buoy	21:16	
Date	2011/7/3		Let go Anchor	0:24	
Weather	d		Sink Top Buoy	0:56	
Wave Hight	1.3	m	Pos. of Start	47°05.15	N
Seabeam Depth	5,212	m		160°04.26	E
Ship Heading	<213>		Pos. of Drop. Anc.	47°00.01	N
Ship Ave.Speed	1.9	knot		159°57.98	E
Wind	<210>	6.0 m/s	Pos. of Mooring	47°00.34	N
Current	<145>	10.3 cm/sec		159°58.42	E



Table 3.1.1-6 Deployment BGC Mooring Record at S-1

Project	Time-Series		Depth	5,920.0	m
Area	North Pacific		Planned Depth	5,915.0	m
Station	S1 BGC		Length	5,752.3	m
Target Position	30°03.8656	N	Depth of Buoy	150	m
	144°58.0275	E	Period	1	year
ACOUCTIC RELEASERS					
Type	Edgetech		Edgetech		
Serial Number	27864		27815		
Receive F.	11.0	kHz	11.0	kHz	
Transmit F.	14.0	kHz	14.0	kHz	
RELEASE C.	344421		344657		
Enable C.	357724		361035		
Disable C.	357762		361073		
Battery	2 years		2 years		
Release Test	OK		OK		
DEPLOYMENT					
Recorder	Toru Idai		Start	5.3	Nmile
Ship	R/V MIRAI		Overshoot	600	m
Cruise No.	MR11-05		Let go Top Buoy	20:13	
Date	2011/7/29		Let go Anchor	23:04	
Weather	bc		Sink Top Buoy	-	
Wave Hight	1.3	m	Pos. of Start	30°07.11	N
Seabeam Depth	5,924	m		145°02.57	E
Ship Heading	<230>		Pos. of Drop. Anc.	30°03.75	N
Ship Ave.Speed	1.8	knot		144°57.68	E
Wind	<265>	9.4 m/s	Pos. of Mooring	30°03.93	N
Current	<315>	10.3 cm/sec		144°58.03	E

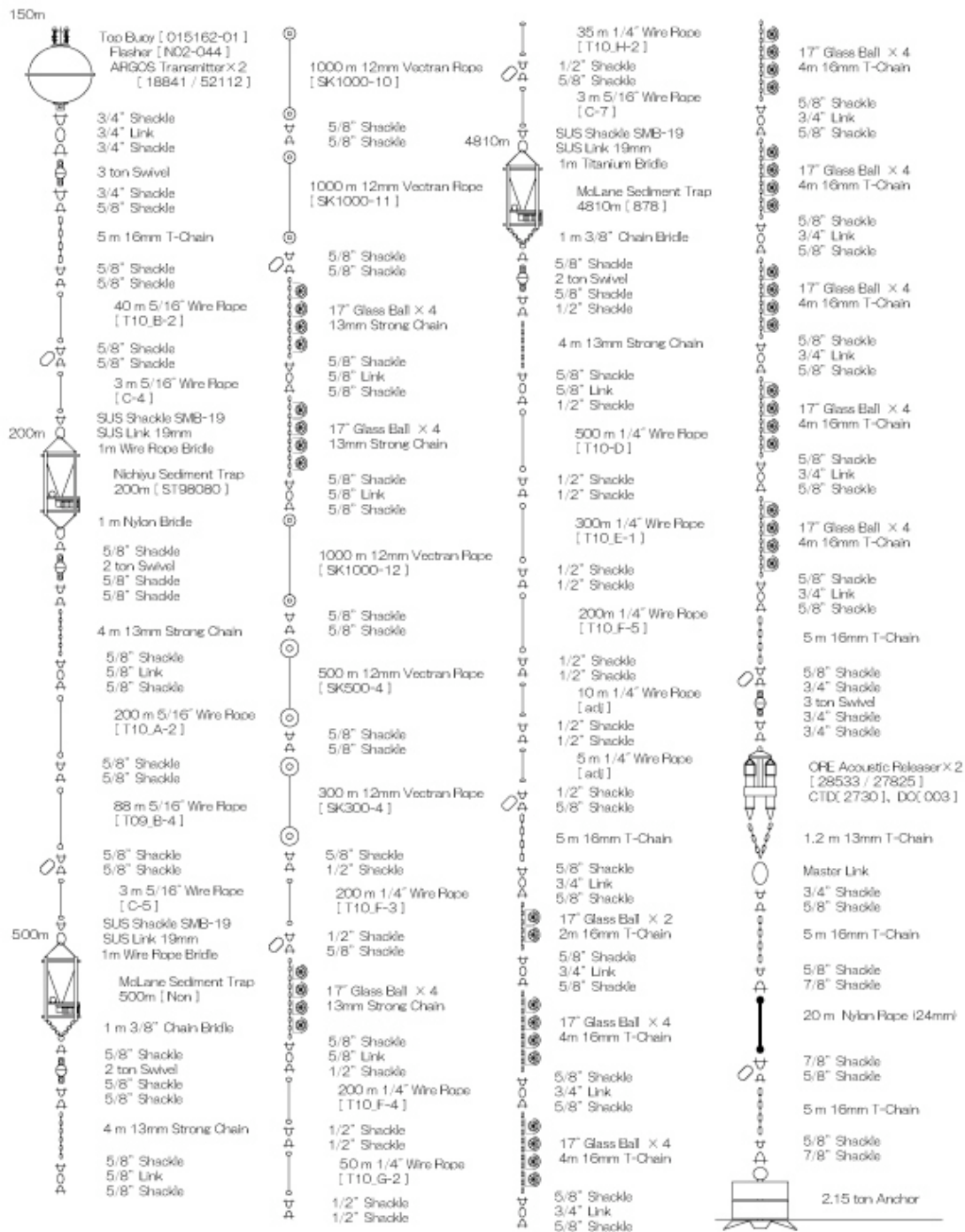
MR11-05 K2 Recovery Final Ver.

JPAC NW-PACIFIC **BGC** Mooring

Station K2, 5206.2m

Fig. 3.1.1-1 Recovery BGC Mooring Figure at K-2

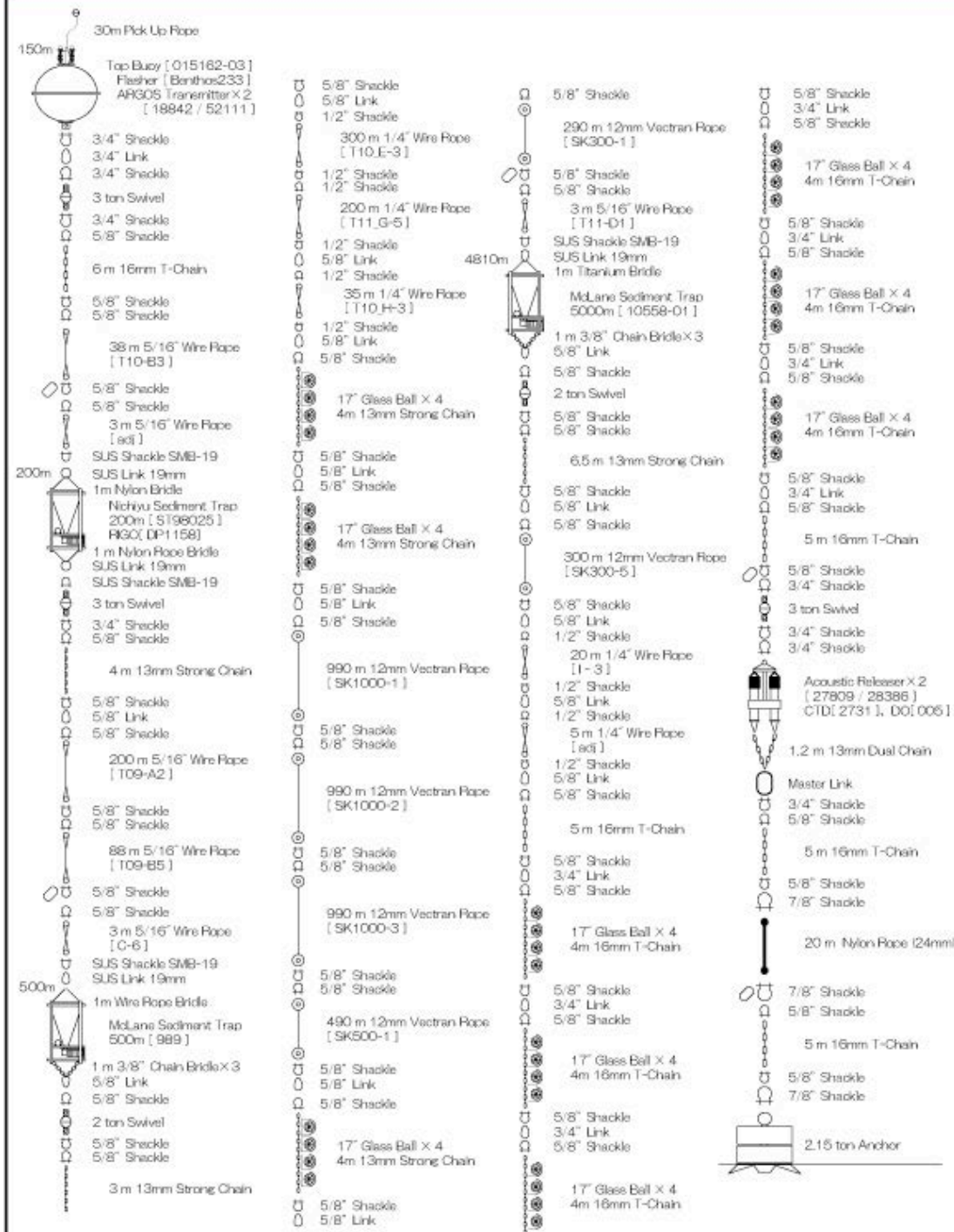
MR11-05 S1 Recovery Final Ver.

JPAC NW-PACIFIC **BGC** Mooring

Station S1, 5920.0m

Fig. 3.1.1-2 Recovery BGC Mooring Figure at S-1

# MR11-05 K2 BGC Deployment Final Ver.

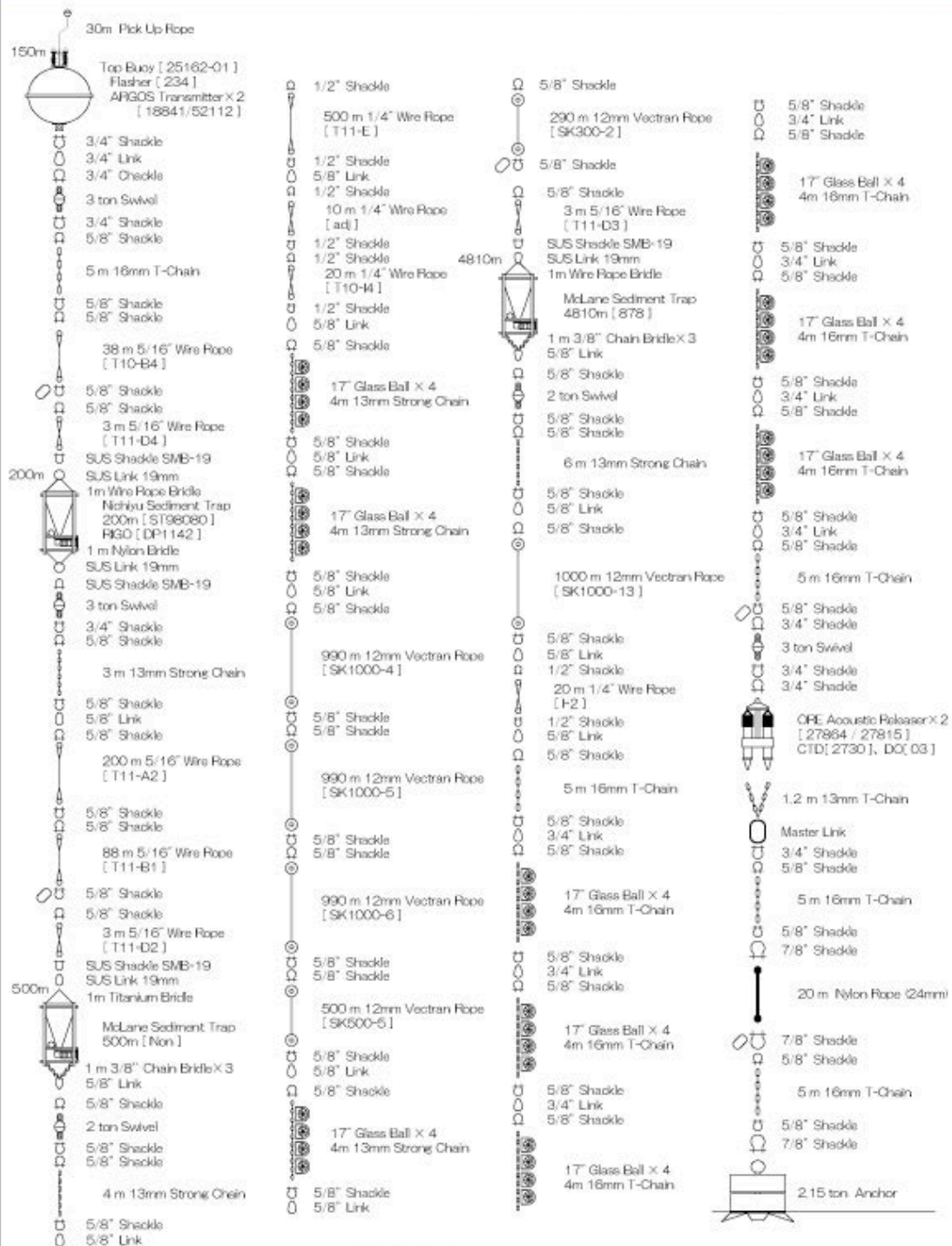


JPAC NW-PACIFIC **BGC** Mooring

Station K2, 5206.2m

Fig. 3.1.1-3 Deployment BGC Mooring Figure at K-2

# MR11-05 S1 BGC Deployment Final Ver.



JPAC NW-PACIFIC **BGC** Mooring

Station S1, 5920.0m

Fig. 3.1.1-4 Deployment BGC Mooring Figure at S-1



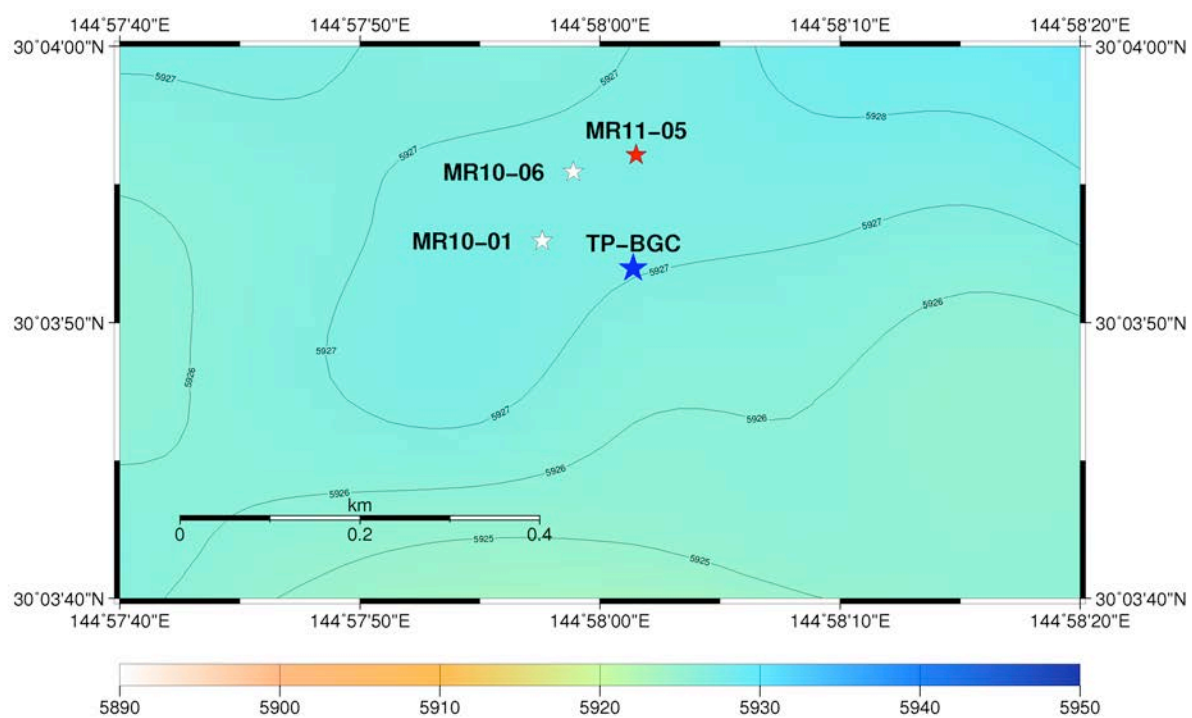
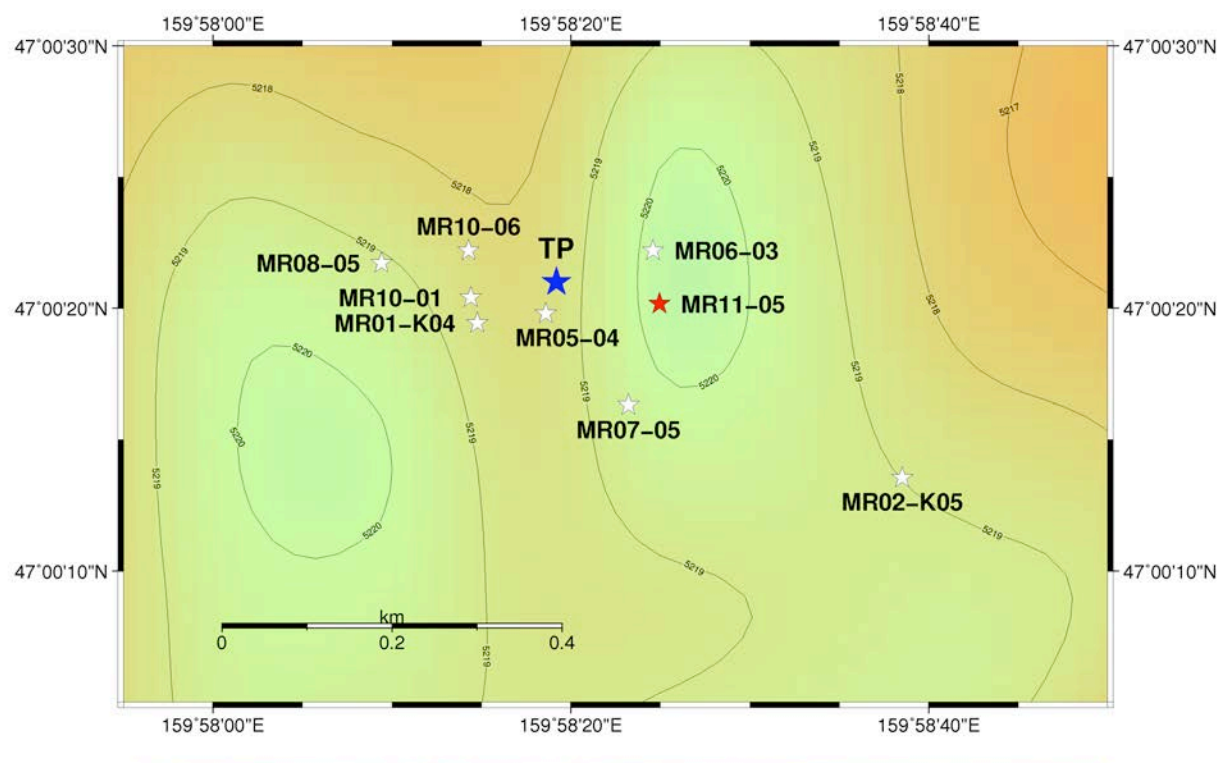


Fig. 3.1.1-5 Deployment position of (a) K2 (b) S1 ST mooring systems

### 3.1.2 Instruments

On mooring systems, the following instruments are installed.

#### (1) ARGOS CML (Compact Mooring Locator)

The Compact Mooring Locator is a subsurface mooring locator based on SEIMAC's Smart Cat ARGOS PTT (Platform Terminal Transmitter) technology. Using CML, we can know when our mooring has come to the surface and its position. The CML employs a pressure sensor at the bottom. When the CML is turned ON, the transmission is started immediately every 90 seconds and then when the pressure sensor works ON by approximately 10 dbar, the transmission is stopped. When the top buoy with the CML comes to the surface, the pressure sensor will work OFF and the transmission will be started. Smart Cat transmissions will be initiated at this time, allowing us to locate our mooring. Depending on how long the CML has been moored, it will transmit for up to 120 days on a 90 second repetition period. Battery life, however, is affected by how long the CML has been moored prior to activation. A longer pre-activation mooring will mean less activation life.

Principle specification is as follows:

#### (Specification)

Transmitter:	Smart Cat PTT
Operating Temp.:	+35 [deg] to -5 [deg]
Standby Current:	80 microamps
Smart Cat Freq.:	401.650 MHz
Battery Supply:	7-Cell alkaline D-Cells
Ratings:	+10.5VDC nom., 10 Amp Hr
Hull:	6061-T6 Aluminum
Max Depth:	1,000 m
Length:	22 inches
Diameter:	3.4 inches
Upper flange:	5.60 inches
Dome:	Acrylic
Buoyancy:	-2.5 (negative) approx.
Weight	12 pounds approx.

#### (2) Submersible Recovery Strobe

The Benthos Recovery Strobe is intended to aid in the marking or recovery of oceanographic instruments, manned vehicles, remotely operated vehicles, buoys or structures. Due to the occulting (firing closely spaced bursts of light) nature of this design, it is much more visible than conventional marker strobes, particularly in poor sea conditions.

#### (Specification)

Repetition Rate:	Adjustable from 2 bursts per second to 1 burst every 3 seconds.
Burst Length:	Adjustable from 1 to 5 flashes per burst. 100 ms between flashes nominal.
Battery Type:	C-cell alkaline batteries.
Life:	Dependent on repetition rate and burst length. 150 hours with a one flash burst every 2 seconds.
Construction:	Awl-grip painted, Hard coat anodized 6061 T-6 aluminum housing.
Max. Depth:	7,300m

Daylight-off:	User selected, standard
Pressure Switch:	On at surface, auto off when submerged below 10m.
Weight in Air:	4 pounds
Weight in Water:	2 pounds
Diameter:	1.7 inches nominal
Length:	21-1/2 inches nominal

### (3) Depth Sensor

RIGO RMD Depth sensor is digital memory type and designed for mounting on the plankton net and instrument for mooring and so on. It is small and right weight for easy handling. Sampling interval is chosen between 2 and 127 seconds or 1 and 127 minutes and sampled Time and Depth data. The data is converted to personal computer using exclusive cable (printer interface).

#### (Specification)

Model:	RMD-500
Operating Depth:	0 ~ 500m
Precision:	0.5% (F.S.)
Accuracy:	1/1300
Memory:	65,534 data (128kbyte)
Battery:	lithium battery (CR2032) DC6V
Battery Life:	65,000 data or less than 1 year
Sample interval:	2 ~ 127 seconds or 1 ~ 127 minutes
Broken Pressure:	20MPa
Diameter:	50mm
Length:	150mm
Main Material:	vinyl chloride resin
Cap material:	polyacetal resin
Weight:	280g

### (4) CTD SBE-37

The SBE 37-SM MicroCAT is a high-accuracy conductivity and temperature (pressure optional) recorder with internal battery and memory. Designed for moorings or other long duration, fixed-site deployments, the MicroCAT includes a standard serial interface and nonvolatile FLASH memory. Constructed of titanium and other non-corroding materials to ensure long life with minimum maintenance, the MicroCAT's depth capability is 7000 meters; it is also available with an optional 250-meter plastic *ShallowCAT* housing.

#### (Specification)

##### Measurement Range

Conductivity: 0 - 7 S/m (0 - 70 mS/cm)

Temperature: -5 to 35 °C

Optional Pressure: 7000 (meters of deployment depth capability)

##### Initial Accuracy

Conductivity: 0.0003 S/m (0.003 mS/cm)

Temperature: 0.002 °C

Optional Pressure: 0.1% of full scale range

Typical Stability (per month)



Conductivity: 0.0003 S/m (0.003 mS/cm)  
Temperature: 0.0002 °C  
Optional Pressure: 0.004% of full scale range

Resolution

Conductivity: 0.00001 S/m (0.0001 mS/cm)  
Temperature: 0.0001 °C  
Optional Pressure: 0.002% of full scale range

Time Resolution 1 second

Clock Accuracy 13 seconds/month

Quiescent Current \* 10 microamps

Optional External Input Power 0.5 Amps at 9-24 VDC

Housing, Depth Rating, and Weight (without pressure sensor)

Standard Titanium, 7000 m (23,000 ft)

Weight in air: 3.8 kg (8.3 lbs)

Weight in water: 2.3 kg (5.1 lbs)

(sampling parameter)

Sampling start time: Oct. 28<sup>th</sup> 2008 01:00:00

Sampling interval: 1800 seconds

(5) AREC DO Sensor

AREC DO (Compact Optode) sensor is digital memory type and designed for mounting on the plankton net and instrument for mooring and so on. It is small and right weight for easy handling. Sampling interval is chosen between 1 and 30 seconds. The data is converted to personal computer using exclusive cable (serial port).

(Specification)

Model:	COMPACT-Optode
Sensor Type:	Fluorescence quenching
Operating Range:	0 ~ 120%
Precision:	0.4%
Accuracy:	within 5%
Memory:	2Mbyte flash memory
Battery:	lithium battery 7Ah
Battery Life:	172800 data
Sample interval:	1,2,5,10,15,20 and 30 seconds
Diameter:	54mm
Length:	272mm
Main Material:	titanium
Weight in water:	0.6kg
Broken Pressure:	60MPa

### 3.1.3 Sampling schedule

Sampling schedule of time-series sediment traps at stations K2 and S1 are as follows:

K2			
	21cup		26cup
	500 m, 4810 m		200m
Int	16		16
1	2011.7.5	1	2011.7.5
2	2011.7.21	2	2011.7.21
3	2011.8.6	3	2011.8.6
4	2011.8.22	4	2011.8.22
5	2011.9.7	5	2011.9.7
6	2011.9.23	6	2011.9.23
7	2011.10.9	7	2011.10.9
8	2011.10.25	8	2011.10.25
9	2011.11.10	9	2011.11.10
10	2011.11.26	10	2011.11.26
11	2011.12.12	11	2011.12.12
12	2011.12.28	12	2011.12.28
13	2012.1.13	13	2012.1.13
14	2012.1.29	14	2012.1.29
15	2012.2.14	15	2012.2.14
16	2012.3.1	16	2012.3.1
17	2012.3.17	17	2012.3.17
18	2012.4.2	18	2012.4.2
19	2012.4.18	19	2012.4.18
20	2012.5.4	20	2012.5.4
21	2012.5.20	21	2012.5.20
	2012.6.5	22	2012.6.5
		23	2012.6.21
		24	2012.7.7
		25	2012.7.23
		26	2012.8.8
			2012.8.24

K2	
Deployment date	2011.7.4
MR12-** start date	ca. 2012.6.01
Recovery date	ca. 2012.6.04

S1			
	21cup		26cup
	500 m, 4810 m		200m
Int	16		16
1	2011.7.30	1	2011.7.30
2	2011.8.15	2	2011.8.15
3	2011.8.31	3	2011.8.31
4	2011.9.16	4	2011.9.16
5	2011.10.2	5	2011.10.2
6	2011.10.18	6	2011.10.18
7	2011.11.3	7	2011.11.3
8	2011.11.19	8	2011.11.19
9	2011.12.5	9	2011.12.5
10	2011.12.21	10	2011.12.21
11	2012.1.6	11	2012.1.6
12	2012.1.22	12	2012.1.14
13	2012.2.7	13	2012.1.22
14	2012.2.23	14	2012.1.30
15	2012.3.10	15	2012.2.7
16	2012.3.26	16	2012.2.15
17	2012.4.11	17	2012.2.23
18	2012.4.27	18	2012.3.2
19	2012.5.13	19	2012.3.10
20	2012.5.29	20	2012.3.18
21	2012.6.14	21	2012.3.26
	2012.6.30	22	2012.4.11
		23	2012.4.27
		24	2012.5.13
		25	2012.5.29
		26	2012.6.14
			2012.6.30

S1	
Deployment date	2011.7.29
MR12-02 start date	ca. 2012.6.01
Recovery date	ca. 2012.6.20

S1-500mは2000年問題に対応していない古いソフトなので、今年（2011年）を1990年として設定した。

### 3.1.4 Preliminary results

#### (1) Water depth of 200m sediment trap and top buoy

Depth of 200 m sediment trap at station K2 and top buoy at station S1 were monitored by a depth sensor (RIGO RMD) each two hours during deployment. Just after sediment trap mooring system at station K2 was deployed, the trap depth was approximately 210 m (Fig. 3.1.4.1). Trap depth gradually decreased toward July 2011 and the depth of 200 m sediment trap became approximately 200 m. Variation of water depth during deployment was at most 5 m at station K2.

Water depth of top buoy, which is located approximately 50 m over 200 m sediment trap, at station S1 was 165 m when mooring system was deployed (Fig. 3.1.4.1). It is indicative of that 200 m sediment trap at station S1 was located at approximately 215 m. Compared to water depth of 200 m sediment trap at K2, variability of top buoy at S1 was larger: amplitude of water depth sometimes became larger than 10 m in last December / January and top buoy was deepened to 190 m (by 30 m) in March 2011. Water depth of top buoy also decreased gradually and the final water depth was approximately 158 m, approximately 7 m shallower than the initial depth. Decrease of water depth at both mooring systems are likely attributed to extension of nylon rope used during approximately 9 months deployment.

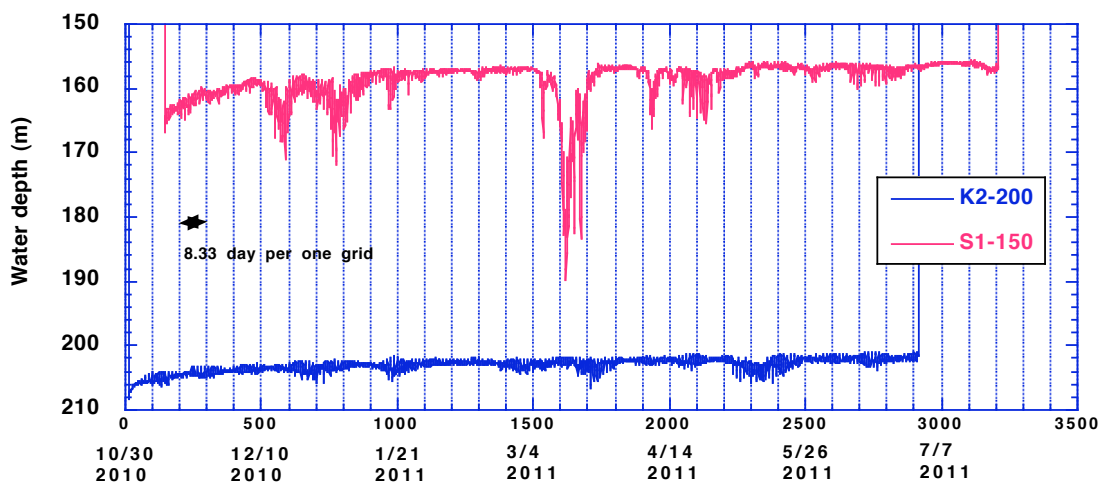


Fig. 3.1.4.1 Seasonal variability in water depths of 200 m sediment trap (K2) and top

#### (2) Sediment trap (Station K2)

Sediment trap mooring system deployed in last October 2010 was recovered at station K2. Time-series sediment traps at 200m, 500m and 4810m collected seasonal sinking particles each 6 – 12 days interval. At 200m, relatively higher flux was observed in the early period after sediment trap started sampling in autumn. However amount of collected materials decreased since then (Fig. 3.1.4.2). Distinct seasonal variability in sediment trap materials at 500 m and 4810 m did not appear. Compared to other years, amount and seasonal variability of sinking materials collected looked smaller. Moreover synchronization of seasonal variability between different depths was not seen either. Based on small decrease of nutrient

concentration from winter (not shown), it was suspected that highly productive period was late this year and sinking particles would increase in near future.

(Station S1)

Sediment trap mooring system deployed in last October 2010 was also recovered successfully at station S1. At 200m, relatively higher flux was observed in late February and April 2011 (Fig. 3.1.4.2). At 500m, similar seasonal variability was observed although variability was small. At 4810 m, high flux was observed in May 2011. Distinct synchronization of seasonal variability between different depths was not observed.

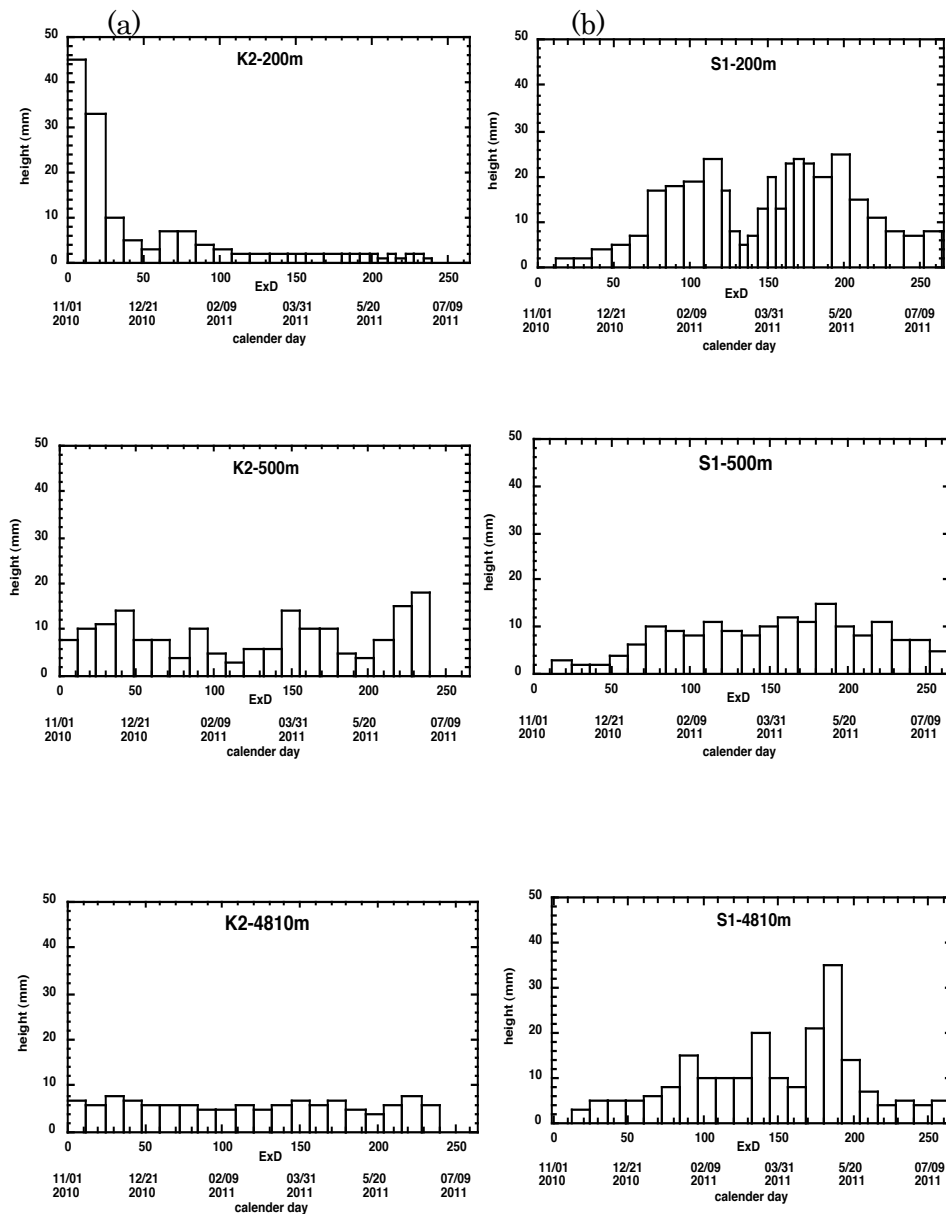


Fig. 3.1.4.2 Seasonal variability in sinking particle flux (a) K2-200m (upper) K2-500m (middle) K2-4810m (lower) and (b) S1-200m (upper) S1-500m (middle) S1-4810m (lower) . Vertical axis is height of collected materials in collecting cups.

### 3.2 Underwater profiling buoy system (Primary productivity profiler)

**Tetsuichi FUJIKI (JAMSTEC)**

**Toru IDAI (MWJ)**

**Tetsuya NAKAMURA (Nichiyu Giken Kogyo)**

#### (1) Objective

An understanding of the variability in phytoplankton productivity provides a basic knowledge of how aquatic ecosystems are structured and functioning. The primary productivity of the world oceans has been measured mostly by the radiocarbon tracer method or the oxygen evolution method. As these traditional methods use the uptake of radiocarbon into particulate matter or changes in oxygen concentration in the bulk fluid, measurements require bottle incubations for periods ranging from hours to a day. This methodological limitation has hindered our understanding of the variability of oceanic primary productivity. To overcome these problems, algorithms for estimating primary productivity by using satellite ocean color imagery have been developed and improved. However, one of the major obstacles to the development and improvement of these algorithms is a lack of *in situ* primary productivity data to verify the satellite estimates.

During the past decade, the utilization of active fluorescence techniques in biological oceanography has brought marked progress in our understanding of phytoplankton photosynthesis in the oceans. Above all, fast repetition rate (FRR) fluorometry reduces the primary electron acceptor ( $Q_a$ ) in photosystem (PS) II by a series of subsaturating flashlets and can measure a single turnover fluorescence induction curve in PSII. The PSII parameters derived from the fluorescence induction curve provide information on the physiological state related to photosynthesis and can be used to estimate gross primary productivity. FRR fluorometry has several advantages over the above-mentioned traditional methods. Most importantly, because measurements made by FRR fluorometry can be carried out without the need for time-consuming bottle incubations, this method enables real-time high-frequency measurements of primary productivity. In addition, the FRR fluorometer can be used in platform systems such as moorings, drifters, and floats.

The current study aimed to assess the vertical and temporal variations in PSII parameters and primary productivity in the western Pacific, by using an underwater profiling buoy system that uses the FRR fluorometer (system name: Primary productivity profiler)

#### (2) Methods

##### a) Primary productivity profiler

The primary productivity profiler (original design by Nichiyu Giken Kogyo) consisted mainly of an observation buoy equipped with a submersible FRR fluorometer (Diving Flash, Kimoto Electric), a scalar irradiance sensor (QSP-2200, Biospherical Instruments), a CTD sensor (MCTD, Falmouth Scientific) and a dissolved oxygen sensor (Compact Optode, Alec Electronics), an underwater winch, an acoustic Doppler current profiler (Workhorse Long Ranger, Teledyne RD Instruments) and an acoustic releaser (Fig. 1). The observation buoy moved between the winch depth and the surface at a rate of  $0.2 \text{ m s}^{-1}$  and measured the vertical profiles of phytoplankton fluorescence, irradiance, temperature, salinity and dissolved oxygen. The profiling rate of the observation buoy was set to  $0.2 \text{ m s}^{-1}$  to detect small-scale variations (approx. 0.5 m) in the vertical profile. To minimize biofouling of instruments, the underwater

winch was placed below the euphotic layer so that the observation buoy was exposed to light only during the measurement period. In addition, the vertical migration of observation buoy reduced biofouling of instruments.

b) Measurement principle of FRR fluorometer

The FRR fluorometer consists of closed dark and open light chambers that measure the fluorescence induction curves of phytoplankton samples in darkness and under actinic illumination. To allow relaxation of photochemical quenching of fluorescence, the FRR fluorometer allows samples in the dark chamber to dark adapt for about 1 s before measurements. To achieve cumulative saturation of PSII within 150  $\mu$ s — i.e., a single photochemical turnover — the instrument generates a series of subsaturating blue flashes at a light intensity of 25 mmol quanta  $\text{m}^{-2} \text{s}^{-1}$  and a repetition rate of about 250 kHz  $\text{s}^{-1}$ . The PSII parameters are derived from the single-turnover-type fluorescence induction curve by using the numerical fitting procedure described by Kolber et al. (1998). Analysis of fluorescence induction curves measured in the dark and light chambers provides PSII parameters such as fluorescence yields, photochemical efficiency and effective absorption cross section of PSII, which are indicators of the physiological state related to photosynthesis. Using the PSII parameters, the rate of photosynthetic electron transport and the gross primary productivity can be estimated.

c) Site description and observations

The primary productivity profiler deployed at station S1 in MR11-02 was recovered on 26 July 2011 (UTC). In addition, the primary productivity profiler was newly-deployed on 29 July 2011 (UTC) (Fig. 2, target position: 29° 56.268 N, 144° 58.513 E, 5915 m; actual position: 29° 55.567 N, 144° 59.560 E, 5901 m). The measurements began on 2 August 2011 and will continue until 31 May 2012.

Measurement schedule at station S1 (Japan time)

1. 11/08/02 02:00	2. 11/08/02 11:00	3. 11/08/05 11:00	4. 11/08/08 02:00
5. 11/08/08 11:00	6. 11/08/11 11:00	7. 11/08/14 02:00	8. 11/08/14 11:00
9. 11/08/17 11:00	10. 11/08/20 02:00	11. 11/08/20 11:00	12. 11/08/23 11:00
13. 11/08/26 02:00	14. 11/08/26 11:00	15. 11/08/29 11:00	16. 11/09/01 02:00
17. 11/09/01 11:00	18. 11/09/04 11:00	19. 11/09/07 02:00	20. 11/09/07 11:00
21. 11/09/10 11:00	22. 11/09/13 02:00	23. 11/09/13 11:00	24. 11/09/16 11:00
25. 11/09/19 02:00	26. 11/09/19 11:00	27. 11/09/22 11:00	28. 11/09/25 02:00
29. 11/09/25 11:00	30. 11/09/28 11:00	31. 11/10/01 02:00	32. 11/10/01 11:00
33. 11/10/04 11:00	34. 11/10/07 02:00	35. 11/10/07 11:00	36. 11/10/10 11:00
37. 11/10/13 02:00	38. 11/10/13 11:00	39. 11/10/16 11:00	40. 11/10/19 02:00
41. 11/10/19 11:00	42. 11/10/22 11:00	43. 11/10/25 02:00	44. 11/10/25 11:00
45. 11/10/28 11:00	46. 11/10/31 02:00	47. 11/10/31 11:00	48. 11/11/03 11:00
49. 11/11/06 02:00	50. 11/11/06 11:00	51. 11/11/09 11:00	52. 11/11/12 02:00
53. 11/11/12 11:00	54. 11/11/15 11:00	55. 11/11/18 02:00	56. 11/11/18 11:00
57. 11/11/21 11:00	58. 11/11/24 02:00	59. 11/11/24 11:00	60. 11/11/27 11:00
61. 11/11/30 02:00	62. 11/11/30 11:00	63. 11/12/03 11:00	64. 11/12/06 02:00
65. 11/12/06 11:00	66. 11/12/09 11:00	67. 11/12/12 02:00	68. 11/12/12 11:00
69. 11/12/15 11:00	70. 11/12/18 02:00	71. 11/12/18 11:00	72. 11/12/21 11:00

73. 11/12/24 02:00	74. 11/12/24 11:00	75. 11/12/27 11:00	76. 11/12/30 02:00
77. 11/12/30 11:00	78. 12/01/02 11:00	79. 12/01/05 02:00	80. 12/01/05 11:00
81. 12/01/08 11:00	82. 12/01/11 02:00	83. 12/01/11 11:00	84. 12/01/14 11:00
85. 12/01/17 02:00	86. 12/01/17 11:00	87. 12/01/20 11:00	88. 12/01/23 02:00
89. 12/01/23 11:00	90. 12/01/26 11:00	91. 12/01/29 02:00	92. 12/01/29 11:00
93. 12/02/01 11:00	94. 12/02/04 02:00	95. 12/02/04 11:00	96. 12/02/07 11:00
97. 12/02/10 02:00	98. 12/02/10 11:00	99. 12/02/13 11:00	100. 12/02/16 02:00
101. 12/02/16 11:00	102. 12/02/19 11:00	103. 12/02/22 02:00	104. 12/02/22 11:00
105. 12/02/25 11:00	106. 12/02/28 02:00	107. 12/02/28 11:00	108. 12/03/02 11:00
109. 12/03/05 02:00	110. 12/03/05 11:00	111. 12/03/08 11:00	112. 12/03/11 02:00
113. 12/03/11 11:00	114. 12/03/14 11:00	115. 12/03/17 02:00	116. 12/03/17 11:00
117. 12/03/20 11:00	118. 12/03/23 02:00	119. 12/03/23 11:00	120. 12/03/26 11:00
121. 12/03/29 02:00	122. 12/03/29 11:00	123. 12/04/01 11:00	124. 12/04/04 02:00
125. 12/04/04 11:00	126. 12/04/07 11:00	127. 12/04/10 02:00	128. 12/04/10 11:00
129. 12/04/13 11:00	130. 12/04/16 02:00	131. 12/04/16 11:00	132. 12/04/19 11:00
133. 12/04/22 02:00	134. 12/04/22 11:00	135. 12/04/25 11:00	136. 12/04/28 02:00
137. 12/04/28 11:00	138. 12/05/01 11:00	139. 12/05/04 02:00	140. 12/05/04 11:00
141. 12/05/07 11:00	142. 12/05/10 02:00	143. 12/05/10 11:00	144. 12/05/13 11:00
145. 12/05/16 02:00	146. 12/05/16 11:00	147. 12/05/19 11:00	148. 12/05/22 02:00
149. 12/05/22 11:00	150. 12/05/25 11:00	151. 12/05/28 02:00	152. 12/05/28 11:00
153. 12/05/31 11:00			

### (3) Preliminary results

The operating condition of observation buoy in the primary productivity profiler recovered from station S1 was shown in figure 3.

### (4) Data archives

The data will be submitted to JAMSTEC Data Management Office.

### (5) References

Kolber, Z. S., O. Prášil and P. G. Falkowski. 1998. Measurements of variable chlorophyll fluorescence using fast repetition rate techniques: defining methodology and experimental protocols. *Biochim. Biophys. Acta*. 1367: 88-106.

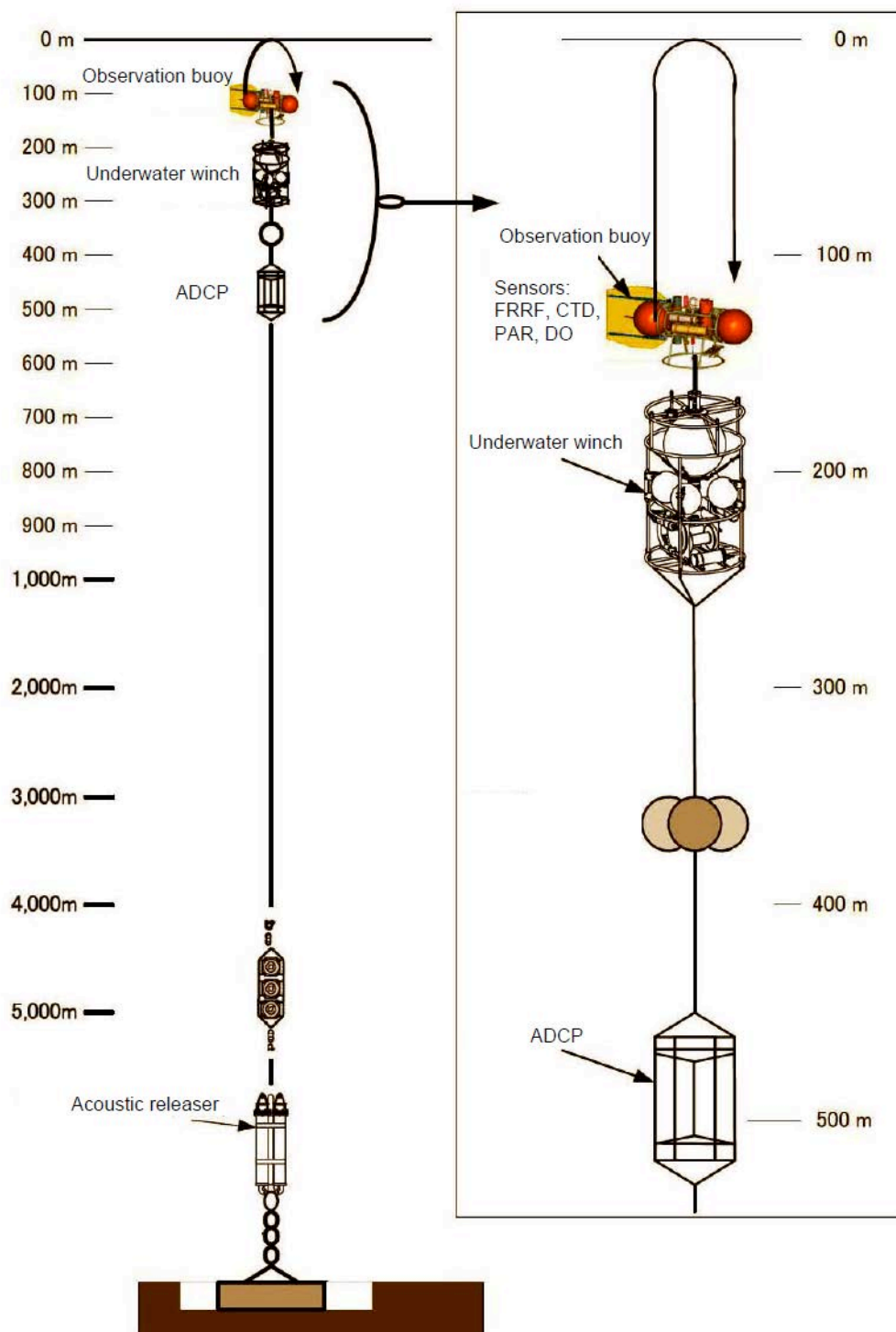
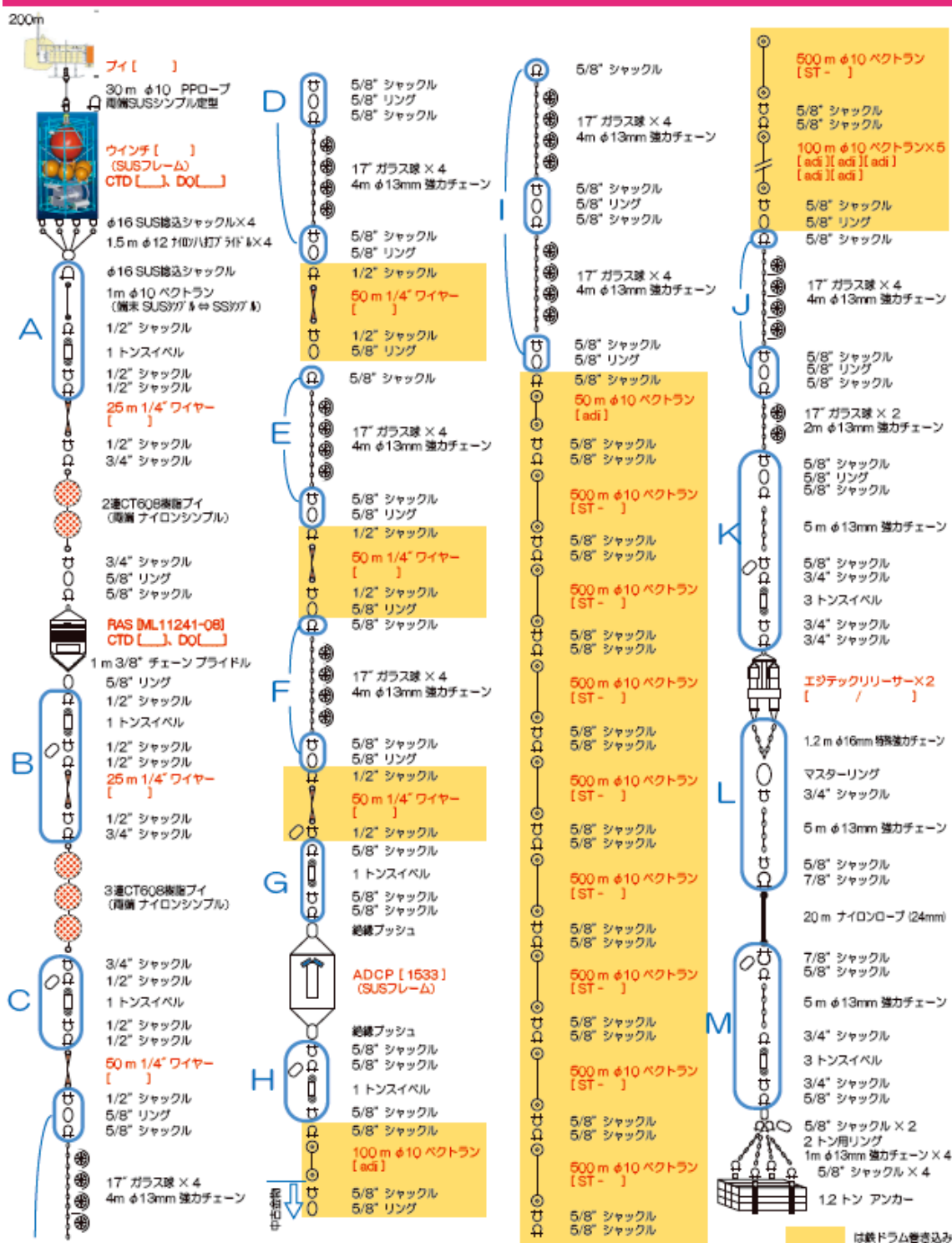


Figure 1. Schematic diagram of the primary productivity profiler.





Project on Ocean Productivity Profiling System

設計水深 5912.0m 2011/06/08 版

Figure 2. Detailed design of the primary productivity profiler deployed at station S1 in MR11-05.

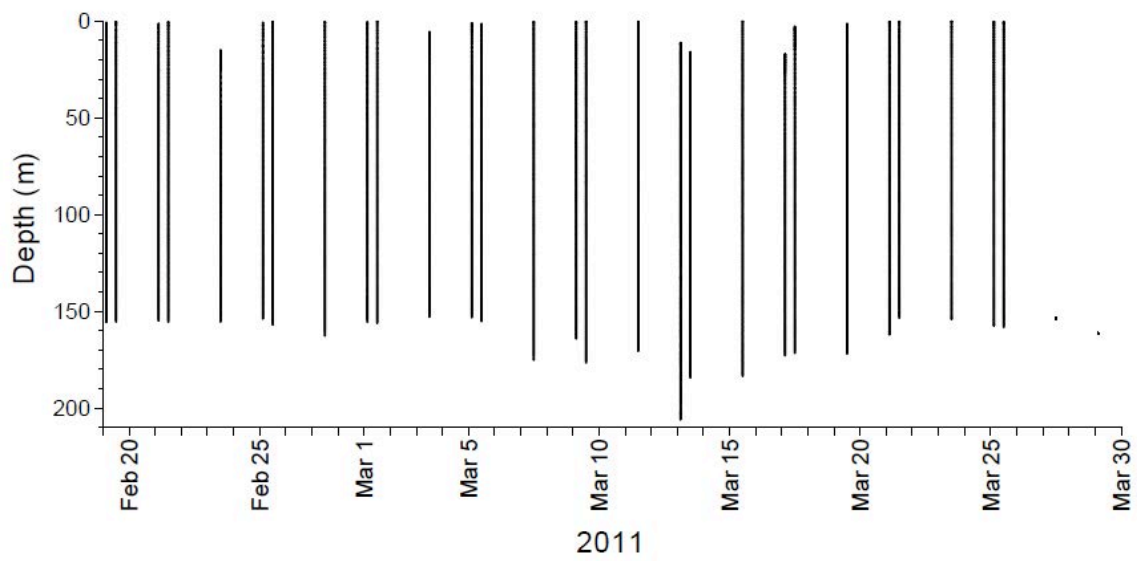


Figure 3. The operating condition of observation buoy in the primary productivity profiler recovered from station S1.

### 3.3 WHOI ST mooring system

**Makio HONDA (JAMSTEC)**

**Cris GERMAN (Woods Hole Oceanographic Institution, WHOI)**

**Steven J. MANGANINI (WHOI)**

In order to collect time-series sinking particle and certify how and when artificial radioactive nuclides are transported vertically near the Fukushima Daiichi nuclear power plant, time-series sediment traps were deployed at approximately 500 m and 1000 m at station F1. Sampling interval are 16 days at 1000 m and 32 days at 500 m (16 days in March and April 2012). Before deployment, collecting cups were filled up with seawater based 10% buffered formalin. This observation is cooperative research with Woods Hole Oceanographic Institution (PI: Cris German). This mooring system will be recovered in June 2012 during MIRAI MR12-02 cruise.

Table 3.3.1 design of ST mooring system



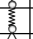


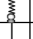


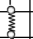


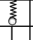
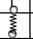
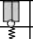


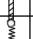
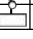







Mooring I.D.		Fukushima WHOI Sediment Trap Mooring (F1)								
Water Depth		1300.00								
Specifications										
Item #	Description	Weight	Quantity	Length	Weight	Length	Bottom	Surface	Mooring	Mooring
		(lb/m,ea)	#	Item	Item	(m)	mab	mbs	(lb)top to bottom	(lb)bottom to top
										no anchor
	1 GLASS BALLS 17"on 1m,3/8 chain	-50.00	18.00	18.00	-900.00	18.00	842.04	457.96	-900.00	-618.56
	2 Current Meter	18.00	1.00	1.00	18.00	19.00	824.04	475.96	-882.00	281.44
	3 wire rope 1/4"	0.27	1.00	20.00	5.32	39.00	823.04	476.96	-876.68	263.44
	4 chain, 3/8"	4.49	1.00	2.00	8.98	41.00	803.04	496.96	-867.70	258.12
	5 bridle (3-wire rope)	10.16	1.00	1.00	10.16	42.00	801.04	498.96	-857.54	249.14
	6 SEDIMENT TRAP MK7	121.00	1.00	1.52	121.00	43.52	800.04	499.96	-736.54	238.98
	7 bridle,(3-1m 3/8 chain)	23.20	1.00	1.00	23.20	44.52	798.52	501.48	-713.34	117.98
	8 chain, 3/8"	4.49	1.00	2.00	8.98	46.52	797.52	502.48	-704.36	94.78
	9 wire rope 1/4"	0.27	1.00	461.00	122.63	507.52	795.52	504.48	-581.73	85.80
	10 GLASS BALLS 17"on 1m,3/8 chain	-50.00	10.00	10.00	-500.00	517.52	334.52	965.48	-1081.73	-36.82
	11 Current Meter	18.00	1.00	1.00	18.00	518.52	324.52	975.48	-1063.73	463.18
	12 wire rope 1/4"	0.15	1.00	20.00	3.00	538.52	323.52	976.48	-1060.73	445.18
	13 chain, 3/8"	4.49	1.00	2.00	8.98	540.52	303.52	996.48	-1051.75	442.18
	14 bridle (3-wire rope)	10.16	1.00	1.00	10.16	541.52	301.52	998.48	-1041.59	433.20
	15 SEDIMENT TRAP MK7	121.00	1.00	1.52	121.00	543.04	300.52	999.48	-920.59	423.04
	16 bridle,(3-1m 3/8 chain)	23.20	1.00	1.00	23.20	544.04	299.00	1001.00	-897.39	302.04
	17 chain, 3/8"	4.49	1.00	2.00	8.98	546.04	298.00	1002.00	-888.41	278.84
	18 wire rope 1/4"	0.27	1.00	176.00	46.82	722.04	296.00	1004.00	-841.60	269.86
	19 chain, 3/8"	4.49	1.00	2.00	8.98	724.04	120.00	1180.00	-832.62	223.04
	20 ACOUSTIC RELEASE (ORE Tandem)	160.00	1.00	1.00	160.00	725.04	118.00	1182.00	-672.62	214.06
	21 chain, 3/8"	4.49	1.00	2.00	8.98	727.04	117.00	1183.00	-663.64	54.06
	22 wire rope 1/4"	0.27	1.00	50.00	13.30	777.04	115.00	1185.00	-650.34	45.08
	23 wire rope 1/4"	0.27	1.00	50.00	13.30	827.04	65.00	1235.00	-637.04	31.78
	24 nylon rope,3/4"	0.05	1.00	10.00	0.52	837.04	15.00	1285.00	-636.52	18.48
	25 chain, 3/8"	4.49	1.00	4.00	17.96	841.04	5.00	1295.00	-618.56	17.96
	26 ANCHOR	0.89	2300.00	1.00	2047.00	842.04	1.00	1299.00	1428.44	

Table 3.3.2 Time-schedule of sampling

F1-ST schedule

	1000m		500m	
	21		13	
	16		32	
1	2011.7.19	1	2011.7.19	
2	2011.8.4	2	2011.8.20	
3	2011.8.20	3	2011.9.21	
4	2011.9.5	4	2011.10.23	
5	2011.9.21	5	2011.11.24	
6	2011.10.7	6	2011.12.26	
7	2011.10.23	7	2012.1.27	
8	2011.11.8	8	2012.2.28	
9	2011.11.24	9	2012.3.15	interval
10	2011.12.10	10	2012.3.31	16
11	2011.12.26	11	2012.4.16	
12	2012.1.11	12	2012.5.2	
13	2012.1.27	13	2012.5.18	
14	2012.2.12		2012.6.19	
15	2012.2.28			
16	2012.3.15			
17	2012.3.31			
18	2012.4.16			
19	2012.5.2			
20	2012.5.18			
21	2012.6.3			
	2012.6.19			

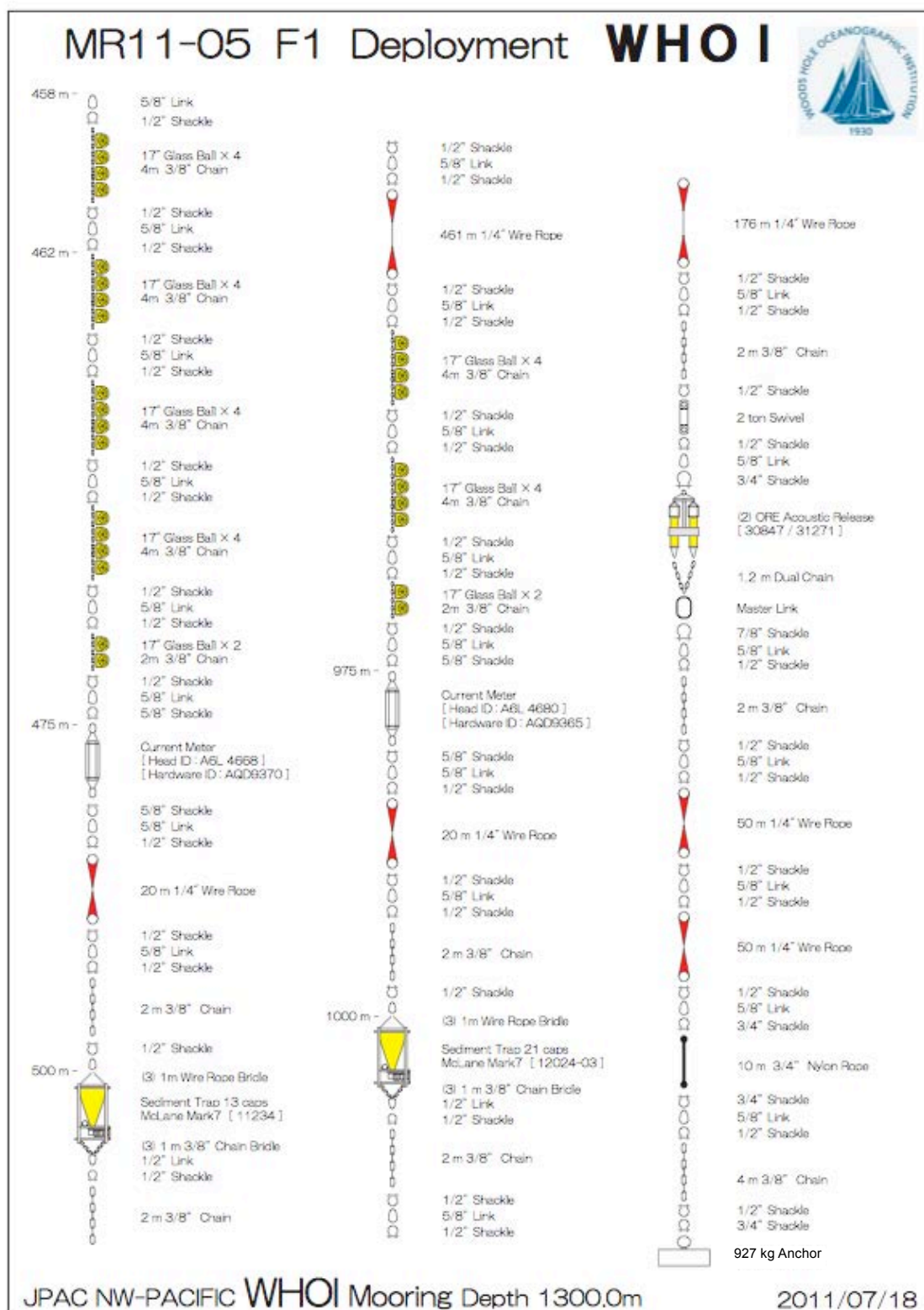


Fig. 3.3.1 Schematic diagram of ST mooring system

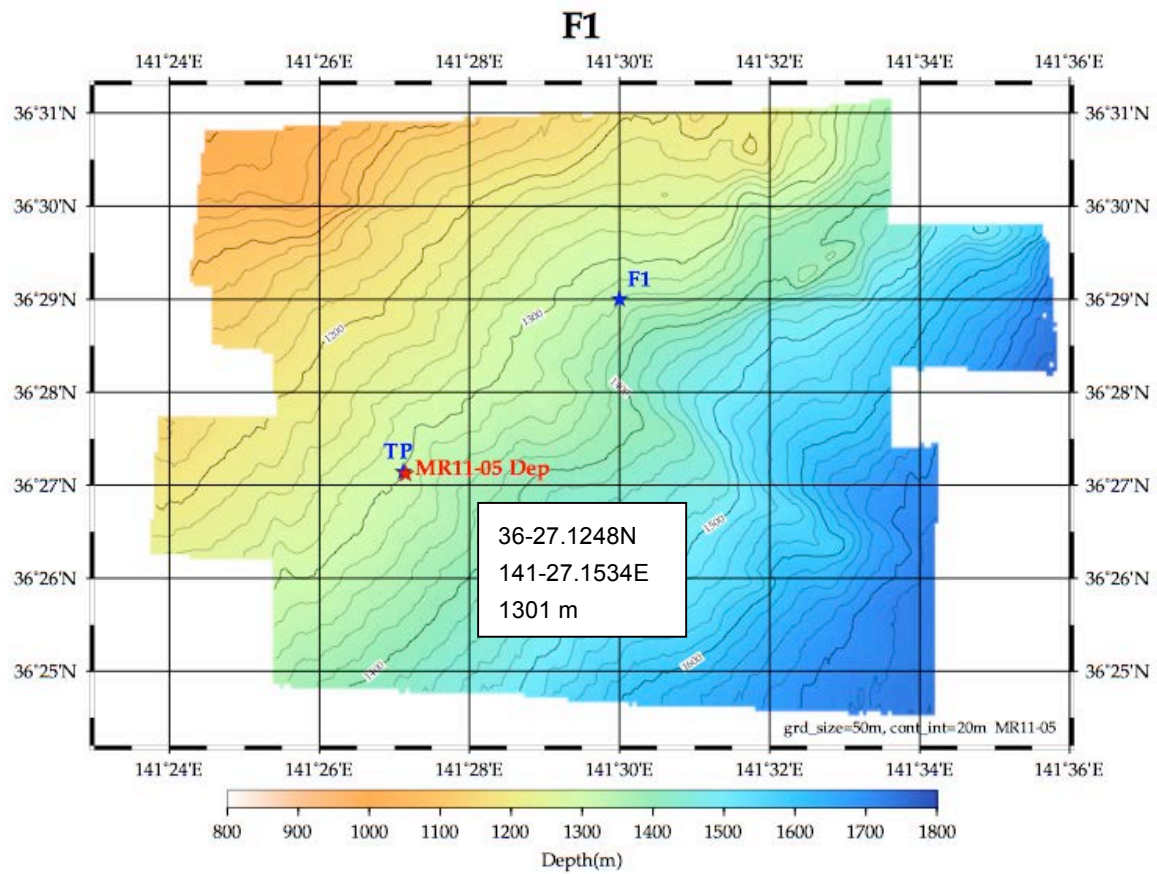


Fig. 3.3.2 Deployment position of F1-ST mooring



### 3.4 Phytoplankton

#### 3.4.1 Chlorophyll *a* measurements by fluorometric determination

Kazuhiko MATSUMOTO (JAMSTEC RIGC)

Shoko TATAMISASHI (MWJ)

##### 1. Objective

Phytoplankton biomass can estimate as the concentration of chlorophyll *a* (chl-*a*), because all oxygenic photosynthetic plankton contain chl-*a*. Phytoplankton exist various species in the ocean, but the species are roughly characterized by their cell size. The objective of this study is to investigate the vertical distribution of phytoplankton and their size fractionations as chl-*a* by using the fluorometric determination.

##### 2. Sampling

Samplings of total chl-*a* were conducted from 16 depths between the surface and 200 m at all observational stations. At the cast for primary production, water samples were collected at about ten depths from among the surface, 0.1%~60% light depths relative to the surface and at about six other depths between the surface and 200 m at the station of S1, K2 and F1.

##### 3. Instruments and Methods

Water samples (0.5L) for total chl-*a* were filtered (<0.02 MPa) through 25mm-diameter Whatman GF/F filter. Size-fractionated chl-*a* were obtained by sequential filtration (<0.02 MPa) of 1-L water sample through 10- $\mu$ m, 3- $\mu$ m and 1- $\mu$ m polycarbonate filters (47-mm diameter) and Whatman GF/F filter (25-mm diameter). Phytoplankton pigments retained on the filters were immediately extracted in a polypropylene tube with 7 ml of N,N-dimethylformamide (Suzuki and Ishimaru, 1990). Those tubes were stored at -20°C under the dark condition to extract chl-*a* for 24 hours or more.

Fluorescences of each sample were measured by Turner Design fluorometer (10-AU-005), which was calibrated against a pure chl-*a* (Sigma-Aldrich Co.). We applied two kind of fluorometric determination for the samples of total chl-*a*: “Non-acidification method” (Welschmeyer, 1994) and “Acidification method” (Holm-Hansen *et al.*, 1965). Size-fractionated samples were applied only “Non-acidification method”. Analytical conditions of each method were listed in table 1.

##### 4. Preliminary Results

The results of total chl-*a* at station S1, K2 and F1 were shown in Figure 1 and 2. The results of total chl-*a* at station KNOT, JKEO and F1 were shown in Figure 3. The results of size fractionated chl-*a* were shown in Figure4.

##### 6. Data archives

The processed data file of pigments will be submitted to the JAMSTEC Data Integration and Analysis Group (DIAG) within a restricted period. Please ask PI for the latest information.

##### 7. Reference

- Suzuki, R., and T. Ishimaru (1990), An improved method for the determination of phytoplankton chlorophyll using N, N-dimethylformamide, *J. Oceanogr. Soc. Japan*, 46, 190-194.
- Holm-Hansen, O., Lorenzen, C. J., Holmes, R.W. and J. D. H. Strickland (1965), Fluorometric determination of chlorophyll. *J. Cons. Cons. Int. Explor. Mer.* 30, 3-15.
- Welschmeyer, N. A. (1994), Fluorometric analysis of chlorophyll *a* in the presence of chlorophyll *b* and pheopigments. *Limnol. Oceanogr.* 39, 1985-1992.

**Table 1.** Analytical conditions of “Non-acidification method” and “Acidification method” for chlorophyll *a* with Turner Designs fluorometer (10-AU-005).

	Non-acidification method	Acidification method
Excitation filter (nm)	436	340-500
Emission filter (nm)	680	>665
Lamp	Blue Mercury Vapor	Daylight White



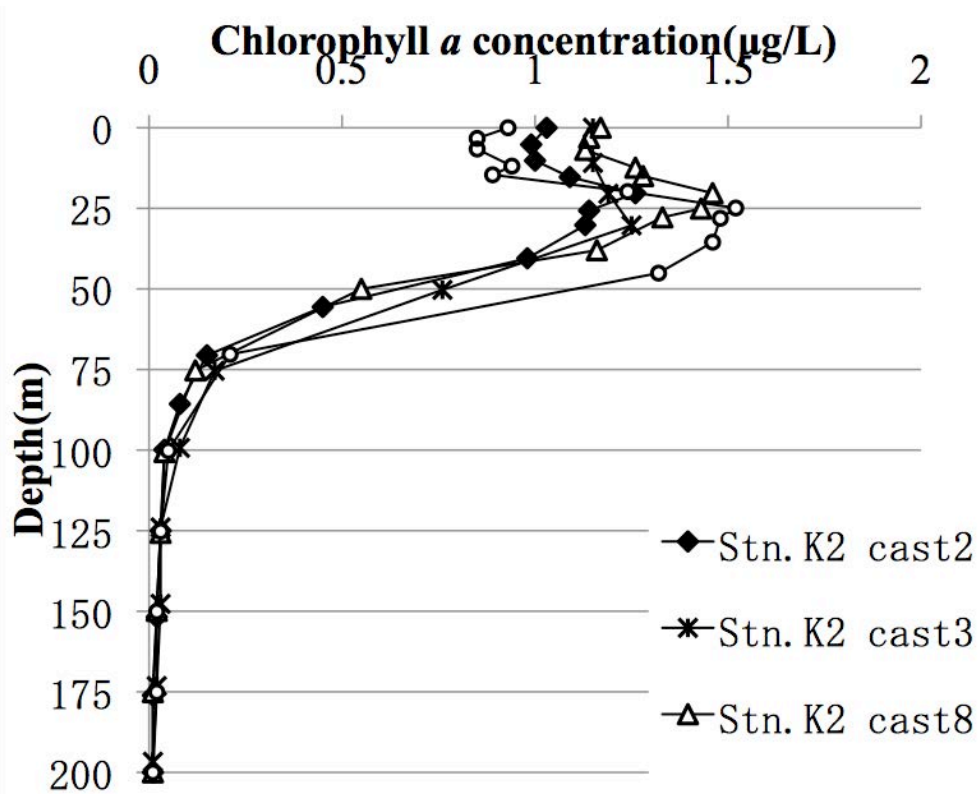


Figure1. Vertical distribution of chlorophyll *a* at Stn.K2

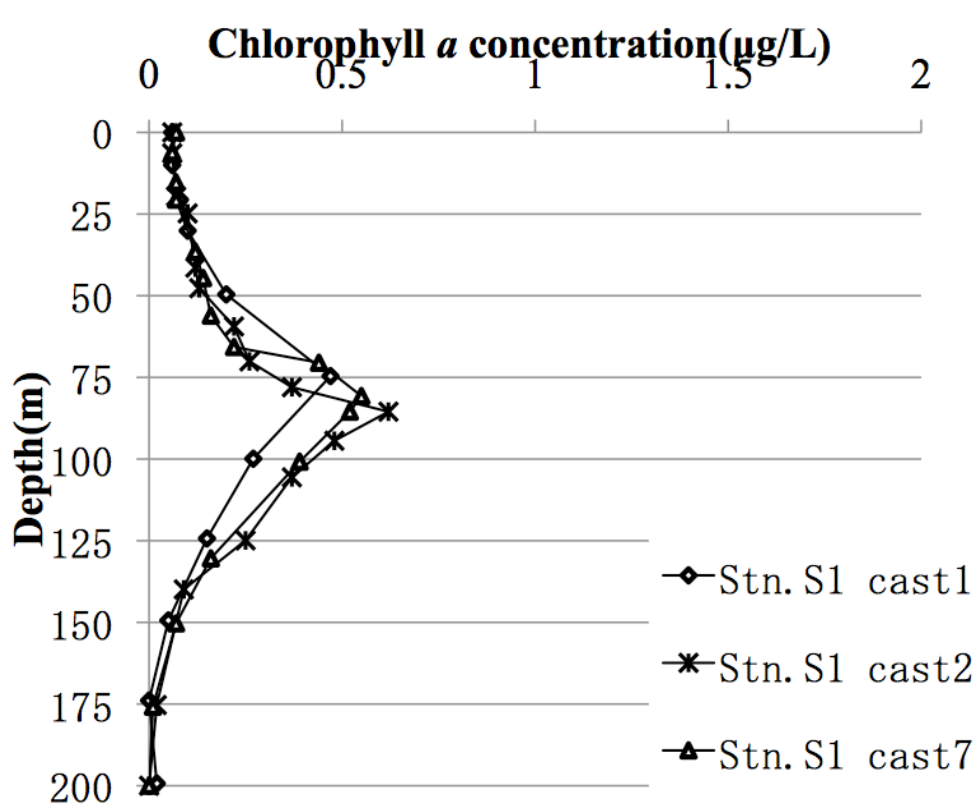
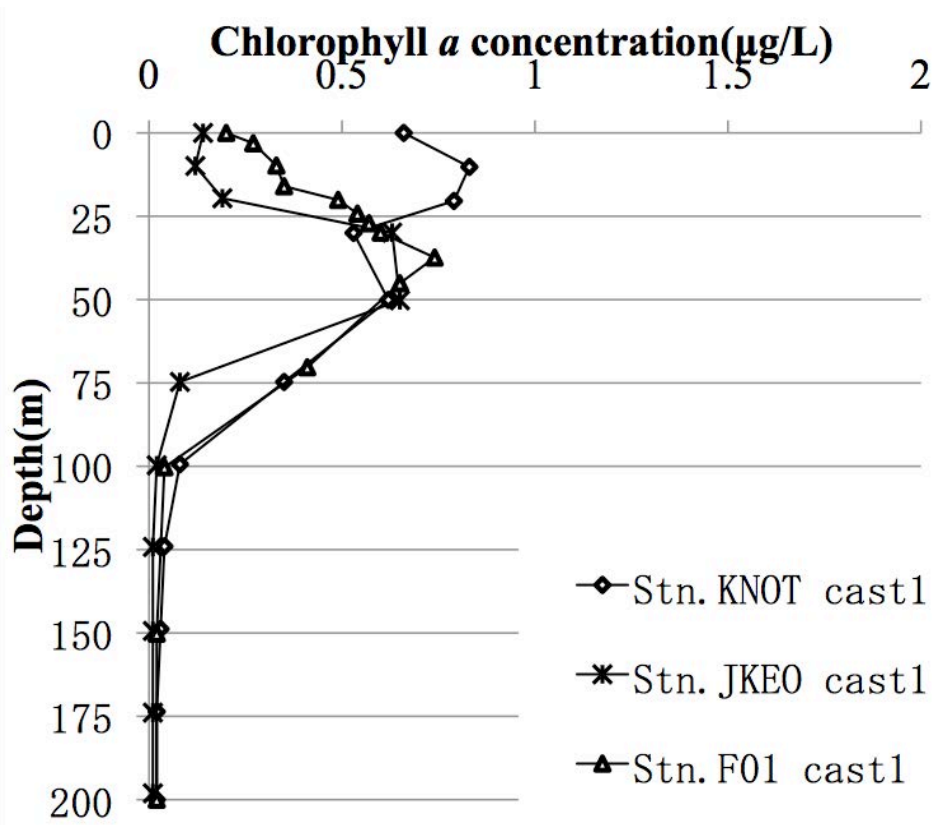


Figure2. Vertical distribution of chlorophyll *a* at Stn.S1



**Figure3.** Vertical distribution of chlorophyll *a* at Stn.KNOT, JKEO and F1

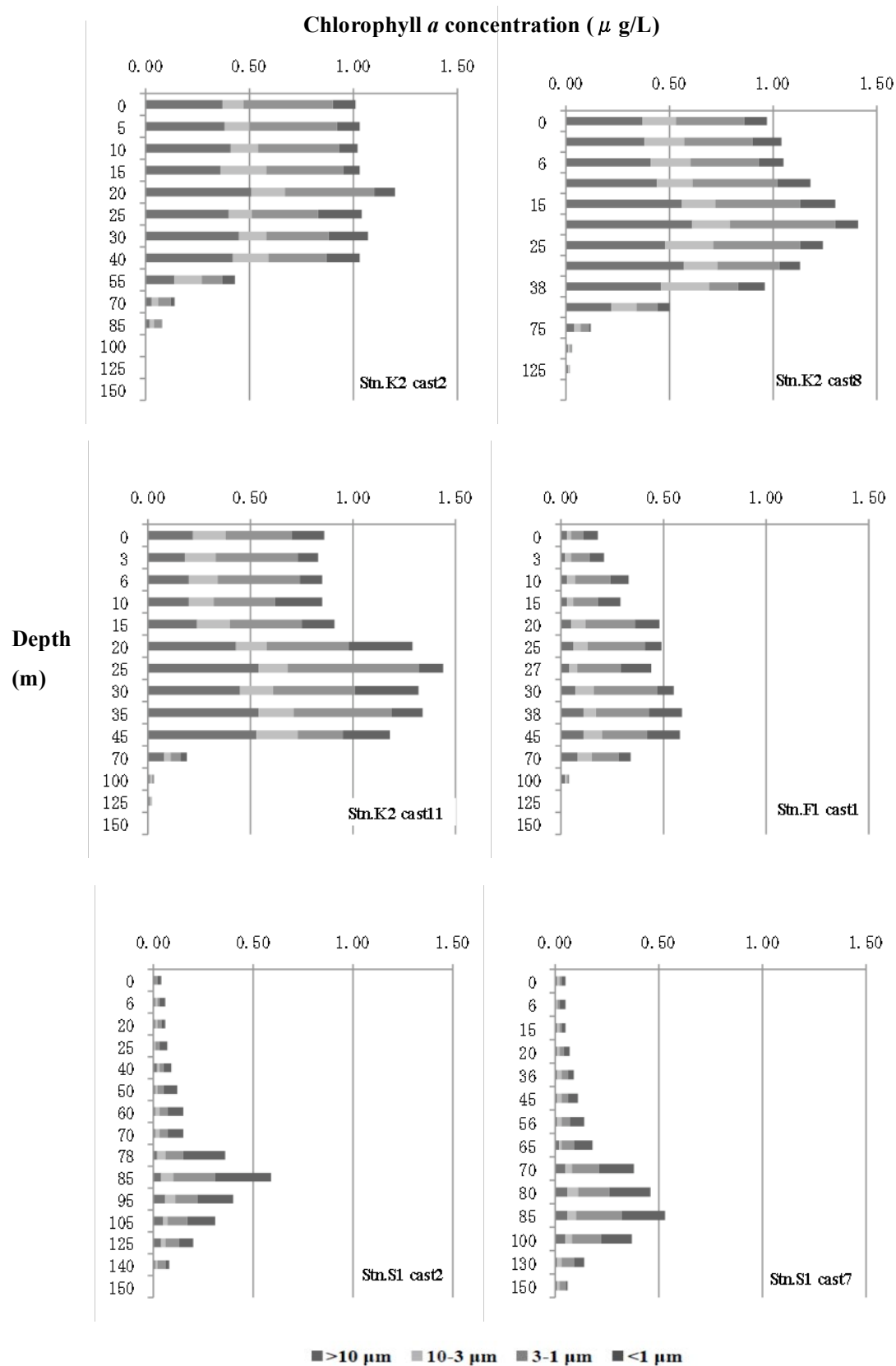


Figure 4 Vertical distribution of size-fractionated chlorophyll *a*

### 3.4.2. HPLC measurements of marine phytoplankton pigments

**Kazuhiko MATSUMOTO (JAMSTEC RIGC)**

**Hironori SATO (MWJ)**

**Shoko TATAMISASHI (MWJ)**

#### (1) Objective

The chemotaxonomic assessment of phytoplankton populations present in natural seawater requires taxon-specific algal pigments as good biochemical markers. A high-performance liquid chromatography (HPLC) measurement is an optimum method for separating and quantifying phytoplankton pigments in natural seawater. In this cruise, we measured the marine phytoplankton pigments by HPLC to investigate the marine phytoplankton community structure in the western North Pacific.

#### (2) Methods, Apparatus and Performance

Seawater samples were collected from 11 depths between the surface and 200 m at the cast for the primary production. Sampling depths were determined by the light intensity at eight depths from among the surface, 0.5%, 1%, 2.5%, 5%, 10%, 25%, 50% light depths relative to the surface and at three other depths between the surface and 200 m. Seawater samples were collected using Niskin bottles, except for the surface water, which was taken by a bucket. Seawater samples were filtered (<0.02 MPa) through the 47-mm diameter Whatman GF/F filter (Filtration volume was adjusted to 2-5 liters). To remove retaining seawater in the sample filters, GF/F filters were vacuum-dried in a freezer (0 °C) within 6 hours. Subsequently, phytoplankton pigments retained on a filter were extracted in a glass tube with 4 ml of N,N-dimethylformamide (HPLC-grade) for at least 24 hours in a freezer (-20 °C), and analyzed by HPLC within a few days.

Residua cells and filter debris were removed through polypropylene syringe filter (pore size: 0.2 µm) before the analysis. The samples injection of 500 µl was conducted by auto-sampler with the mixture of extracted pigments (350 µl), pure water (150 µl) and internal standard (10 µl). Phytoplankton pigments were quantified based on C<sub>8</sub> column method containing pyridine in the mobile phase (Zapata *et al.*, 2000).

##### (i) HPLC System

HPLC System was composed by Agilent 1200 modular system, G1311A Quaternary pump (low-pressure mixing system), G1329A auto-sampler and G1315D photodiode array detector.

##### (ii) Stationary phase

Analytical separation was performed using a YMC C<sub>8</sub> column (150×4.6 mm). The column was thermostatted at 35 °C in the column heater box.

##### (iii) Mobile phases

The eluant A was a mixture of methanol: acetonitrile: aqueous pyridine solution (0.25M pyridine), (50:25:25, v:v:v). The eluant B was a mixture of methanol: acetonitrile: acetone (20:60:20, v:v:v). Organic solvents for mobile phases were used reagents of HPLC-grade.

(iv) Calibrations

HPLC was calibrated using the standard pigments (Table 1). The solvents of pigment standards were displaced to N,N-dimethylformamide, but the concentrations were determined with spectrophotometer by using its extinction coefficient in ethanol or acetone.

(v) Internal standard

Ethyl-apo-8'-carotenoate was added into the samples prior to the injection as the internal standard. The mean chromatogram area and its coefficient of variation (CV) of internal standard were estimated as the following two samples:

Standard samples (Figure 1):  $225.2 \pm 3.2$  (n = 56), CV=1.4%

Seawater samples:  $232.7 \pm 6.8$  (n = 106), CV=2.9%

(vi) Pigment detection and identification

Chlorophylls and carotenoids were detected by photodiode array spectroscopy (350~800 nm). Pigment concentrations were calculated from the chromatogram area at different five channels (Table 1). First channel was allocated at 409 nm of wavelength for the absorption maximum of Pheophorbide *a* and Pheophytin *a*. Second channel was allocated at 431 nm for the absorption maximum of chlorophyll *a*. Third channel was allocated at 440 nm for the absorption maximum of [3,8-divinyl]-protochlorophyllide. Fourth channel was allocated at 450 nm for other pigments. Fifth channel was allocated at 462 nm for chlorophyll *b*.

(3) Preliminary results

Vertical profiles of major pigments (Chlorophyll *a*, Chlorophyll *b* (including divinyl chlorophyll *b*), Divinyl Chlorophyll *a*, Fucoxanthin 19'-hexanoyloxyfucoxanthin, 19'-butanoyloxyfucoxanthin, and Zeaxanthin) at the station K2, S1 and F1 were shown in Figure 2,3 and 4.

(4) Data archives

The processed data file of pigments will be submitted to the JAMSTEC Data Integration and Analyses Group (DIAG) within a restricted period. Please ask PI for the latest information.

(5) Reference

Zapata M, Rodriguez F, Garrido JL (2000), Separation of chlorophylls and carotenoids from marine phytoplankton: a new HPLC method using a reversed phase C<sub>8</sub> column and pyridine-containing mobile phases, *Mar. Ecol. Prog. Ser.*, 195, 29-45.

**Table 1.** Retention time and wavelength of identification for pigment standards.

No.	Pigment	Productions	Retention Time (minute)	Wavelength of identification (nm)
1	Chlorophyll <i>c3</i>	DHI Co.	8.3	462
2	Chlorophyllide <i>a</i>	DHI Co.	10.4	431
3	[3,8-Divinyl]-Protochlorophyllide	DHI Co.	11.1	440
4	Chlorophyll <i>c2</i>	DHI Co.	11.7	450
5	Peridinin	DHI Co.	14.6	450
6	Pheophorbide <i>a</i>	DHI Co.	17.0	409
7	19'-butanoyloxyfucoxanthin	DHI Co.	18.2	450
8	Fucoxanthin	DHI Co.	19.4	450
9	Neoxanthin	DHI Co.	19.8	440
10	Prasinoxanthin	DHI Co.	21.1	450
11	19'-hexanoyloxyfucoxanthin	DHI Co.	22.0	450
12	Violaxanthin	DHI Co.	21.9	440
13	Diadinoxanthin	DHI Co.	24.5	450
14	Antheraxanthin	DHI Co.	26.0	450
15	Alloxanthin	DHI Co.	27.2	450
16	Diatoxanthin	DHI Co.	28.1	450
17	Zeaxanthin	DHI Co.	28.8	450
18	Lutein	DHI Co.	29.0	450
19	Ethyl-apo-8'-carotenoate	Sigma-Aldrich Co.	30.9	462
20	Crococanthin	DHI Co.	33.0	450
21	Chlorophyll <i>b</i>	Sigma-Aldrich Co.	33.4	462
22	Divinyl Chlorophyll <i>a</i>	DHI Co.	34.6	440
23	Chlorophyll <i>a</i>	Sigma-Aldrich Co.	35.0	431
24	Pheophytin <i>a</i>	DHI Co.	37.4	409
25	Alpha-carotene	DHI Co.	38.2	450
26	Beta-carotene	Sigma-Aldrich Co.	38.4	450

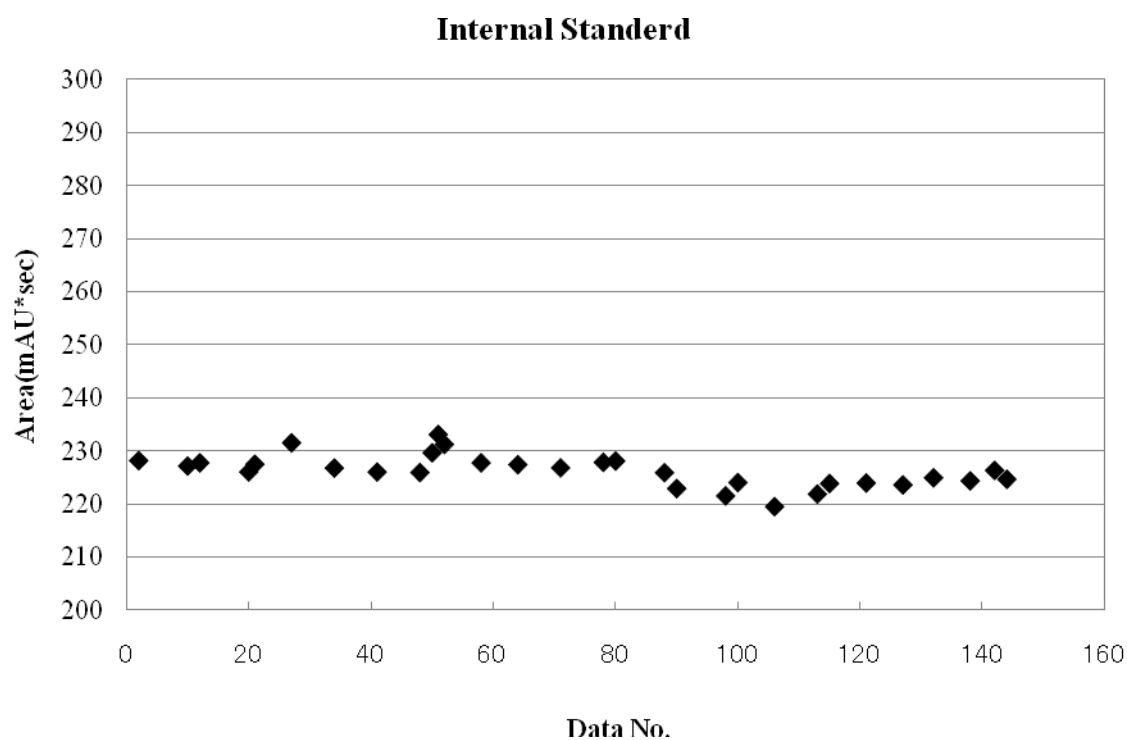


Figure 1. Variability of chromatogram areas for the internal standard.

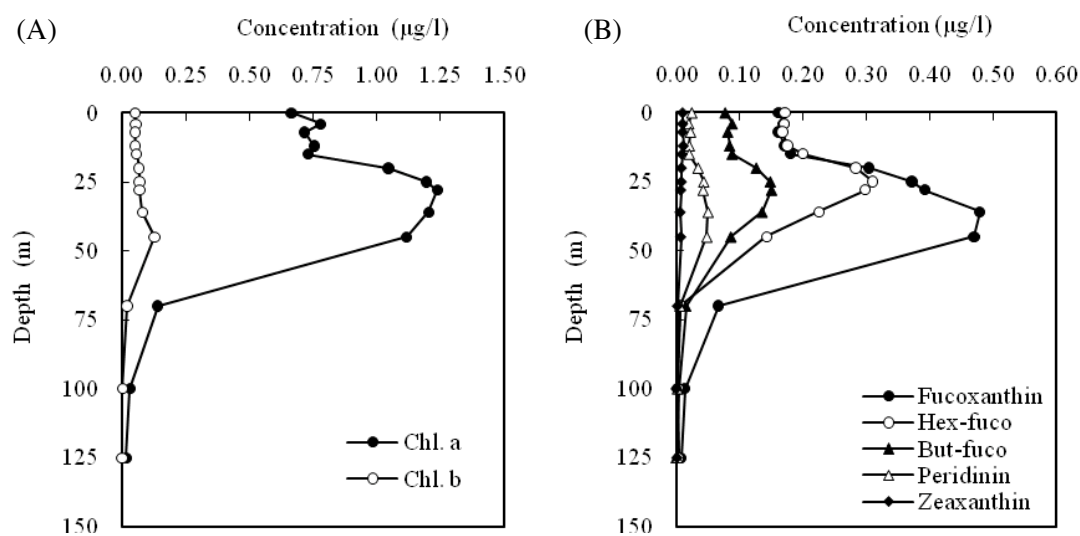


Figure 2-(A). Vertical distributions of major phytoplankton pigments (Chlorophyll *a*, Chlorophyll *b*) at Stn.K2 cast11.

Figure 2-(B). Vertical distributions of major phytoplankton pigments (Fucoxanthin, 19'-hexanoyloxyfucoxanthin, 19'-butanoyloxyfucoxanthin, Peridinin and Zeaxanthin) at Stn.K2 cast11.

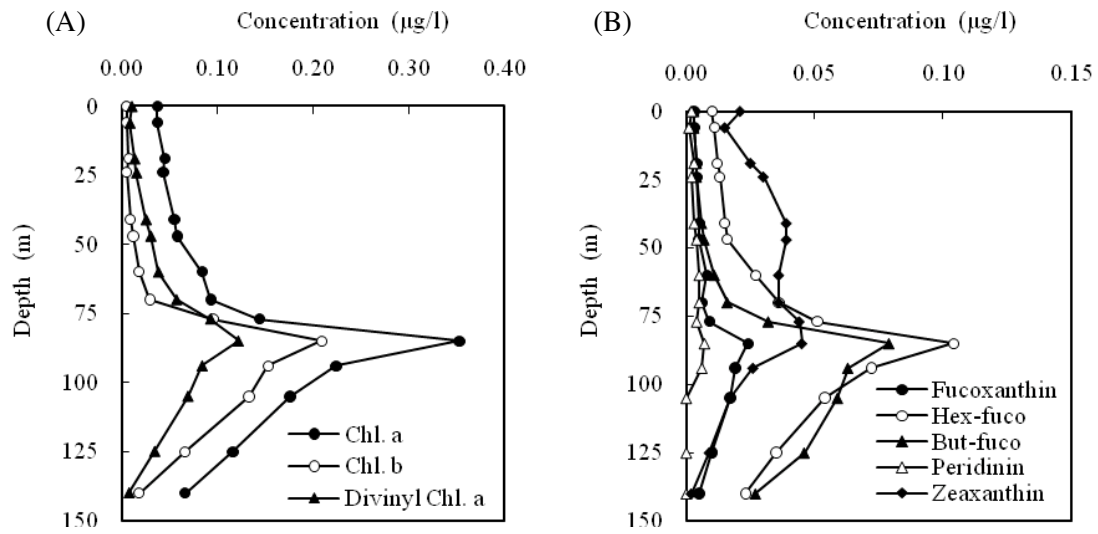


Figure 3-(A). Vertical distributions of major phytoplankton pigments (Chlorophyll *a*, Chlorophyll *b*, Divinyl Chlorophyll *a*) at Stn.S1 cast2.

Figure 3-(B). Vertical distributions of major phytoplankton pigments (Fucoxanthin, 19'-hexanoyloxyfucoxanthin, 19'-butanoyloxyfucoxanthin, Peridinin and Zeaxanthin) at Stn.S1 cast2.

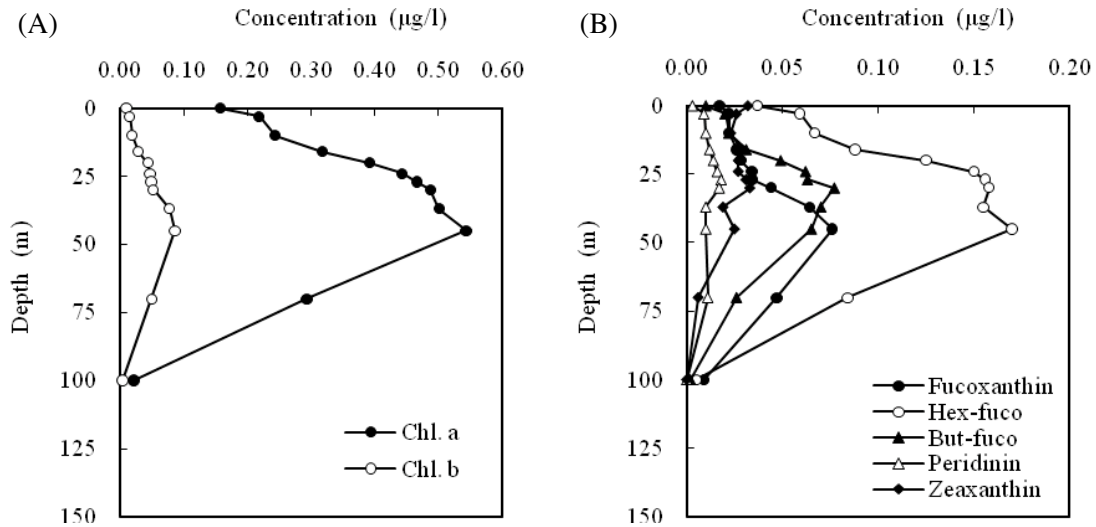


Figure 4-(A). Vertical distributions of major phytoplankton pigments (Chlorophyll *a*, Chlorophyll *b*) at Stn.F1 cast1.

Figure 4-(B). Vertical distributions of major phytoplankton pigments (Fucoxanthin, 19'-hexanoyloxyfucoxanthin, 19'-butanoyloxyfucoxanthin, Peridinin and Zeaxanthin) at Stn.F1 cast1.



### 3.4.3. Phytoplankton abundance

#### Kazuhiko MATSUMOTO (JAMSTEC RIGC)

##### (1) Objectives

The main objective of this study is to estimate phytoplankton abundances and their taxonomy in the subarctic gyre and the subtropical gyre in the western North Pacific. Phytoplankton abundances were measured with two kinds of methods: microscopy for large size phytoplankton and flowcytometry for small size phytoplankton.

##### (2) Sampling

Samplings were conducted using Niskin bottles, except for the surface water, which was taken by a bucket. Samplings were carried out at the three observational stations of K2, F1 and S1.

##### (3) Methods

###### 1) Microscopy

Water samples were placed in 500 ml plastic bottle at station K2, F1 and in 1000 ml plastic bottle at station S1. Samples were fixed with neutral-buffered formalin solution (1% final concentration). The microscopic measurements are scheduled after the cruise.

###### 2) Flowcytometry

###### 2)-1 Equipment

The flowcytometry system used in this research was BRYTE HS system (Bio-Rad Laboratories Inc). System specifications are follows:

Light source: 75W Xenon arc lamp

Excitation wavelength: 350-650 nm

Detector: high-performance PMT

Analyzed volume: 75  $\mu$ l

Flow rate: 10  $\mu$ l min<sup>-1</sup>

Sheath fluid: Milli-Q water

Filter block: B2 as excitation filter block, OR1 as fluorescence separator block

B2 and OR1 have ability as follows:

B2:           Excitation filter   390-490 nm

              Beam-splitter     510 nm

              Emission filter   515-720 nm

OR1:       Emission filter 1   565-605 nm

              Beam-splitter     600 nm

              Emission filter 2   >615 nm

###### 2)-2 Measurements

The water samples were fixed immediately with glutaraldehyde (1% final concentration) and stored in the dark at 4°C. The analysis by the flow cytometer was acquired on board within 24 hours after the sample fixation. Calibration was achieved with standard beads of 0.356 – 9.146  $\mu$ m (Polysciences, Inc.). Standard beads of 2.764  $\mu$ m were added into each sample prior to the injection of flow cytometer as internal standard. Phytoplankton cell populations were estimated from the forward light scatter signal. Acquired data were

stored in list mode file and analyzed with WinBryte software. Phytoplankton are classified with prokaryotic cyanobacteria (*Prochlorococcus* and *Synechococcus*) and other eukaryotes on the basis of scatter and fluorescence signals. *Synechococcus* is discriminated by phycoerythrin as the orange fluorescence, while other phytoplankton are recognized by chlorophylls as the red fluorescence without the orange fluorescence. *Prochlorococcus* and picoeukaryotes were distinguished with their cell size, but it was difficult to identify the abundance of *Prochlorococcus* accurately in the surface mixed layer due to its decreased chlorophyll fluorescence. The cell size was estimated using the empirically-determined relationship between cell diameter ( $d_{\text{cell}}$ ) and bead diameter ( $d_{\text{bead}}$ ) with the forward light scatter signal (FS) by Blanchot *et al.*, (2001) as follows.

$$d_{\text{cell}} = d_{\text{bead}} (\text{FS})^{1/5}$$

#### (4) Preliminary result

The vertical profile of phytoplankton group identified by flow cytometer at station K2 (cast 2) is shown in Figure 1.

*Prochlorococcus* was not observed in this station. The mean cell size of *Synechococcus* (SYN) was estimated to 0.8 – 1.0  $\mu\text{m}$ . The mean cell size of eukaryotic phytoplankton of EUK-1, EUK-2 and EUK-3 were estimated to 1.0 – 1.5  $\mu\text{m}$ , 2.1 – 2.9  $\mu\text{m}$  and 3.0 – 3.7  $\mu\text{m}$ , respectively. The population of EUK-4 was isolated in cell size of >5.4  $\mu\text{m}$ .

#### (5) Data Archive

All data will be submitted to Data Integration and Analysis Group (DIAG), JAMSTEC.

#### (6) Reference

Blanchot J, André J-M, Navarette C, Neveux J, Radenac M-H (2001), Picophytoplankton in the equatorial Pacific: vertical distributions in the warm pool and in the high nutrient low chlorophyll conditions, *Deep-Sea Research I* 48, 297-314.

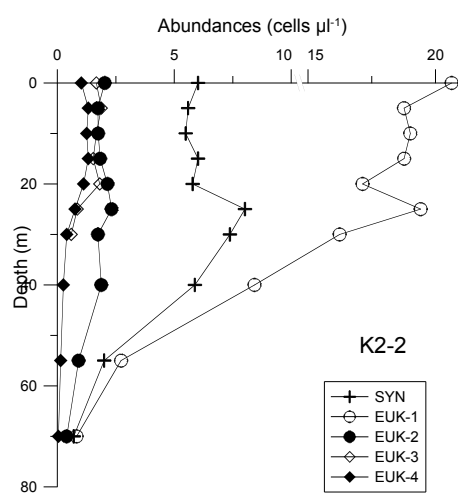


Figure 1. Vertical profile of phytoplankton abundances at K2

### 3.4.4 Primary production and new production

**Kazuhiko MATSUMOTO (JAMSTEC RIGC)**

**Miyo IKEDA (MWJ)**

**Kanako YOSHIDA (MWJ)**

**Hatsumi AOYAMA (MWJ)**

#### (1) Objective

Quantitative assessment of temporal and spatial variation in carbon and nitrate uptake in the surface euphotic layer should be an essential part of biogeochemical studies in the western North Pacific. Primary production (PP) was measured as incorporation of inorganic  $C^{13}$ , and new production (NP), measurement of nitrate uptake rate was conducted with  $^{15}N$  stable isotope tracer at K2, F1 and S1 stations.

#### (2) Methods

##### 1) Sampling, incubation bottle and filter

Sampling was begun at predawn immediately before the incubation experiment. Seawater samples were collected using Teflon-coated and acid-cleaned Niskin bottles, except for the surface water, which was taken by a bucket. Samplings were conducted at eight depths between the surface and 1% light depth in response to the light levels of the incubation containers adjusted with the blue acrylic plate. Two kinds of baths were prepared for PP and NP (bath-1), and for oxygen evolution (bath-2). The light levels of the incubation containers in each bath were shown in Table 3.4.4-1. The light depths relative to the surface had been estimated by SPMR sensor on the previous day of the sampling. Seawater samples were placed into acid-cleaned clear polycarbonate bottles in duplicate for PP and NP, and in a single for the dark and the time-zero samples. The time-zero sample was filtered immediately after the addition of  $^{13}C$  and  $^{15}N$  solution. The PP incubation was conducted in a single for bath-2. Filtration of seawater sample was conducted with pre-combusted glass fiber filters (Whatman GF/F 25 mm) with temperature of 450 degree C for at least 4 hours.

##### 2) Incubation

Each bottle was spiked with sufficient  $NaH^{13}CO_3$  just before incubation so that  $^{13}C$  enrichment was about 10% of ambient dissolved inorganic carbon as final concentration of  $0.2 \text{ mmol dm}^{-3}$  (Table 3.4.4-2). The  $^{15}N$ -enriched  $NO_3$ ,  $K^{15}NO_3$  solution, was injected to the incubation bottles (except PP bottles), resulting that the final concentration of  $^{15}N$  enrichment was about 10% of ambient nitrate (Table 3.4.4-3). Incubation was begun at predawn and continued for 24 h. The simulated *in situ* method was conducted in the on-deck bath cooled by running surface seawater or by immersion cooler. The incubation by the *in situ* method was conducted for PP at the station of K2. In the *in situ* method, bottles were placed appropriate depths on a line attached to a drifting mooring system (see the chapter 3.6.1).

##### 3) Measurement

After 24 hours incubation, samples were filtered though GF/F filter, and the filters were kept in a freezer (-20 degree C) on board until analysis. Before analysis, the filters were dried in the oven (45 degree C) for at least 20 hours, and inorganic carbon was removed by acid treatment in a HCl vapor bath for 30 minutes. All samples were measured by a mass spectrometer ANCA-SL system at MIRAI during this cruise.

Instruments: preprocessing equipment ROBOPLEP-SL (Europa Scientific Ltd.; now SerCon Ltd.)  
stable isotope ratio mass spectrometer EUROPA20-20 (Europa Scientific Ltd.; now SerCon Ltd.)

Methods: Dumas method, Mass spectrometry

Precision: All specifications are for n=5 samples.

It is a natural amount and five time standard deviation of the analysis as for amount 100 µg of the sample. We measured repeatability 4 times in this cruise.  $^{13}\text{C}$  (0.1 - 0.2 ‰),  $^{15}\text{N}$  (0.1 - 0.3 ‰)

Reference Material: The third-order reference materials L-aspartic acid (SHOKO Co., Ltd.)

#### 4) Calculation

##### (a) Primary Production

Based on the balance of  $^{13}\text{C}$ , assimilated organic carbon ( $\Delta\text{POC}$ ) is expressed as follows (Hama *et al.*, 1983):

$$^{13}\text{C}_{(\text{POC})} * \text{POC} = ^{13}\text{C}_{(\text{sw})} * \Delta\text{POC} + (\text{POC} - \Delta\text{POC}) * ^{13}\text{C}_{(0)}$$

This equation is converted to the following equation;

$$\Delta\text{POC} = \text{POC} * (^{13}\text{C}_{(\text{POC})} - ^{13}\text{C}_{(0)}) / (^{13}\text{C}_{(\text{sw})} - ^{13}\text{C}_{(0)})$$

where  $^{13}\text{C}_{(\text{POC})}$  is concentration of  $^{13}\text{C}$  of particulate organic carbon after incubation, *i.e.*, measured value(%).  $^{13}\text{C}_{(0)}$  is that of particulate organic carbon before incubation, *i.e.*, that for samples as a blank.

$^{13}\text{C}_{(\text{sw})}$  is concentration of  $^{13}\text{C}$  of ambient seawater with a tracer. This value for this study was determined based on the following calculation;

$$^{13}\text{C}_{(\text{sw})} (\%) = [(\text{TDIC} * 0.011) + 0.0002] / (\text{TDIC} + 0.0002) * 100$$

where TDIC is concentration of total dissolved inorganic carbon at respective bottle depth(mol dm<sup>-3</sup>) and 0.011 is concentration of  $^{13}\text{C}$  of natural seawater (1.1%). 0.0002 is added  $^{13}\text{C}$  (mol) as a tracer. Taking into account for the discrimination factor between  $^{13}\text{C}$  and  $^{12}\text{C}$  (1.025), primary production (PP) was, finally, estimated by

$$\text{PP} = 1.025 * \Delta\text{POC}$$

##### (b) New production

$\text{NO}_3$  uptake rate or new production (NP) was estimated with following equation:

$$\text{NP} (\mu\text{g dm}^{-3} \text{ day}^{-1}) = (^{15}\text{N}_{\text{excess}} * \text{PON}) / (^{15}\text{N}_{\text{enrich}}) / \text{day}$$

where  $^{15}\text{N}_{\text{excess}}$ , PON and  $^{15}\text{N}_{\text{enrich}}$  are excess  $^{15}\text{N}$  (measured  $^{15}\text{N}$  minus  $^{15}\text{N}$  natural abundance, 0.366 atom%) in the post-incubation particulate sample (%), particulate nitrogen content of the sample after incubation (mg dm<sup>-3</sup>) and  $^{15}\text{N}$  enrichment in the dissolved fraction (%), respectively.

(3) Preliminary results

Fig. 3.4.4.1 and 3.4.4.2 show the vertical profile of primary production (PP) and the diurnal change of photosynthetically available radiation (PAR) observed by PUV-510B (Biospherical Instruments Inc.).

(4) Data archives

All data will be submitted to JAMSTEC Data Integration and Analyses Group (DIAG).

Table 3.4.4-1 Light intensity of simulated *in situ* bath

Number	Bath 1	Bath 2 (with oxygen evolution)
#1	100%	96%
#2	59%	56%
#3	38%	33%
#4	17%	12%
#5	13%	7.8%
#6	7%	4.8%
#7	3.8%	3%
#8	1%	1%

Table 3.4.4-2 Sampling cast table and spike  $^{13}\text{C}$  concentration

Incubation type	CTD cast	$\text{NaH}^{13}\text{CO}_3$ ( $\mu\text{mol dm}^{-3}$ )
SIS/IS	K02M02	200
SIS	K02M08	200
SIS	K02M11	200
SIS	F01M01	200
SIS	S01M02	200
SIS	S01M07	200

Table 3.4.4-3 Sampling cast table and spike  $^{15}\text{N}$  concentration

Incubation type	CTD cast	Light Intensity	$\text{K}^{15}\text{NO}_3$ ( $\mu\text{mol dm}^{-3}$ )
SIS	K02M02	All layers	1.5
SIS	K02M08	100% - 3.8%	1.8
		1%	2.2
SIS	K02M11	100% - 3.8%	1.7
		1%	2.1
SIS	F01M01	All layers	0.1
SIS	S01M02	100% - 3.8%	0.01
		1%	0.1
SIS	S01M07	100% - 3.8%	0.01
		1%	0.1

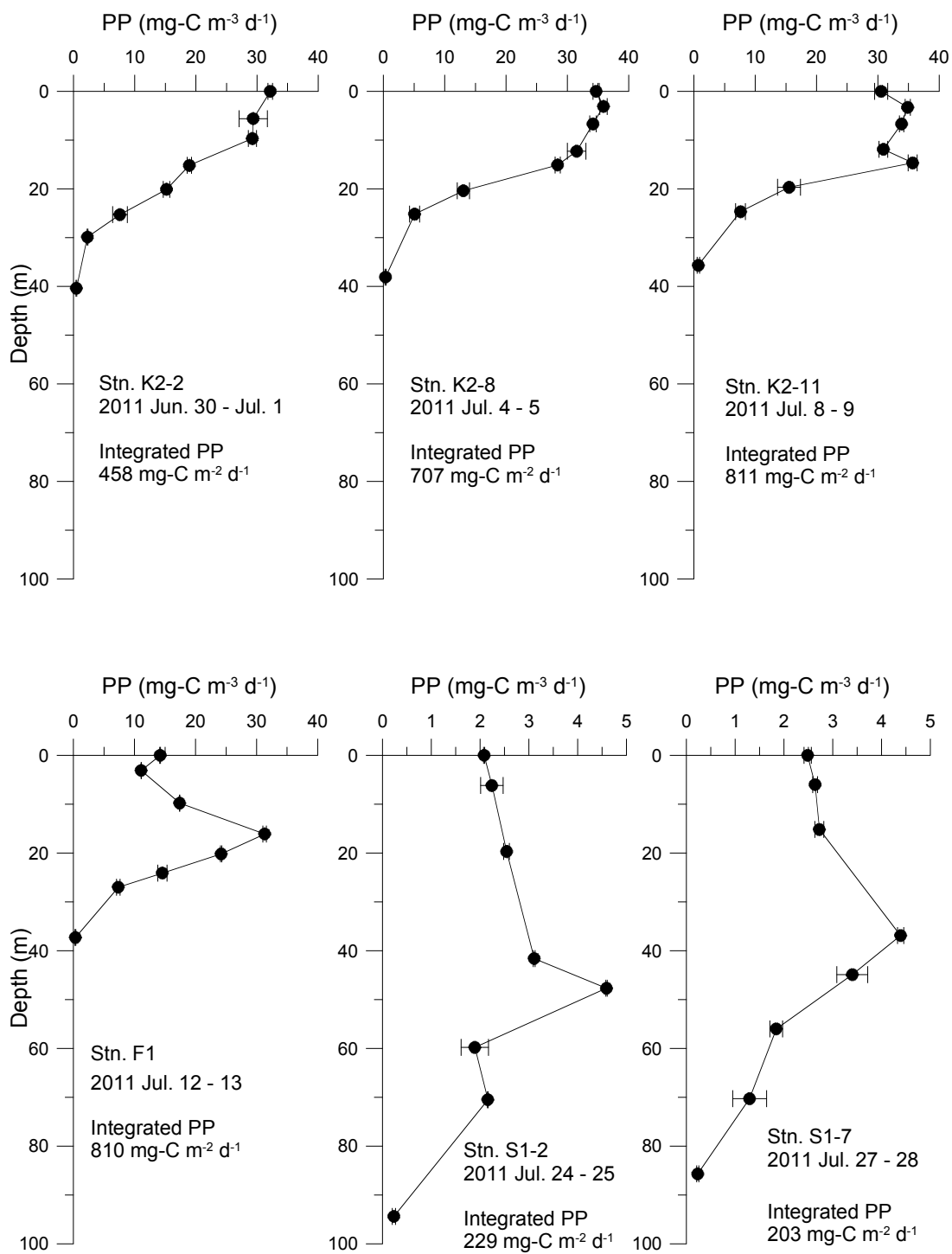


Figure 3.4.4.1 Vertical profile of primary production



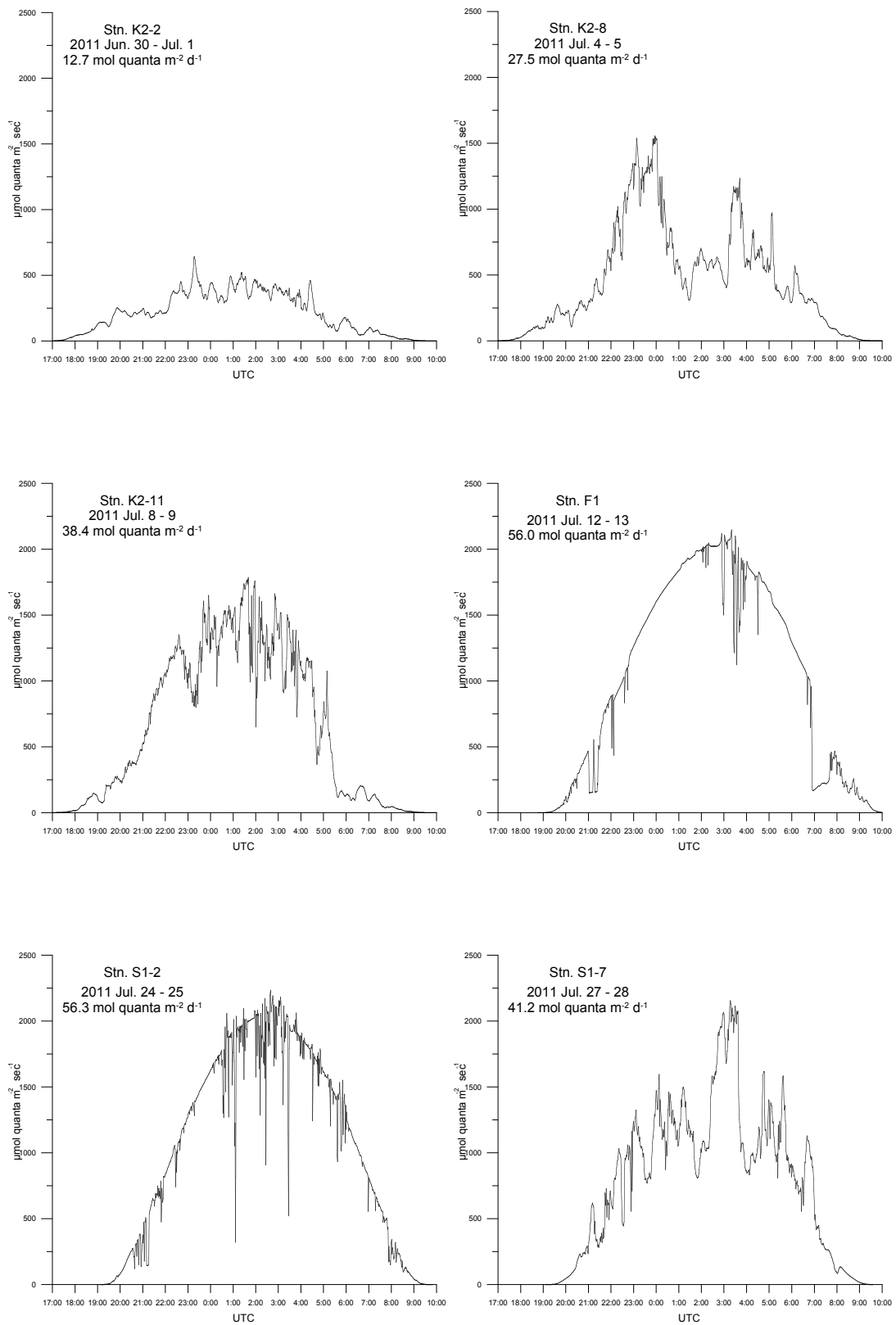


Figure 3.4.4.2 Photosynthetically available radiation (PAR) during incubation experiment

### 3.4.5 P vs. E curve

**Kazuhiko MATSUMOTO (JAMSTEC RIGC)**

**Miyo IKEDA (MWJ)**

**Kanako YOSHIDA (MWJ)**

**Hatsumi AOYAMA (MWJ)**

#### (1) Objectives

The objective of this study is to estimate the relationship between phytoplankton photosynthetic rate (P) and scalar irradiance (E) in the western North Pacific.

#### (2) Methods

##### 1) Sampling

Samplings were carried out at two observational stations of K2 and S1. Sample water was collected at three depths of different irradiance level, using Teflon-coated and acid-cleaned Niskin bottles.

##### 2) Incubation

Three incubators filled in water were used, illuminated at one end by a 500W halogen lamp. Water temperature was controlled by circulating water cooler (Fig. 3.4.5-1). Water samples were poured into acid-cleaned clear nine flasks (approx. 1 liter) and arranged in the incubator linearly against the lamp after adding the isotope solutions. The isotope solutions of  $0.2 \text{ mmol dm}^{-3}$  (final concentration) of  $\text{NaH}^{13}\text{CO}_3$  solution were spiked. All flasks were controlled light intensity by shielding with a neutral density filter on lamp side. The light intensities inside the flasks were shown in Table 3.4.5. The incubations were begun at about local noon and continued for 3 h. Filtration of seawater sample was conducted with glass fiber filters (Whatman GF/F 25 mm) which precombusted with temperature of 450 degree C for at least 4 hours.

##### 3) Measurement

After the incubation, samples were treated as same as the primary production experiment. During the cruise, All incubator samples were measured by a mass spectrometer ANCA-SL system at MIRAI. The analytical function and parameter values used to describe the relationship between the photosynthetic rate (P) and scalar irradiance (E) are best determined using a least-squares procedure from the following equation.

$$P = P_{\max}(1 - e^{-\alpha E/P_{\max}})e^{-b\alpha E/P_{\max}} : (\text{Platt et al., 1980})$$

where,  $P_{\max}$  is the light-saturated photosynthetic rate,  $\alpha$  is the initial slope of the P vs. E curve, b is a dimensionless photoinhibition parameter.

#### (3) Preliminary results

The P vs. E curve obtained at the station of K2 and S1 (3m) is shown in Fig. 3.4.5-2.

#### (4) Data archives

All data will be submitted to JAMSTEC Data Integration and Analyses Group (DIAG) .

(5) Reference

Platt, T., Gallegos, C.L. and Harrison, W.G., 1980. Photoinhibition of photosynthesis in natural assemblages of marine phytoplankton. *Journal of Marine Research*, 38, 687-701.

Table 3.4.5 Light Intensity of P vs. E measurements

	Bath A	Bath B	Bath C
Bottle No.	Light intensity ( $\mu\text{E m}^{-2} \text{sec}^{-1}$ )		
1	2000	2000	1950
2	950	1050	930
3	410	500	440
4	185	230	195
5	85	110	87
6	40	45	38
7	18	20	16
8	6.8	8.6	6.5
9	0	0	0

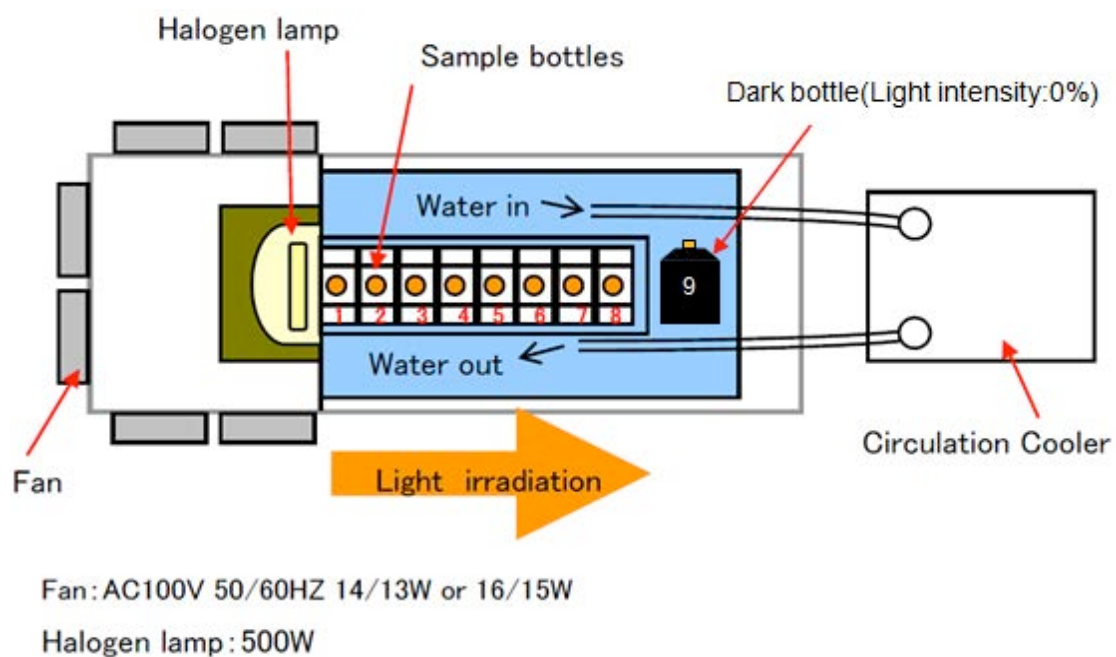


Fig. 3.4.5-1 Look down view of Incubator for Photosynthesis and irradiation curve

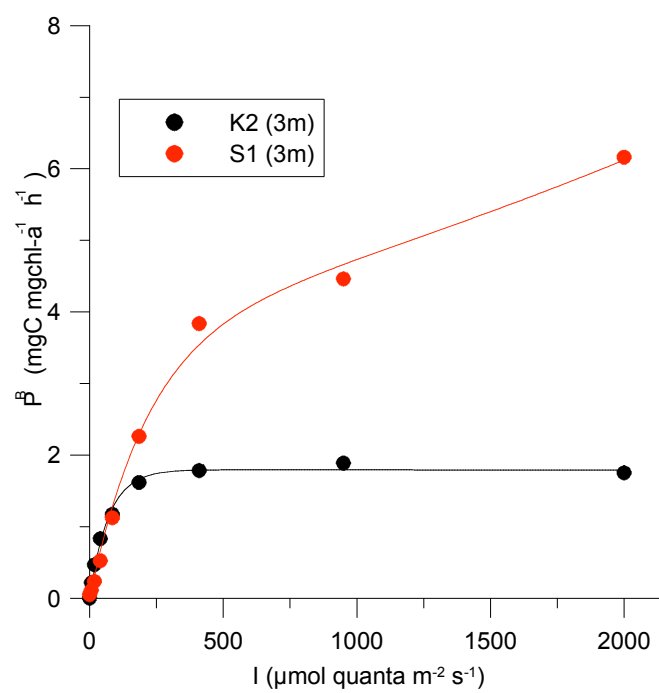


Fig. 3.4.5-2

### 3.4.6. Oxygen evolution (gross primary productivity)

**Tetsuichi FUJIKI (JAMSTEC)**  
**Osamu ABE (Nagoya University)**  
**Misato KUWAHARA (MWJ)**  
**Hideki YAMAMOTO (MWJ)**

#### (1) Objective

An understanding of the variability in phytoplankton productivity provides a basic knowledge of how aquatic ecosystems are structured and functioning. Primary productivity in the world's oceans has been measured mostly by the carbon tracer or oxygen evolution methods. In incubations of 24 hours, the former method provides the values closest to net primary productivity (NPP), while the latter comes closest to gross primary productivity (GPP). The GPP is defined as total amount of oxygen released by phytoplankton photosynthesis. The NPP/GPP ratio provides fundamental information on the metabolic balance and carbon cycle in the ocean. In the MR11-05, the GPP were measured using the light-dark bottle and  $^{18}\text{O}$  spike methods and fast repetition rate (FRR) fluorometry.

#### (2) Methods

##### Sampling

Seawater samples were collected from eight depths corresponding to light levels of approximately 100, 60, 35, 13, 7, 5, 3 and 1 % of surface light intensity, using a bucket (surface only) and 12-L Niskin-X bottles attached to a CTD rosette system. Seawater samples were carefully transferred from Niskin bottle into volume calibrated flasks (ca. 100 cm<sup>3</sup>).

##### Light-dark bottle method

At each light depth, three light and three dark bottles were incubated under light condition that simulated those of the original sampling depth. The dark bottles were wrapped with aluminum foil. After 24 h incubation, the light and dark bottles were fixed immediately. Fixing, storage, reagent preparation, measurement and standardization were followed the dissolve oxygen section. The GPP was estimated by adding the dark respiration in dark bottles to the net oxygen evolution in light bottles.

##### $^{18}\text{O}$ spike method

The samples were spiked with enriched  $^{18}\text{O}$ -labeled water (Cambridge Isotope Laboratories) and incubated for 24 h under light condition that simulated those of the original sampling depth as the light-dark bottle method. After incubation, ~100 mL of subsample were drawn into preevacuated gas extraction vessels and capped.

After measurements of the isotopic composition of  $\text{O}_2$  in the laboratory on land, the GPP is calculated from the isotopic composition of dissolved oxygen in initial and incubated samples using the following equation (Bender et al. 2000).

$$\text{GPP} = \{[\delta^{18}\text{O}(\text{O}_2)_f - \delta^{18}\text{O}(\text{O}_2)_i] / [\delta^{18}\text{O}_{\text{water}} - \delta^{18}\text{O}(\text{O}_2)_i]\} \times (\text{O}_2)_i$$

where the subscripts i and f are the isotopic composition of  $\text{O}_2$  in initial and final samples,  $(\text{O}_2)_i$  is the oxygen concentration of the initial water sample, and  $\delta^{18}\text{O}_{\text{water}}$  is the isotopic composition of the enriched water.

### FRR fluorometry

Measurement principle of FRR fluorometer can be found in the section 3.2 (POPPS mooring). The FRR fluorometer together with a scalar irradiance sensor (QSP-2200, Biospherical Instruments) and a pressure gauge (ABH500PSC1B, Honeywell International) were deployed several times a day using a ship winch. These instrument packages lowered gently through the water column to 100m (200m for S1) depth and up again at a rate of  $0.2 \text{ m s}^{-1}$  and measured vertical profiles of GPP.

### (3) Preliminary results

At stations K2, S1 and F1, the vertical profiles of GPP measured with the light-dark bottle method were shown in figure 3.4.6.1.

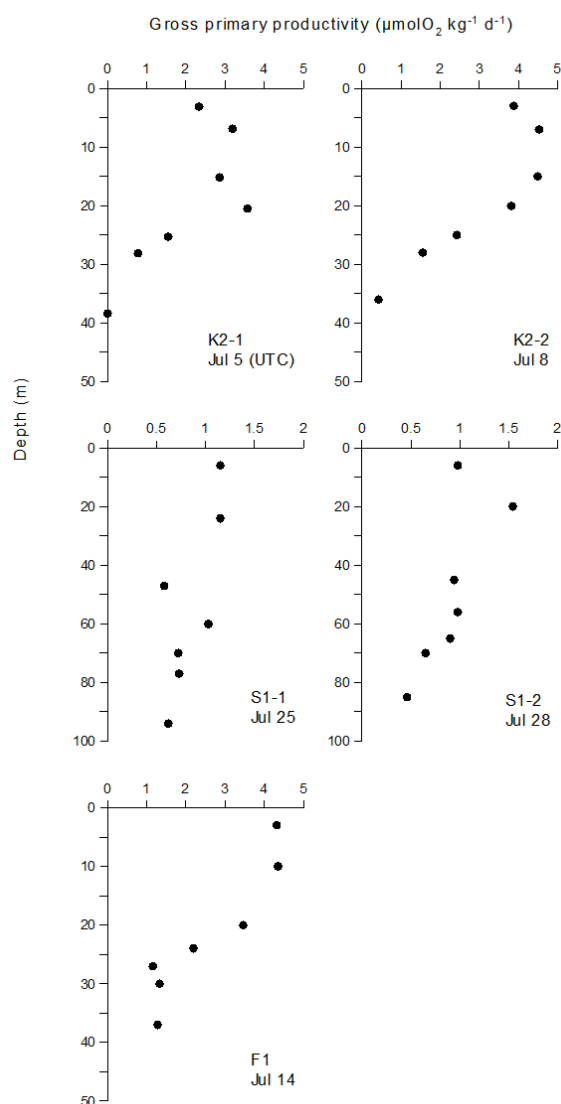


Figure 3.1.6.1. Vertical profiles of GPP at stations K2, S1 and F1, measured with the light-dark bottle method.

(4) Data archives

The data will be submitted to Data Integration and Analyses Group (DIAG), JAMSTEC.

(5) References

Bender, M. L., M. L. Dickson and J. Orchardo. 2000. Net and gross production in the Ross Sea as determined by incubation experiments and dissolved O<sub>2</sub> studies. *Deep-Sea Res.* II 47: 3141–3158.

### 3.5 Optical measurement

**Makio HONDA (JAMSTEC RIGC)**

**Kazuhiko MATSUMOTO (JAMSTEC RIGC)**

#### (1) Objective

The objective of this measurement is to investigate the air and underwater light conditions at respective stations and to determine depths for *in situ* or simulated *in situ* measurement of primary production by using carbon stable isotope (C-13) during late autumn. In addition, optical data can be used for the validation of satellite data.

#### (2) Description of instruments deployed

The instrument consisted of the SeaWiFS Profiling Multichannel Radiometer (SPMR) and SeaWiFS Multichannel Surface Reference (SMSR). The SPMR was deployed in a free fall mode through the water column (see right picture). The SPMR profiler called “Free Fall” has a 13 channel irradiance sensors (Ed), a 13 channel radiance sensors (Lu), tilt sensor, and fluorometer. The SMSR has a 13 channel irradiance sensors (Es) and tilt meter (Table 1). These instruments observed the vertical profiles of visible and ultra violet light and chlorophyll concentration.



Table 1. Center wavelength (nm) of the SPMR/SMSR

Es	379.5	399.6	412.2	442.8	456.1	490.9	519.0	554.3	564.5	619.5	665.6	683.0	705.9
Ed	380.0	399.7	412.4	442.9	455.2	489.4	519.8	554.9	565.1	619.3	665.5	682.8	705.2
Lu	380.3	399.8	412.4	442.8	455.8	489.6	519.3	554.5	564.6	619.2	665.6	682.6	704.5

Optical measurements by Free Fall were conducted at our time-series station K2 and S1. Measurements should be ideally conducted at median time. However observations were conducted irregularly because of limited ship-time and other observation's convenience (Table 2). The profiler was dropped twice a each deployment to a depth of 200 m. The SMSR was mounted on the anti-rolling system's deck and was never shadowed by any ship structure. The profiler descended at an average rate of 1.0 m/s with tilts of less than 3 degrees except near surface.

Observed data was analyzed by using software “Satlantic PPROSOFT 6” and extinction rate and photosynthetically available radiation (PAR) were computed.



Table 2 Locations of optical observation and principle characteristics  
(Date and Time in LST: UTC+11hr at station K2, UTC+10hr at station S1 and  
UTC+9hr at station F1)

Date and Time	Station	Lat./Long.	Surface PAR (quanta cm <sup>-2</sup> sec <sup>-1</sup> )	Euphotic layer* (m)	Memo
2011.06.30 10:50	K2	47N/160E	4.7 x 10 <sup>16</sup>	~ 46	1 day before PP incubation #1
2011.07.01 11:18	K2	47N/160E	3.0 x 10 <sup>16</sup>	~ 42	during PP incubation #1
2011.07.04 11:03	K2	47N/160E	2.8 x 10 <sup>16</sup>	~ 47	1 day before PP incubation #2
2011.07.05 11:03	K2	47N/160E	7.4 x 10 <sup>16</sup>	~ 46	during PP incubation #2
2011.07.7 11:03	K2	47N/160E	5.0 x 10 <sup>16</sup>	~ 45	1 day before PP incubation #3
2011.07.8 11:03	K2	47N/160E	9.3 x 10 <sup>16</sup>	~ 45	during PP incubation #3
2011.07.12 11:03	Before F1	36-40 N / 142-01E	5.3 x 10 <sup>16</sup>	~ 45	1 day before PP incubation at station F1
2011.07.13 11:06	F1	36-29N / 141-30E	1.2 x 10 <sup>17</sup>	~ 67	during PP incubation #1
2011.07.24 13:06	S1	30N/145E	1.2 x 10 <sup>17</sup>	~ 107	1 day before PP incubation #1
2011.07.24 13:06	S1	30N/145E	1.2 x 10 <sup>17</sup>	~ 104	during PP incubation #1
2011.07.27 11:01	S1	30N/145E	1.1 x 10 <sup>17</sup>	~ 96	1 day before PP incubation #2
2011.07.28 10:36	S1	30N/145E	8.8 x 10 <sup>16</sup>	~ 95	during PP incubation #2

\* Euphotic layer: 0.5% of surface PAR

### (3) Preliminary result

We deployed “Free Fall sensor” five times at station K2 and four times at station S1 (Table 2). Surface PAR ranged from approximately 2.8 x 10<sup>16</sup> to 1.2 x 10<sup>17</sup> quanta cm<sup>-2</sup> sec<sup>-1</sup> and surface PAR at S1 was two times higher than that at K2 on average (5.4 x 10<sup>16</sup> and 1.1 x 10<sup>16</sup> quanta cm<sup>-2</sup> sec<sup>-1</sup> at K2 and S1, respectively). The euphotic layers, that is defined as water depth with 0.5 % of surface PAR, were approximately 45 m at station K2 and 100 m at station S1. It is likely attributed to the amount of particulate materials, *i.e.* phytoplankton, in the water column: the amount of phytoplankton was likely smaller at S1 than those at K2 although surface PAR was higher at S1. This was supported by the fact that higher chlorophyll-a and primary productivity at station K2.

### (4) Data archive

Optical data were filed on two types of file.  
(BIN file) digital data of upwelling radiance and downwelling irradiance each 1 m from near

surface to approximately 150 m for respective wave-lengths with surface PAR data during “Free Fall” deployment

(PAR file) in situ PAR each 1 m from near surface to approximately 100 m with extinction coefficient with surface PAR data during “Free Fall” deployment

These data files will be submitted to JAMSTEC Data Integration and Analyses Group (DIAG).

### **3.6 Drifting sediment trap**

#### **3.6.1 Drifting mooring system**

**Hajime KAWAKAMI (JAMSTEC MIO)**  
**Makio C. HONDA (JAMSTEC RIGC)**  
**Hideki FUKUDA (University of Tokyo)**  
**Mario UCHIMIYA (University of Tokyo)**  
**Jaeho SONG (University of Tokyo)**  
**Shotaro SUZUKI (University of Tokyo)**  
**Yoshihisa MINO (Nagoya University)**  
**Toru KOBARI (Kagoshima University)**  
**Yuichi HAYASAKI (Kagoshima University)**  
**Sachi MIYAKE (Kagoshima University)**  
**Rie NAKAMURA (Kagoshima University)**  
**Miyo IKEDA (MWJ)**  
**Kanako YOSHIDA (MWJ)**  
**Toru IDAI (MWJ)**  
**Masaki FURUHATA (MWJ)**  
**Tomoyuki TAKAMORI (MWJ)**

In order to conduct drifting sediment trap experiment at stations K2 and S1, drifting mooring system (drifter) was deployed. This drifter consists of radar reflector, GPS radio buoy (Taiyo TGB-100), flush light, surface buoy, ropes and sinker. On this system, “Knauer” type sediment trap at 10 layers were installed together (Traps of JAMSTEC: 60, 100, 150, and 200 m; traps of Nagoya University: 90, 95, 180, and 190 m; traps of University of Tokyo: 105 and 210 m). Thanks to the effort by MWJ technicians, drifting mooring system was upgraded on board. The configuration is shown in Fig. 3.6.1-1.

The drifter was deployed at 18:10 on 1 July (UTC) at station K2 and at 20:00 on 25 July (UTC) at station S1. The drifter was recovered at 18:20 on 6 July at stations K2 and at 3:10 on 30 July at station S1. The drifter’s position was monitored by using GPS radio. Fig. 3.6.1-2 shows tracks of the drifter. In general, the drifter tended to drift eastward and westward at stations K2 and S1, respectively.

## Station: K2

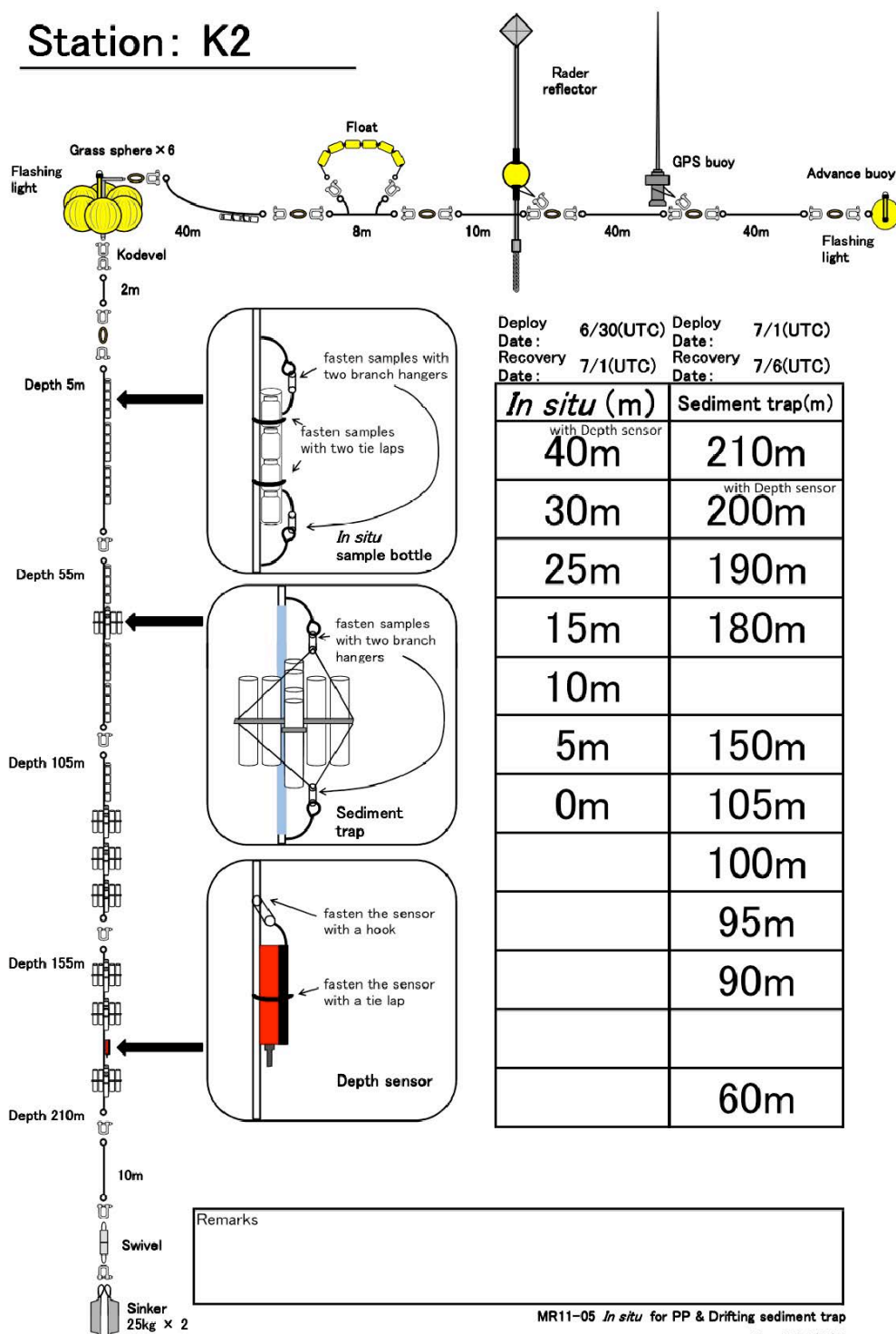


Fig. 3.6.1-1 Drifting mooring system at stations K2 and S1.

# Station: S1

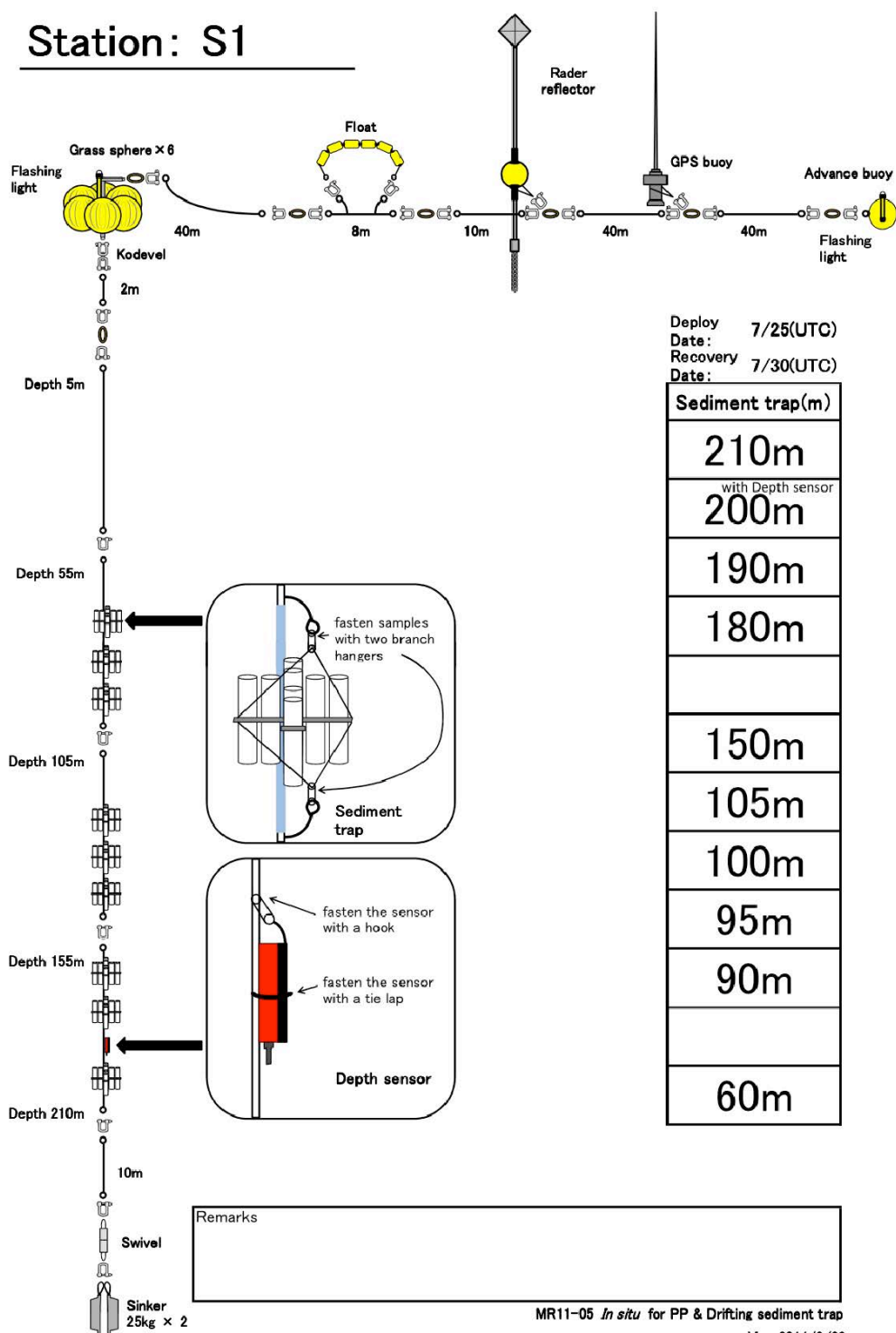


Fig. 3.6.1-1 Continued.

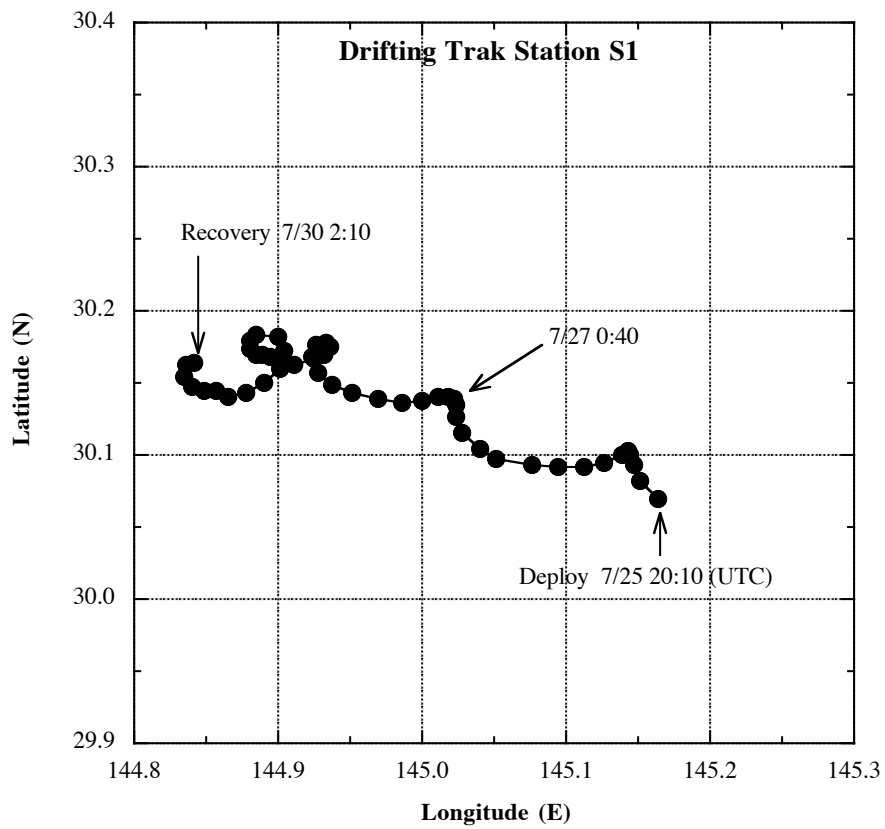
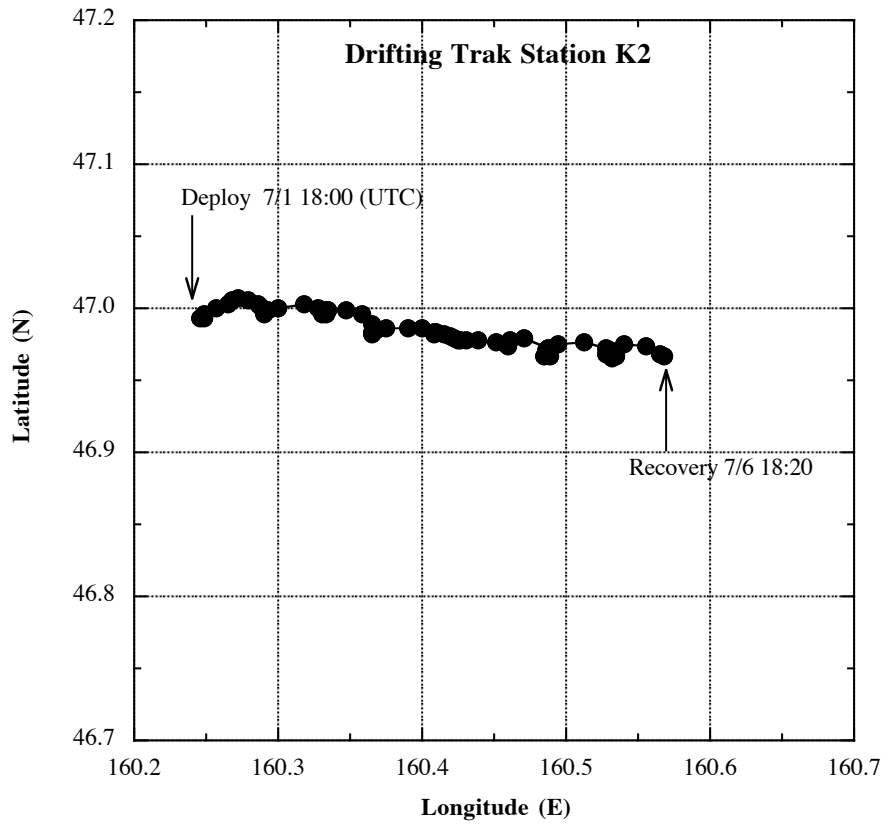


Fig. 3.6.1-2 Track of drifter (GPS buoy) at stations K2 and S1.

### 3.6.2 Drifting sediment trap of JAMSTEC

**Hajime KAWAKAMI (JAMSTEC MIO)**

**Makio C. HONDA (JAMSTEC RIGC)**

In order to collect sinking particles and measure carbon flux, and zooplankton, “Knauer type” cylindrical sediment trap (Photo 3.6.2-1) was deployed at stations K2 and S1 where measurement of primary productivity was conducted. This trap consists of 8 individual transparent polycarbonate cylinders with baffle (collection area: ca. 0.0038 m<sup>2</sup>, aspect ratio: 620 mm length / 75 mm width = 8.27), which was modified from Knauer (1979). Before deployment, each trap was filled with filtrated surface seawater, which salinity is adjusted to ~ 39 PSU by addition of NaCl (addition of 100 g NaCl to 20 L seawater) were placed in tubes. These were located at approximately 60, 100, 150, and 200 m. After recovery, sediment traps were left for half hour to make collected particles settle down to the bottle. After seawater in acrylic tube was dumped using siphonic tube, collecting cups were took off. Two cups of samples at each layer were given to the team of Kagoshima University to determine fecal pellets. Four cups of samples at each layer were filtered thorough Nuclepore filter with a nominal pore size of 0.4µm and GF/F filter by two cups, for respective purposes (total mass flux, trace elements, total particulate carbon, and particulate organic carbon). The other samples were added buffered formalin for archive. The filter and archive samples were kept in freezer and refrigerator by the day when these were analyzed, respectively.

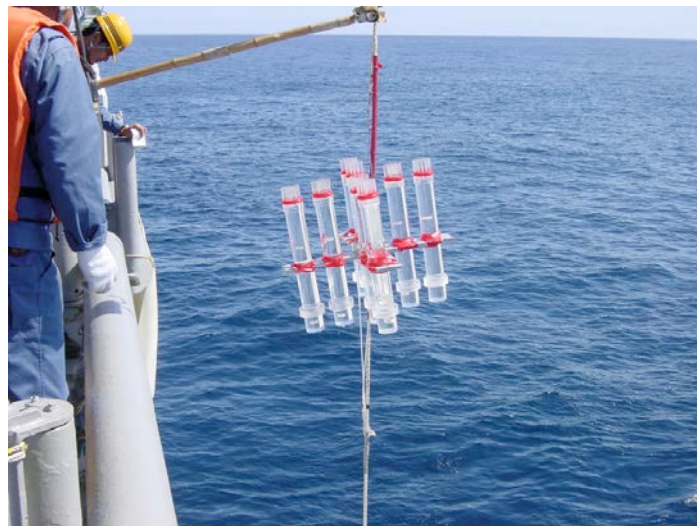


Photo 3.6.2-1 Drifting Sediment Trap.

### 3.6.3 Vertical changes of fecal pellets

**Toru KOBARI (Kagoshima University)**

#### (1) Objective

Sinking particles includes phytoplankton aggregates, zooplankton fecal pellets, feeding mucus, carcass and crustacean molts (e.g. Flower and Knauer, 1986). Especially, fecal pellets significantly contribute to downward flux of particulate organic carbon (POC) and are a key component of the biological pump mediated by zooplankton community (Bishop et al., 1977; Lampitt et al., 1990; Silver and Gowing, 1991; Carroll et al., 1998; Turner, 2002). Fecal pellets are changed by zooplankton ingestion (coprophagy), fragmentation via sloppy feeding or swimming activity (coprorhexy) and loosening of membrane (coprochaly) during sinking (Paffenhöfer and Strickland, 1970; Lampitt et al., 1990; Noji et al., 1991). These processes largely affect transfer efficiency of POC flux (Wilson et al., 2008). It has been believed that fecal pellets are declined by bacterial decomposition (Honjo and Roman, 1978; Aristegui et al., 2002) and/or coprophagy/coprorhexy of small copepods such as cyclopoids and poecilostomatoids for last two decades (González and Smetacek, 1994; Suzuki et al., 2003; Svensen and Nejstgaard, 2003; Huskin et al., 2004; Poulsen and Kiørboe, 2006). In recent years, however, these copepods showed minor contributions to coprophagy/coprorhexy from the field observations (Iversen and Poulsen, 2007) and laboratory experiments (Reigstad et al., 2005). Alternatively, heterotrophic microbes consumed fecal pellets (Poulsen and Iversen, 2008). Thus, we should re-consider how fecal pellets are declined or changed during sinking from surface to mesopelagic depths.

In the present study, we investigated vertical changes in flux, shape and volume of fecal pellets from drifting sediment trap experiments to evaluate how fecal pellets were changed or declined.

#### (2) Methods

Knauer-type sediment traps were deployed at 60, 100, 150 and 200 m at K2 and S1 in the Northwestern Pacific Ocean for 96 hours during the Mirai cruise (MR11-05) from 27 June to 4 August 2011. The sediment traps were constructed from 8 cylinders (collection area: ca. 0.0038 m<sup>2</sup>, aspect ratio: 620 mm length / 75 mm width = 8.27) with a baffle to reduce turbulence, mounted on a polyvinylchloride frame. Approximately 250-mL polycarbonate sample cup was attached to the bottom of each cylinder via screw threads. The sample cup was filled with a brine solution.

Once traps were recovered, samples for particle organic carbon (POC) flux were preserved at 4°C until filtration. To avoid pellet breakage during processing, samples for POC flux were not screened; i.e. swimmers were picked out under a stereo-dissecting microscope. These samples were filtered through a pre-combusted and pre-weighed Whatman GF/F filter under vacuum pressure less than 10kPa and rinsed with Milli-Q water. Samples for fecal pellet (FP) flux were fixed with 5% buffered formaldehyde solution.



Table 1. Summary list of oceanographic observations, plankton samplings and experiments at K2 during MR11-05							
Samplings/Observations	Analyses	Stat Date	Time	End Date	Time	Depth (m)	No. of samples
Drifting Sediment Trap	FPD	02 Jul	05:00	07 Jul	05:00	60/100/150/200	4
	CFlux	02 Jul	05:00	07 Jul	05:00	60/100/150/200	4
Bucket	DE	01 Jul	03:30	02 Jul	03:30		48
	DE	05 Jul	04:00	06 Jul	04:00		48
	DE	08 Jul	04:00	09 Jul	04:00		48
CTD-CMS	Pico	01 Jul	03:30			0/5/10/15/20/25/30/40	24
	Nano	01 Jul	03:30			0/5/10/15/20/25/30/40	8
	Micro	01 Jul	03:30			0/5/10/15/20/25/30/40	8
CTD-CMS	TC	02 Jul	22:00	03 Jul	22:00	20	45
	CHL	02 Jul	22:00	03 Jul	22:00	20	20
	FPD	02 Jul	22:00	03 Jul	22:00	20	30
	TC	06 Jul	17:00	07 Jul	17:00	20	45
	CHL	06 Jul	17:00	07 Jul	17:00	20	20
	FPD	06 Jul	17:00	07 Jul	17:00	20	30
Single NORPAC	FPD	01 Jul	11:30	01 Jul	11:40	0-100	-
	FPD	05 Jul	11:30	05 Jul	11:40	0-100	-
Twin NORPAC	Macro + GP	30 Jun	22:00	30 Jun	22:10	0-200	1
	Macro + GP	01 Jul	11:30	01 Jul	11:40	0-200	1
	Macro + GP	01 Jul	22:00	01 Jul	22:10	0-200	1
	Macro + GP	04 Jul	22:00	04 Jul	22:10	0-200	1
	Macro + GP	05 Jul	11:30	05 Jul	11:40	0-200	1
	Macro + GP	06 Jul	11:30	06 Jul	11:40	0-200	1
IONESS	Macro+DM	02 Jul	11:00	02 Jul	14:00	0-1000	16
	Macro+DM	02 Jul	22:00	02 Jul	01:00	0-1000	16
	Macro+DM	03 Jul	11:00	03 Jul	14:00	0-1000	16
	Macro+DM	03 Jul	22:00	03 Jul	01:00	0-1000	16
	Macro+DM	07 Jul	11:00	07 Jul	12:30	0-125	8
	Macro+DM	08 Jul	23:00	08 Jul	00:30	0-100	8
Abbreviations	FPD	Fecal pellet analyses					
	DE	Dilution experiments					
	Pico	Microscopic analyses for picoplankton					
	Nano	Microscopic analyses for nanozooplankton					
	Micro	Microscopic analyses for microplankton					
	Macro	Microscopic analyses for macrozooplankton					
	GP	Gut pigment analyses					
	FPD	Fecal pellet decomposition					
	TC	Trophic cascading					
	DM	Dry mass measurement					
	CHL	Chlorophyll measurement					

### (3) Preliminary results

During the cruise, we collected 8 samples for POC flux and 8 samples for FP flux (Tables 1 and 2). In the land laboratory, carbon and nitrogen contents will be measured from these filter samples. For fixed samples, number, shape and volume will be measured under a stereo dissecting microscope.

Samplings/Observations Analyses		Stat	End	Depth (m)		No. of	Reference
		Date	Time	Date	Time	samples	
Drifting Sediment Trap	FPD	02 Jul	05:00	07 Jul	05:00	60/100/150/200	4
	CFlux	02 Jul	05:00	07 Jul	05:00	60/100/150/200	4
Bucket	DE	01 Jul	03:30	02 Jul	03:30		48
	DE	05 Jul	04:00	06 Jul	04:00		48
	DE	08 Jul	04:00	09 Jul	04:00		48
CTD-CMS	Pico	01 Jul	03:30			0/5/10/15/20/25/30/40	24
	Nano	01 Jul	03:30			0/5/10/15/20/25/30/40	8
	Micro	01 Jul	03:30			0/5/10/15/20/25/30/40	8
CTD-CMS	TC	02 Jul	22:00	03 Jul	22:00	20	45
	CHL	02 Jul	22:00	03 Jul	22:00	20	20
	FPD	02 Jul	22:00	03 Jul	22:00	20	30
	TC	06 Jul	17:00	07 Jul	17:00	20	45
	CHL	06 Jul	17:00	07 Jul	17:00	20	20
	FPD	06 Jul	17:00	07 Jul	17:00	20	30
Single NORPAC	FPD	01 Jul	11:30	01 Jul	11:40	0-100	-
	FPD	05 Jul	11:30	05 Jul	11:40	0-100	-
Twin NORPAC	Macro + GP	30 Jun	22:00	30 Jun	22:10	0-200	1
	Macro + GP	01 Jul	11:30	01 Jul	11:40	0-200	1
	Macro + GP	01 Jul	22:00	01 Jul	22:10	0-200	1
	Macro + GP	04 Jul	22:00	04 Jul	22:10	0-200	1
	Macro + GP	05 Jul	11:30	05 Jul	11:40	0-200	1
	Macro + GP	06 Jul	11:30	06 Jul	11:40	0-200	1
IONESS	Macro+DM	02 Jul	11:00	02 Jul	14:00	0-1000	16
	Macro+DM	02 Jul	22:00	02 Jul	01:00	0-1000	16
	Macro+DM	03 Jul	11:00	03 Jul	14:00	0-1000	16
	Macro+DM	03 Jul	22:00	03 Jul	01:00	0-1000	16
	Macro+DM	07 Jul	11:00	07 Jul	12:30	0-125	8
	Macro+DM	08 Jul	23:00	08 Jul	00:30	0-100	8
Abbreviations	FPD	Fecal pellet analyses					
	DE	Dilution experiments					
	Pico	Microscopic analyses for picoplankton					
	Nano	Microscopic analyses for nanozooplankton					
	Micro	Microscopic analyses for microplankton					
	Macro	Microscopic analyses for macrozooplankton					
	GP	Gut pigment analyses					
	FPD	Fecal pellet decomposition					
	TC	Trophic cascading					
	DM	Dry mass measurement					
	CHL	Chlorophyll measurement					

### (4) Reference

- Aristegui, J., Duarte, C.M., Agusti, S., Doval, M., Alvarez-Salgado, X.A., Hansell, D.A. (2002). Dissolved organic carbon support of respiration in the dark ocean. *Science*, 298, 1967-1967.
- Bishop, J.K., Edmond, J.M., Ketten, D.R., Bacon, M.P., Silker, W.B. (1977). The chemistry, biology, and vertical flux of particulate matter from the upper 400m of the equatorial Atlantic Ocean. *Deep-Sea Research*, 24, 511-548.
- Carroll, M.L., Miquel, J.-C., Fowler, S.W. (1998). Seasonal patterns and depth-specific trends of zooplankton fecal pellet fluxes in the Northwestern Mediterranean Sea. *Deep-Sea Research I*, 45, 1303-1318.
- González, H. E., Smetacek, V. (1994). The possible role of the cyclopoid copepod *Oithona* in retarding vertical flux of zooplankton fecal material. *Marine Ecology Progress Series*, 113, 233-246.
- Flower, S.W., Knauer, G.A. (1986). Role of large particles in the transport of elements and organic compounds through the oceanic water column. *Progress in Oceanography*, 16, 147-194.
- Honjo, S., Roman, M. R. (1978). Marine copepod fecal pellets: production, preservation and sedimentation. *Journal of Marine Research*, 36, 45-57.

- Huskin, I., Viesca, L., Anado' n, R. (2004). Particle flux in the Subtropical Atlantic near the Azores: influence of mesozooplankton. *Journal of Plankton Research*, 26, 403-415.
- Iversen, M. H., Poulsen, M. R. (2007). Coprorhexy, coprophagy, and coprochaly in the copepods *Calanus helgolandicus*, *Pseudocalanus elongatus*, and *Oithona similis*. *Marine Ecology Progress Series*, 350, 79-89.
- Lampitt, R.S., Noji, T.T., von Bodungen, B. (1990). What happens to zooplankton faecal pellets? Implications for material flux. *Marine Biology*, 104, 15-23.
- Noji, T. T., Estep, K. W., MacIntyre, F., Norrbin, F. (1991). Image analysis of faecal material grazed upon by three species of copepods: evidence for coprohexy, coprophagy, and coprochaly. *Journal of the Marine Biological Association of the United Kingdom*, 71, 465-480.
- Paffenhöfer, G.-A., Strickland, J. D. H. (1970). A note on the feeding of *Calanus helgolandicus* on detritus. *Marine Biology*, 5, 97-99.
- Poulsen, L. K., Kiørboe, T. (2006). Vertical flux and degradation rates of copepod fecal pellets in a zooplankton community dominated by small copepods. *Marine Ecology Progress Series*, 323, 195-204.
- Poulsen, M. R., Iversen, M. H. (2008). Degradation of copepod fecal pellets: key role of protozooplankton. *Marine Ecology Progress Series*, 367, 1-13.
- Reigstad, M., Riser, C. W., Svensen, C. (2005). Fate of copepod faecal pellets and the role of *Oithona* spp. *Marine Ecology Progress Series*, 304, 265-270.
- Silver, M.W., Gowing, M.M. (1991). The "particle" flux: origins and biological components. *Oceanography*, 26, 75-113.
- Suzuki, H., Sasaki, H., Fukuchi, M. (2003). Loss processes of sinking fecal pellets of zooplankton in the mesopelagic layers of the Antarctic marginal ice zone. *Journal of Oceanography*, 59, 809-818.
- Svensen, C., Nejstgaard, J. C. (2003). Is sedimentation of copepod faecal pellets determined by cyclopoids? Evidence from enclosed ecosystems. *Journal of Plankton Research*, 25, 917-926.
- Turner, J.T. (2002). Zooplankton fecal pellets, marine snow and sinking phytoplankton blooms. *Aquatic Microbial Ecology*, 27, 57-102.
- Wilson, S. E., Steinberg, D. K., Buesseler, K. O. (2008). Changes in fecal pellet characteristics with depth as indicators of zooplankton repackaging of particles in the mesopelagic zone of the subtropical and subarctic North Pacific Ocean. *Deep-Sea Research II*, 55, 1636-1647.

### 3.7 Po-210 and export flux

**Hajime KAWAKAMI (JAMSTEC MIO)**  
**Makio C. HONDA (JAMSTEC RIGC)**

#### (1) Purpose of the study

The fluxes of POC were estimated from Particle-reactive radionuclide ( $^{210}\text{Po}$ ) and their relationship with POC in the western North Pacific Ocean.

#### (2) Sampling

Seawater and suspended particulate sampling for  $^{210}\text{Po}$ ,  $^{210}\text{Pb}$ , and POC: 2 stations (stations K2 and S1) and 16 depths (10, 20, 30, 50, 75, 100, 150, 200, 300, 400, 500, 600, 700, 800, 900, and 1000 m) at each station.

Seawater samples (10 L for  $^{210}\text{Po}$  and  $^{210}\text{Pb}$ ) were taken from Hydrocast at each depth. The seawater samples for  $^{210}\text{Po}$  were filtered through polypropylene cartridge filters with a nominal pore size of 0.8  $\mu\text{m}$  on board immediately after water sampling.

*In situ* filtering (suspended particulate) samples were taken from large volume pump sampler (Large Volume Water Transfer System WTS-6-1-142LV04, McLane Inc.). Approximately 200 and 1000 L seawater was filtered through glass-fiber filter with a nominal pore size of 0.7  $\mu\text{m}$  at each station at 10–200m depths and 300–1000m depths, respectively. The filter samples were divided for  $^{210}\text{Po}$  and POC.

#### (3) Chemical analyses

Dissolved and particulate  $^{210}\text{Po}$  was absorbed on 25 mm silver disks electrically, and were measured by  $\alpha$ -ray counter (Octéte, Seiko EG&G Co. Ltd.). For total (dissolved + particulate)  $^{210}\text{Pb}$  measurement, the same procedure was applied to the seawater samples 18 months later, when  $^{210}\text{Po}$  come to radioactive equilibrium with  $^{210}\text{Pb}$ .

POC was measured with an elemental analyzer (Perkin-Elmer model 2400II) in land-based laboratory.

#### (4) Preliminary result

The distributions of  $^{210}\text{Po}$  and POC will be determined as soon as possible after this cruise. This work will help further understanding of particle dynamics at the euphotic layer and twilight zone.

### 3.8 Settling velocity of particles in the twilight zone

**Yoshihisa MINO (NAGOYA UNIV. HyARC)**

**Chiho SUKIGARA (NAGOYA UNIV. HyARC)**

#### (1) Objective

Sinking particles have been considered as the most important vehicle, by which the biological pump sequesters carbon in the ocean interior (Buesseler et al., 2007). As the particles sink they undergo the remineralization processes (fragmented into non-sinking ones and consumed by bacteria etc.) in the twilight zone, which leads to POC flux attenuation with depth. A large number of sediment trap studies have revealed that POC flux attenuation varied seasonally and regionally (Berelson, 2001), so it is required to understand this variability in order to better quantify the magnitude of biological pump. Recent studies pointed out the significance of particle settling velocity, varying three orders of magnitude, as a parameter affecting the flux attenuation (Armstrong et al., 2002, 2009; Trull et al., 2008).

This study aims to determine the settling velocity (SV) of particles collected by sediment trap at ~100 and 200 m depth for the subarctic (station K2) and subtropical (S1) North Pacific Ocean, for further understanding the carbon transfer in the twilight zone.

#### (2) Materials and methods

Particulate samples were collected in the drifting sediment trap experiments conducted during this cruise (see the chapter 3.6 for details on the sediment trap experiments). The depth of sample collection is 90-95, 180-190m at both stations (K2 and S1).

Here we applied the elutriation method (Peterson et al. 2005) to fractionate particles into SV classes using countercurrents of varying speeds. A portion of the sediment trap samples was introduced into the custom-built polycarbonate elutriator and separated into 5 fractions with SVs of >500, 150-500, 50-150, 15-50, <15 m d<sup>-1</sup>. After the swimmers are removed using the tweezers under microscope, each SV-fraction sample was filtrated onto pre-combusted GF/F filter and stored frozen. The organic carbon content in samples will be determined on shore, which derive the settling velocity spectra of the trapped particles. The carbon and nitrogen isotope abundances are also determined for each SV-fraction.

#### (3) Data archive

The experimental data sets from this study will be submitted to JAMSTEC Data Integration and Analyses Group (DIAG).

#### (4) References

- Armstrong et al. (2002), *Deep-Sea Res. II*, 49, 219-236.
- Armstrong et al. (2009), *Deep-Sea Res. II*, 56, 1470-1478.
- Berelson, (2001), *Oceanography*, 14, 59-67.
- Buesseler et al. (2007), *Science*, 316, 567-570.
- Peterson et al. (2005), *Limnol. Oceanogr.: Methods*, 3, 520-532.
- Trull et al. (2008), *Deep-Sea Res. II*, 55, 1684-1695.

### 3.9 Zooplankton

#### 3.9.1 Community structure and ecological roles

**Minoru KITAMURA(JAMSTEC)**

**Kazuhiko MATSUMOTO (JAMSTEC)**

**Toru KOBARI (Kagoshima Univ.)**

##### (1) Objective

Subarctic western North Pacific is known to be a region with high biological draw down of atmospheric CO<sub>2</sub>. And time-series biogeochemical observations conducted at the station K2 have revealed high annual material transportation efficiency to the deep compared to the other time-series sites set in the subtropical regions. Importance of not only sinking particle but also ‘active transport’ by zooplankton on vertical material transport is recently suggested in several area such as Oyashio region, the station BATS or Antarctic Ocean. However, biogeochemical role of zooplankton is not fully estimated in western subarctic gyre, North Pacific. With these backgrounds, goal of the research is to investigate roles of mesozooplankton and micronekton in vertical material transport in the station K2, western subarctic North Pacific. We deployed two types of plankton nets to investigate species and size composition of zooplankton from the surface to the greater deep.

Material transport through microbial food web is one of the pathways which is little understood. To estimate ecological roles of the nano- and microzooplankton we will also analyze abundance, vertical distribution and grazing pressure of them.

For comparison to K2 ecosystem, we also conducted same samplings at a new time-series station, S1

##### (2) Materials and methods

###### *Mesozooplankton and micronekton samplings (IONESS Sampling)*

For collection of stratified sample sets, multiple opening/closing plankton net system, IONESS, was used. This is a rectangular frame trawl with nine nets. Area of the net mouth is 1.5 m<sup>2</sup> when the net frame is towed at 45° in angle, and mesh pore size is 0.33-mm. Volume of filtering water of each net is estimated using area of net mouth, towing distance, and filtering efficiency. The area of net mouth is calibrated from frame angle during tow, the towing distance is calculated from revolutions of flow-meter, and the filtering efficiency is 96% which was directly measured. The net system is towed obliquely. Ship speed during net tow was about 2 knot, speeds of wire out and reeling were 0.1-0.7 m/s and 0.1-0.3 m/s, respectively.

Total ten tows (except three tows for collection of RI samples) of IONESS were done. The stratified sampling layers at stations K2 and S1 were summarized in the Table 3.9.1-1. To understand diel vertical migration of mesozooplankton and micronekton, the samplings were conducted during both day and night. Towing data such as date, time, position, sampling layers are summarized in Table 3.5.1-1.

###### *NORPAC net sampling*

A twin-type NORPAC net with fine mesh (100 mm) and flow meters was used. The net was vertically towed 0-50 m and 0-150 m at the Stations K2 and S1. Zooplankton samples were preserved in the 5% buffered formalin seawater for the later analysis.

### Nano- and microzooplankton sampling

Seawater samples were collected at eight depths within the euphotic and three depths within the aphotic zones in both the stations K2 and S1. The former eight depths corresponded to nominal specific optical depths approximately 100, 50, 35, 17, 12, 7, 3 and 1% light intensity relative to the surface irradiance as determined from the optical profiles obtained by PAR sensor attached on CTD system. And the latter three depths were 200, 400 and 800 m.

Seawater samples were immediately treated with the final concentration of 1% glutaraldehyde and were kept at 4°C until filtering. Each seawater sample were filtered through 1µm pore size Nuclepore filter, pre-stained by irgalan black, at the low vacuum of 15 cmHg, and were double-stained using DAPI (4'-diamidino-2-phenylindole dihydrochloride) and proflavine (3-6-diamidino-acridine hemisulfate). Just before the finish of filtering, DAPI was added to sample in filtering funnel for the staining DNA. After the DAPI staining, proflavine was also added for the staining of flagella. Both the staining time is five minute. The working solution of DAPI (10 µg/ml) and proflavine (0.033%) were pre-filtered through 0.45 µm pore size of non-pyrogenic Durapore membrane filter (Millipore, Millex-GX). After the filtering, sample filters put on a slide-glass with one drop of immersion oil, and covered with micro cover glass. All preparations were stored in the deep freezer (-80°C) until the observation.

Sampling data such as depths or filtering volume are summarized in Table 3.9.1-2.

**Table 3.9.1-1. Summary of IONESS samplings.**

#### MR11-05 IONESS Samplings

including filtering efficiency, 96%, in calculations of filtering volume of water

Stn.	Tow ID	Date & Time			Position	Sampling layer (upper, m) and filtering volume (bottom, m³)									Remarks	
		LST	in out	UTC	in out	Net No. 0	1	2	3	4	5	6	7	8		
K2	I110702A	2011.7.2	11:05	2011.7.2	0:05	47°00.00'N, 160°04.90'E	0-1074-1000	1000-750	750-500	500-300	300-200	200-150	150-100	100-50	50-0	RI-IONESS
		13:59	2:59		46°55.14'N, 160°08.80'E		2673.3	2846.7	1696.3	823.5	546.7	345.1	622.8	724.3		
	I110702B	2011.7.2	22:06	2011.7.2	11:06	46°59.79'N, 160°04.92'E	0-1085-1000	1000-750	750-500	500-300	300-200	200-150	150-100	100-50	50-0	
		2011.7.3	1:00		14:00	46°54.81'N, 160°07.90'E		2149.3	2585.9	2235	1006.6	608.3	1109.1	942.9	911.4	
	I110703A	2011.7.3	11:08	2011.7.3	0:08	46°59.85'N, 160°05.03'E	0-1085-1000	1000-750	750-500	500-300	300-200	200-150	150-100	100-50	50-0	
		13:55	2:55		46°55.60'N, 160°08.07'E		2868.9	3039.1	1989	627.8	545.9	337.3	423.6	976.7		
	I110703B	2011.7.3	22:00	2011.7.3	11:00	46°59.90'N, 160°04.68'E	0-1055-1000	1000-750	750-500	500-300	300-200	200-150	150-100	100-50	50-0	
		2011.7.4	0:55		13:55	46°54.73'N, 160°03.81'E		3525.5	3089.1	1856.5	936.3	518.7	816.6	682.2	661.3	
	I110705A	2011.7.5	22:06	2011.7.5	11:06	46°59.82'N, 160°04.96'E	0-200-100	100-25	25-0	0-100	100-25	25-0	0-100	100-25	25-0	
		2011.7.6	1:00		14:00	46°54.73'N, 160°02.70'E		3158.2	1816.8	1184.7	3190.1	1950.2	1298.8	1313.8	480	
FI	I110707A	2011.7.7	11:44	2011.7.7	0:44	46°59.79'N, 160°04.32'E	0-300-125	125-100	100-75	75-50	50-40	40-30	30-20	20-10	10-0	Shallow-IONESS
		12:37	1:37		13:37	46°58.94'N, 160°02.33'E		377.2	440.4	623.5	151	125	170.9	156.3	106	
	I110708A	2011.7.8	23:00	2011.7.8	12:00	46°59.99'N, 160°05.11'E	0-300-100	100-75	75-50	50-40	40-30	30-20	20-10	10-0	0	
		2011.7.9	0:09		13:09	46°57.69'N, 160°05.16'E		449.3	402.1	131.4	175.2	110.9	160.4	70.8	-	
S1	I110713A	2011.7.13	22:06	2011.7.13	11:06	36°28.52'N, 141°29.15'E	0-200-100	100-30	30-0	0-100	100-30	30-0	0-100	100-30	30-0	RI-IONESS
		2011.7.14	0:04		13:04	36°28.89'N, 141°30.14'E		2409.7	1061.9	809.6	1830.4	496	811.3	1186.3	1137.1	
S1	I110726A	2011.7.26	21:00	2011.7.26	11:00	29°59.97'N, 144°59.67'E	0-1052-1000	1000-750	750-500	500-300	300-200	200-150	150-100	100-50	50-0	RI-IONESS
		23:51	13:51		13:51	30°00.46'N, 145°42.95'E		3388.2	2764.7	1733.5	1127.7	532.8	722.2	225.7	579.8	
	I110727A	2011.7.27	11:40	2011.7.27	1:40	29°58.26'N, 144°58.52'E	0-1053-1000	1000-750	750-500	500-300	300-200	200-150	150-100	100-50	50-0	
		14:29	4:29		4:29	30°02.44'N, 145°02.44'E		2744.0	2889.6	1740.6	1235.6	1071.0	975.6	489.1	507.6	
	I110728A	2011.7.28	21:14	2011.7.28	11:14	29°59.87'N, 144°59.25'E	0-150-100	100-25	25-0	0-100	100-25	25-0	0-100	100-25	25-0	
		23:56	13:56		13:56	30°02.31'N, 145°03.53'E		2426.4	1420.8	726.4	2171.1	1434.3	697.1	2307.1	2337.1	
	I110729A	2011.7.29	11:57	2011.7.29	1:57	30°00.00'N, 144°59.86'E	0-1065-1000	1000-750	750-500	500-300	300-200	200-150	150-100	100-50	50-0	
		14:46	4:46		4:46	30°02.05'N, 144°54.34'E		2560.1	2469.6	1992.0	1195.7	976.1	981.4	772.8	899.5	
	I110729B	2011.7.29	20:56	2011.7.29	10:56	29°59.90'N, 144°56.34'E	0-1051-1000	1000-750	750-500	500-300	300-200	200-150	150-100	100-50	50-0	
		23:47	13:47		13:47	30°04.52'N, 144°53.34'E		2608.4	2505.8	2033.1	1386.9	1210.7	890.4	975.1	1036.9	

**Table 3.9.1-2. Summary of water samplings for nano- and microzooplankton abundance**

MR11-05

Water samplings for analysis of nano- and microzooplankton abundance

\* Local ship time

Stn.	Date*	Time*	CTD cast ID	Depth (m)	Irradiance (%)	Sample No.	Filtering vol. (ml)	Funnel No.
K2	2011.7.1	2:00	K2_2 Shallow cast (PP 1st)	40	1	K2-1	265	2
				30	4	K2-2	275	3
				25	7	K2-3	290	4
				20	13	K2-4	210	1
				15	17	K2-5	210	2
				10	35	K2-6	220	3
				5	60	K2-7	235	4
				0	100	K2-S	190	1
K2	2011.7.1	6:00	K2_3 Deep cast (Routine)	200	-	K2-200	500	1
				400	-	K2-400	500	3
				800	-	K2-800	500	4
S1	2011.7.24	15:30	S1_1 Deep cast (Routine)	200	-	S1-200	500	2
				400	-	S1-400	500	3
				800	-	S1-800	500	4
S1	2011.7.25	3:30	S1_2 Shallow cast (PP 1st)	94	1	S1-1	443	1
				77	3	S1-2	365	2
				70	5	S1-3	330	3
				60	7	S1-4	350	4
				47	13	S1-5	305	1
				24	33	S1-6	345	2
				6	60	S1-7	380	3
				0	100	S1-S	390	4

### (3) Future plans and sample/data archives

#### *Community structure and ecological role of mesozooplankton*

Subsamples are stored at JAMSTEC or Kagoshima Univ. Environmental (T, S) and net status (net number, towing distance, etc.) data, which were recorded during each tow, is stored under Kitamura and Kobari. Using the IONESS samples, we will analyze about

- (a) vertical distribution of bulk biomass of zooplankton,
- (b) composition of major taxa (copepods, euphausiids, etc.) in each depth strata,
- (c) community structure in species level for dominant taxa (eg. copepods, krill),
- (d) identification of vertical migrants (diel and ontogenetic)
- (e) carbon flux by the migrants.

#### *Vertical distribution of microzooplankton*

Sample analysis is consigned to Marine Biological Research Institute of Japan Co. LTD., Shinagawa, Tokyo.



### 3.9.2 Grazing pressure of microzooplankton

**Minoru KITAMURA(JAMSTEC)**  
**Kazuhiko MATSUMOTO (JAMSTEC)**  
**Toru KOBARI (Kagoshima Univ.)**

#### (1) Objective

To understand material export from surface to deep ocean, not only estimations of primary productivity or vertical flux but also evaluation of grazing impacts at surface is needed. Grazing by larger organisms might bring about efficient vertical carbon transport through repacking phytoplankton into fecal pellets or active carbon transport by diel and ontogenetic migrator. On the other hand, grazing by smaller organisms might have small or negative impact to vertical export. Identification of influential grazers and quantitative estimation of their grazing rates are essential to discuss the carbon cycle in the ocean. Recently, large grazing pressure of not only the crustacean plankton but also microzooplankton has been recognized in the several area. Based on this background, we estimated grazing rate of them.

#### (2) Materials and methods

Eight dilution incubation experiments were done through the cruise (Table 3.9.2-1). For each experiment 40 l of water were collected from Niskin bottle or bucket. Water was pre-screened through 200 µm mesh to exclude larger zooplankton. Dilution series were prepared with 25, 50, 75, and 100% of natural seawater. Filtered water was obtained by direct gravity flow through a compact cartridge filter (ADVANTEC, MCS-020-D10SR). Incubation of the dilute water was done in transparent polycarbonate bottle. Duplicate or triplicate bottle were prepared. Incubation lasted for 24 or 48 h in a tank with continuous flow of surface seawater under natural light conditions. All the water samplings, filtering, and incubate items were soaked in 10% HCl and rinsed Milli-Q water between each use on board. Nutrient was added in the incubation bottles. To measure initial and final chl. *a* concentration, experiment water were filtered onto GF/F filter and extracted 6 ml DMF at -20°C until measurement. Chl. *a* was measured fluorometrically (Welshmeyer method) with a Turner Design fluorometer. Phytoplankton cell numbers were also counted using flowcytometry.

Apparent phytoplankton growth rate ( $d^{-1}$ ) were calculated using following equation:

$$\text{Apparent growth rate} = (1/t)\ln(P_t/P_0)$$

where *t* is incubation time (day),  $P_t$  and  $P_0$  are final and initial Chl. *a* concentration or cell number, respectively. When the apparent phytoplankton growth rate is plotted as a function of dilution factor, the y-intercept and negative slope of the approximate line means true phytoplankton growth ( $k$ ;  $d^{-1}$ ) and grazing coefficient of microzooplankton ( $g$ ;  $d^{-1}$ ), respectively. According to Verity et al. (1993) and Zhang et al. (2006), microzooplankton grazing pressure on primary production ( $P_p$ ; %) is calculated as the following equation:

$$P_p = (e^{kt} - e^{(k-g)t}) / (e^{kt} - 1) * 100$$

Through the three incubation experiments, we tried to estimate true growth rate of phytoplankton, grazing rate of microzooplankton and grazing pressure of microzooplankton on primary production. Incubation states are summarized in Table

### 3.9.2-2.

**Table 3.9.2-1. Dilution experiments, list of samplings.**

Station	Date*	Exp. ID.	Water sampling							
			Time*	Position	Depth m	Irradiance %	Temp. °C	Chl. <i>a</i> µg/l	CTD cast No.	Sampler
K2	2011.7.1	K2-1	2:00	46°59.87'N, 160°12.11'E	0	100	6.5	1.03	K2_2 Shallow cast (PP 1st)	Bucket
	2011.7.5	K2-2	2:30	47°00.01'N, 160°04.96'E	0	100	6.9	1.18	K2_8 Shallow cast (PP 2nd)	Bucket
	2011.7.5	K2-3	8:30	47°00.01'N, 160°04.96'E	25*	5	6.5	1.21	K2_9 Shallow cast (PE)	Clean Niskin
	2011.7.8	K2-4	2:30	47°00.33'N, 160°04.69'E	0	100	7.8	1.00	K2_11 Shallow cast (PP 3rd)	Bucket
S1	2011.7.25	S1-1	3:30	30°00.10'N, 144°59.97'E	0	100	26.94	0.06	S1_2 Shallow cast (PP 1st)	Bucket
	2011.7.28	S1-2	3:30	30°00.09'N, 144°59.93'E	0	100	27.1	0.08	S1_7 Shallow cast (PP 2nd)	Bucket
	2011.7.28	S1-3	9:00	30°00.49'N, 144°59.75'E	70*	3	19.7	0.67	S1_8 Shallow cast (PE/Paleo)	Clean Niskin
	2011.7.31	S1-4	5:30	29°44.02'N, 144°42.91'E	80*	ca 2	19.4	0.34	S1_13 Deep cast (ARGO#9)	Clean Niskin

\*Local ship time

# Chl. *a* max. depth

**Table 3.9.2-2. Dilution experiments, summary of incubation states.**

Station	Date*	Exp. ID.	Incubation						Remarks
			Time* start	Time* end	Incubation bottle	Temp. °C	Irradiance %	Nutrients addition	
K2	2011.7.1-2	K2-1	1 July 3:40	2 July 3:30	1L	6.5-6.7	100	+	Matsumoto FCM, Kobari FCM
	2011.7.5-6	K2-2	5 July 3:45	6 July 4:30	1L	6.8-7.5	100	+	Matsumoto FCM, Kobari FCM
	2011.7.5-6	K2-3	5 July 11:00	6 July 11:00	1L	6.8-7.5	2.5	+	Matsumoto FCM
	2011.7.8-9	K2-4	8 July 4:00	9 July 4:20	1L	7.7-9.3	100	+	Matsumoto FCM, Kobari FCM
S1	2011.7.25-26	S1-1	25 July 5:00	26 July 5:20	2L	26.8-27.7	100	++	Matsumoto FCM, Kobari FCM
	2011.7.28-29	S1-2	28 July 4:50	29 July 5:30	2L	27.0-28.3	100	++	Matsumoto FCM, Kobari FCM
	2011.7.28-29	S1-3	28 July 11:00	29 July 10:30	1L	20.5	2.5	++	Matsumoto FCM, Kobari FCM
	2011.7.31-8.1	S1-4	31 July 9:15	1 Aug. 9:30	1L	20.5	2.5	++	Matsumoto FCM

\*Local ship time

### (3) Preliminary results

All measurements of Chl. *a* and phytoplankton cell numbers were finished on board. Preliminary results of four experiments conducted in the station K2 are shown in the Figure 3.9.2-1.

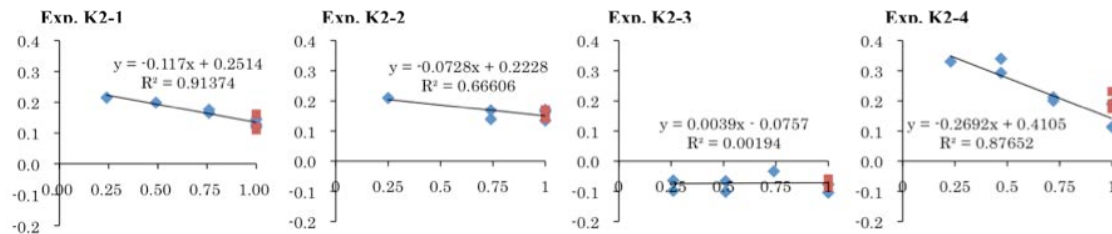


Fig.3.9.2-1. Correlation between apparent growth rates of phytoplankton community (y axis) and dilution factors (x axis). Apparent growth rates were estimated from Chl. *a* measurements. Slops of the regression line means grazing rates ( $d^{-1}$ ) of the microzooplankton community.

### References

- Verity, P.G., D.K. Stoecker, M.E. Sieracki & J.R. Nelson. 1996. Grazing, growth and mortality of microzooplankton during the 1989 North Atlantic spring bloom at 47°N, 18°W. *Deep-Sea Res.*, 40: 1793-1814.
- Zhang, W., H. Li, T. Xiao, J. Zhang, C. Li & S. Sun. 2006. Impact of microzooplankton and copepods on the growth of phytoplankton in the Yellow Sea and East China Sea. *Hydrobiologia*, 553: 357-366.

### 3.10 Effects of zooplankton on sinking carbon flux

**Toru KOBARI (Kagoshima University)**

#### 3.10.1 Active carbon flux

##### (1) Objective

It has been long accepted that sinking particles are major pathway of vertical carbon flux into the ocean interior and support mesopelagic carbon demand (Fowler and Knauer, 1986; Zhang and Dam, 1997; Aristegui et al., 2002). In the past decade, a number of studies have also shown that diurnally vertical migrants significantly contribute to carbon flux by consuming POC in surface waters and respiring and excreting the metabolized POC at depth. This “actively transported carbon flux” is equivalent to 3 to 127%, of the sinking POC flux in tropical to subarctic waters (Al-Mutairi and Landry, 2001; Dam et al., 1995; Longhurst et al., 1990; Le Borgne and Rodier, 1997; Steinberg et al., 2000, 2008; Zhang and Dam, 1997). Thus, we should evaluate how mesozooplankton community transports carbon to mesopelagic depth as active carbon flux.

In the present study, we compare abundance, biomass and taxonomic composition of mesozooplankton community between day and night at K2 and S1 in Northwestern Pacific Ocean to estimate active carbon flux.

##### (2) Methods

Samplings were carried out during the RV Mirai cruise (MR11-05) from 27 June to 4 August 2011 at K2 and S1 in the Northwestern Pacific Ocean. Mesozooplankton were collected from 200 m to sea surface using Twin North Pacific Standard net (Motoda 1957: diameter 45 cm, mesh size 0.1 mm) at a speed of 1 m sec<sup>-1</sup>. One sample was preserved in borax-buffered 5% formaldehyde for microscopic identification. Another sample was immediately anesthetized with soda water. Sample was frozen in liquid nitrogen after blotting adhering seawater on paper towels and stored at -80°C for measurement of gut pigments.

##### (3) Preliminary results

During the cruise, 6 samples at K2 and 5 samples at S1 were collected for microscopic identification (Tables 1 and 2). Simultaneously, 6 samples at K2 and 5 samples at S1 were collected for gut pigments. In the land laboratory, major taxa and predominant copepods will be identified under a stereo dissecting microscope from fixed samples. For frozen samples, gut pigments of the predominant copepods will be measured by fluorometer.

##### (4) Reference

- Al-Mutairi, H., Landry, M.R. (2001). Active export of carbon and nitrogen at Station ALOHA by diel migrant zooplankton. *Deep-Sea Research II*, 48, 2083–2103.
- Aristegui, J., Duarte, C.M., Agustí, S., Doval, M., A'lvarez-Salgado, X.A., Hansell, D.A. (2002). Dissolved organic carbon support of respiration in the dark ocean. *Science*, 298, 1967.
- Dam, H.G., Roman, M.R., Youngbluth, M.J. (1995). Downward export of respiratory carbon and dissolved inorganic nitrogen by diel-migrant mesozooplankton at the JGOFS Bermuda time-series station. *Deep-Sea Research I*, 42, 1187–1197.
- Fowler, S.W. Knauer, G.A. (1986). Role of large particles in the transport of elements and organic

- compounds through the oceanic water column. *Progress in Oceanography*. 16, 147–194.
- Le Borgne, R., Rodier, M. (1997). Net zooplankton and the biological pump: a comparison between oligotrophic and mesotrophic equatorial Pacific. *Deep-Sea Research II*, 44, 2003–2023.
- Longhurst, A.R., Bedo, A.W., Harrison, W.G., Head, E.J.H., Sameoto, D.D. (1990). Vertical flux of respiratory carbon by oceanic diel migrant biota. *Deep-Sea Research*, 37, 685–694.
- Motoda, S., (1957). North Pacific standard net. *Information Bulletin of Planktology in Japan*, 4, 13-15.
- Steinberg, D.K., Carlson, C.A., Bates, N.R., Goldthwait, S.A., Madin, L.P., Michaels, A.F. (2000). Zooplankton vertical migration and the active transport of dissolved organic and inorganic carbon in the Sargasso Sea. *Deep-Sea Research I*, 47, 137–158.
- Steinberg, D.K., Cope, J.S., Wilson, S.E., Kobari, T. (2008). A comparison of mesopelagic mesozooplankton community structure in the subtropical and subarctic North Pacific Ocean. *Deep-Sea Research II*, 55, 1615– 1635.
- Zhang, X., Dam, H.G. (1997). Downward export of carbon by diel migrant mesozooplankton in the central equatorial Pacific. *Deep-Sea Research II*, 44, 2191–2202.

### 3.10.2 Production and consumption of fecal pellets

#### (1) Objective

Fecal pellets are changed by zooplankton ingestion (coprophagy), fragmentation via sloppy feeding or swimming activity (coprorhexy) and loosening of membrane (coprochaly) during sinking (Paffenhöfer and Strickland, 1970; Lampitt et al., 1990; Noji et al., 1991). These processes largely affect transfer efficiency of POC flux (Wilson et al., 2008). It has been believed that fecal pellets are declined by bacterial decomposition (Honjo and Roman, 1978; Aristegui et al., 2002) and/or coprophagy/coprorhexy of small copepods such as cyclopoids and poecilostomatoids for last two decades (González and Smetacek, 1994; Suzuki et al., 2003; Svensen and Nejstgaard, 2003; Huskin et al., 2004; Poulsen and Kiørboe, 2006). In recent years, however, these copepods showed minor contributions to coprophagy/coprorhexy from the field observations (Iversen and Poulsen, 2007) and laboratory experiments (Reigstad et al., 2005), and heterotrophic microbes consume fecal pellets (Poulsen and Iversen, 2008). Thus, we should re-consider how fecal pellets are declined or changed during sinking from surface to mesopelagic depths.

In the present study, we carried out on-board experiments to evaluate how heterotrophic microbes and copepods affect fecal pellets at K2 and S1 in Northwestern Pacific Ocean.

#### (2) Methods

Samplings were carried out during the RV Mirai cruise from 27 June to 4 August 2011 at K2 and S1 in the Northwestern Pacific Ocean. Live copepods were collected from the depth at 1% light intensity to sea surface using North Pacific Standard net (Motoda 1957: diameter 45 cm, mesh size 0.1 mm) at a speed of 0.5 m sec<sup>-1</sup>.

We carried out on-board experiments to evaluate effects of heterotrophic microbes and copepods on fecal pellets at both stations. Live copepods were identified under stereomicroscope and transferred into chambers (9-mL glass bottle with GF/F filtered seawater) and placed at ambient temperature under dark condition. Fecal pellets were gently collected from incubation bottle from *Artemia salina*. Following the methods of Poulsen and Iversen (2008), bottle incubations were done.

#### (3) Preliminary results

During the cruise, on-board experiments were carried out twice at S1 and K2. Each sample will be brought back to the land laboratory for microscopic analysis on number, shape and volume for fecal pellets.

#### (4) Reference

- Aristegui, J., Duarte, C.M., Agusti, S., Doval, M., Alvarez-Salgado, X.A., Hansell, D.A. (2002). Dissolved organic carbon support of respiration in the dark ocean. *Science*, 298, 1967-1967.
- González, H. E., Smetacek, V. (1994). The possible role of the cyclopoid copepod *Oithona* in retarding vertical flux of zooplankton fecal material. *Marine Ecology Progress Series*, 113, 233-246.
- Honjo, S., Roman, M. R. (1978). Marine copepod fecal pellets: production, preservation and sedimentation. *Journal of Marine Research*, 36, 45-57.
- Huskin, I., Viesca, L., Anado' n, R. (2004). Particle flux in the Subtropical Atlantic near the

- Azores: influence of mesozooplankton. *Journal of Plankton Research*, 26, 403-415.
- Iversen, M. H., Poulsen, M. R. (2007). Coprorhexy, coprophagy, and coprochaly in the copepods *Calanus helgolandicus*, *Pseudocalanus elongatus*, and *Oithona similis*. *Marine Ecology Progress Series*, 350, 79-89.
- Lampitt, R.S., Noji, T.T., von Bodungen, B. (1990). What happens to zooplankton faecal pellets? Implications for material flux. *Marine Biology*, 104, 15-23.
- Motoda, S., (1957). North Pacific standard net. *Information Bulletin of Planktology in Japan*, 4, 13-15.
- Noji, T. T., Estep, K. W., MacIntyre, F., Norrbin, F. (1991). Image analysis of faecal material grazed upon by three species of copepods: evidence for coprohexy, coprophagy, and coprochaly. *Journal of the Marine Biological Association of the United Kingdom*, 71, 465-480.
- Paffenhöfer, G.-A., Strickland, J. D. H. (1970). A note on the feeding of *Calanus helgolandicus* on detritus. *Marine Biology*, 5, 97-99.
- Poulsen, L. K., Kiørboe, T. (2006). Vertical flux and degradation rates of copepod fecal pellets in a zooplankton community dominated by small copepods. *Marine Ecology Progress Series*, 323, 195-204.
- Poulsen, M. R., Iversen, M. H. (2008). Degradation of copepod fecal pellets: key role of protozooplankton. *Marine Ecology Progress Series*, 367, 1-13.
- Reigstad, M., Riser, C. W., Svensen, C. (2005). Fate of copepod faecal pellets and the role of *Oithona* spp. *Marine Ecology Progress Series*, 304, 265-270.
- Suzuki, H., Sasaki, H., Fukuchi, M. (2003). Loss processes of sinking fecal pellets of zooplankton in the mesopelagic layers of the Antarctic marginal ice zone. *Journal of Oceanography*, 59, 809-818.
- Svensen, C., Nejstgaard, J. C. (2003). Is sedimentation of copepod faecal pellets determined by cyclopoids? Evidence from enclosed ecosystems. *Journal of Plankton Research*, 25, 917-926.
- Wilson, S. E., Steinberg, D. K., Buesseler, K. O. (2008). Changes in fecal pellet characteristics with depth as indicators of zooplankton repackaging of particles in the mesopelagic zone of the subtropical and subarctic North Pacific Ocean. *Deep-Sea Research II*, 55, 1636-1647.

### 3.11 Biological study for phytoplankton and zooplankton

**Katsunori KIMOTO (RIGC, JAMSTEC)**

**Michelle TIGCHELAAR (Hawaii Univ. / RIGC, JAMSTEC)**

#### 3.11.1 Planktic Foraminifers and radiolarians

##### (1) Objective

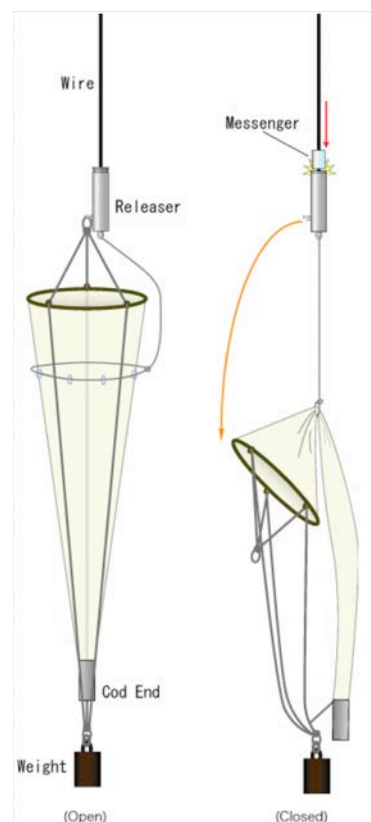
Planktic foraminifers and radiolarians produce calcium carbonate and siliceous tests respectively and contribute to the material cycles. Planktic foraminifers show wide distributions in the surface water. Recent molecular biological studies revealed the high genetic variations within many planktic foraminifera species. These intra-specific genetic variations considered be the indications of the cryptic speciation and their ecologies could be different among these cryptic species. Moreover, morphological variations which correspond to the genetic populations is confirmed on several species. The water mass structure is considered as one of the factors which affect the distribution of the genetic populations. However, the genetic variability of the planktic foraminifers is not fully understood. In this study, we collected living planktic foraminifer in order to reveal the genetic populations of the planktic foraminifera in the North Pacific Subpolar gyre and the Subtropical gyre.

##### (2) Methods

Living planktic foraminifera samples were collected by filtration of surface seawater and vertical towing of a NORPAC net (Fig. 3-11-1). Surface seawater taken from onboard seawater tap was filtered using filtration apparatus (100  $\mu\text{m}$  opening). The NORPAC net towing was conducted at station K2 and S1. A closing NORPAC net (63  $\mu\text{m}$  opening) was used in order to obtain depth-stratified samples. The sampling depths of the NORPAC net tows are summarized in Table 3.11.1. Obtained NORPAC net samples were divided using sample separation apparatus and the half volume of the sample were used for DNA analysis.

The divided samples were stored at 4 °C and living planktic foraminifer and radiolarian individuals were picked under a stereomicroscope. Picked specimens were cleaned in filtered seawater with fine brushes. Specimens were air dried on the faunal slides and stored at -80 °C.

Fig.3-11-1 Schematic illustration of closing NORPAC net. Plankton net is open during towing (left), and closed at the top of the sampling depth range by deploying a messenger (right).



(3) Preliminary result on shipboard

Species identifications under stereomicroscope show that planktic foraminifer species at K2 consist of subpolar species while species at S1 is consist of subtropical species. Samples collected station K2 contained *Globigerina bulloides*, *Neogloboquadrina pachyderma*, *Turborotalita quinqueloba*, and *Globigerinita uvula*. Planktic foraminifera species observed in the samples collected in the Subtropical Gyre region include *Globigerinoides ruber*, *Globigerinoides sacculifer*, *Globigerinoides conlobatus*, *Orbulina universa*, *Hastigerina pelagica*, *Globorotalia truncatulinoides*, *Globorotalia menardii*, and *Streptochilus globulosus*. The number of individuals collected at S1 was very few compared to the samples collected at K2.

(4) Data archive

The planktic foraminifer samples are stored at JAMSTEC. Molecular phylogenetic analyses and morphological observations will be conducted.



Table 3-11-1. Summary of plankton tow sampling.

Station	Latitude	Longitude	Depth (m)	Date	Time	Station	Latitude	Longitude	Depth (m)	Date	Time
K2	47 0 N	160 0 E	0-20	2011 6 30	7:00 UTC	S1	30 0 N	145 0 E	750-1000	2011 7 26	24:00 UTC
K2	47 0 N	160 0 E	20-50	2011 6 30	7:10 UTC	S1	30 0 N	145 0 E	500-750	2011 7 26	24:00 UTC
K2	47 0 N	160 0 E	50-100	2011 6 30	7:20 UTC	S1	30 0 N	145 0 E	300-500	2011 7 26	24:00 UTC
K2	47 0 N	160 0 E	100-150	2011 6 30	7:30 UTC	S1	30 0 N	145 0 E	200-300	2011 7 26	24:00 UTC
K2	47 0 N	160 0 E	150-200	2011 6 30	7:40 UTC	S1	30 0 N	145 0 E	150-200	2011 7 26	24:00 UTC
K2	47 0 N	160 0 E	200-300	2011 6 30	8:00 UTC	S1	30 0 N	145 0 E	100-150	2011 7 26	24:00 UTC
K2	47 0 N	160 0 E	300-500	2011 7 1	4:00 UTC	S1	30 0 N	145 0 E	50-100	2011 7 26	24:00 UTC
K2	47 0 N	160 0 E	500-700	2011 7 1	5:00 UTC	S1	30 0 N	145 0 E	0-50	2011 7 26	24:00 UTC
K2	47 0 N	160 0 E	700-1000	2011 7 1	6:00 UTC	S1	30 0 N	145 0 E	750-1000	2011 7 26	24:00 UTC
K2	47 0 N	160 0 E	0-20	2011 7 2	3:00 UTC	S1	30 0 N	145 0 E	500-750	2011 7 26	24:00 UTC
K2	47 0 N	160 0 E	20-50	2011 7 2	3:10 UTC	S1	30 0 N	145 0 E	300-500	2011 7 26	24:00 UTC
K2	47 0 N	160 0 E	50-100	2011 7 2	3:20 UTC	S1	30 0 N	145 0 E	200-300	2011 7 26	24:00 UTC
K2	47 0 N	160 0 E	100-150	2011 7 2	3:30 UTC	S1	30 0 N	145 0 E	150-200	2011 7 26	24:00 UTC
K2	47 0 N	160 0 E	150-200	2011 7 2	3:40 UTC	S1	30 0 N	145 0 E	100-150	2011 7 26	24:00 UTC
K2	47 0 N	160 0 E	200-300	2011 7 2	4:00 UTC	S1	30 0 N	145 0 E	50-100	2011 7 26	24:00 UTC
K2	47 0 N	160 0 E	300-500	2011 7 3	21:00 UTC	S1	30 0 N	145 0 E	0-50	2011 7 26	24:00 UTC
K2	47 0 N	160 0 E	500-700	2011 7 3	21:30 UTC	S1	30 0 N	145 0 E	750-1000	2011 7 27	12:00 UTC
K2	47 0 N	160 0 E	700-1000	2011 7 3	22:20 UTC	S1	30 0 N	145 0 E	500-750	2011 7 27	12:00 UTC
K2	47 0 N	160 0 E	200-300	2011 7 5	4:10 UTC	S1	30 0 N	145 0 E	300-500	2011 7 27	12:00 UTC
K2	47 0 N	160 0 E	150-200	2011 7 5	4:20 UTC	S1	30 0 N	145 0 E	200-300	2011 7 27	12:00 UTC
K2	47 0 N	160 0 E	100-150	2011 7 5	4:30 UTC	S1	30 0 N	145 0 E	150-200	2011 7 27	12:00 UTC
K2	47 0 N	160 0 E	50-100	2011 7 5	4:40 UTC	S1	30 0 N	145 0 E	100-150	2011 7 27	12:00 UTC
K2	47 0 N	160 0 E	20-50	2011 7 5	4:50 UTC	S1	30 0 N	145 0 E	50-100	2011 7 27	12:00 UTC
K2	47 0 N	160 0 E	0-20	2011 7 5	5:10 UTC	S1	30 0 N	145 0 E	0-50	2011 7 27	12:00 UTC
K2	47 0 N	160 0 E	0-50	2011 7 5	5:30 UTC	S1	30 0 N	145 0 E	750-1000	2011 7 27	12:00 UTC
K2	47 0 N	160 0 E	500-1000	2011 7 6	2:00 UTC	S1	30 0 N	145 0 E	500-750	2011 7 27	12:00 UTC
K2	47 0 N	160 0 E	300-500	2011 7 6	2:40 UTC	S1	30 0 N	145 0 E	300-500	2011 7 27	12:00 UTC
K2	47 0 N	160 0 E	200-300	2011 7 6	3:00 UTC	S1	30 0 N	145 0 E	200-300	2011 7 27	12:00 UTC
K2	47 0 N	160 0 E	100-200	2011 7 6	3:20 UTC	S1	30 0 N	145 0 E	150-200	2011 7 27	12:00 UTC
K2	47 0 N	160 0 E	50-100	2011 7 6	3:40 UTC	S1	30 0 N	145 0 E	100-150	2011 7 27	12:00 UTC
K2	47 0 N	160 0 E	0-50	2011 7 6	4:00 UTC	S1	30 0 N	145 0 E	50-100	2011 7 27	12:00 UTC
K2	47 0 N	160 0 E	200-300	2011 7 6	21:00 UTC	S1	30 0 N	145 0 E	0-50	2011 7 27	12:00 UTC
K2	47 0 N	160 0 E	150-200	2011 7 6	21:20 UTC	S1	30 0 N	145 0 E	750-1000	2011 7 29	12:00 UTC
K2	47 0 N	160 0 E	100-150	2011 7 6	21:40 UTC	S1	30 0 N	145 0 E	500-750	2011 7 29	12:00 UTC
K2	47 0 N	160 0 E	50-100	2011 7 6	21:50 UTC	S1	30 0 N	145 0 E	300-500	2011 7 29	12:00 UTC
K2	47 0 N	160 0 E	20-50	2011 7 6	22:00 UTC	S1	30 0 N	145 0 E	200-300	2011 7 29	12:00 UTC
K2	47 0 N	160 0 E	0-20	2011 7 6	22:10 UTC	S1	30 0 N	145 0 E	150-200	2011 7 29	12:00 UTC
K2	47 0 N	160 0 E	500-1000	2011 7 7	3:45 UTC	S1	30 0 N	145 0 E	100-150	2011 7 29	12:00 UTC
K2	47 0 N	160 0 E	300-500	2011 7 7	4:30 UTC	S1	30 0 N	145 0 E	50-100	2011 7 29	12:00 UTC
K2	47 0 N	160 0 E	150-300	2011 7 7	5:00 UTC	S1	30 0 N	145 0 E	0-50	2011 7 29	12:00 UTC
K2	47 0 N	160 0 E	50-150	2011 7 7	5:20 UTC	S1	30 0 N	145 0 E	750-1000	2011 7 29	24:00 UTC
K2	47 0 N	160 0 E	0-50	2011 7 7	5:45 UTC	S1	30 0 N	145 0 E	500-750	2011 7 29	24:00 UTC
						S1	30 0 N	145 0 E	300-500	2011 7 29	24:00 UTC
						S1	30 0 N	145 0 E	200-300	2011 7 29	24:00 UTC
						S1	30 0 N	145 0 E	150-200	2011 7 29	24:00 UTC
						S1	30 0 N	145 0 E	100-150	2011 7 29	24:00 UTC
						S1	30 0 N	145 0 E	50-100	2011 7 29	24:00 UTC
						S1	30 0 N	145 0 E	0-50	2011 7 29	24:00 UTC

### 3.11.2 Shell-bearing phytoplankton studies in the western North Pacific

#### (1) Objectives

Shell-bearing phytoplanktons (Diatoms, Silicoflagellates, and Coccolithophorids) are main primary producer of the ocean, therefore it is important to know their seasonal distribution, interactions, and transgressions of assemblages. Furthermore, hard skeletons of phytoplankton remains in the deep sea sediments and it provide useful information for paleoceanographic changes of sea surface water conditions. In this study, we collected water samples from Stn. K2 and S1 to investigate vertical distributions and ecological features of each phytoplankton.

#### (2) Methods

Seawater samples were obtained from upper 200 m water depths at all hydrocast stations by CTD/Niskin systems of 12 L bottle capacity. The locations that were collected seawater were listed in Table 2.

For coccolithophorid separations, maximally 10 litter seawaters were filtered using 0.8  $\mu\text{m}$  membrane filter (ADVANTEC MFS, Inc., JAPAN) immediately after collection. For diatoms and silicoflagellates separations, maximally 5 litter seawaters were also filtered using 0.45  $\mu\text{m}$  membrane filter.

#### (3) Future works

Collected samples were analyzed assemblages, diversities and spacial distributions for each taxon at onshore laboratory. These data will be compared with the sediment trap datasets that are moored at St. S1 and K2, same locations with water sampling points in this time. That should be provided the important information of seasonal and spacial variability of phytoplankton related with oceanographic changes in the western north Pacific.

Table3-11-2. Summary of seawater filtration sampling.

Station	Latitude			Longitude			Depth (m)		Date			Time	
K2	47	0	N	160	0	E	200	2011	7	1	21:00	UTC	
K2	47	0	N	160	0	E	150	2011	7	2	21:00	UTC	
K2	47	0	N	160	0	E	100	2011	7	2	21:00	UTC	
K2	47	0	N	160	0	E	75	2011	7	2	21:00	UTC	
K2	47	0	N	160	0	E	50	2011	7	2	21:00	UTC	
K2	47	0	N	160	0	E	30	2011	7	2	21:00	UTC	
K2	47	0	N	160	0	E	10	2011	7	2	21:00	UTC	
K2	47	0	N	160	0	E	0	2011	7	2	21:00	UTC	
S1	30	0	N	145	0	E	200	2011	7	28	23:00	UTC	
S1	30	0	N	145	0	E	150	2011	7	28	23:00	UTC	
S1	30	0	N	145	0	E	100	2011	7	28	23:00	UTC	
S1	30	0	N	145	0	E	75	2011	7	28	23:00	UTC	
S1	30	0	N	145	0	E	50	2011	7	28	23:00	UTC	
S1	30	0	N	145	0	E	30	2011	7	28	23:00	UTC	
S1	30	0	N	145	0	E	10	2011	7	28	23:00	UTC	
S1	30	0	N	145	0	E	0	2011	7	28	23:00	UTC	

### **3.12 Community structures and metabolic activities of microbes**

**Jeho SONG**

**(Atmosphere and Ocean Research Institute, The University of Tokyo)**

**Shotaro SUZUKI (AORI)**

**Mario UCHIMIYA (AORI)**

**Hideki FUKUDA (AORI)**

**Hiroshi OGAWA (AORI)**

**Toshi NAGATA (AORI)**

**Kazuhiro KOGURE (AORI)**

**Koji HAMASAKI (AORI)**

#### **(1) Objective**

A significant fraction of dissolved and particulate organic matter produced in the euphotic layer of oceanic environments is delivered to meso- and bathypelagic layers, where substantial transformation and decomposition of organic matter proceeds due to the actions of diverse microbes thriving in these layers. Statio-temporal variations in organic matter transformation and decomposition in the ocean's interior largely affect patterns in carbon cycling in the global ocean. Thus elucidating diversity, activities and distribution patterns of microbes in deep oceanic waters is fundamentally important in order to better understand major controls of oceanic material cycling in the ocean.

The objective of this study is to determine seasonal variability of microbial diversity and activities during the time-series observation of vertical fluxes at the two distinctive oceanic stations located in the subarctic and subtropical western North Pacific. We investigated i) full-depth profiles of prokaryotic abundance and related biogeochemical parameters including dissolved organic carbon and nitrogen concentrations (potential resources of prokaryotes), and the abundances of viruses (potential predators of prokaryotes), ii) community structures of Bacteria and Archaea and their metabolic activities, iii) sinking velocity and physico-chemical properties of suspended particles in the mixing layer.

#### **(2) Method**

Seawater samples were collected from predetermined depths of two CTD casts, i.e. the Atmosphere and Ocean Research Institute (AORI) cast and the Routine cast, conducted at Stations K2 and S1 (see the meta-data sheet for details). Sinking particles were collected by drifting traps to determine fluxes of sinking POC/PON and their weight (see the meta-data sheet for details).

#### **i) Full-depth profiles of prokaryotic activity and abundance and related biogeochemical parameters**

- a) Prokaryotic abundance: Flow cytometry
- b) Prokaryotic production: <sup>3</sup>H-leucine incorporation
- c) Virus abundance: Flow cytometry
- d) DOC/DON: Concentrations of dissolved organic carbon and total dissolved nitrogen were determined by the high temperature catalytic oxidation (HTCO) method. The concentration of dissolved organic nitrogen was calculated by subtracting the concentration of dissolved inorganic nitrogen (determined by Auto-analyzer) from that of total dissolved nitrogen.

ii) Relationship between community structures of Bacteria and Archaea and their metabolic activities

- a) Bacterial community structures: PCR-DGGE method after extracting DNA from particles collected on 0.22  $\mu\text{m}$ -pore-size filters (Sterivex).
- b) Activities of bacteria: Bromodeoxyuridine-incorporating methods
- c) Isolation of bacteria: The high-through-put dilution culture method as well as conventional agar plating.

iii) Sinking velocity and physic-chemical properties of suspended particles

- a) Concentrations of particulate organic carbon and nitrogen: Determined using an elemental analyzer for samples collected on GF/F filters.
- b) Weight of suspended solid: Determined by weighing samples collected on pre-weighted GF/F filter.
- c) Particle size distribution of suspended particles in upper layer (0-200 m): Determined by an *in situ* particle sizing instrument, LISST-100 (Sequoia Scientific Inc., USA).

(3) All results will be submitted to Data Management Office, JAMSTEC after analysis and validation and be opened to public via the web site.

### 3.13 Dissolved organic carbon

**Masahide WAKITA (Mutsu Institute for Oceanography, JAMSTEC)**

#### (1) Purpose of the study

Fluctuations in the concentration of dissolved organic carbon (DOC) in seawater have a potentially great impact on the carbon cycle in the marine system, because DOC is a major global carbon reservoir. A change by < 10% in the size of the oceanic DOC pool, estimated to be ~ 700 GtC, would be comparable to the annual primary productivity in the whole ocean. In fact, it was generally concluded that the bulk DOC in oceanic water, especially in the deep ocean, is quite inert based upon  $^{14}\text{C}$ -age measurements. Nevertheless, it is widely observed that in the ocean DOC accumulates in surface waters at levels above the more constant concentration in deep water, suggesting the presence of DOC associated with biological production in the surface ocean. This study presents the distribution of DOC during summer in the northwestern North Pacific Ocean.

#### (2) Sampling

Seawater samples were collected at stations K2 (Cast 3, 4, 7, 8 and 11) and S1 (Cast 1, 7 and 10) and brought the total to ~260.  $\Delta^{14}\text{C}$  of DOC and DIC are also sampled to estimate the  $^{14}\text{C}$ -age of DOC at station K2 (Cast 4 and 7). Seawater from each Niskin bottle was transferred into 60 ml High Density Polyethylene bottle (HDPE) (for DOC) or 1000 ml Duran glass bottle (for  $\Delta^{14}\text{C}$  of DOC) rinsed with same water three times. Water taken from the surface to 250 m is filtered using precombusted (450°C) GF/F inline filters as they are being collected from the Niskin bottle. At depths > 250 m, the samples are collected without filtration. After collection, samples are frozen upright and preserved at ~ -20 °C cold until analysis in our land laboratory. Before use, all glassware was muffled at 550 °C for 5 hrs.

#### (3) Analysis

Prior to analysis, samples are returned to room temperature and acidified to pH < 2 with concentrated hydrochloric acid. DOC analysis was basically made with a high-temperature catalytic oxidation (HTCO) system improved a commercial unit, the Shimadzu TOC-V (Shimadzu Co.). In this system, the non-dispersive infrared was used for carbon dioxide produced from DOC during the HTCO process (temperature: 680 °C, catalyst: 0.5% Pt-Al<sub>2</sub>O<sub>3</sub>).

#### (4) Preliminary result

The distributions of DOC will be determined as soon as possible after this cruise.

#### (5) Data Archive

All data will be submitted to JAMSTEC Data Management Office (DMO) within 2 years.

### 3.14 Chlorofluorocarbons

Ken'ichi SASAKI (JAMSTEC MIO)

Masahide WAKITA (JAMSTEC MIO)

#### (1) Objective

Chlorofluorocarbons (CFCs) and sulfur hexafluoride (SF<sub>6</sub>) are chemically and biologically stable gases that have been synthesized at 1930's and 1960's, respectively. The atmospheric CFCs and SF<sub>6</sub> can slightly dissolve in sea surface water by air-sea gas exchange and then are spread into the ocean interior. The chemical species of CFCs (CFC-11 (CCl<sub>3</sub>F), CFC-12 (CCl<sub>2</sub>F<sub>2</sub>), CFC-113 (C<sub>2</sub>Cl<sub>3</sub>F<sub>3</sub>)) and SF<sub>6</sub> can be used as transient chemical tracers for the ocean circulation on timescale of several decades. We measured concentrations of CFCs in seawater and perform the tentative analysis of SF<sub>6</sub> in the seawater on board.

#### (2) Apparatus

Dissolved CFCs are measured by an electron capture detector (ECD) – gas chromatograph attached with a purging & trapping system.

Table 3-14-1 Instruments

Gas Chromatograph:	GC-14B (Shimadzu Ltd.)
Detector:	ECD-14 (Shimadzu Ltd)
Analytical Column:	
Pre-column:	Silica Plot capillary column [i.d.: 0.53mm, length: 8 m, film thickness: 0.25µm]
Main column:	Connected two capillary columns (Pola Bond-Q [i.d.: 0.53mm, length: 9 m, film thickness: 6.0µm] followed by Silica Plot [i. d.: 0.53mm, length: 14 m, film thickness: 0.25µm])
Purging & trapping:	Developed in JAMSTEC. Cold trap columns are 1/16" SUS tubing packed with Porapak T.

#### (3) Procedures

##### 3-1 Sampling

Seawater sub-samples for CFC measurements were collected from 12 liter Niskin bottles to 300 ml glass bottles at stations K2 (Cast 3), KNOT (Cast 1), and S1 (Cast 1). The test samples of SF<sub>6</sub> were collected to 400ml glass bottles at station K2 (Cast 4) and S1 (Cast 5). The bottles were filled by nitrogen gas before sampling. Two times of the bottle volumes of seawater sample were overflowed. The bottles filled by seawater sample were kept in water bathes controlled at 7°C until analysis. The CFCs concentrations were determined within 48 hr.

In order to confirm CFC concentrations of standard gases and their stabilities and also to check CFC saturation levels in sea surface water, CFC mixing ratios in background air were also analyzed. Air samples were collected into a 200ml glass cylinder on deck.

##### 3-2 Analysis

The analytical system is modified from the original design of Bullister and Weiss (1988). Constant volume of sample water (50ml) is taken into a sample loop. The sample is sent into stripping chamber and dissolved CFCs are de-gassed by N<sub>2</sub> gas purging for 8 minutes. The gas sample is dried by magnesium perchlorate desiccant and concentrated on a trap column cooled down to -50 °C. Stripping efficiencies of CFCs are confirmed by re-stripping of surface layer samples and more than 99.5 % of dissolved CFCs are extracted on the first purge. Following purging & trapping, the trap column is isolated and electrically heated to 140 °C. Desorbed CFCs are lead into the pre-column. CFCs are roughly separated from other compounds in the pre-column and are sent to main analytical column. And then the pre-column is switched to another line and flushed by counter flow of pure nitrogen gas. CFCs sent into main column are separated further and detected by an electron capture detector (ECD). Nitrogen gases used in this system was filtered by gas purifier tube packed Molecular Sieve 13X (MS-13X).

Table 3-14-2 Analytical conditions of dissolved CFCs in seawater.

---

Temperature	
Analytical Column:	95 °C
Detector (ECD):	240°C
Trap column:	-50 °C (at adsorbing) & 140 °C (at desorbing)
Mass flow rate of nitrogen gas (99.99995%)	
Carrier gas:	12 ml/min
Detector make-up gas:	25 ml/min
Back flush gas:	20 ml/min
Sample purge gas:	130 ml/min
Standard gas (Japan Fine Products co. ltd.)	
Base gas:	Nitrogen
CFC-11:	300 ppt (v/v)
CFC-12:	160 ppt (v/v)
CFC-113:	30 ppt (v/v)

---

#### (4) Preliminary result

CFC concentrations were slightly over saturation with respect to overlying air in mixing layer, rapidly decreased with depth. CFCs were not detected in denser water than 27.7  $\sigma_\theta$ . Precisions estimated from replicate analyses were better than +/- 0.01pmol kg<sup>-1</sup> or +/- 0.5% (whichever is greater) for CFC-11 and CFC-12 and +/- 0.01pmol kg<sup>-1</sup> or +/- 2% (whichever is greater) for CFC-113. The standard gases used in this analysis will be calibrated with respect to SIO scale standard gases and then the data will be corrected.

A large and broad peak was interfered determining CFC-113 peak area for samples collected from surface mixing layer in station S1. Retention time of the interfering peak was around 3 % shorter than that of CFC-113. We could not determine CFC-113 peak area for these samples and give quality flag of "5".

#### (5) Data archive

All CFC data will be submitted to JAMSTEC Data Management office (DMO) and under its control.

(6) Reference

Bullister, J.L and Weiss R.F. 1988. Determination of  $\text{CCl}_3\text{F}$  and  $\text{CCl}_2\text{F}_2$  in seawater and air. Deep Sea Research, 35, 839-853.



### 3.15 Argo float

**Toshio SUGA (JAMSTEC RIGC C, not on board): Principal Investigator**

**Taiyo KOBAYASHI (JAMSTEC RIGC) Operation Leader**

**Shigeki HOSODA (JAMSTEC RIGC: not on board)**

**Kanako SATO (JAMSTEC RIGC: not on board)**

**Mizue HIRANO (JAMSTEC RIGC: not on board)**

**Toru IDAI (MWJ)**

**Masaki FURUHATA (MWJ)**

**Shungo OSHITANI (MWJ)**

**Tomoyuki TAKAMORI (MWJ)**

**Sayaka KAWAMURA (MWJ)**

#### (1) Objective

The recent studies have shown that the oceanic physical phenomena of a small scale from tens to hundreds kilometers such as meso-scale eddies have the potential to affect significantly the transport of material such as nutrient salts and the biological activity of phytoplankton. In order to clarify the relationship between meso-scale eddies and the biological activity, we deploy 22 Argo floats equipped with dissolved oxygen sensors with a cycle of 2 days in the 150-km square area centered at the mooring buoy S1 (30N, 145E). This scientific project is the western North Pacific Integrated Physical-Biogeochemical Ocean Observation Experiment (INBOX). This enable for us to get data observed by Argo floats with 30-km horizontal resolution every 2 days. The observational frequency is equivalent to five hundreds times the horizontal and temporal resolution of the core Argo Project. This observation with finer horizontal and temporal resolution will make it possible to resolve meso-scale eddies with a horizontal scale from tens to hundreds kilometers and with a temporal scale from several days to months. We can evaluate the relationship between meso-scale eddies and the biological activity by analyzing temperature, salinity and dissolved oxygen data together with the data of mooring buoys and research vessels.

#### (2) Method

We launched twenty NEMO floats manufactured by Optimare and two APEX floats by Teledyne Webb Research. Each float except one APEX float equips two sensors: one is a SBE41 CTD sensor manufactured by Sea-Bird Electronics Inc (SBE) to measure temperature, salinity, and pressure and the other is an Optode 3830 sensor manufactured by Aanderaa Data Instruments (AADI) to measure dissolved oxygen. One of APEX float equips a SBE41 CTD sensor and two dissolved oxygen sensors manufactured by SBE and AADI. CTD observation were conducted at 5 points where floats were launched (shown Table 3.15-4).

The float usually drifts at a depth of 1500 dbar (called the parking depth), then it dives to a depth of 2000 dbar. During the ascent to the sea surface with increasing its volume to change its buoyancy, the float measures sea water temperature, salinity, pressure and dissolved oxygen. To send the measured data to the Argo data center via the Iridium transmitting system in real time, the float stays at the sea surface for enough time, approximately 1 hour (the time out period), except for the APEX float with two oxygen sensors which transmits its data by the ARGOS system and stays at the sea surface for 10 hours. Finally the float returns to the parking depth with decreasing volume.

The cycle of each float except the APEX float equipped with two dissolved oxygen sensors is 1 day just after it was launched. The cycle of the float moving repeats every days generally for about 2 years. The floats with the Iridium transmitting system can change their operation by commands which operators on land sent and we arranged that all floats measure profiles simultaneously with 2 days cycle on August 6. The specification of the floats is shown in Table 3.15-1, 3.15-2, and 3.15-3.

### (3) Float recovery

A NEMO float (S/N 202) had drifted on the sea surface since its launch on July 23. Thus, we tried to pick it up and the trial succeeded at 06:25 on July 31 (UTC) at 30-37.94 [N], 145-09.06 [E]. A bladder cover of the recovered float had been removed and it may be the cause for no dive to the depth due to less float weight.

Table 3.15-1: Specification of launched float (NEMO)

Float Type	Provor float manufactured by Optimare.
CTD sensor	SBE41 manufactured by Sea-Bird Electronics Inc.
Dissolved oxygen	Optode 3830 manufactured by Aanderaa Data Instruments
Cycle	2days
Iridium transmit timeout	90 minutes (The timeout period at the sea surface)
Target Parking Pressure	1500 dbar
Sampling layers	116
	(2010,2000,1950,1900,1850,1800,1750,1700,1650,1600,1550,1500,1450,1400,1350,1300,1250,1200,1150,1100,1050,1000,980,960,940,920,900,880,860,840,820,800,780,760,740,720,700,680,660,640,620,600,580,560,540,520,500,490,480,470,460,450,440,430,420,410,400,390,380,370,360,350,340,330,320,310,300,290,280,270,260,250,240,230,220,210,200,195,190,185,180,175,170,165,160,155,150,145,140,135,130,125,120,115,110,105,100,95,90,85,80,75,70,65,60,55,50,45,40,35,30,25,20,15,10,6 dbar)

Table 3.15-2: Specification of launched float (APEX with Iridium transmission system)

Float Type	Provor float manufactured by Teledyne Webb Research.
CTD sensor	SBE41cp manufactured by Sea-Bird Electronics Inc.
Dissolved oxygen	Optode 3830 manufactured by Aanderaa Data Instruments
Cycle	2days
Iridium transmit timeout	90 minutes (The timeout period at the sea surface)
Target Parking Pressure	1500 dbar
Sampling layers	Pressure, temperature, and salinity: Each 2dbar from 2000dbar to surface (High resolution mode) Pressure, temperature, salinity, and dissolved oxygen:75 layers
	(2000,1900,1800,1700,1600,1500,1450,1400,1350,1300,1250,1200,1150,1100,1050,1000,950,900,850,800,750,700,650,625,600,575,550,525,500,475,450,425,400,375,350,340,330,320,310,300,290,280,270,260,250,240,230,220,210,200,190,180,170,160,150,140,130,120,110,100,90,80,70,60,50,45,40,35,30,25,20,15, 10,6,and surface,dbar)

Table 3.15-3: Specification of launched float (APEX with ARGOS transmission system)

Float Type	Provor float manufactured by Teledyne Webb Research.
CTD sensor	SBE41 manufactured by Sea-Bird Electronics Inc.
Dissolved oxygen	Optode 3830 manufactured by Aanderaa Data Instruments SBE-43I manufactured by Sea-Bird Electronics Inc.
Cycle	2days
ARGOS transmit interval	30 seconds
Target Parking Pressure	1500 dbar
Sampling layers	71
	(2000,1950,1900,1850,1800,1750,1700,1650,1600,1550,1500,1450,1400,1350,1300,1250,1200,1150,1100,1050,1000,950,900,850,800,750,700,650,600,550,500,450,400,380,360,350,340,330,320,310,300,290,280,270,260,250,240,230,220,210,200,190,180,170,160,150,140,130,120,110,100,90,80,70,60,50,40,30,20,8,4 or surf., dbar)

## (4) Preliminary result

The Float S/N, ARGOS ID or IMEI Number, launched date/ time, launched position observation cycle of the float is summarized in Table. 3.15-4. The data will be measured automatically each observation cycle.

All floats observe at the western part of an anti-cyclonic eddy. The data of the float drifting nearest the center of the anti-cyclonic eddy shows that salinity and oxygen maximum layer lie near the seasonal thermocline at the depth of about 50 dbar. Another oxygen maximum shows in about 200 dbar, where is the upper part of the Subtropical Mode Water in the North Pacific.

Table 3.15-4: Launching area and date/time

Float S/N	ARGOS/IMEI ID	Date and Time of Reset (UTC)	Date and Time of launch (UTC)	Location of launch	Observation cycle	Remarks
199	3000 340 135 48640	2011/7/23 04 : 41	2011/7/23 05:38	29-44.29 [N] 144-56.69[E]	2 days	NEMO
168	3000 340 135 44640	2011/7/23 05 : 42	2011/7/23 06:57	29-28.49 [N] 145-00.02[E]	2 days	NEMO
193	3000 340 139 19680	2011/7/23 07 : 00	2011/7/23 08:15	29-28.00 [N] 145-17.86[E]	2 days	NEMO
4267	86579	2011/7/23 08 : 21	2011/7/23 09:29	29-27.84 [N] 145-35.67[E]	2 days	APEX with 2 oxygen sensors
194	3000 340 135 46630	2011/7/23 09 : 33	2011/7/23 10:48	29-43.8275 [N] 145-35.9552[E]	2 days	NEMO
196	3000 340 135 47630	2011/7/23 10 : 56	2011/7/23 12 : 15	29-59.9279 [N] 145-35.9717[E]	2 days	NEMO
195	3000 340 135 46640	2011/7/23 12 : 21	2011/7/23 13 : 39	30-15.8312 [N] 145-35.9945[E]	2 days	NEMO

197	3000 340 135 47640	2011/7/23 13 : 45	2011/7/23 14 : 58	30-31.99[N] 145-35.93[E]	2 days	NEMO
201	3000 340 135 49640	2011/7/23 15 : 06	2011/7/23 16 : 13	30-32.01[N] 145-18.09[E]	2 days	NEMO Failure at the launch
202	3000 340 130 25610	2011/7/23 16 : 21	2011/7/23 17 : 31	30-32.07 [N] 145-00.16[E]	2 days	NEMO Surface drifting and then recovered
198	3000 340 135 48630	2011/7/23 17 : 38	2011/7/23 18 : 55	30-16.05[N] 145-00.00[E]	2 days	NEMO
162	3000 340 135 41650	2011/7/23 21 : 02	2011/7/23 22 : 04	29-59.9661[N] 144-24.6235[E]	2 days	NEMO
161	3000 340 135 41640	2011/7/23 22 : 08	2011/7/23 23 : 25	29-44.2814[N] 144-24.0581[E]	2 days	NEMO
200	3000 340 135 49630	2011/7/23 23 : 28	2011/7/24 00 : 46	29-28.1741[N] 144-24.0082[E]	2 days	NEMO
164	3000 340 135 42650	2011/7/24 00 : 50	2011/7/24 01 : 57	29-28.0337[N] 144-41.8502[E]	2 days	NEMO
4985	8816 9375 7490	2011/7/30 06 : 37	2011/7/30 08 : 28	29-59.55[N] 145-00.21[E]	2 days	APEX CTD observation
170	3000 340 135 45640	2011/7/30 10 : 25	2011/7/30 12 : 17	30-15.45[N] 145-17.65[E]	2 days	NEMO CTD observation
169	3000 340 135 45630	2011/7/30 12 : 22	2011/7/30 13 : 39	30-00.00[N] 145-17.96[E]	2 days	NEMO
167	3000 340 135 44630	2011/7/30 15 : 34	2011/7/30 16 : 59	29-44.04[N] 145-17.43[E]	2 days	NEMO CTD observation
166	3000 340 135 43640	2011/7/30 20 : 18	2011/7/30 21 : 35	29-44.47[N] 144-41.65[E]	2 days	NEMO CTD observation
163	3000 340 135 42640	2011/7/30 21 : 40	2011/7/30 22 : 50	30-00.10[N] 144-41.98[E]	2 days	NEMO
165	3000 340 135 43630	2011/7/31 00 : 47	2011/7/31 02 : 07	30-16.04[N] 144-42.00[E]	2 days	NEMO CTD observation

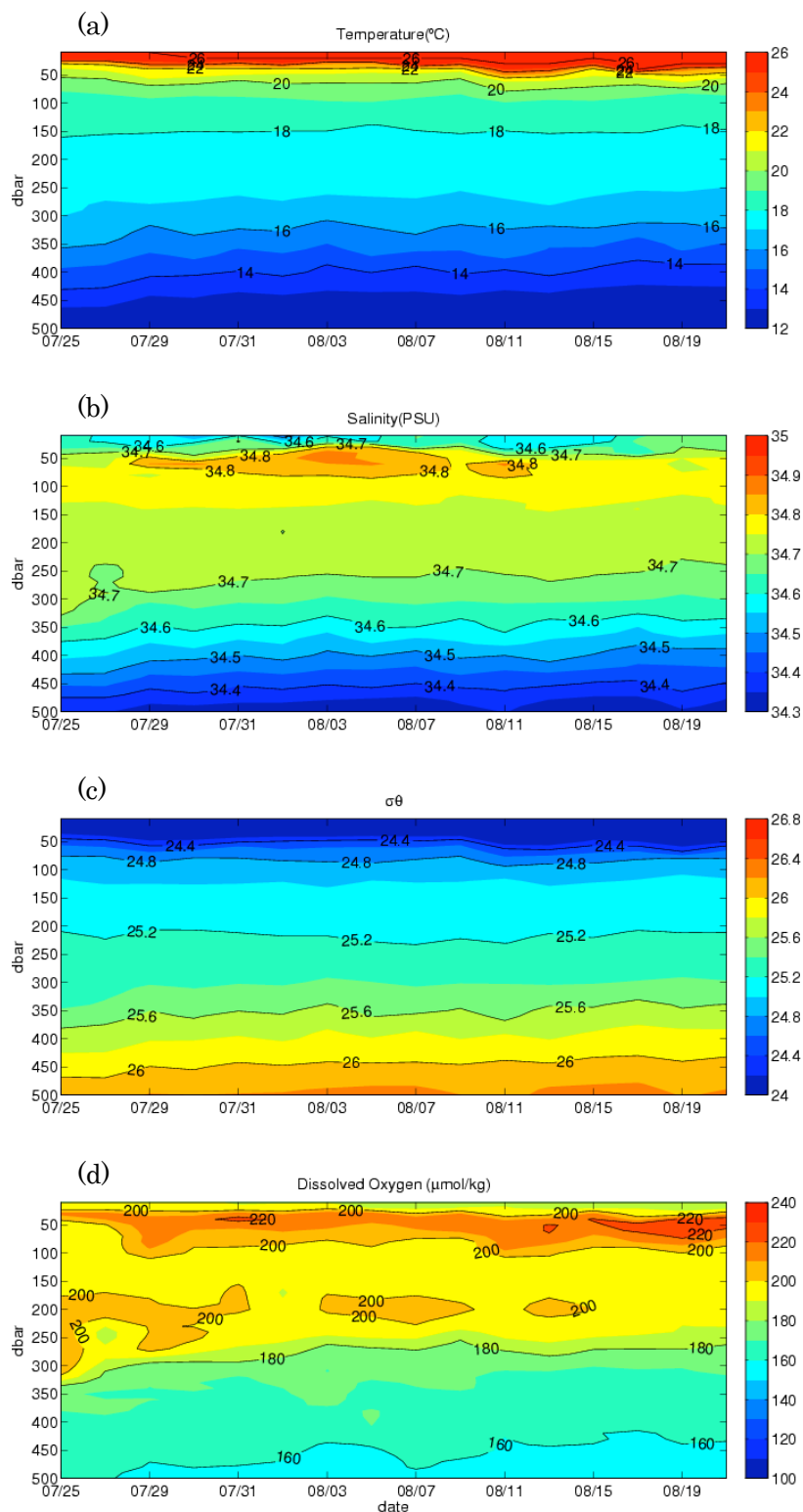


Figure 3.15-1. Time series of temperature (a), salinity (b), and density (c), and dissolved oxygen (d) in the upper 500 dbar of NEMO S/N 196.

(5) Data archive

The data observed by floats will be released via Global Data Assembly Center (GDAC: <http://www.usgodae.org/argo/argo.html>, or <http://www.coriolis.eu.org/>) and Global Telecommunication System (GTS) by November, 2011.

### 3.16 Optical measurement of marine snow: Visual Plankton Recorder (VPR)

**Makio HONDA (JAMSTEC RIGC)**

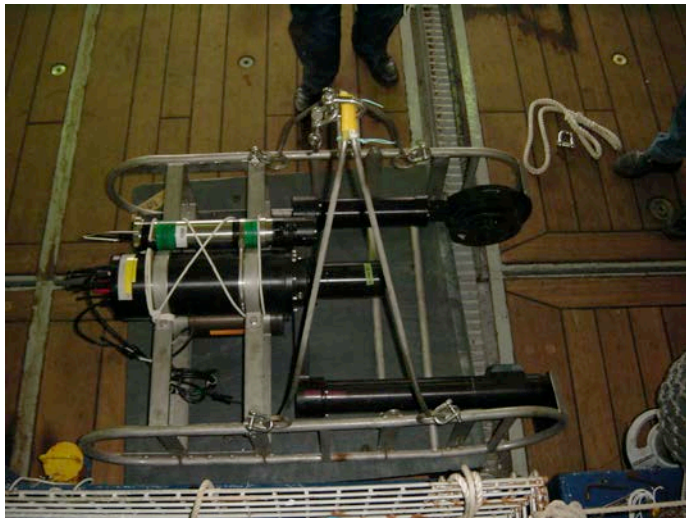
#### (1) Objective

Aggregated sinking particles, namely “marine snow”, play an important role in transporting atmospheric CO<sub>2</sub> to the ocean interior. The study of marine snow has been traditionally conducted by collecting these with “sediment trap” and by chemical and biological analysis in laboratory. On the other hand, in situ qualitative observations of marine snow such as measurement of turbidity and light attenuation have also been conducted. Bishop et al. (2009) tried to estimate abundance and flux of particulate organic carbon (POC) by using the “carbon explorer”, that is “ARGO float” type optical method. Recently application of visual plankton recorder (VPR) to marine snow observation (Lindsay et al., 2008) has been examined. In addition, in situ laser raman spectrometry (LR) has been also examined (Brewer et al., 2004) in order to know chemical composition of seawater and sea-floor sediment (see appendix). In order to conduct the research and development of optical measurement of marine snow, I have started to evaluate VPR and LR.

#### (2) Method

In this cruise, Visual Plankton Recorder (VPR) (picture 1) was deployed twice at stations S1.

VPR takes approximately 12 dark-field images per second. Field of view is approximately 5 cm x 5 cm (S3 mode) and 1 cm x 1 cm (S1 mode). In order to take pictures under same light condition, VPR was deployed at night. Deployment record is shown in Table 1. During this cruise, VPR descended to 500 m with downward velocity of 0.5 m/sec. Depth of VPR and vertical profiles in water temperature and salinity was monitored with CTD with sampling time of 0.5 seconds.



Station	S1-1	S1-2
Date (LST*)	28 July 2011	29 July 2011
Battery connect	19:26	19:47
CTD connect	19:31	19:48
Switch ON (Mode S3)	19:44	19:48
Water In	19:59 *	20:01
Start Descend (0.5m/sec ↓ )	20:01	20:03
Bottom (500m)	20:18	20:20
Start Ascend (1.0m/sec ↑ )	20:19	20:22
Water out	20:28	20:30
On deck	20:29	20:31
Switch ON (Mode S1)	20:29	20:31*
Water In	20:31	
Start Descend (0.5m/sec ↓ )	20:32	
Bottom (500m)	20:49	
Start Ascend (1.0m/sec ↑ )	20:50	
Water out	21:00	
On deck	21:00	
Switch OFF	21:03	
memo	* Irregular light flushing	*System stopped when mode was changed from S3 to S1.

LST= JST + 1 hr = UTC + 10 hr

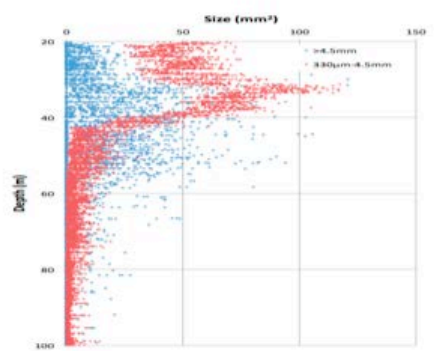
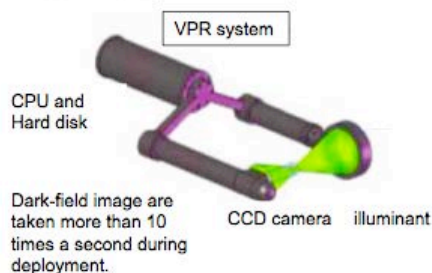
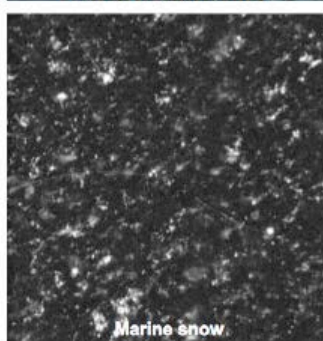
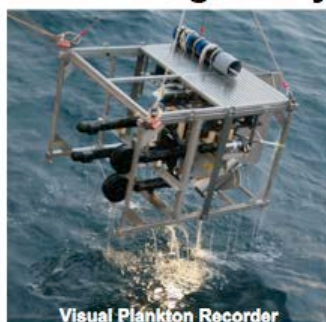
### (3) Data analysis

Data stored in hard disk will be analyzed with image-analysis software (Image pro) on land.



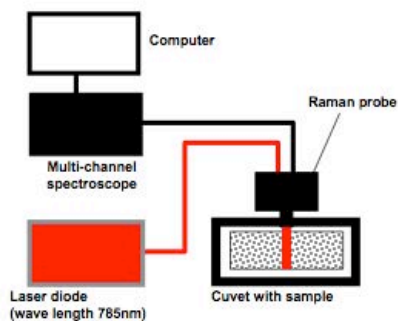
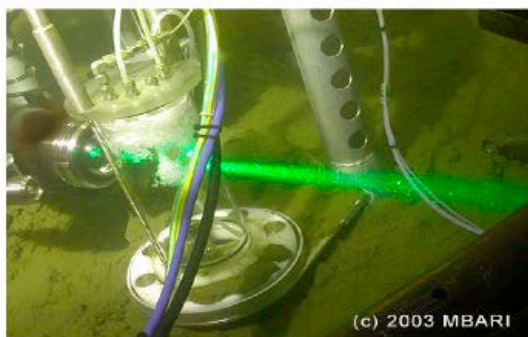
## Visual Plankton Recorder

### Image analysis of marine snow

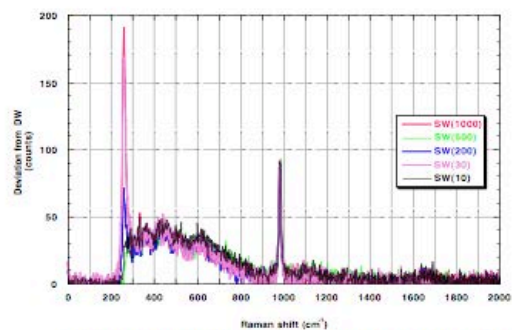


Vertical distribution of particulate materials

## Laser Raman Spectrometry



Conceptual diagram of PLRS



Raman shift of seawater collected from 10 m to 1000m

### **3.17 Observational research on air-sea interaction in the Kuroshio-Oyashio Extension region**

**Yoshimi KAWAI (JAMSTEC) Principal Investigator**  
**Katsuhisa MAENO (GODI)**  
**Harumi OHTA (GODI)**  
**Ryo OHYAMA (GODI)**

#### **3.8.1 Radiosonde observation**

##### **(1) Objective**

Investigation of atmospheric vertical structure of pressure, temperature, humidity, wind direction and wind speed, responding to the ocean temperature front of the Kuroshio Extension and Oyashio.

##### **(2) Parameters**

According to the manufacturer, the range and accuracy of parameters measured by the radiosonde sensor (RS92-SGPD) are as follows;

Parameter	Range	Accuracy
Pressure	3~1080 hPa	+/- 1 hPa (1080-100 hPa), +/- 0.6 hPa (100-3 hPa)
Temperature	-90~60 °C	+/- 0.5 °C
Humidity	0~100 %	5 %

##### **(3) Method**

Atmospheric soundings by radiosondes were carried out between KNOT and JKEO sites (N line), between JKEO and FI sites (W line), and at K2 site in the northwestern Pacific Ocean. In total, 36 soundings were carried out (Table 3.8.1-1, Figure 3.8.1-1). The main system consisted of processor (Vaisala, DigiCORA Ver.3.64.1), GPS antenna (GA20), UHF antenna (RB21), ground check kit (GC25), balloon launcher (ASAP), and GPS radiosonde sensor (RS92-SGPD).

##### **(4) Preliminary results**

Longitude-height cross sections of air temperature, specific humidity, zonal and meridional wind speeds along the ship track are shown in Figures 3.8.1-2~3.8.1-9. At most of the observation points, sea surface temperature was cooler than or nearly close to the near-surface air temperature, and relative humidity was higher than 90 %. In fact, the radiosonde observations showed that the atmosphere was stable or neutral in the observation period.

##### **(5) Data archive**

Raw data were recorded in ASCII format every 2 seconds during ascent. These raw data were submitted to the Data Integration and Analysis Group (DIAG) of JAMSTEC just after the cruise.

Table 3.8.1-1. Radiosonde launch log.

Sounding No.	Station No.	Launching				Maximum		Duration (sec)
		Date (UT)	Time	Lon	Lat	Altitude	hPa	
RS001	K2	2011/06/30	23:30:17	160.084	46.999	23610	33.0	6096
RS002	K2	2011/07/01	02:30:05	160.999	47.000	23395	34.1	5718
RS003	N3	2011/07/10	06:05:47	150.516	41.433	14271	151.2	3694
RS004	N4	2011/07/10	07:30:47	150.276	41.298	13133	181.0	3708
RS005	N5	2011/07/10	08:59:04	150.054	41.159	13589	168.3	3698
RS006	N6	2011/07/10	10:30:24	149.816	40.965	14523	144.7	3692
RS007	N7	2011/07/10	11:59:21	149.540	40.742	12878	188.2	3706
RS008	N8	2011/07/10	13:30:28	149.311	40.538	13035	183.8	3702
RS009	N9	2011/07/10	15:00:45	149.063	40.331	13436	172.2	3688
RS010	N10	2011/07/10	16:30:10	148.807	40.121	14653	141.3	3696
RS011	N11	2011/07/10	18:00:27	148.557	39.901	13867	160.5	3696
RS012	N12	2011/07/10	19:30:37	148.288	39.682	13413	172.8	3704
RS013	N13	2011/07/10	20:58:36	148.050	39.460	13446	171.8	3692
RS014	N14	2011/07/10	22:28:58	147.789	39.251	12351	204.2	3736
RS015	N15	2011/07/11	00:01:53	147.520	39.012	12688	193.9	3720
RS016	N16	2011/07/11	01:27:25	147.284	38.818	12169	210.1	3718
RS017	N17	2011/07/11	02:59:11	147.013	38.594	12760	192.0	3708
RS018	N18	2011/07/11	04:28:43	146.784	38.382	12830	190.0	3716
RS019	JKEO	2011/07/11	06:24:49	146.428	38.137	24015	30.8	6290
RS020	JKEO	2011/07/11	10:00:23	146.423	38.069	11880	220.2	3730
RS021	W1	2011/07/11	11:29:07	146.305	38.036	12935	187.1	3692
RS022	W2	2011/07/11	12:59:18	146.052	37.948	12383	203.8	3704
RS023	W3	2011/07/11	14:29:06	145.728	37.851	12742	192.3	3706
RS024	W4	2011/07/11	15:58:12	145.384	37.745	13328	175.2	3696
RS025	W5	2011/07/11	17:30:15	145.070	37.634	12906	186.9	3706
RS026	W6	2011/07/11	18:58:39	144.710	37.520	13902	159.4	3700
RS027	W7	2011/07/11	20:30:20	144.398	37.422	14009	156.4	3706
RS028	W8	2011/07/11	21:58:55	144.059	37.313	13544	168.4	3710
RS029	W9	2011/07/11	23:29:44	143.740	37.223	12358	203.3	3716
RS030	W10	2011/07/12	00:59:05	143.399	37.099	13757	163.0	3704
RS031	W11	2011/07/12	02:28:52	143.055	36.992	13365	173.7	3704
RS032	W12	2011/07/12	03:58:49	142.749	36.882	12593	196.2	3720
RS033	W13	2011/07/12	05:29:00	142.417	36.782	11910	218.2	3732
RS034	W14	2011/07/12	06:58:56	142.041	36.675	13367	173.8	3706
RS035	W15	2011/07/12	08:58:57	141.741	36.570	12920	186.4	3710
RS036	F1	2011/07/12	10:29:07	141.498	36.482	21647	44.5	5570

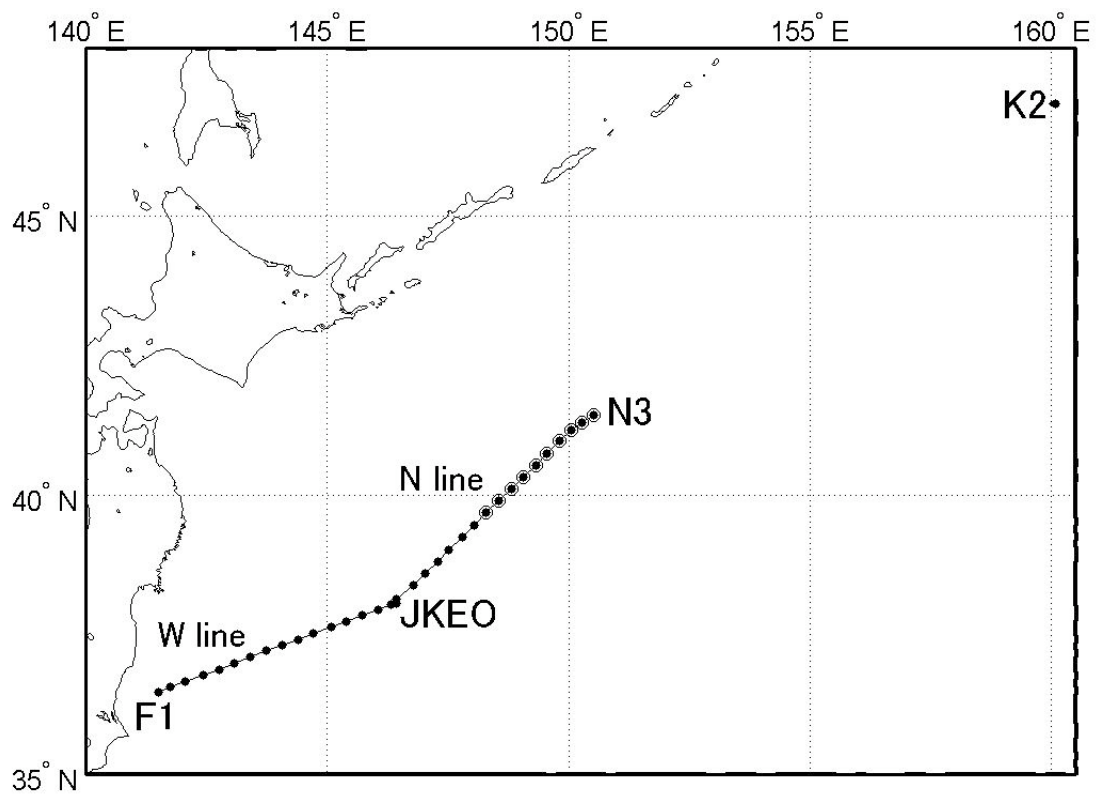


Figure 3.8.1-1. Positions of the GPS radiosonde (dots) and XCTD observations (open circles).

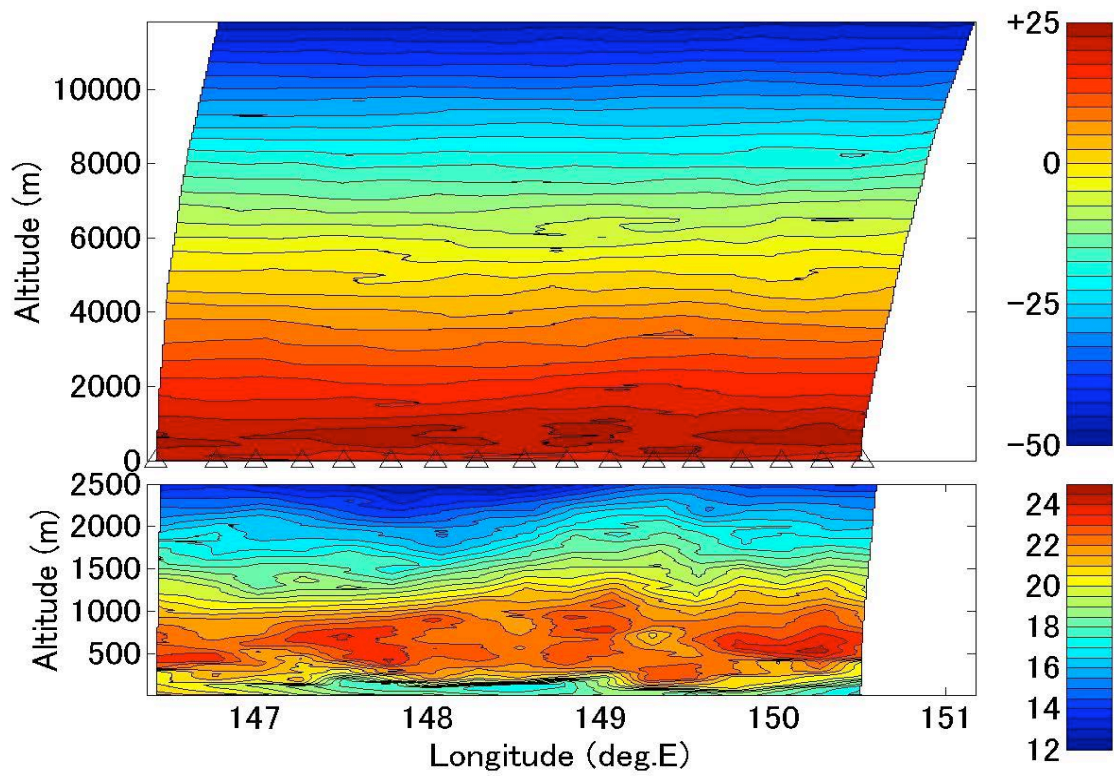


Figure 3.8.1-2. Section of temperature ( $^{\circ}\text{C}$ ) observed with GPS radiosondes along the N line (N3 to JKEO). Contour intervals are  $2.5^{\circ}\text{C}$  (upper) and  $0.5^{\circ}\text{C}$  (lower).

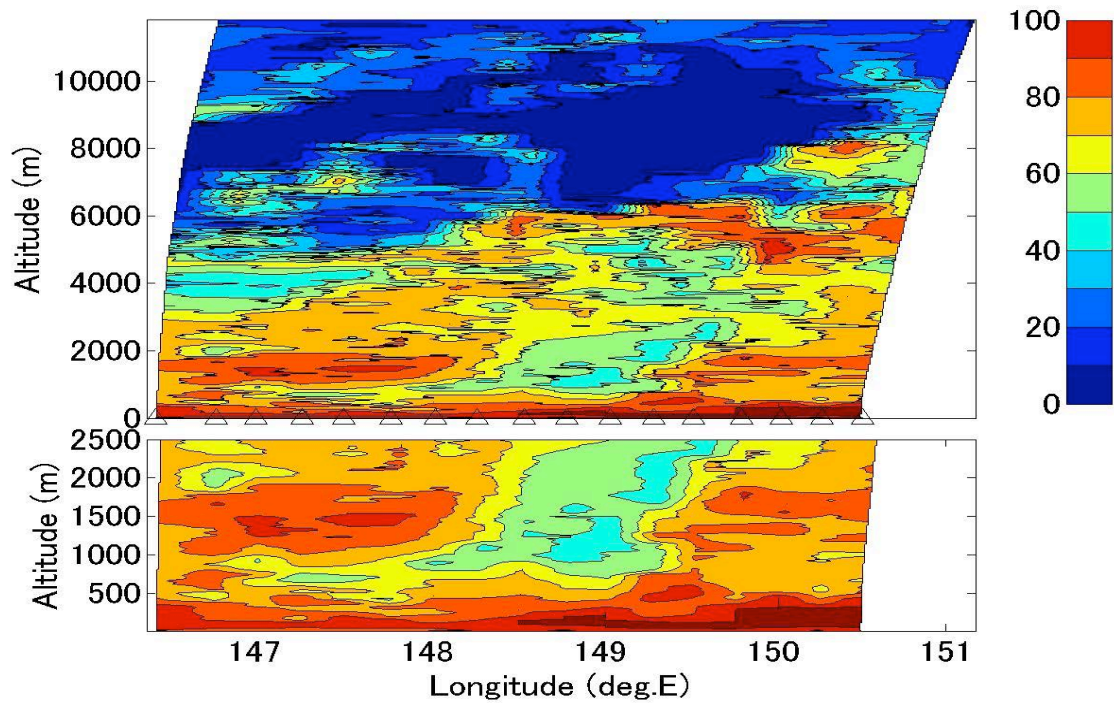


Figure 3.8.1-3. Section of relative humidity (%) observed with GPS radiosondes along the N line (N3 to JKEO). Contour interval is 10 %.



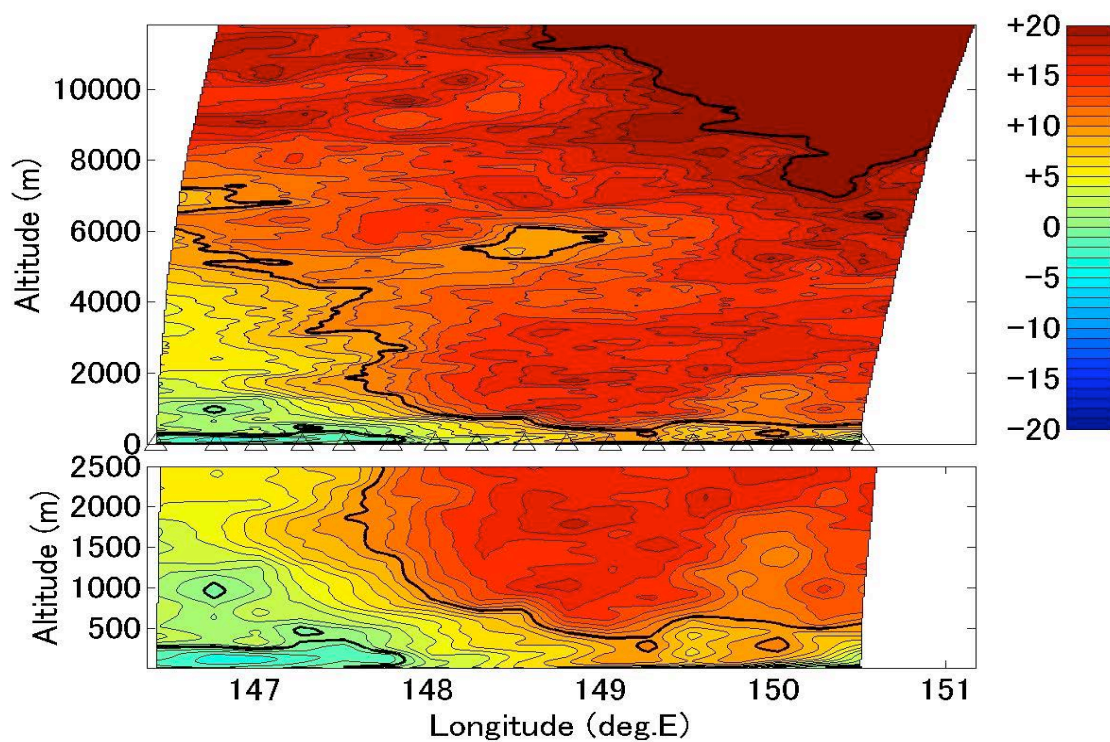


Figure 3.8.1-4. Section of zonal wind speed (m/s) observed with GPS radiosondes along the N line (N3 to JKEO). Intervals of thin and thick contours are 1 m/s and 10 m/s, respectively.

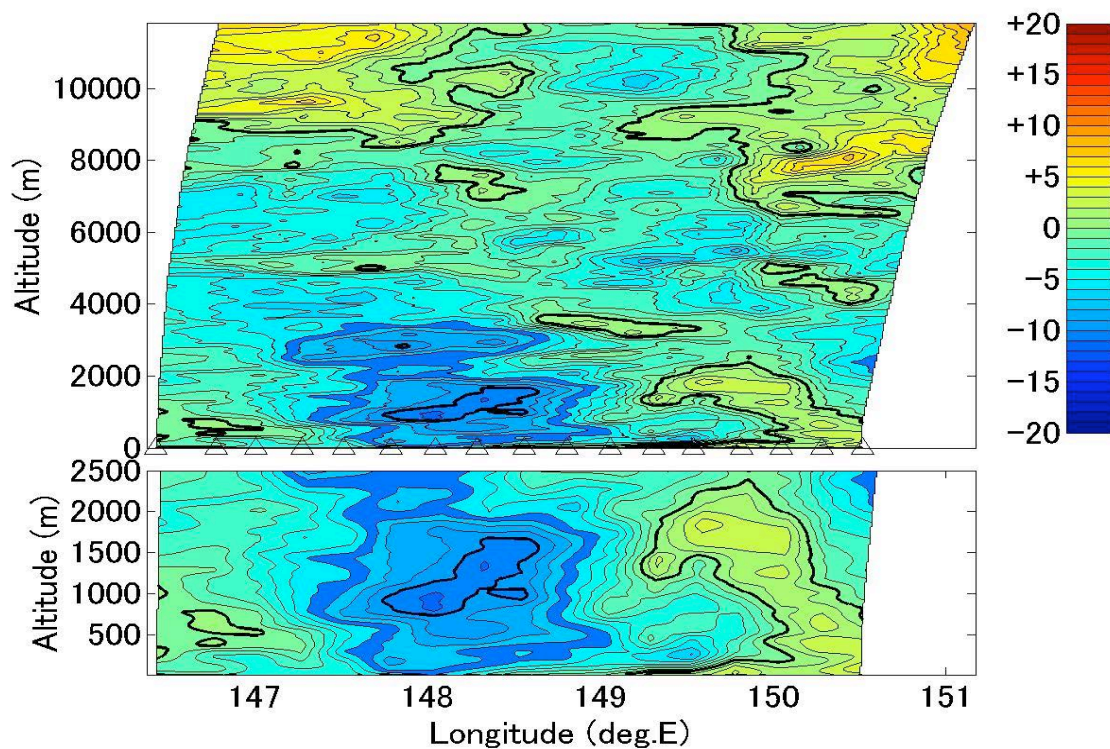


Figure 3.8.1-5. Section of meridional wind speed (m/s) observed with GPS radiosondes along the N line (N3 to JKEO). Intervals of thin and thick contours are 1 m/s and 10 m/s, respectively.

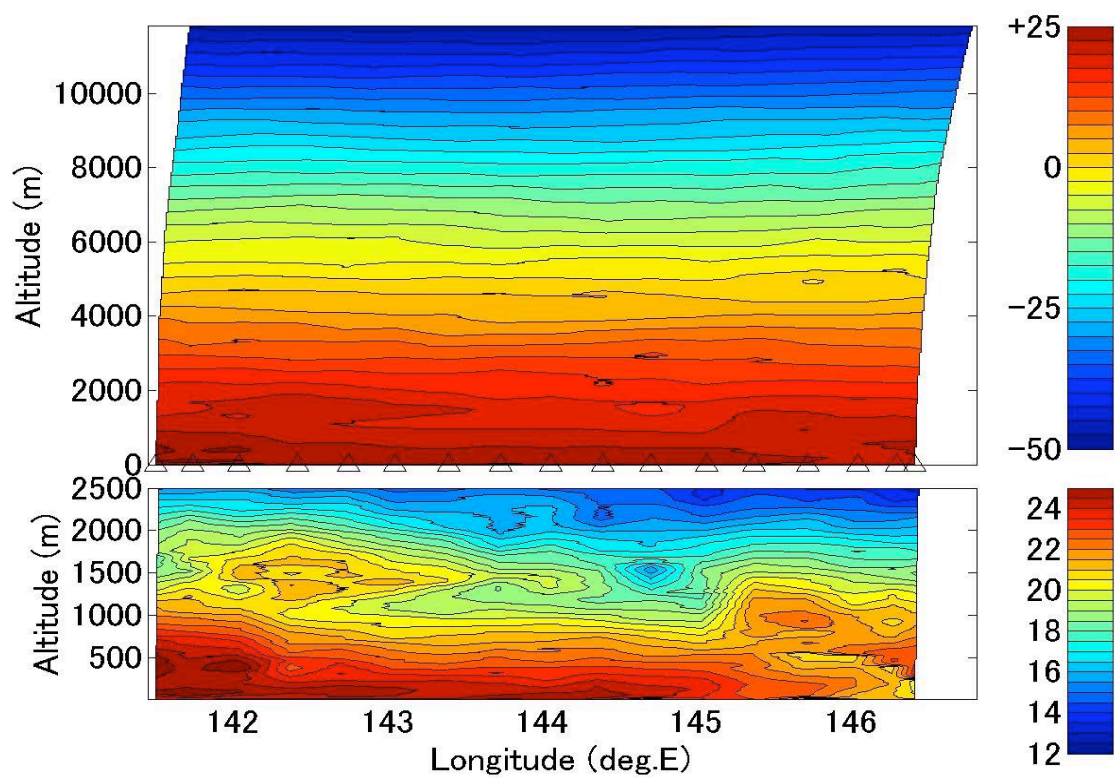


Figure 3.8.1-6. Section of temperature ( $^{\circ}\text{C}$ ) observed with GPS radiosondes along the W line (JKEP to F1). Contour intervals are  $2.5^{\circ}\text{C}$  (upper) and  $0.5^{\circ}\text{C}$  (lower).

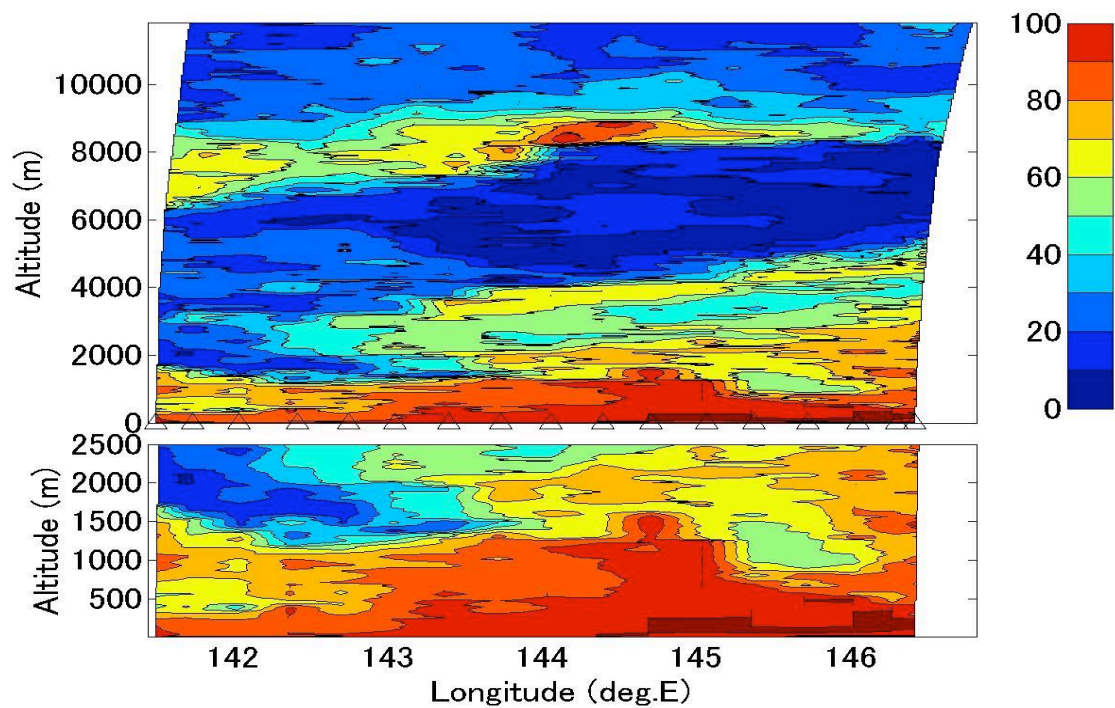


Figure 3.8.1-7. Section of relative humidity (%) observed with GPS radiosondes along the W line (JKEP to F1). Contour interval is 10 %.



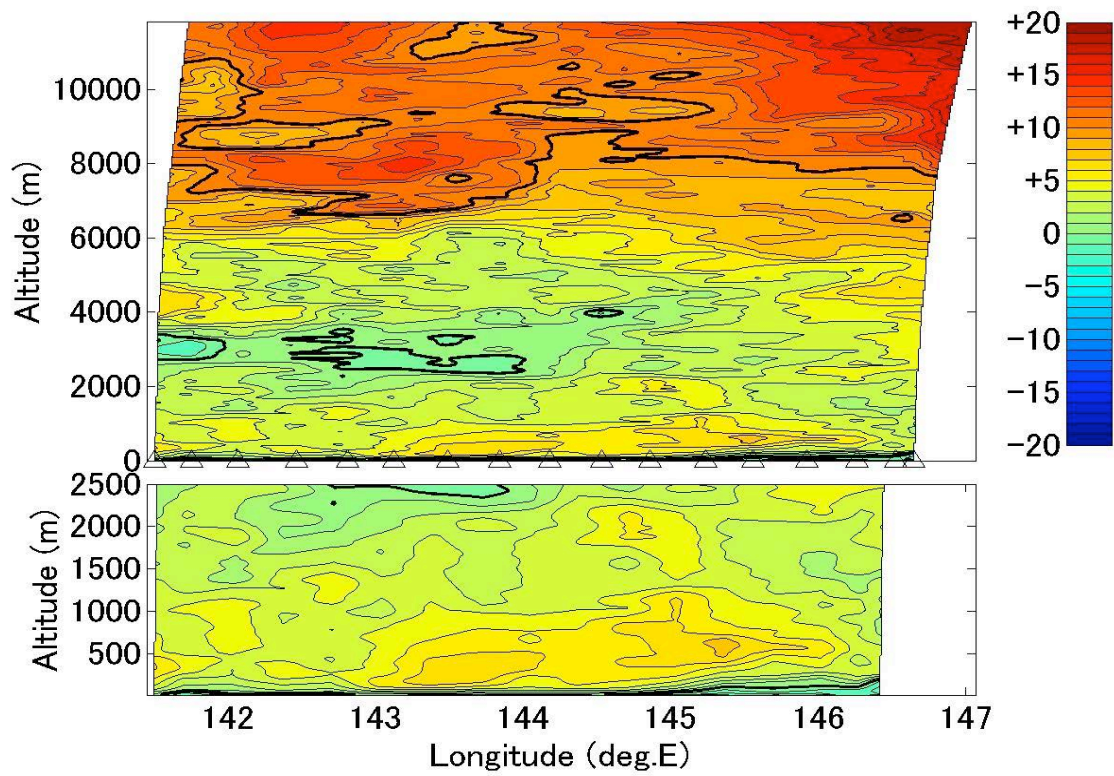


Figure 3.8.1-8. Section of zonal wind speed (m/s) observed with GPS radiosondes along the W line (JKEP to F1). Intervals of thin and thick contours are 1 m/s and 10 m/s, respectively.

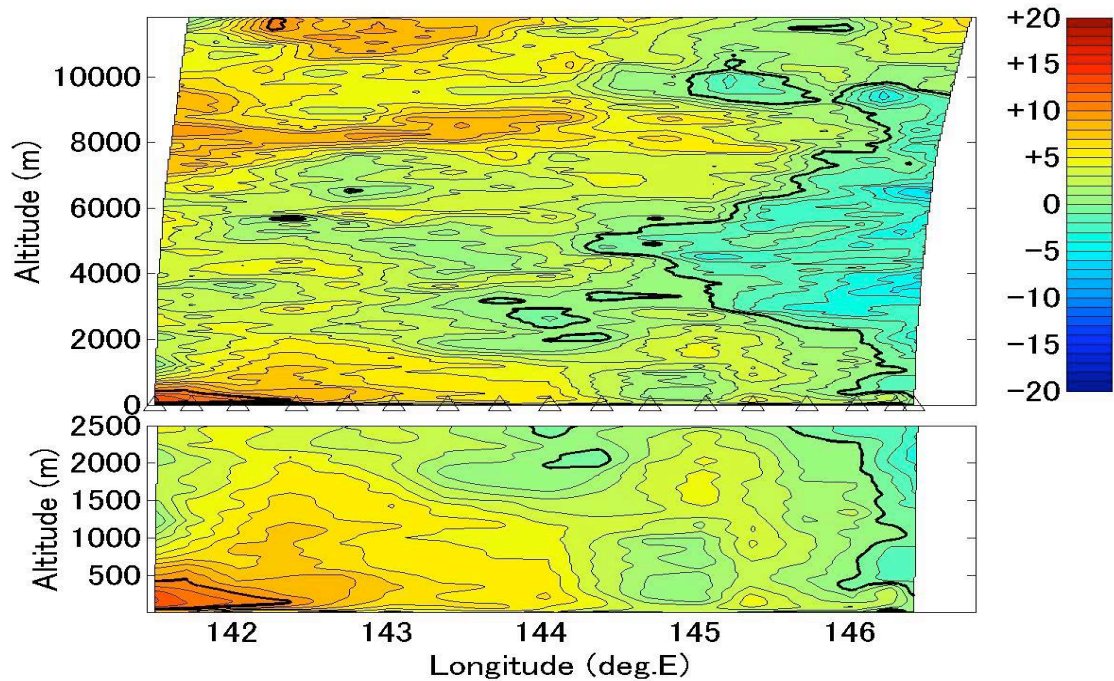


Figure 3.8.1-9. Section of meridional wind speed (m/s) observed with GPS radiosondes along the W line (JKEP to F1). Intervals of thin and thick contours are 1 m/s and 10 m/s, respectively.



### 3.8.2 XCTD observation

#### (1) Objectives

Investigation of the hydrographic and current structures across the subarctic front, focusing on air-sea interaction.

#### (2) Parameters

According to the manufacturer, Tsurumi-Seiki Co., Ltd., the range and accuracy of parameters measured by the XCTD (eXpendable Conductivity, Temperature, and Depth profiler) are as follows;

Parameter	Range	Accuracy
Conductivity	0-60 mS	$\pm 0.03$ mS/cm
Temperature	-2 - 35 °C	$\pm 0.02$ °C
Depth	0-1000 m	5 m or 2 % at depth, whichever is greater

#### (3) Methods

We measured temperature and salinity from the sea surface to the depth of 1100 m by using XCTD-1 probes and an on-board data converter, MK-130 (Tsurumi-Seiki Co., Ltd.). We intersected the subarctic front, casting probes by an automatic launcher. A total of 10 casts were performed, as shown in the observation summary (Table 3.8.2-1) and the XCTD site map (see Figure 3.8.1-1).

#### (4) Preliminary results

Both temperature and salinity profiles down to 1100 m were obtained at 10 sites. A sharp temperature/salinity front was formed around 41°00'N, 149°50'E below about 20m in depth (Figures 3.8.2-1~3.8.2-2). Near-surface water was very light (warm and low saline), and formed stable stratification. The warmer, humid air covering the sea surface would contribute to forming the shallow stratification.

#### (5) Data archives

These XCTD data were submitted to the Data Integration and Analysis Group (DIAG) of JAMSTEC just after the cruise.

Table 3.8.2-1. Summary of the XCTD observations

Station No.	Date* (YYYY/MM/DD)	Time (UT)	Latitude	Longitude	Depth (m)
N3	2011/07/10	06:13	41-25.80N	150-28.34E	5214
N4	2011/07/10	07:38	41-16.69N	150-13.84E	5256
N5	2011/07/10	09:07	41-07.65N	149-58.99E	5205
N6	2011/07/10	10:38	40-54.78N	149-44.06E	5511
N7	2011/07/10	12:07	40-42.94N	149-29.13E	5324
N8	2011/07/10	13:38	40-29.95N	149-14.61E	5262
N9	2011/07/10	15:08	40-17.27N	148-59.77E	5688
N10	2011/07/10	16:35	40-03.82N	148-46.12E	5437
N11	2011/07/10	18:06	39-50.00N	148-30.31E	5533
N12	2011/07/10	19:36	39-36.22N	148-15.95E	5492

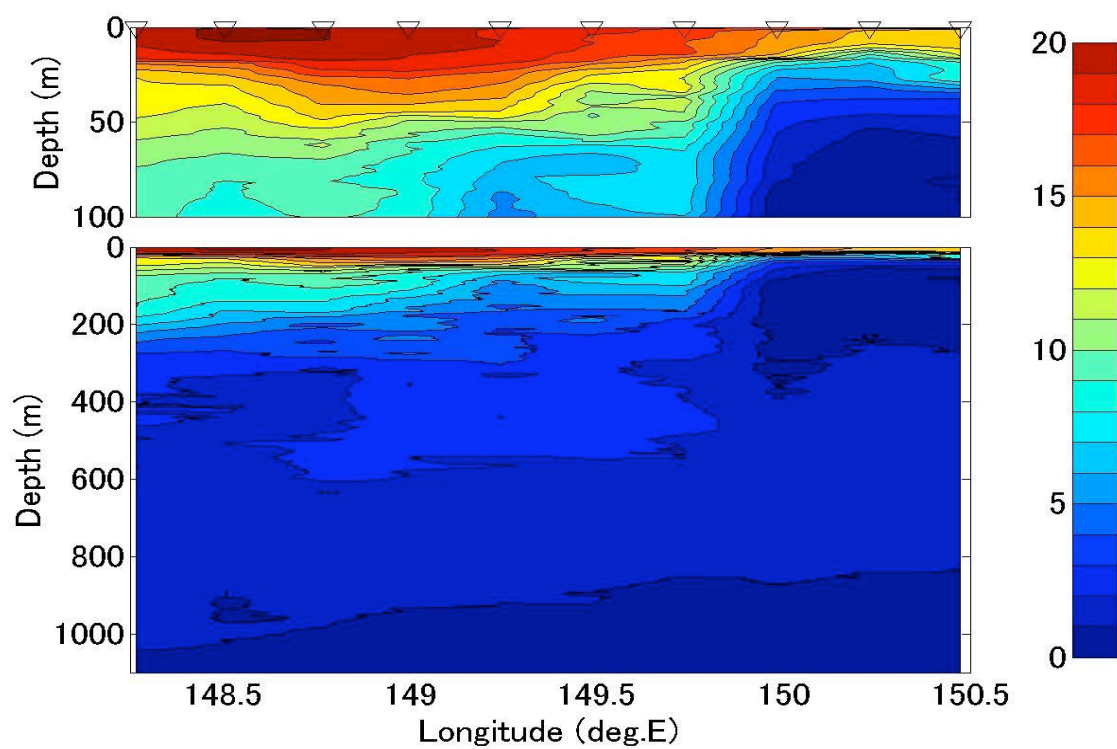


Figure 3.8.2-1. Section of in situ temperature observed with XCTDs. Contour interval is 1°C.

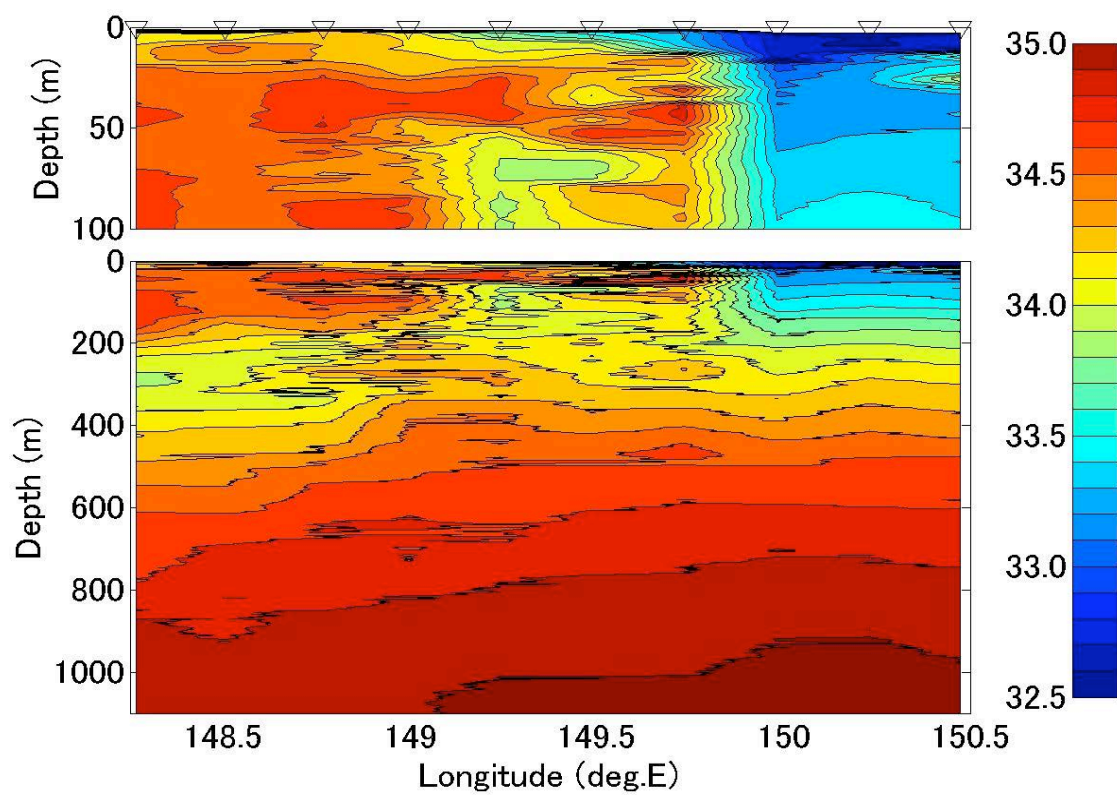


Figure 3.8.2-2. Section of salinity observed with XCTDs. Contour interval is 0.1.

### **3.18 Temporal changes in water properties of abyssal water in the western North Pacific**

**Hiroshi UCHIDA (JAMSTEC RIGC) (Principal Investigator; not on board)**

**Masahide WAKITA (JAMSTEC MIO)**

**Akihiko MURATA (JAMSTEC RIGC) (not on board)**

#### **(1) Objective**

The objective of this study is to clarify temporal changes in water properties of abyssal water in the western North Pacific by means of moored CTD/O<sub>2</sub> observations. The time series data will be used to evaluate observational error caused by short-term temperature fluctuation for the estimation of bottom water warming in recent decades derived from land-to-land repeat hydrographic data, and to monitor long-term fluctuation of water properties of the abyssal water.

#### **(2) Materials and methods**

CTDs used in the mooring observations were SBE-37 SM (Sea-Bird Electronics, Inc., Bellevue, Washington, USA). The SBE-37s had no pump, but included an optional pressure sensor with a range of 7000 m, developed by Paine Electronics, LLC, East Wenatchee, Washington, USA, except for the SBE-37 used in the first mooring period. Oxygen sensors used in the mooring observations were Oxygen Optode model 3830 (Aanderaa Data Instruments AS, Bergen, Norway). The optode sensor was attached to a datalogger with an internal battery and memory in a titanium housing designed for mooring observation (Compact OPTODE; Alec Electronics Co., Ltd., Kobe, Japan) (Uchida et al., 2008b).

The SBE-37 and Oxygen Optode were attached to the acoustic releaser of the BGC mooring system (Table 3.9.1). Depth of the acoustic releasers was 34 m above the sea floor. The SBE-37 and Oxygen Optode data were obtained at a sampling interval of 30 minutes for the first mooring period and of 1 hour for the other mooring periods.

For in situ calibration during a hydrographic cast before mooring deployment or after mooring recovery, these sensors were attached to the water-sampling frame at station S01\_2 during MR10-01. These data will be compared with the simultaneously obtained shipboard CTDO<sub>2</sub> data.

#### **(3) Preliminary result**

Time series of potential temperature and oxygen saturation obtained from the mooring observations were shown in Fig. 3.9.1. The CTD data for the first period (from October 2008 to January 2010) is not available due to leakage of the CTD sensor. Quality control is not yet performed for the data and will be performed by using a method similar to that of Uchida et al. (2008a, 2009). The data were low-pass-filtered by the running mean with a window of 25 hours. The oxygen data were drifted in time during the mooring period, probably due to a slow time-dependent, pressure-induced effect. Similar drifts were observed for the AADI Oxygen Optodes moored in the deep ocean (Uchida et al., 2009).

#### **(4) Data archive**

The quality-controlled moored CTD/O<sub>2</sub> data will be submitted to JAMSTEC Data Integration and Analyses Group (DIAG).

(5) References

- Uchida, H., T. Kawano and M. Fukasawa (2008a): In situ calibration of moored CTDs used for monitoring abyssal water. *J. Atmos. Oceanic Technol.*, 25, 1695-1702.
- Uchida, H., T. Kawano, I. Kaneko and M. Fukasawa (2008b): In situ calibration of optode-based oxygen sensors. *J. Atmos. Oceanic Technol.*, 25, 2271-2281.
- Uchida, H., H. Yamamoto, K. Ichikawa, M. Kawabe and M. Fukasawa (2009): Wake Island Passage Flux Experiment Data Book, JAMSTEC, Yokosuka, Japan, 93 pp.

Table 3.9.1. Summary of mooring observations for the abyssal water.

Cruise	Mooring	K2	S1
MR08-05	Deployment	2008/10/28 01:13 (K-2 BGC) 47-00.36 N, 159-58.16 E, 5206 m SBE37 S/N 2757 (5172 m) OPTODE S/N 5 (5172 m)	None
MR10-01	Recovery	2010/01/24 11:20 The SBE 37 was leaked and no data is available for the SBE 37.	None
	Deployment	2010/02/15 05:05 (K2 BGC) 47-00.34 N, 159-58.24 E, 5206 m SBE37 S/N 2731 (5172 m) OPTODE S/N 5 (5172 m)	2010/02/03 03:06 (S1 BGC) 30-03.88 N, 144-57.96 E, 5926 m SBE37 S/N 2730 (5892 m) OPTODE S/N 3 (5892 m)
MR10-06	Recovery	2010/10/25 01:41	2010/11/06 01:44
	Deployment	2010/10/31 05:35 (K2 BGC) 47-00.37 N, 159-58.24 E, 5218 m SBE37 S/N 2731 (5184 m) OPTODE S/N 5 (5184 m)	2010/11/10 01:52 (S1 BGC) 30-03.92 N, 144-57.98 E, 5927 m SBE37 S/N 2730 (5893 m) OPTODE S/N 3 (5893 m)
MR11-05	Recovery	2011/06/30 02:04	2011/07/24 21:19
	Deployment	2011/07/04 00:24 (K2 BGC) 47-00.34 N, 159-58.42 E, 5218 m SBE37 S/N 2731 (5184 m) OPTODE S/N 5 (5184 m)	2011/07/28 23:04 (S1 (BGC) 30-03.93 N, 144-58.03 E, 5924 m SBE37 S/N 2730 (5890 m) OPTODE S/N 3 (5890 m)

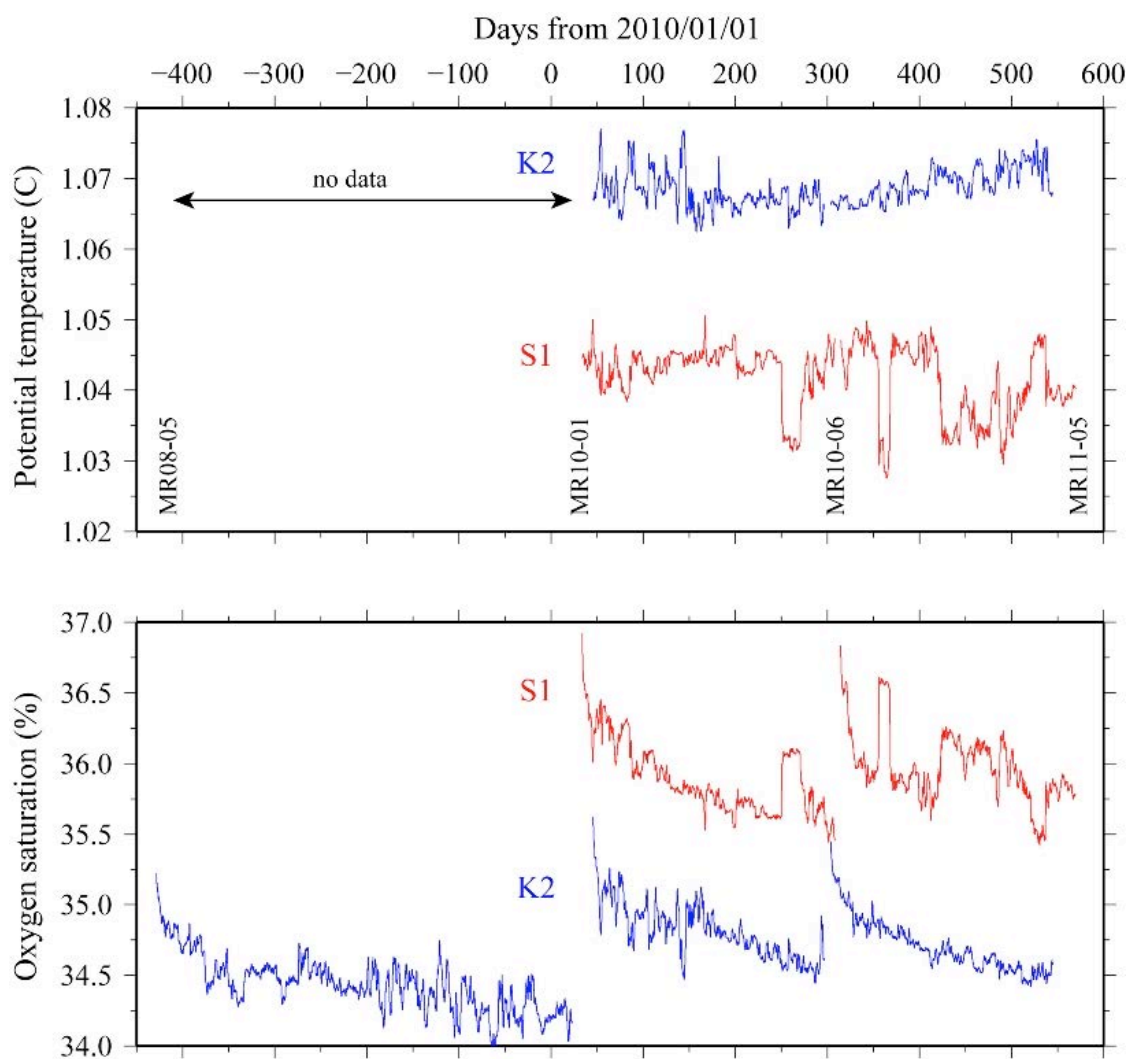


Fig. 3.9.1. Time series of potential temperature and oxygen saturation at 34 m above the sea floor of K2 and S1 stations.

## 4. Studies of artificial radioactive nuclide

### 4.1 Verification of DNA damage in microorganisms by the radioactive contamination

Hideki KOBAYASHI (Biogeos, JAMSTEC)

#### 1. Introduction

The accidents in Fukushima nuclear plants released large amounts of radioactive materials to environments including marine environment from 11/March/2011. For example, about 4.7 PBq of the radioactive materials was released to marine environment during 5 days from 2/April (1). Effects of these radioactive materials on organisms should be checked for the safety of social life all over the world. In general, the bioaccumulation of radioactive materials starts from small organisms including bacteria. The bioaccumulation of radioactive materials would provide DNA damage in the cell. Bacterial cells activate SOS network of genetic system to restore DNA damages (2). The *recA* gene is one of key genes in SOS network, and widely distributed among bacterial species. In addition, DNA sequence of *recA* gene is homologous between species. So, we planned to detect activation of SOS network caused by radioactive materials with *recA* mRNA. DNA sequence of *recA* would show bacterial species, which tend to accumulate radioactive materials.

#### 2. Materials and methods

**Filtration of seawater sample.** Seawater sample was obtained from seawater intake system (depth; 6 m), bucket sampling (depth; 0 m) and Niskin sampler (depth; 30, 50, 100 m). All seawater samples were filtrated with 0.45 and 1  $\mu$ m pore cellulose filter to collect microorganisms. All filters were stored in -80°C freezer.

**Construction of PCR primer for amplification of *recA* gene.** We collected *recA* DNA sequences of various bacterial species from DNA database in NCBI. We constructed forward primer Rec-k4-F (GCNTTYATYGAYGCNGARCA) and Rec-k4-r (AARGTNGTNAARAAYAARRT). The amplification of *recA* gene of *Caulobacter* strain was conformed.

**Check mitomycin C (MMC) resistance of bacteria.** Seawater samples (100  $\mu$ l) were spread on MarineBroth 2216 agar plate with or without 2  $\mu$ l of MMC (1 mg/ml). Then MarineBroth 2216 agar plates were incubated at room temperature for 3 days. The number of colonies grown on MarineBroth 2216 agar plates was counted and calculated a frequency of MMC resistant cells.

#### 3. Results

First, we checked a frequency of MMC resistant cells in seawater. MMC works as DNA damage agent in a cell, and activates SOS network. This mechanism was similar with that of radioactive materials. If released radioactive materials already activated SOS network, environmental bacteria are resistant to MMC. The frequency of MMC resistant cells in seawater was shown in Table 1.

The frequency of MMC resistant cells was significantly high in the surface seawater of D2 and D4. About 80% and 30% of bacterial cells were resistant to MMC in surface seawater of D4 and D2, respectively. More bacterial cells were also detected from surface water of D2 and D4. The MMC resistant cells were preliminarily identified with 16S rDNA sequence, and found that *Photobacterium* sp., *Pseudomonas* sp., and *Stenotrophomonas* sp. were main species (data not shown).

#### 4. Discussion

Preliminary analysis presented here showed clearly increase of MMC resistant cells off Fukushima nuclear plants. However, we can detect no radioactive material in filters used for collection of microorganisms with Geiger counter ( $<0.02 \mu\text{S/h}$ ). In addition, MMC resistant cells are isolated from only surface seawater. The radioactive materials released from Fukushima nuclear plant would activate transiently SOS network of environmental microorganisms. In fact, *Photobacterium* sp is one of major marine bacterial species, and *Pseudomonas* sp. and *Stenotrophomonas* sp. are also isolated from seawater. There was no extremophiles reported as high radioactive materials resistant microorganisms like *Deinococcus radiodurans*. These results indicated activation of SOS network in bacterial cells. We will try checking *recA* mRNA from collect bacteria in next stage.

#### References

- 1) <http://www.meti.go.jp/press/2011/04/20110425002/20110425002-2.pdf>
- 2) Frederick C. N., eds. *Escheichia coli* and *Salmonella*; Cellular and Molecular Biology (second edition), vol. I, ASM press, 1999.



Table 1 Sampling point of seawater and a frequency of MMC resistant cell <sup>1)</sup>

Date	18-Jul	18-Jul	19-Jul	20-Jul	20-Jul	20-Jul
point	F1	D4	D2	Off miyagi	Off miyagi	Off Iwate
latitude	36° 28'02	36° 41'49	37° 19'930	38° 6'1	38° 46'6	39° 15'950
longitude	141° 27'51	141° 9'8	141° 27'9366	142° 31'92	142° 29'301	142° 30'420
depth (m)						
0			13/45			
6	0/22	71/90	1/31	1/35	2/16	0/24
30	0/15	1/15	1/9			
50	0/34	3/15	1/10			
100	2/74	3/20	1/10			

Date	21-Jul	30-Jul	1-Aug	1-Aug	2-Aug
point	Off Fukushima	S1	Pacific ocean	Pacific ocean	Pacific ocean
latitude	37° 6'0521	29° 55'8252	32° 31'1359	34° 26'6541	36° 38'1777
longitude	142° 42'741	144° 58'6662	144° 31'7472	143° 58'8343	143° 20'6400
depth (m)					
0					
6	1/27	1/16	1/21	0/17	0/32
30					
50					
100					

1) MMC resistant cells/all cells in 0.1 ml of seawater

## **4.2 The concentration of radionuclides in the western North Pacific**

**Tatsuo AONO (National Institute for Radiological Sciences: NIRS)**

**Jian ZHENG (NIRS)**

**Hajime KAWAKAMI (JAMSTEC)**

**Makio HONDA (JAMSTEC)**

The most part of artificial radionuclides ( $^{134}\text{Cs}$ ,  $^{137}\text{Cs}$  and Pu isotopes etc.) in the ocean were delivered by global fallout and nuclear weapons testing before the earthquake on March 11<sup>th</sup>. The accidents of Fukushima Daiichi nuclear power plant (FNPP) caused emission of radionuclides to atmosphere and ocean after the Great East Japan Earthquake, and the large volume of pollution water include the high concentrations of radionuclides were flowed to ocean from the FNPP. In order to clarify the distributions and behaviors of radionuclides in the western North Pacific, seawater samples were collected during in this cruise. The collected samples have been determined of Cs and Pu in the laboratory.

Radioactive Cs is measured with a gamma spectrometry using extended range coaxial Ge detector, and Pu isotopes are measured with an alpha spectrometry and ICP-MS.

### **4.3 Estimation of radionuclides' deposition into the ocean in the western Pacific by using a regional chemical model**

**Masayuki TAKIGAWA (JAMSTEC) Principal Investigator (not on-board)**

#### **(1) Objectives**

Total amount of cesium 137 that has been discharged into the atmosphere from the Fukushima Daiichi Power Plant has been estimated to be  $1.2 \times 10^{16}$  Bq by using SPEEDI-II. There were several explosive releases of radionuclides in March 2011, and some of this event might affect the horizontal distribution of radionuclides in the Pacific via the transport in the atmosphere and the dry and wet deposition. It is our objectives to estimate the impact of atmospheric transport and deposition on the horizontal and vertical distributions of radionuclides in the ocean.

#### **(2) Method**

We have developed a Eulerian transport model for radionuclides based on a regional chemical transport model WRF/Chem version 3.1.1. It considers the transport, dispersion, and deposition of radionuclides. As the chemical modules for radionuclides such as decay and deposition have been implemented into the meteorological framework in the WRF model, the convective transport of radionuclides and the vertical mixing by planetary boundary layer are diagnosed based on the meteorologic stability at every model timestep (1 minutes for this study). The model domain covers the oceanic transport model JCOPE domain with the horizontal resolution of 10 km. The model has 34 vertical layers up to 100 hPa. The atmospheric transport and deposition of cesium 137 and iodine 131 is taken into account. Dry deposition velocity for cesium 137 and iodine 131 is taken from Maryon et al. (1991) and Klug et al. (1992), respectively. Wet deposition is based on Maryon et al. (1996), and the three-dimensional rain and snow flux distributions are taken from that in the every model timestep. The precipitation intensity has strong effect on the wet deposition, and the large-scale condensation scheme and the convection scheme have been chosen from preliminary calculations by comparing the meteorological outputs with ground-based observations by JMA (Japan Meteorological Agency). The calculation has been done from 11 March 2011 to 3 May 2011. The emission from Fukushima Daiichi Power Plant is taken from Chino et al. (2011) until 6 April 2011. The emission from 7 April to 3 May was linearly interpolated by using Chino et al (2011) and the estimated value on 20-28 June estimated by TEPCO (Tokyo Electric Power Company).

#### **(3) Preliminary results**

Figure 1 denotes the horizontal distribution of 1-hour accumulated deposition of cesium 137 at 00Z 15 March 2011. Unit is Bq/m<sup>2</sup>. Red and blue lines denote the model domain for WRF/Chem and JCOPE2, respectively.

#### **(4) Data archives**

The model output will be submitted to the Data Management Group in JAMSTEC, and will be archived there.

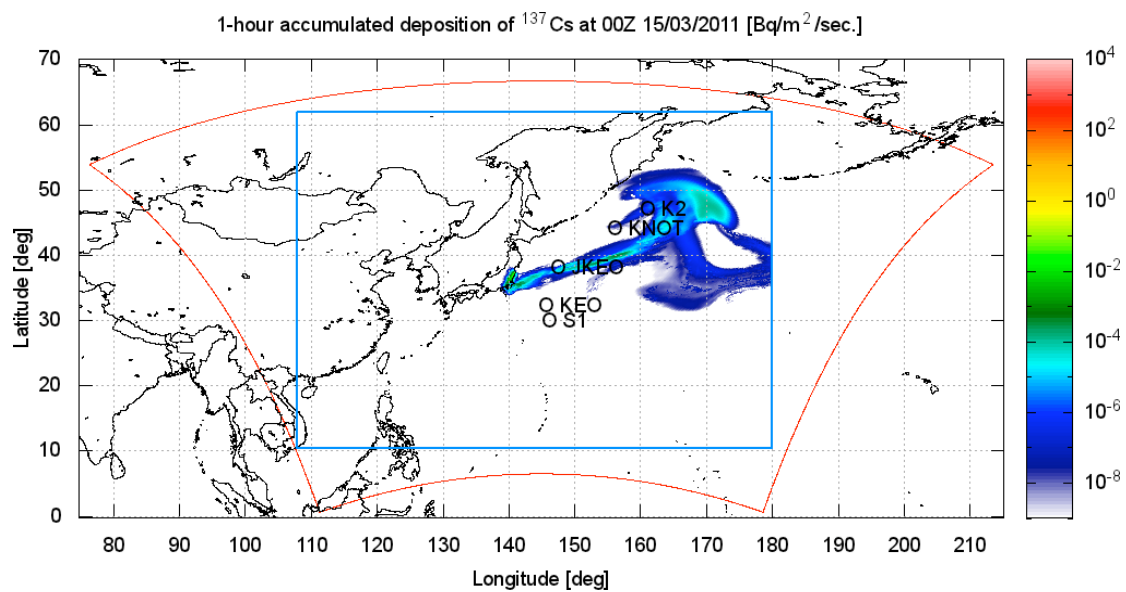


**Fig. 1 : 1-hour accumulated deposition of cesium 137 at 00Z 15 March 2011.**

#### **4.4 Model-observation comparison study on upper-ocean conditions and radionuclide dispersion off Tohoku**

**Yukio MASUMOTO (JAMSTEC)**

To investigate radionuclide dispersion off Tohoku in the northwestern Pacific Ocean after the tragic accident of Fukushima Dai-ichi nuclear power plant, a comparison study for  $^{134}\text{Cs}$  and  $^{137}\text{Cs}$  radioactivity observed during the MR11-05 cruise and that from simulated results is being conducted. Simulated radionuclide dispersion is obtained by a particle-tracking model using surface currents reproduced by Japan Coastal Ocean Predictability Experiment 2 (JCOPE2) model. Source information for  $^{134}\text{Cs}$  and  $^{137}\text{Cs}$  in the model is adopted from observed values obtained by Tokyo Electricity Power Corporation (TEPCO), while atmospheric fallout is excluded for preliminary calculations.

Results from the preliminary calculations tend to show a complicated dispersion pattern with strong influences of coastal current system, offshore geostrophic currents, meso-scale eddy activities, Kuroshio, and local wind stresses. Most of the radionuclides flow southeastward and subsequently extend to eastward along the Kuroshio extension. They spread widely within the mixed-water region between Kuroshio and Oyashio, with the eastern edge near the dateline, though the concentration becomes rather low by the end of August in most of the regions.

Detailed comparison with the observed data will be conducted and processes responsible for the dispersion, including impacts of the atmospheric fallout, will be investigated.

## **4.5 Geochemical behavior of radionuclides from Fukushima Daiichi Nuclear Power Plant in marine environment**

**S. NAGAO (LLRL Kanazawa University)**

**M. INOUE (LLRL Kanazawa University)**

**Y. HAMAJIMA (LLRL Kanazawa University)**

**M. YAMAMOTO (LLRL Kanazawa University)**

### **(1) Objectives**

Nuclear accident at the Fukushima Daiichi Nuclear Power Plant (NPP) was occurred after the 2011 Tohoku Earthquake and Tsunami. About 370-630 PBq of radionuclides was released from the Fukushima Daiichi NPP due to vent and hydrogen explosion (NSC and NISA). To assess radiation dose in marine environment, distribution and activity level of radionuclides are needed for seawater and bottom sediments from coastal to pelagic ocean. In this study, spatial and vertical distributions of  $^{134}\text{Cs}$ ,  $^{137}\text{Cs}$ ,  $^{238}\text{U}$  and  $^{239,240}\text{Pu}$  are measured for surface seawaters and bottom sediments to understand to distribution and geochemical behavior of radionuclides released from the Fukushima Daiichi NPP in western Pacific Ocean.

### **(2) Samplings**

A multiple core sampler was used for taking the surface sediment. This core sampler consists of a main body of 620kg-weight and 4 or 6 sub-core samplers (I.D. 74mm and length of 60cm). Sediment samples for the radionuclide analyses were collected at four stations, Stns. F1, D2, D4 and S1. Each sediment core sample was cut into 2-cm interval on board the ship.

Vertical water samplings were conducted at two stations, Stn. F1 and S1, from 0, 50, 100, and 200 m depth. About 20 L of vertical seawater samples were also collected from 0, 50, and 100 m at Stns. D1, D2, D3, and D4. Surface water samples were collected at Stn. KNOT, JKEO, K2 and KEO.

### **(3) Analytical methods**

The  $^{134}\text{Cs}$ ,  $^{137}\text{Cs}$  and  $^{210}\text{Pb}$  radioactivities of sediment samples are measured by gamma-ray spectrometry using low BKG Ge detectors at LLRL and ultra-low BKG Ge detectors at Ogoya Underground Laboratory of Kanazawa University. Uranium and plutonium analyses were conducted by alpha-ray spectrometry after the pretreatments such as decomposition with mixed acids and separation with ion exchange resin.

Seawater samples were measured for radioactivity of  $^{134}\text{Cs}$  and  $^{137}\text{Cs}$  with low BKG and ultra-low BKG Ge detectors after the coprecipitation with ammonium phosphomolybdate (AMP). The radioactivity of  $^{238}\text{Pu}$  and  $^{239,240}\text{Pu}$  was also measured with alpha-ray spectrometry after the separation and purification by ion exchange techniques.

### **(4) Preliminary results**

Our group will be analyzed for radioactivity of  $^{134}\text{Cs}$  and  $^{137}\text{Cs}$  in seawater and sediment samples collected at each site. Some of seawater and sediment samples at Fukushima Site (D1, D2, D3, and D4) will be measured for radioactivity of  $^{238}\text{U}$  and  $^{238, 239, 240}\text{Pu}$ .

## 4.6 Distribution of radioisotopes in sediments off Fukushima, Japan

**Yoshihisa Kato (School of Marine Science and Technology, Tokai University)**

### (1) Objective

Serious artificial radioactive contamination in the offshore of East Japan was caused by the accident in the Fukushima Nuclear Plant Daiichi. After the accident, it has already been known that the radioisotopes,  $^{134}\text{Cs}$  (half-life  $T = 2.06$  years) and  $^{137}\text{Cs}$  ( $T = 30.01$  years), were highly concentrated in the near shore bottom sediment. These isotopes in the sediment will pollute benthic organisms throughout their life cycle. Particularly, we should keep the behavior and distribution of  $^{137}\text{Cs}$  in benthic environment under observation over a span of 100, because of its long half life. This study aims to clear the down-core and lateral distributions of  $^{134}\text{Cs}$  and  $^{137}\text{Cs}$  in the near-shore sediment off Fukushima just after the nuclear plant accident.

### (2) Sampling

Surface sediment cores were taken from the 4 stations, D1, D2, D4 and F1, in the offshore of the Fukushima Nuclear Power Plant Daiichi using a multiple corer (see Table 4-7-1). For radioactivity measurement, the sediment cores were extruded at 0.5-cm intervals in the top 2 cm-layer and at the 1.0-cm in the depth from 2 to 10 cm on board.

### (3) Shore-based program

Activities of  $^{134}\text{Cs}$ ,  $^{137}\text{Cs}$  and total  $^{210}\text{Pb}$  (supported + unsupported) will be measured using an EG&G Ortec model GWL-120230 well type HPGe detector. The specific gamma rays at 604.7 keV and 795.86 keV for  $^{134}\text{Cs}$ , 661.7 keV for  $^{137}\text{Cs}$  and 46.5 keV for  $^{210}\text{Pb}$  will be counted for 48 h using a Seiko EG&G model 7800 multi-channel analyzer. The efficiencies are able to be calibrated using Uranium-Thorium Ore DL-1a for  $^{210}\text{Pb}$  (the activity is equal to  $23.3 \text{ Bq kg}^{-1}$ ; Canada Center for Mineral and Energy Technology) and the house reference material for  $^{137}\text{Cs}$  ( $45 \text{ Bq kg}^{-1}$ ) prepared by adsorption of a known activity  $^{137}\text{Cs}$  standard solution (Japan Radioisotope Association) on to a powdered sediment prepared from the deeper portion of a deep-sea piston core.

#### 4.7 Detection of radioactive sulfur in the maritime air and surface seawater

**Naohiro YOSHIDA (PI, Tokyo Institute of Technology, not on board)**

**Sakae TOYODA (Tokyo Institute of Technology, not on board)**

**Keita YAMADA (Tokyo Institute of Technology, not on board)**

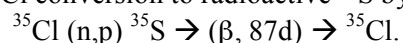
**Chisato YOSHIKAWA (Tokyo Institute of Technology, not on board)**

**Sebastian O. DANIELACHE (Tokyo Institute of Technology, not on board)**

##### (1) Objectives

A massive earthquake (magnitude 9.0) hit Japan near the east coast of Honshu on 11th March 2011. The earthquake followed by a deadly tsunami extensively damaged the Fukushima nuclear power plant situated in Fukushima, 177 km from the epicenter. The Fukushima nuclear power plant has six boiling water reactor (BWR). The earthquake triggered the automatic shutdown of the three operating reactors - Units 1, 2 and 3 and the control rods were completely inserted to terminate the nuclear fission reaction occurring within the fuel core. However, residual heat produced at the reactor core due to the radioactive decay of fission products requires extended time period to cool.

As reported, maintaining enough cooling to remove the decay heat from the reactor and spent fuel pool was the main challenge at the affected reactor site after the March 11th tsunami. Since both in-site and off-site power to the plant was disabled, sea water mixed with boric acid (to reduce the neutron flux in the core and thus slow down the nuclear reaction) was pumped into reactor vessel of Unit 1, 2 and 3 continuously for 13 days from period 13th March to 26th March 2011. Sea water was also sprayed by helicopters and concrete pump on the spent fuel containment. Nearly few hundred tones of sea water was used as a coolant before switching to fresh water after realizing the potential or corrosional processes. Another disadvantage is that salts and minerals present in sea water may also become radioactive by reacting with thermal neutrons emitted from the reactor. A specific example is  $^{35}\text{Cl}$  conversion to radioactive  $^{35}\text{S}$  by an (n,p) reaction:



Radioactive  $^{35}\text{S}$  ( $\beta$  decay to  $^{35}\text{Cl}$ , half life  $\sim 87$  days) is also produced in atmosphere by cosmic ray spallation of  $^{40}\text{Ar}$ . The  $^{35}\text{S}$  production rate has both altitudinal and latitudinal dependence and the polar troposphere has the maximum production rate and equatorial troposphere the minimum. Once produced,  $^{35}\text{S}$  rapidly oxidizes to  $^{35}\text{SO}_2$  ( $\sim 1\text{sec}$ ) which is removed from the atmosphere by wet and dry deposition.  $^{35}\text{SO}_2$  may undergo gas and aqueous phase oxidation to produce  $^{35}\text{SO}_4^{2-}$  aerosols which are removed from the atmosphere.  $^{35}\text{S}$  is the only radioactive isotope which simultaneously exists in gas and particle phases and has a suitably short half life to detect air motions which renders it a sensitive tracer in understanding boundary layer chemistry and air mass transport on short time scales.  $^{35}\text{S}$  measurements have been done on atmospheric sulfate and  $\text{SO}_2$  gas at the coastal and inland site to understand boundary layer chemistry and to calculate the dry deposition rate of  $\text{SO}_2$ .

The Fukushima nuclear plant uniquely served as a point source of artificially made  $^{35}\text{S}$  into the atmosphere for a considerably long time period which provided an excellent opportunity to understand the gas ( $^{35}\text{SO}_2$ ) to particle ( $^{35}\text{SO}_4^{2-}$ ) conversion and its long range transport over the Pacific. The simultaneous gas and particle speciation and 87 day half life render it a unique isotope to clock transformation and transportation, particularly given the unique point source and its magnitude. Other fission products e.g.  $^{137}\text{Cs}$ ,  $^{131}\text{I}$  behave as a solid particle, becoming attached to



aerosol surface subsequent to their radiogenic formation and do not strictly reflect the atmospheric gas phase chemistry.

The purpose of this study is to understand the chemical evolution of radioactive  $^{35}\text{S}$  to aerosols during the long range transport and clock the sulfur chemistry in the environment by measuring  $^{35}\text{S}$  activity in atmospheric sulfate collected from aerosol and sea water, and by comparing the results with those in soil, rain water, stream from various locations in Japan and at the west coast of USA (Scripps Institute of Oceanography, California). Present work will also help us in predicting the diffusion pathways of other radioactive contamination in the atmosphere and its future use for the evaluation of the environmental problems.

## (2) Methods

Aerosols were collected onto a quartz filter (Pallflex, 2500QAT-UP, 8\*10 inches) using a high-volume air sampler (Kimoto Electric Co. Ltd., 123SL) at the air flow rate of 1020 L/min. Surface seawater was collected into a 5-L plastic bottle using a bucket (when the ship was staying) or continuous sampling system (when the ship was underway).

Aerosol samples will be analyzed by a Ge-detector for  $\gamma$ -emitting nuclides ( $^{137}\text{Cs}$ ,  $^{134}\text{Cs}$ , etc.) at the Radioisotope Center, Tokyo Institute of Technology, and then by a low-level liquid scintillation spectroscopy for  $^{35}\text{S}$  at University of California, San Diego (Dr. M. Thiemens), where extraction of  $^{35}\text{S}$  and preparation of  $\text{BaSO}_4$  will be also conducted. Seawater samples will be treated to precipitate  $^{35}\text{S}$  as  $\text{BaSO}_4$  and measured at UCSD similarly to the aerosol samples.

## (3) Results

Collected samples are listed in Tables 1 and 2. They will be analyzed as described in Methods.

## (4) Data archives

The data of  $^{35}\text{S}$  concentrations in aerosol and seawater will be submitted to the JAMSTEC DMO (Data Management Office)

Table 1. List of aerosol samples.

Sample ID	Date&time (UTC)		Site		Flow rate (L/min)		Air volume (m3)	Personel	Notes
	Start	Stop	Start	Stop	Initial	Final			
MR11-05-TT-HV#1	2011/7/16 4:20	2011/7/17 22:00	Yokohama	F1	1017	1018	2531.6	Honda	Sunny
MR11-05-TT-HV#2	2011/7/17 22:02	2011/7/20 9:01	F1	off Kamaishi	1021	1018	3610.8	Honda	Storm wind (typhoon) on Jul 19-20
MR11-05-TT-HV#3	2011/7/20 9:03	2011/7/20 4:13	off Kamaishi	S1	1018	1021	4128.8	Honda	Black aerosols (contamination by ship's smoke?)
MR11-05-TT-HV#4	2011/7/20 4:19	2011/7/25 22:53	S1	S1	1026	1023	4096.5	Honda	
MR11-05-TT-HV#5	2011/7/25 22:55	2011/7/28 1:48	S1	S1	1021	1023	3137.2	Honda	
MR11-05-TT-HV#6	2011/7/28 1:50	2011/7/31 1:42	S1	S1	1023	1022	4440.6	Honda	Rainy at the stop time
MR11-05-TT-HV#7	2011/7/31 1:44	2011/8/1 22:52	S1	?	1023	1019	2790.6	Honda	
MR11-05-TT-HV#8	2011/8/1 22:53	2011/8/3 22:56	?	Sekinehama	1021	1019	5763.9	Honda	Mist at the stop time

Table 2. List of surface seawater samples.

Sample ID	Month	Day	Time (UTC)	Latitude (N) °	Longitude (E) °	Station	Personel	Notes
MR11-05-TT-SW#1	7	1	22:38	47	160	K2	Wakita	CTD Cast.4
MR11-05-TT-SW#2	7	9	11:36	44	155	KNOT	Wakita	CTD Cast.1
MR11-05-TT-SW#3	7	11	10:32	38	5 146	25 JKEO	Wakita	CTD Cast.1
MR11-05-TT-SW#4	7	13	1:05	36	29 141	30 F1	Wakita	CTD Cast.2
MR11-05-TT-SW#5	7	15	9:50	35	41.72 141	14.02 Off Choshi	Wakita	Surface pump
MR11-05-TT-SW#6	7	15	17:26	34	48.26 140	15.82 Off Tateyama	Wakita	Surface pump
MR11-05-TT-SW#7	7	18	7:05	36	41.44 141	9 D4	Wakita	CTD Cast.1
MR11-05-TT-SW#8	7	18	22:02	36	59.98 141	16.97 D3	Wakita	CTD Cast.1
MR11-05-TT-SW#9	7	19	1:11	37	19.93 141	27.93 D2	Wakita	CTD Cast.1
MR11-05-TT-SW#10	7	19	5:00	37	35.01 141	30.95 D1	Wakita	CTD Cast.1
MR11-05-TT-SW#11	7	19	9:58	37	48.7 142	18.8 Off Kinkazan	Wakita	Surface pump
MR11-05-TT-SW#12	7	20	9:01	39	18.3 142	30.5 Off Kamaishi	Wakita	Surface pump
MR11-05-TT-SW#13	7	24	8:24	30	0.1 144	59.97 S1	Wakita	CTD Cast.2
MR11-05-TT-SW#14	8	2	23:05	40	41.84 141	56.55 Off Hachinohe	Wakita	Surface pump

#### 4.8. Multiple Corer (MC)

**Katsunori KIMOTO (RIGC, JAMSTEC)**

**Sayaka KAWAMURA (Marine Works Japan Co. Ltd): Operation Leader**

**Tomoyuki TAKAMORI (Marine Works Japan Co. Ltd)**

##### (1) Objective

After the hit of East Japan Huge Earthquake occurred in 11, March, 2011, the artificial radioactive leakage has been continued from the Fukushima Daiichi Nuclear plants. Huge amount of artificial radioactive nuclides that is emitting from the atomic reactors flow into the Pacific Ocean, and pollute ambient environments. Observation of diffusion of radionuclides is quite important to evaluate affection to natural environments, especially marine biosphere. In this cruise, we collected bottom sediments from 5 stations near the Fukushima Daiichi Nuclear Power Plants (~50 km far from coast at minimum) to observe the concentrations of radionuclides on the seafloor and evaluate the pollution of the bottom water environments.

##### (2) Instruments and methods

A Multiple core sampler (Rigo co. ltd., Japan) was used for taking the surface sediment. This core sampler consists of a main body of 620kg-weight and 4 or 8 sub-core samplers (I.D. 74mm and length of 60cm).

##### Winch operation

When we started lowering PC and MC, a speed of wire out was set to be 0.3 m/s, and then gradually increased to the maximum of 1.0 m/s. The corers were stopped at a depth about 50 m above the seafloor for 5 minutes to reduce some pendulum motion of the system. After the corers were stabilized, the wire was stored out at a speed of 0.3 m/s and we carefully watched a tension meter. When the corers touched the bottom, wire tension abruptly decreases by the loss of the corer weight. Immediately after confirmation that the corers hit the bottom, wire out was stopped and winding of the wire was started at a speed of 0.3m/s until the tension gauge indicates that the corers were lifted off the bottom. After leaving the bottom, winch wire was wound in at the maximum speed.

##### (3) Results

Results of MC recoveries were summarized in table 4-8-1. Main lithologies of sediments in Stn. D-1 (MC05), D-2 (MC04), and D-4 (MC02) were fine to very fine sand. The sediment in Stn. F-1 (MC01), deeper site of off Fukushima, was composed of silt with very fine sand. These sediments were basically massive and it was not observed typical sedimentological features. In Stn. S1 (MC06), very far from Fukushima and deepest site in this cruise, sediment was composed of massive siliceous clay. It was observed black colored two volcanic ash layers at ~20 and 25cm of core.

##### (4) Future works

Recovered core materials were distributed to some institutes. Measuring  $^{134}\text{Cs}$  and  $^{137}\text{Cs}$ ,  $^{238}\text{U}$ ,  $^{239}\text{Pu}$ ,  $^{240}\text{Pu}$  will be performed by Tokai University, Kanazawa University, and National Institute of Radiological Sciences (NIRS).

Table 4-8-1. Coring summary of the MC.

Date (mmddyy)	Core ID	St.	Location	Latitude	Longitude	water depth (m)	HAND	Length (cm)	Distribution
2011.7.18	MC01	F-1	Off Fukushima	36°28.9658' N	141°29.9313' E	1327	HAND1	13.0	JAMSTEC
							HAND2	13.5	Kanazawa Univ.
							HAND4	15.0	Tokai Univ.
							HAND5	15.5	-
							HAND6	15.0	Kanazawa Univ.
							HAND8	14.0	NIRS
2011.7.18	MC02	D-4	Off Fukushima	36°41.4423' N	141°09.0083' E	206	HAND1	25.0	Tokai Univ.
							HAND4	25.0	Kanazawa Univ.
							HAND5	25.0	-
							HAND8	25.5	JAMSTEC
2011.7.18	MC03	D-3	Off Fukushima	36°59.9849' N	141°16.9764' E	154	HAND1	0.0	no recovery
							HAND4	0.0	
							HAND5	0.0	
							HAND8	0.0	
2011.7.19	MC04	D-2	Off Fukushima	37°19.9387' N	141°27.9335' E	158	HAND1	15.0	JAMSTEC
							HAND4	14.7	Tokai Univ.
							HAND5	13.3	Kanazawa Univ.
							HAND8	0.0	-
2011.7.19	MC05	D-1	Off Fukushima	37°35.0121' N	141°30.9534' E	141	HAND1	22.7	Tokai Univ.
							HAND4	37.7	JAMSTEC
							HAND5	45.0	-
							HAND8	23.0	NIRS
2011.7.25	MC06	S1	NW Pacific	30°11.9763' N	145°05.9590' E	5939	HAND1	36.5	Kanazawa Univ.
							HAND4	37.0	Kanazawa Univ.
							HAND5	36.0	-
							HAND8	38.0	JAMSTEC

## (5) Observation log

Observation logs are shown in table 4-8-2~4-8-7.

Table 4-8-2. Observation log of the MC01.

Cruise Name:		MR11-05 Leg2		Operator:		Sayaka Kawamura(MWJ)		
Date: (UTC)		2011/7/18						
Core Number:		MC01						
Area:		Off Fukushima						
Sampling Site:		St.F1						
Weather:		Fine						
Wind direction:		220deg		Wind speed:		4.2m/s		
Current direction:		8.4deg		Current speed:		0.2knot		
Time*	Depth	Wire length	Latitude	Longitude	Tension	Wire speed	Wire in/out	Remarks
(UTC)	(m)	(m)			(ton)	(m/s)	( ↑ / ↓ )	
228	1328	-			-	-	-	Start the operation.
229	1333	0	36°29.0007' N	141°29.9601' E	0.5	0.0	-	MC on surface. Reset the wire length. Wire out (-0.9m/s).
240	1328	500			0.9	0.0	-	Start the swell compensator. Wire out (-0.9m/s).
251	1331	1000			1.3	0.9	↓	
256	1327	1280			1.7	0.0	-	Wire stop.
302	1329	1280			1.6	~0.3	↓	Wire out.
3:04:57	1327	1324	36°28.9658' N	141°29.9313' E	Min. 1.0	0.3	↓	MC hit the bottom**, Wire out 5m.
305	1327	1328			1.1	0.0	-	Wire stop. Wait 30 seconds.
306	1328	1328			1.1	~0.3	↑	Wire in.
3:07:04	1327	1317	36°28.9627' N	141°29.9290' E	Max. 2.1	0.3	↑	MC left the bottom** Wire in (-1.0m/s).
312	1328	1000			1.5	1.0	↑	
321	1329	500			0.9	0.0	-	Stop the swell compensator. Wire in (-0.9m/s).
332	1326	0	36°28.9381' N	141°29.9296' E	0.6	0.1	↑	MC on surface.
334	-	-			-	-	-	MC on deck.
*LST: UTC +9h								
**Latitude and Longitude was used the ship position.								

Table 4-8-3. Observation log of the MC02.

Cruise Name:	MR11-05_Leg2	Operator:	Sayaka Kawamura(MWJ)				
Date: (UTC)	2011/7/18						
Core Number:	MC02						
Area:	Off Fukushima						
Sampling Site:	St.D4						
Weather:	Cloudy						
Wind direction:	196deg	Wind speed:	2.9m/s				
Current direction:	312deg	Current speed:	0.1knot				

Table 4-8-4. Observation log of the MC03.

Cruise Name:	MR11-05_Leg2		Operator:	Sayaka Kawamura(MWJ)				
Date: (UTC)	2011/7/18							
Core Number:	MC03							
Area:	Off Fukushima							
Sampling Site:	St.D3							
Weather:	Cloudy							
Wind direction:	189deg		Wind speed:	6.7m/s				
Current direction:	260.3deg		Current speed:	0.4knot				
Time*	Depth	Wire length	Latitude	Longitude	Tension	Wire speed	Wire in/out	Remarks
(UTC)	(m)	(m)			(ton)	(m/s)	(↑ / ↓)	
2056	154	-			-	-	-	Start the operation.
2058	155	0	36°59.9883' N	141°16.9838' E	0.4	0.0	-	MC on surface. Reset the wire length. Wire out (~0.9m/s).
2104	154	100			0.5	0.0	-	Wire stop.
2109	154	100			0.5	~0.3	↓	Wire out.
21:12:32	154	148	36°59.9849' N	141°16.9764' E	Min. 0.0	0.3	↓	MC hit the bottom**, Wire out 6m.
2112	154	153			0.0	0.0	-	Wire stop. Wait 60 seconds.
2114	154	153			0.0	~0.3	↑	Wire in.
21:15:11	154	140	36°59.9843' N	141°16.9752' E	Max. 1.1	0.3	↑	MC left the bottom** Wire in (~9.0m/s).
2120	154	0	36°59.9807' N	141°16.9642' E	0.6	0.2	↑	MC on surface.
2122	-	-			-	-	-	MC on deck.
*LST: UTC +9h								
**Latitude and Longitude was used the ship position.								

Table 4-8-5. Observation log of the MC04.

Cruise Name:	MR11-05_Leg2	Operator:	Sayaka Kawamura(MWJ)					
Date: (UTC)	2011/7/19							
Core Number:	MC04							
Area:	Off Fukushima							
Sampling Site:	St.D2							
Weather:	Rain							
Wind direction:	193deg	Wind speed:	4.6m/s					
Current direction:	138.3deg	Current speed:	0.4knot					
Time*	Depth	Wire length	Latitude	Longitude	Tension	Wire speed	Wire in/out	Remarks
(UTC)	(m)	(m)			(ton)	(m/s)	(↑ / ↓)	
006	160	-			-	-	-	Start the operation.
009	159	0	37°19.9324' N	141°27.9420' E	0.4	0.0	-	MC on surface. Reset the wire length. Wire out (~0.9m/s).
013	160	110			0.5	0.0	-	Wire stop.
018	158	110			0.6	~0.3	↓	Wire out.
0:20:52	158	152	37°19.9387' N	141°27.9335' E	Min. 0.0	0.3	↓	MC hit the bottom**, Wire out 6m.
021	158	157			0.0	0.0	-	Wire stop. Wait 60 seconds.
022	159	157			0.0	~0.3	↑	Wire in.
0:23:00	159	146	37°19.9353' N	141°27.9347' E	Max. 1.1	0.3	↑	MC left the bottom** Wire in (~9.0m/s).
027	159	0	37°19.9367' N	141°27.9407' E	0.6	0.1	↑	MC on surface.
028	159	-			-	-	-	MC on deck.
*LST: UTC +9h								
**Latitude and Longitude was used the ship position.								

Table 4-8-6. Observation log of the MC05.

Cruise Name:	MR11-05_Leg2		Operator:	Sayaka Kawamura(MWJ)				
Date: (UTC)	2011/7/19							
Core Number:	MC05							
Area:	Off Fukushima							
Sampling Site:	St.D1							
Weather:	Rain							
Wind direction:	197deg		Wind speed:	11.2m/s				
Current direction:	194.5deg		Current speed:	0.5knot				
Time*	Depth	Wire length	Latitude	Longitude	Tension	Wire speed	Wire in/out	Remarks
(UTC)	(m)	(m)			(ton)	(m/s)	(↑ / ↓)	
3:58	140	-			-	-	-	Start the operation.
4:00	140	0	37°35.0164' N	141°30.9590' E	0.5	0.0	-	MC on surface. Reset the wire length. Wire out (~0.9m/s).
4:07	141	91			0.5	0.0	-	Wire stop.
4:12	141	91			0.5	~0.3	↓	Wire out.
4:15:04	141	136	37°35.0121' N	141°30.9534' E	Min. 0.0	0.3	↓	MC hit the bottom**, Wire out 6m.
4:15	140	142			0.0	0.0	-	Wire stop. Wait 60 seconds.
4:16	140	142			0.0	~0.3	↑	Wire in.
4:17:27	140	129	37°35.0092' N	141°30.9522' E	Max. 1.4	0.3	↑	MC left the bottom** Wire in (~9.0m/s).
4:24	140	0	37°35.0037' N	141°30.9330' E	0.6	0.0	↑	MC on surface.
4:25	140	-			-	-	-	MC on deck.
*LST: UTC +9h								
**Latitude and Longitude was used the ship position.								

Table 4-8-7. Observation log of the MC06.

Cruise Name:		MR11-05 Leg2		Operator:		Sayaka Kawamura(MWJ)			
Date: (UTC)		2011/7/25							
Core Number:		MC06							
Area:		The Western North Pacific							
Sampling Site:		St.S1							
Weather:		Fine but cloudy							
Wind direction:		60deg		Wind speed:		3.0m/s			
Current direction:		4.3deg		Current speed:		0.8knot			
Time*	Depth	Wire length	Latitude	Longitude	Tension	Wire speed	Wire in/out	Remarks	
(UTC)	(m)	(m)			(ton)	(m/s)	(↑ / ↓)		
21:57	5941	-			-	-	-	Start the operation.	
21:59	5940	0	30°11.9526' N	145°05.9612' E	0.5	0.0	-	MC on surface. Reset the wire length. Wire out (~1.0m/s).	
22:10	5943	500			0.9	0.0	-	Start the swell compensator. Wire out (~1.0m/s).	
22:19	5941	1000			1.3	1.0	↓		
22:28	5940	1500			1.7	1.0	↓		
22:36	5941	2000			2.1	1.0	↓		
22:44	5943	2500			2.5	1.0	↓		
22:53	5940	3000			3.0	1.0	↓		
23:01	5942	3500			3.4	1.0	↓		
23:10	5940	4000			3.9	1.0	↓		
23:19	5936	4500			4.3	1.0	↓		
23:26	5941	5000			4.6	1.0	↓		
23:35	5940	5500			5.1	1.0	↓		
23:42	5937	5890			5.6	0.0	-	Wire stop.	
23:47	5939	5890			5.5	~0.3	↓	Wire out.	
23:50:31	5939	5937	30°11.9763' N	145°05.9590' E	Min. 4.8	0.3	↓	MC hit the bottom**, Wire out 5m.	
23:50	5939	5942			4.9	0.0	-	Wire stop. Wait 30 seconds.	
23:51	5937	5942			4.9	~0.3	↑	Wire in.	
23:52:49	5940	5917	30°11.9783' N	145°05.9585' E	Max. 6.1	0.3	↑	MC left the bottom** Wire in (~1.1m/s).	
23:59	5939	5500			5.4	1.1	↑		
00:07	5938	5000			5.0	1.1	↑		
00:14	5939	4500			4.6	1.1	↑		
00:21	5939	4000			4.2	1.1	↑		
00:29	5945	3500			3.7	1.1	↑		
00:37	5942	3000			3.3	1.1	↑		
00:44	5945	2500			2.9	1.1	↑		
00:52	5939	2000			2.4	1.1	↑		
01:00	5937	1500			1.9	1.1	↑		
01:07	5938	1000			1.5	1.1	↑		
01:16	5940	500			1.0	0.0	-	Stop the swell compensator. Wire in (~0.9m/s).	
01:25	5942	0	30°11.9659' N	145°05.9954' E	0.6	0.1	↑	MC on surface.	
01:28	5944	-			-	-	-	MC on deck.	
*LST: UTC +10h									
**Latitude and Longitude was used the ship position.									

## 5. Geophysical observation

### 5.1 Swath Bathymetry

**Takeshi MATSUMOTO (University of the Ryukyus): Principal Investigator (not on-board)**

**Masao NAKANISHI (Chiba University): Principal Investigator (not on-board)**

**Katsuhisa MAENO (Global Ocean Development Inc.: GODI)**

**Harumi OTA (GODI)**

**Ryo OYAMA (Mirai Crew)**

#### (1) Introduction

R/V MIRAI is equipped with a Multi narrow Beam Echo Sounding system (MBES), SEABEAM 2112.004 (SeaBeam Instruments Inc.). The objective of MBES is collecting continuous bathymetric data along ship's track to make a contribution to geological and geophysical investigations and global datasets.

#### (2) Data Acquisition

The "SEABEAM 2100" on R/V MIRAI was used for bathymetry mapping during the MR11-05 cruise from 27 June to 3 August 2011.

To get accurate sound velocity of water column for ray-path correction of acoustic multibeam, we used Surface Sound Velocimeter (SSV) data to get the sea surface (6.2m) sound velocity, and the deeper depth sound velocity profiles were calculated by temperature and salinity profiles from CTD and XCTD data by the equation in Del Grosso (1974) during the cruise.

Table 5.1-1 shows system configuration and performance of SEABEAM 2112.004 system.

Table 5.1-1 System configuration and performance

#### SEABEAM 2112.004 (12 kHz system)

Frequency:	12 kHz
Transmit beam width:	2 degree
Transmit power:	20 kW
Transmit pulse length:	3 to 20 msec.
Depth range:	100 to 11,000 m
Beam spacing:	1 degree athwart ship
Swath width:	150 degree (max)
	120 degree to 4,500 m
	100 degree to 6,000 m
	90 degree to 11,000 m
Depth accuracy:	Within < 0.5% of depth or +/-1m, whichever is greater, over the entire swath. (Nadir beam has greater accuracy; typically within < 0.2% of depth or +/-1m, whichever is greater)

#### (3) Preliminary Results



The results will be published after primary processing.

(4) Data Archives

Bathymetric data obtained during this cruise will be submitted to the Data Management Group (DMG) in JAMSTEC, and will be archived there.

## 5.2 Sea surface gravity

**Takeshi MATSUMOTO (University of the Ryukyus): Principal Investigator (not on-board)**

**Masao NAKANISHI (Chiba University): Principal Investigator (not on-board)**

**Katsuhisa MAENO (Global Ocean Development Inc.: GODI)**

**Harumi OTA (GODI)**

**Ryo OYAMA (Mirai Crew)**

### (1) Introduction

The local gravity is an important parameter in geophysics and geodesy. We collected gravity data at the sea surface.

### (2) Parameters

Relative Gravity [CU: Counter Unit]

[mGal] = (coef1: 0.9946) \* [CU]

### (3) Data Acquisition

We measured relative gravity using LaCoste and Romberg air-sea gravity meter S-116 (Micro-g LaCoste, LLC) during the MR11-05 cruise from 27 June 2011 to 4 August 2011.

To convert the relative gravity to absolute one, we measured gravity using portable gravity meter (Scintrex gravity meter CG-5), at Yokohama as the reference points.

### (4) Preliminary Results

Absolute gravity table is shown in Table 5.2-1.

Table 5.2-1

No.	Date	U.T.C.	Port	Absolute Gravity [mGal]	Sea Level [cm]	Draft [cm]	Gravity at Sensor * <sup>1</sup> [mGal]	L&R * <sup>2</sup> Gravity [mGal]
#1	26 Jun. 08:25		Sekinehama	980371.94	277	643	980372.84	12653.44
#2	05 Aug.00:15		Sekinehama	980371.94	267	638	980372.81	12653.16

\*<sup>1</sup>: Gravity at Sensor = Absolute Gravity + Sea Level\*0.3086/100 + (Draft-530)/100\*0.0431

\*<sup>2</sup>: LaCoste and Romberg air-sea gravity meter S-116

### (5) Data Archives

Surface gravity data obtained during this cruise will be submitted to the Data Management Group (DMG) in JAMSTEC, and will be archived there.

### 5.3 Sea Surface magnetic field

**Takeshi MATSUMOTO**(University of the Ryukyus): Principal Investigator (not on-board)

**Masao NAKANISHI** (Chiba University): Principal Investigator (not on-board)

**Katsuhisa MAENO** (Global Ocean Development Inc.: GODI)

**Harumi OTA** (GODI)

**Ryo OYAMA** (Mirai Crew)

#### 1) Three-component magnetometer

##### (1) Introduction

Measurements of magnetic force on the sea are required for the geophysical investigations of marine magnetic anomaly caused by magnetization in upper crustal structure. We measured geomagnetic field using a three-component magnetometer during the MR11-05 cruise from 27 June 2011 to 4 August 2011.

##### (2) Principle of ship-board geomagnetic vector measurement

The relation between a magnetic-field vector observed on-board, **H<sub>ob</sub>**, (in the ship's fixed coordinate system) and the geomagnetic field vector, **F**, (in the Earth's fixed coordinate system) is expressed as:

$$\mathbf{H}_{ob} = \mathbf{A} \mathbf{R} \mathbf{P} \mathbf{Y} \mathbf{F} + \mathbf{H}_p \quad (a)$$

where **R**, **P** and **Y** are the matrices of rotation due to roll, pitch and heading of a ship, respectively. **A** is a 3 x 3 matrix which represents magnetic susceptibility of the ship, and **H<sub>p</sub>** is a magnetic field vector produced by a permanent magnetic moment of the ship's body. Rearrangement of Eq. (a) makes

$$\mathbf{B} \mathbf{H}_{ob} + \mathbf{H}_{bp} = \mathbf{R} \mathbf{P} \mathbf{Y} \mathbf{F} \quad (b)$$

where **B** = **A**<sup>-1</sup>, and **H<sub>bp</sub>** = -**B H<sub>p</sub>**. The magnetic field, **F**, can be obtained by measuring **R**, **P**, **Y** and **H<sub>ob</sub>**, if **B** and **H<sub>bp</sub>** are known. Twelve constants in **B** and **H<sub>bp</sub>** can be determined by measuring variation of **H<sub>ob</sub>** with **R**, **P** and **Y** at a place where the geomagnetic field, **F**, is known.

##### (3) Instruments on R/V MIRAI

A shipboard three-component magnetometer system (Tierra Technica SFG1214) is equipped on-board R/V MIRAI. Three-axes flux-gate sensors with ring-cored coils are fixed on the fore mast. Outputs of the sensors are digitized by a 20-bit A/D converter (1 nT/LSB), and sampled at 8 times per second. Ship's heading, pitch, and roll are measured utilizing a Inertial Navigation System (Fiber Optical Gyro) installed for controlling attitude of a Doppler radar. Ship's position (GPS) and speed data are taken from LAN every second.

##### (4) Data Archives

These data obtained during this cruise will be submitted to the Data Management Group (DMG) in JAMSTEC, and will be archived there.

##### (6) Remarks

1. For calibration of the ship's magnetic effect, we made a "Figure eight" turn (a pair of clockwise and anti-clockwise rotation). The periods were follows;
  - i) 23:52UTC 14 Jul. - 00:19 UTC 17 Jul. around at 37-36N, 141-43E
  - ii) 03:59UTC 03 Aug. - 04:31 UTC 03 Aug. around at 41-29N, 141-43E

## 2) Cesium magnetometer

### (1) Introduction

Measurement of total magnetic force on the sea is required for the geophysical investigations of marine magnetic anomaly caused by magnetization in upper crustal structure.

### (2) Data Period

09 Jul. 2011, 12:12UTC – 11 Jul. 2011, 05:23UTC

11 Jul. 2011, 10:21UTC – 12 Jul. 2011, 06:50UTC

### (3) Specification

We measured total geomagnetic field using a cesium marine magnetometer (Geometrics Inc., G-882) and recorded by G-882 data logger (Clovertech Co., Ver.1.0.0). The G-882 magnetometer uses an optically pumped Cesium-vapor atomic resonance system. The sensor fish towed 500 m behind the vessel to minimize the effects of the ship's magnetic field. Table 5.3-1 shows system configuration of MIRAI cesium magnetometer system.

Table 5.3-1 System configuration of MIRAI cesium magnetometer system.

Dynamic operating range:	20,000 to 100,000 nT
Absolute accuracy:	$< \pm 2$ nT throughout range
Setting: Cycle rate;	0.1 sec
Sensitivity;	0.001265 nT at a 0.1 second cycle rate
Sampling rate;	1 sec

### (4) Data Archive

Total magnetic force data obtained during this cruise was submitted to the Data Management Group (DMG) of JAMSTEC, and archived there.

### (5) Remarks

1. In the following period, data acquisition was suspended due to PC trouble.  
11 Jul. 2011, 15:08UTC – 11 Jul. 2011, 16:41UTC

## **6. Satellite Image Acquisition (MCSST from NOAA/HRPT)**

<b>Makio HONDA</b>	<b>(JAMSTEC)</b>
<b>Katsuhisa MAENO</b>	<b>(Global Ocean Development Inc.: GODI)</b>
<b>Harumi OTA</b>	<b>(GODI)</b>
<b>Ryo OYAMA</b>	<b>(Mirai Crew)</b>

### **(1) Objectives**

It is our objectives to collect data of sea surface temperature in a high spatial resolution mode from the Advance Very High Resolution Radiometer (AVHRR) on the NOAA polar orbiting satellites and to build a time and depth resolved primary productivity model.

### **(2) Method**

We receive the down link High Resolution Picture Transmission (HRPT) signal from NOAA satellites. We processed the HRPT signal with the in-flight calibration and computed the sea surface temperature by the Multi-Channel Sea Surface Temperature (MCSST) method. A daily composite map of MCSST data is processed for each day on the R/V MIRAI for the area, where the R/V MIRAI located.

We received and processed NOAA data throughout MR11-05 cruise from 27 June 2011 to 3 August 2011.

The sea surface temperature data will be applied for the time and depth resolved primary productivity model to determine a temperature field for the model.

### **(3) Data archives**

The raw data obtained during this this cruise will be submitted to the Data Management Group (DMG) in JAMSTEC, and will be archived there.